ΕΘΝΙΚΟ ΜΕΤΣΟΒΙΟ ΠΟΛΥΤΕΧΝΕΙΟ
ΣΧΟΛΗ ΕΦΑΡΜΟΣΜΕΝΩΝ ΜΑΘΗΜΑΤΙΚΩΝ
ΚΑΙ ΦΥΣΙΚΩΝ ΕΠΙΣΤΗΜΩΝ

ΜΕΛΕΤΗ ΕΝΑΛΛΑΚΤΙΚΩΝ ΘΕΩΡΙΩΝ ΒΑΡΥΤΗΤΑΣ ΣΤΗΝ ΚΟΣΜΟΛΟΓΙΑ, ΕΝΟΨΕΙ ΤΩΝ ΝΕΩΝ ΠΑΡΑΤΗΡΗΣΕΩΝ ΑΠΟ ΒΑΡΥΤΙΚΑ ΚΥΜΑΤΑ

Διδακτορικη Διατριβη

Στυλιανου Σ. Καρυδα
Πτυχιουχου του Τμηματος Φυσικης του Πανεπιστημιου Αθηνων

ΕΠΙΒΛΕΠΩΝ:
ΕΛΕΥΘΕΡΙΟΣ ΠΑΠΑΝΤΩΝΟΠΟΥΛΟΣ
Ομ. Καθηγητής ΕΜΠ

Αθήνα, 2023

ΕΘΝΙΚΟ ΜΕΤΣΟΒΙΟ ΠΟΛΥΤΕΧΝΕΙΟ
ΣΧΟΛΗ ΕΦΑΡΜΟΣΜΕΝΩΝ ΜΑΘΗΜΑΤΙΚΩΝ
ΚΑΙ ΦΥΣΙΚΩΝ ΕΠΙΣΤΗΜΩΝ

ΜΕΛΕΤΗ ΕΝΑΛΛΑΚΤΙΚΩΝ ΘΕΩΡΙΩΝ ΒΑΡΥΤΗΤΑΣ ΣΤΗΝ ΚΟΣΜΟΛΟΓΙΑ, ΕΝΟΨΕΙ ΤΩΝ ΝΕΩΝ ΠΑΡΑΤΗΡΗΣΕΩΝ ΑΠΟ ΒΑΡΥΤΙΚΑ ΚΥΜΑΤΑ

Διδακτορικη Διατριβη

Στυλιανου Σ. Καρυδα
Πτυχιουχου του Τμηματος Φυσικης του Πανεπιστημιου Αθηνων

ΤΡΙΜΕΛΗΣ ΣΥΜΒΟΥΛΕΥΤΙΚΗ ΕΠΙΤΡΟΠΗ:
1....Ελευθέριος Παπαντωνόπουλος, Ομ. Καθ. ΕΜΠ (Επιβλέπων)
2....Γεώργιος Κουτσούμπας, Ομ. Καθ. ΕΜΠ
3....Νικόλαος Ήργες, Καθ. ΕΜΠ

ΕΠΤΑΜΕΛΗΣ ΣΥΜΒΟΥΛΕΥΤΙΚΗ ΕΠΙΤΡΟΠΗ:
1....Ελευθέριος Παπαντωνόπουλος, Ομ. Καθ. ΕΜΠ (Επιβλέπων)
2....Γεώργιος Κουτσούμπας, Ομ. Καθ. ΕΜΠ
3....Νικόλαος Ήργες, Καθ. ΕΜΠ
4....Κωνσταντίνος Αναγνωστόπουλος, Αν. Καθ. ΕΜΠ
5....Κωνσταντίνος Φαράκος, Καθ. ΕΜΠ
6....Νικόλαος Μαυρόματος, Καθ. ΕΜΠ
7....Λεωνίδας Τσέτσερης, Καθ. ΕΜΠ

Αθήνα, 2023

Contents

List of Figures

Ευχαριστίες

Κατά τη διάρκεια της εκπόνησης αυτής της διατριβής έχουν υπάρξει πολλές συνεργασίες και συζητήσεις που βοήθησαν στο να ολοκληρωθεί. Όλη αυτή η διαδρομή έχει οδηγήσει σε μια ωρίμανση, τόσο σε προσωπικό όσο και σε επιστημονικό επίπεδο και το να μην ευχαριστήσω αυτούς που σε μικρότερο ή μεγαλύτερο βαθμό συνεισέφεραν, θα ήταν ασυγχώρητη παράλειψη . Η βασικότερη συνεισφορά, ήταν αυτή του επιβλέποντος καθηγητή μου κ. Ελευθέριου Παπαντωνόπουλου, υπό τη συνεχή καθοδήγηση του οποίου κατέστη δυνατή αυτή η εργασία και ωρίμανση. Επιπλέον, ευχαριστώ τους καθηγητές Γεώργιο Κουτσούμπα και Νικόλαο Ήργε που συναποτέλεσαν την τριμελή επιτροπή, οι οποίοι ήταν πάντα διαθέσιμοι όταν τους χρειαζόμουν. Όμως όλη αυτή η διαδρομή ξεκίνησε στο τμήμα Φυσικής του Ε.Κ.Π.Α. όπου ο σημαντικότερος καθοδηγητής μου ήταν ο καθηγητής κ. Βασίλειος Γεωργαλάς, σε συνεργασία με τον οποίο έγινε και η πρώτη μου δημοσίευση. Ιδιαίτερη μνεία θα ήθελα να αφιερώσω στο Δρ. Γιάννη Νταλιάνη σε συνεργασία με τον οποίο έγινε η δεύτερη δημοσίευση. Από την αλληλεπίδρασή μου μαζί του, θεωρώ ότι έμαθα, ίσως, τα περισσότερα πράγματα που αποτελούν τον πυρήνα της επιστημονικής βάσης αυτής της εργασίας, και γι' αυτό τον ευχαριστώ θερμά. Αντίστοιχα θα ήθελα να ευχαριστήσω το Δρ. Μάνο Σαριδάκη με την πολύτιμη συμβολή και συνεργασία του οποίου κατέστη δυνατή η τρίτη δημοσίευση της διατριβής. Θα ήταν παράλειψη να μην ευχαριστήσω και τους συνοδοιπόρους και συνεργάτες, καθ' όλη αυτή τη διαδρομή, Στέλλα Κιορπελίδη, Θανάση Καρακάση και Cristian Erices, με τους οποίους με τον ένα ή τον άλλο τρόπο συνεργαστήκαμε. Θέλω, ακόμα, να ευχαριστήσω το Δρ. Πραξιτέλη Ντόκο με τον οποίο πέραν της φιλίας που μας συνδέει, έχω αφιερώσει ατελείωτες ώρες συζήτησης σε θέματα Φυσικής και Μαθηματικών. Χωρίς αυτές τις συζητήσεις η όποια κατανόηση έχω αναπτύξει σε αυτές τις επιστήμες, σίγουρα δε θα ήταν η ίδια. Η εργασία αυτή αφιερώνεται στους γονείς μου, στους φίλους μου και στη σύντροφό μου που όλα αυτά τα χρόνια με έχουν ενθαρρύνει και στηρίξει χωρίς όρους. Σας ευχαριστώ όλους θερμά.

Abstract

General Relativity has proven to be an exceptionally successful theory in describing the dynamics of Gravity, with verifiable predictions in both short and long-distance experiments. However, it still remains an incomplete theory, since it is unable to model a variety of behaviors both in the early and late stages of the Universe's life. We are thus naturally led to investigate ways of complementing or modifying General Relativity in order to resolve this kind of tensions against observations, while at the same time we have a limit to which a modified theory of gravity must reduce to.

Among the variety of possible ways to modify it, perhaps the simplest is that of including a scalar field in the action that describes the gravitational dynamics. The dynamics of this field can, then, enrich the corresponding phenomenology and possibly offer ways to resolve the tensions of General Relativity with observations. Including a scalar field has to be done in such a manner that Ostrogradsky's theorem is respected, or theories with instabilities will be produced. The most general non-degenerate Lagrangian that respected this was found by Horndeski in 1974 and brought to a more modern form in the context of Galileon theory. This theory provides a suitable framework to modify General Relativity both at short and long distances, in early and late stages of the Universe's life. Within this context, a prominent position is held by the Scalar-Tensor theories that produce primordial inflation, which plays a crucial role in the Universe's evolution. Thus, we are motivated to look further into specific Galileon terms and their effects.

The extensive study of this kind of theories has unveiled that the inclusion of what is referred to as non-minimal derivative coupling (NMDC) has shown a promising change in dynamics, since, among other effects, it offers a lengthening in the inflationary era through the gravitational friction effect. In this way, the scalar field remains in slow roll for a very long period of time ensuring that a large number of e-folds is achieved, without having to resort to large initial field values. NMDC brings forward the fact that a deviation from the speed of gravitational waves is to be expected in such theories. The recent observation of gravitational waves, however, has strictly constrained their speed, rendering late time deviations from a speed $c_{GW} = 1$ invalid.

Hence, for what is presented in Chapter 1 of this thesis, we are motivated to maintain the positive effects of NMDC, while trying to ameliorate or possibly completely heal its shortcomings. Specifically, in the first chapter of this thesis, we will focus on studying the G_5 term of the Galileon Lagrangian, which corresponds to the class of derivative coupling theories. We focus on modifying G_5 to include a dependence on ϕ, so that a richer phenomenology is obtained. Thus, a possible solution to the late-time deviation from General Relativity will be presented, which at the same time addresses one of the main shortcomings of derivative coupling theories: late-time instabilities due to scalar perturbations' oscillations. We construct specific models that yield predictions successfully tested against observations. Finally, we highlight another aspect of a richer G_5 term: the fact that for a suitable choice, it is capable of producing Primordial Black Holes, in a different manner than the usual inflection point potentials.

Moving on to Chapter 2, we explore the idea of combining two different Galileon terms, specifically G_4 and G_5. We show that the combination of these two terms may have a healing effect on both of the standalone cases' problems, while being able to maintain their corresponding advantages. The inclusion of the G_4 term can immediately solve late-time instability problems, and at the same time produce cosmologically viable observables without having to resort to particularly large field values, due to the gravitational friction effect of the G_5 term.

In Chapter 3 we focus on late-time Cosmology, specifically looking into a scenario of a Universe that contains extra dimensions, within the framework of Kaluza-Klein compactifications. Specifically, we aim to study whether the observed transition from an era of decelerating to an era of accelerating expansion could be the result of the dynamics of an "internal" space. We produce the general solution of the setup chosen, which we prove that is unavoidably attracted to one of three specific, Kasner-type, solutions. By making sure that the internal space is stabilized so as not to fail observational tests of fundamental coupling constants, we show that all such possible scenarios are realized for exotic types of matter.

Σύντομη Περίληψη

Η Γενική Σχετικότητα έχει αποδειχθεί εξαιρετικά επιτυχημένη θεωρία, όσον αφορά στην περιγραφή της δυναμικής της Βαρύτητας, με επαληθεύσιμες προβλέψεις σε πειράματα τόσο σε μικρές, όσο και σε μεγάλες αποστάσεις. Παρόλα αυτά, παραμένει μια ατελής θεωρία, καθώς δεν είναι ικανή να περιγράψει μια πληθώρα συμπεριφορών τόσο στο πρώιμο, όσο και στο ύστερο Σύμπαν. Επομένως, οδηγούμαστε στο να εξερευνήσουμε τρόπους επέκτασης ή τροποποίησής της, ώστε να λυθούν αυτού του είδους τα προβλήματα, ενώ παράλληλα έχουμε ένα χειροπιαστό σενάριο, με το οποίο μπορούμε να συγκρίνουμε τις οριακές συμπεριφορές μιας τροποποιημένης θεωρίας.

Ανάμεσα σε πολλούς τρόπους να τροποποιήσει κανείς τη θεωρία της Βαρύτητας, ίσως ο πιο απλός είναι το να συμπεριλάβει ένα βαθμωτό πεδίο, του οποίου οι αλληλεπιδράσεις με τη βαρύτητα εμπλουτίζουν τη δυναμική του συστήματος των εξισώσεων και την αντίστοιχη φαινομενολογία, προσφέροντας ενδεχόμενα διεξόδους στα προβλήματα της Γενικής Σχετικότητας. Όμως, η συμπερίληψη ενός βαθμωτού πεδίου πρέπει να γίνει με τέτοιο τρόπο που σέβεται το θεώρημα Ostrogradsky, αλλιώς η θεωρία θα είναι ασταθής. Η πιο γενική, μη εκφυλισμένη, Λαγκρανζιανή που σέβεται αυτό το θεώρημα είναι η Λαγκρανζιανή Horndeski, από το 1974, που σε σύγχρονη μορφή ονομάζεται θεωρία Galileon. Η θεωρία αυτή προσφέρει ένα κατάλληλο πλαίσιο για τροποποίηση της θεωρίας της βαρύτητας, τόσο σε μικρές όσο και σε μεγάλες αποστάσεις, σε όλα τα στάδια της ζωής του Σύμπαντος. Ανάμεσα σε αυτές τις τροποποιήσεις, κυριαρχούν οι θεωρίες Βαθμωτού-Τανυστή που προκαλούν πρωταρχικό πληθωρισμό, ο οποίος είναι κρίσιμος για να περιγράψει την εξέλιξη του Σύμπαντος.

Η εκτεταμένη μελέτη τέτοιου τύπου θεωριών, έχει δείξει ότι η συμπερίληψη μιας ζεύξης του κινητικού όρου του πεδίου με τη Βαρύτητα, οδηγεί σε μια ενδιαφέρουσα τροποποίηση της δυναμικής του συστήματος, καθώς ανάμεσα σε άλλα αποτελέσματα, προκαλεί μια εύκολη επέκταση της διάρκειας του πληθωρισμού μέσα από το φαινόμενο της βαρυτικής τριβής. Με αυτό τον τρόπο, το πεδίο παραμένει στην περιοχή slow roll για αρκετά μεγάλο χρονικό διάστημα ώστε να επιτευχθεί ένας σημαντικός αριθμός e-folds, χωρίς να χρειάζονται υπερβολικά μεγάλες τιμές για τις αρχικές συνθήκες. Παράλληλα, με αυτή τη ζεύξη, πρέπει να αναμένεται μια απόκλιση της ταχύτητας των βαρυτικών κυμάτων από αυτή της ταχύτητας του φωτός, κάτι που όμως με βάση τις πρόσφατες παρατηρήσεις δε μπορεί να ισχύει, τουλάχιστον για ύστερες περιόδους της ζωής του Σύμπαντος.

Με βάση τα παραπάνω, στο κεφάλαιο 1 αυτής της διατριβής, γίνεται μια προσπάθεια να διατηρηθούν τα θετικά αποτελέσματα της παραπάνω ζεύξης, ενώ παράλληλα γίνεται μια προσπάθεια να ιαθούν οι παθογένειές της. Συγκεκριμένα, επικεντρωνόμαστε στη μελέτη του όρου G_5 της Λαγκρανζιανής Galileon, που αντιστοιχεί σε αυτή την ομάδα θεωριών. Επικεντρωνόμαστε σε μορφές του G_5 που περιλαμβάνουν ϕ-εξάρτηση, ώστε να δίνει μια πλουσιότερη φαινομενολογία. Μέσω αυτού, θα παρουσιαστεί μια λύση για τους ύστερους χρόνους σε σχέση την απόκλιση των αποτελεσμάτων από τη Γενική Σχετικότητα, που αντιμετωπίζει ένα από τα κύρια προβλήματα αυτών των θεωριών, τις αστάθειες λόγω των αρνητικών τιμών στο τετράγωνο της ταχύτητας μετάδοσης των βαθμωτών διαταραχών. Κατασκευάζουμε συγκεκριμένα μοντέλα που προβλέπουν παρατηρήσιμα μεγέθη σε πολύ καλή συμφωνία με τις παρατηρήσεις. Τέλος, ασχολούμαστε με μια άλλη πλευρά του όρου G_5: αυτή της παραγωγής Πρωταρχικών Μελανών Οπών με έναν εναλλακτικό τρόπο, σε σχέση με τη συνήθη στη βιβλιογραφία επιλογή ενός κατάλληλου δυναμικού.

Συνεχίζοντας, στο κεφάλαιο 2, εξερευνούμε την ιδέα του συνδυασμού δύο διαφορετικών όρων Galileon, συγκεκριμένα του όρου G_4 και του όρου G_5. Δείχνουμε ότι ο συνδυασμός των δύο μπορεί να έχει μια ευεργετική επίδραση στις αδυναμίες των θεωριών όπου ο κάθε όρος δρα μεμονωμένα, ενώ διατηρούνται τα επιμέρους πλεονεκτήματα. Η συμπερίληψη του όρου G_4 λύνει αμέσως τα προβλήματα με τις αστάθειες στο τέλος του πληθωρισμού, παράγοντας παράλληλα, παρατηρήσιμα μεγέθη που είναι σε καλή συμφωνία με τις παρατηρήσεις, χωρίς να χρειάζονται υψηλές τιμές για τις αρχικές συνθήκες της θεωρίας, και αποφεύγοντας έτσι ενδεχόμενα προβλήματα με την κβάντωσή της.

Τέλος, στο κεφάλαιο 3 επικεντρωνόμαστε στην ύστερη Κοσμολογία, συγκεκριμένα σε ένα σενάριο που περιέχει επιπλέον διαστάσεις, στα πλαίσια της θεωρίας Kaluza-Klein. Σκοπός μας είναι να μελετήσουμε το κατά πόσο η παρατηρημένη μετάβαση από μια εποχή επιβραδυνόμενης διαστολής σε μια εποχή επιταχυνόμενης διαστολής, θα μπορούσε να είναι το αποτέλεσμα της δυναμικής των επιπλέον διαστάσεων. Παράγουμε τη γενική λύση της θεωρίας, για την οποία αποδεικνύουμε ότι καταλήγει σε μια λύση ελκυστή, τύπου Kasner. Παράλληλα δείχνουμε ότι για να διαφυλαχθούν οι παρατηρησιακές προβλέψεις πρέπει οι επιπλέον διαστάσεις να είναι σταθεροποιημένες, κάτι που μπορεί να συμβαίνει μόνο για εξωτικούς τύπους ύλης.

Εκτεταμένη Περίληψη

Εισαγωγή

Η Γενική Θεωρία της Σχετικότητας (GR), έθεσε τα θεμέλια για το σύγχρονο τρόπο μελέτης της Βαρύτητας και του χωροχρόνου. Εντός ολίγων χρόνων από τη διατύπωσή της, βρέθηκαν, στο πλαίσιο που αυτή έθεσε, σενάρια (λύσεις) που περιγράφουν ένα σύμπαν το οποίο είτε διαστέλλεται είτε συστέλλεται και πράγματι, από τις παρατηρήσεις του Hubble, αποδείχθηκε ότι το Σύμπαν βρίσκεται σε μια διαστελλόμενη φάση της εξέλιξής του.

Στα μέσα του 20ου αιώνα, η μελέτη της νουκλεοσύνθεσης από τον Gamow έδειξε ότι το Σύμπαν πρέπει να έχει προέλθει από μια πρωταρχική υπέρθερμη και υπέρπυκνη αρχική κατάσταση. Αυτό με τη σειρά του υπονοεί την ύπαρξη μιας παραμένουσας *Κοσμικής Μικροκυματικής Ακτινοβολίας Υποβάθρου* (CMBR) που θα αποτελεί εικόνα του πρωταρχικού Σύμπαντος. Πράγματι, αυτή η ακτινοβολία ανιχνεύθηκε και οι επιτυχίες αυτές οδήγησαν στη Θεωρία της Μεγάλης Έκρηξης, με βάση την οποία το Σύμπαν έχει γεννηθεί και εξελιχθεί ξεκινώντας από μια πολύ πυκνή και θερμή αρχική κατάσταση.

Παρόλες αυτές τις επιτυχίες, έχουν διατυπωθεί εναλλακτικές, της Γενικής Σχετικότητας, θεωρίες που έχουν προσπαθήσει να γενικεύσουν ακόμα περισσότερα τα αποτελέσματά της, ενδεχομένως ενσωματώνοντάς την σε μια πιο πλατιά, ενοποιημένη θεωρία, που ίσως περιλαμβάνει και τις υπόλοιπες θεμελιώδεις αλληλεπιδράσεις της Φύσης, ενώ παράλληλα επιλύει και κάποια από τα προβλήματα που παρουσιάζονται.

Επι παραδείγματι, ο Brans και ο Dicke ανέπτυξαν τις πρώτες θεωρίες σύζευξης ενός βαθμωτού πεδίου με τον τανυστή Ricci, γνωστές ως *Θεωρίες Βαθμωτού-Τανυστή*. Σε τέτοιου τύπου θεωρίες, συμπεριλαμβάνεται ένα βαθμωτό πεδίο και οι αλληλεπιδράσεις του με τη Βαρύτητα. Από τότε, αυτές οι θεωρίες έχουν μελετηθεί ενδελεχώς σε διάφορα πλαίσια. Η πιο συστηματική μελέτη έγινε από τον Horndeski το 1974, που απέδειξε ότι αν κανείς συμπεριλάβει μόνο ένα βαθμωτό πεδίο στη ζεύξη με τη βαρύτητα, για να παράγονται θεωρίες χωρίς παθογενείς αστάθειες, πρέπει η Λαγκρανζιανή να μπορεί να έρθει με κατάλληλο μετασχηματισμό στη μορφή της Λαγκρανζιανής Horndeski.

Η θεωρία Horndeski έχει από τότε μελετηθεί και κατέχει μια περίοπτη θέση ανάμεσα στις πιθανές τροποποιήσεις της Γενικής Σχετικότητας, ως η πιο γενική, μη εκφυλισμένη θεωρία Βαθμωτού-Τανυστή. Η σύγχρονη μορφή της, ισοδύναμη με κατάλληλο μετασχηματισμό με την παραπάνω, είναι αυτή του Γενικευμένου πεδίου Galileon:

$$\begin{aligned}\mathcal{L} =& G_2(\phi, X) - G_3(\phi, X)\Box\phi + G_4(\phi, X)R + G_{4X}\left[(\Box\phi)^2 - \phi^{\mu\nu}\phi_{\mu\nu}\right] \\ & G_5(\phi, X)G^{\mu\nu}\phi_{\mu\nu} - \frac{G_{5X}}{6}\left[(\Box\phi)^3 - 3\Box\phi\phi^{\mu\nu}\phi_{\mu\nu} + 2\phi_{\mu\nu}\phi^{\nu\lambda}\phi^{\mu}_{\lambda}\right]\end{aligned}$$

όπου οι συναρτήσεις G_i είναι αυθαίρετες, εν γένει, συναρτήσεις του πεδίου ϕ και του $X = -\nabla^\nu\phi\nabla_\nu\phi/2$.

Βεβαίως υπάρχουν και προσεγγίσεις τροποποίησης της Γενικής Σχετικότητας που ξεκινούν από τελείως διαφορετική αφετηρία. Επί παραδείγματι, ο Sakharov παρατήρησε ότι η δράση Einstein-Hilbert από την οποία προκύπτουν οι δυναμικές εξισώσεις της Γενικής Σχετικότητας, ενδεχομένως αποτελεί απλώς μια πρώτη προσέγγιση, μιας πιο περίπλοκης δράσης που συμπεριλαμβάνει όρους υψηλότερης τάξης στο βαθμωτό Ricci. Το πιο γνωστό και επιτυχημένο παράδειγμα αυτής της κατηγορίας θεωριών είναι η θεωρία Starobinsky.

Παρόλα αυτά, μετά από παραπάνω από έναν αιώνα, η Γενική Σχετικότητα παραμένει ίδια, όντας η πιο επιτυχημένη θεωρία ως προς την περιγραφή της δυναμικής της Βαρύτητας σε μεγάλες κλίμακες, παρότι η προκύπτουσα από αυτήν, περιγραφή της εξέλιξης του Σύμπαντος, παραμένει ανεπαρκής. Με βάση τις παρατηρήσεις γνωρίζουμε ότι ένα μεγάλο μέρος του περιεχομένου του Σύμπαντος είναι *Σκοτεινής Φύσης*. Πράγματι, μελετώντας το Σύμπαν με βάση τα πρότυπα της Γενικής Σχετικότητας, αν ο μόνος τύπος ύλης που αλληλεπιδρά βαρυτικά είναι η ορατή, σε εμάς, βαρυονική ύλη, τότε δε θα έπρεπε να παρατηρούμε τις Μεγάλης Κλίμακας Δομές, όπως οι γαλαξίες. Επομένως, είναι εύλογο να υποθέσει κανείς ότι είτε η Γενική Σχετικότητα δεν είναι πλήρης, είτε υπάρχει κάποιο είδος ύλης, που αλληλεπιδρά μόνο βαρυτικά και γι' αυτό παραμένει αόρατη σε εμάς, οδηγώντας στη δημιουργία αυτών των δομών. Οι πιθανοί υποψήφιοι για αυτό το άγνωστο περιεχόμενο του Σύμπαντος ονομάζονται συλλογικά *Σκοτεινή Ύλη*.

Επιπλέον, στα τέλη του προηγούμενου αιώνα, παρατηρήθηκε ότι η διαστολή του Σύμπαντος είναι επιταχυνόμενη. Η παρατήρηση αυτή, έδειξε ότι το Σύμπαν διήλθε από μια επιβραδυνόμενη σε μια επιταχυνόμενη διαστολή πριν από 6 με 7 δισεκατομμύρια χρόνια. Αυτό αποτελεί ένα αξεπέραστο εμπόδιο για τη Γενική Σχετικότητα και συνήθως αποδίδεται ως πρόβλημα της *Σκοτεινής Ενέργειας*.

Πέρα από τα άγνωστα περιεχόμενα του Σύμπαντος, παρουσιάζονται και άλλα σημαντικά προβλήματα σχετικά με τα πρωταρχικά στάδια της ζωής του. Η θεωρία της Μεγάλης Έκρηξης δεν εξηγεί μια σειρά

από παρατηρήσεις, όπως για παράδειγμα η αξιοσημείωτη ομογένεια και ισοτροπία που παρατηρείται στο CMBR, ή η παρατήρηση ότι το Σύμπαν ακολουθεί με πολύ μεγάλη ακρίβεια τη γεωμετρία ενός επίπεδου χωροχρόνου (Minkowski) σε μεγάλες κλίμακες.

Για να επιλυθούν αυτά τα προβλήματα, προτάθηκε η θεωρία του *πληθωρισμού* από τον Guth. Με βάση αυτή, στα πρώτα στάδια της Κοσμικής εξέλιξης, έλαβε χώρα μια εκθετική αύξηση του μεγέθους του Σύμπαντος, που απέμπλεξε αιτιακά, σημεία του χωροχρόνου που μέχρι τότε ήταν αιτιακά συνδεδεμένα. Συνηθίζεται αυτό να αποδίδεται στην τροποποίηση της δυναμικής που προκύπτει από τη συμπερίληψη των αλληλεπιδράσεων ενός βαθμωτού πεδίου στη μελέτη της Βαρύτητας. Αν πράγματι αυτή είναι η αιτία του πληθωρισμού, τότε μπορεί κανείς να εργαστεί στα πλαίσια της θεωρίας Horndeski.

Γίνεται λοιπόν σαφές, ότι μπορεί να διατυπωθεί μια πληθώρα θεωριών που τροποποιούν τη Γενική Σχετικότητα και η πραγματοποίηση πειραμάτων και παρατηρήσεων που διακρίνουν τη μια τροποποιημένη θεωρία από την άλλη, αποτελεί κεντρικής σημασίας παράγοντα στη διατύπωση τς σωστής Θεωρίας της Βαρύτητας. Σε αυτή την κατεύθυνση βοηθούν οι ακριβείς παρατηρήσεις της Κοσμικής Ακτινοβολίας Υποβάθρου αλλά και η πρόσφατη παρατήρηση βαρυτικών κυμάτων, που αποτέλεσε άλλη μια πανηγυρική επιβεβαίωση της ισχύος της Γενικής Σχετικότητας.

Βασικός σκοπός αυτής της διατριβής είναι να μελετήσει Θεωρίες Βαθμωτού-Τανυστή, στα πλαίσια της θεωρίας Horndeski, ώστε να εξεταστούν τροποποιήσεις που εμπλουτίζουν και ενδεχομένως διορθώνουν αποτελέσματα που εμπεριέχονται στο φάσμα της φαινομενολογίας που προκύπτει από ένα πληθωριστικό μοντέλο και επιχειρεί να απαντήσει σε ερωτήματα όπως αυτά που τέθηκαν πιο πάνω. Επιπλέον, μελετάται μια περίπτωση τροποποίησης της ύστερης εξέλιξης του Σύμπαντος που τίθεται αντιμέτωπη με τις παρατηρήσεις που σχετίζονται με το *Σκοτεινό Περιεχόμενό* του.

Σε αυτή την κατεύθυνση θέτουμε πρώτα το σύνηθες πλαίσιο μελέτης στην Κοσμολογία και κατόπιν, παρουσιάζουμε τη θεωρία του πεδίου Galileon και τις υπό εξέταση, σε αυτή τη διατριβή, τροποποιήσεις της, μαζί με τα αποτελέσματα που προκύπτουν. Παράγονται τα συγκριτικά πλεονεκτήματα και μειονεκτήματα τους, ενώ παράλληλα παράγεται πληθώρα προβλέψεων που μπορεί να τεθεί αντιμέτωπη με τις παρατηρήσεις. Τέλος, εξετάζεται μια εφαρμογή στα πλαίσια της θεωρίας Kaluza-Klein στην Κοσμολογία. Παράγονται οι ειδικές και η γενική λύση και αποδεικνύεται ότι οι ειδικές λύσεις λειτουργούν σαν ελκυστές της γενικής λύσης, κάτι που αποτελεί ένα πολύ χρήσιμο εφόδιο στη μελέτη αντίστοιχων μοντέλων.

Για να κατασκευάσει κανείς ένα κοσμολογικό μοντέλο, πρέπει να περιγράψει πρώτα τον υπό μελέτη χωρόχρονο, με τη χρήση κατάλληλης μετρικής. Η συνήθης μετρική Friedmann-Lemaitre-Robertson-Walker είναι η:

$$ds^2 = g_{\mu\nu}dx^\mu dx^\nu = -dt^2 + a^2(t)\left[\frac{dr^2}{1-Kr^2} + r^2(d\theta^2 + sin^2\theta d\phi^2)\right]$$

και περιγράφει έναν χωρόχρονο με μέγιστα συμμετρικό χώρο που αντιστοιχεί σε ένα σύμπαν ομογενές και ισότροπο. Όλες οι παρατηρήσεις, προς όλες τις κατευθύνσεις του ουρανού δείχνουν ότι το Σύμπαν πράγματι είναι ομογενές και ισότροπο σε αποστάσεις της τάξης των 100 Mpc και πάνω. Δε φαίνεται λοιπόν να υπάρχουν σοβαρές ενδείξεις, παρατηρησιακές ή θεωρητικές, που να οδηγούν στο συμπέρασμα ότι το Σύμπαν δεν ακολουθεί σε μεγάλες κλίμακες την *Κοσμολογική Αρχή*, δηλαδή την υπόθεση ότι δεν υπάρχει κάποιο προτιμητέο σημείο μέσα σε αυτό.

Η μεταβλητή t συμβολίζει τον κοσμικό χρόνο και η συνάρτηση $a(t)$ είναι ο κοσμικός παράγοντας κλίμακας, ενώ η παράμετρος K δείχνει την εσωτερική γεωμετρία του χώρου. Από τις παρατηρήσεις, αυτή η γεωμετρία είναι επίπεδη με πολύ μεγάλη ακρίβεια, και επομένως επιλέγουμε $K = 0$.

Το μέγεθος $a(t)$ περιγράφει την εξέλιξη του Σύμπαντος. Επιπλέον, ορίζουμε την παράμετρο Hubble:

$$H(t) = \frac{\dot{a}(t)}{a(t)}$$

της οποίας το πρόσημο δείχνει το αν το Σύμπαν διαστέλλεται ή συστέλλεται. Η επιτάχυνση ή επιβράδυνση της όποιας εξέλιξης, δίνεται από το πρόσημο της παραμέτρου q:

$$q = -\frac{\ddot{a}(t)a(t)}{\dot{a}^2(t)}$$

Η σημερινή τιμή της παραμέτρου Hubble μετράται από πολλά υπό εξέλιξη πειράματα. Επί παραδείγματι, η μέτρηση του Planck 2018 ήταν:

$$H_0 = 67,7\ km \cdot s^{-1} \cdot Mpc^{-1}.$$

Για τη δυναμική μελέτη, ξεκινάμε από τη δράση Einstein-Hilbert, από όπου προκύπτουν οι εξισώσεις πεδίου της Βαρύτητας:

$$G_{\mu\nu} \equiv R_{\mu\nu} - \frac{1}{2} g_{\mu\nu} R = 8\pi G T_{\mu\nu} - \Lambda g_{\mu\nu}$$

όπου $T_{\mu\nu}$ είναι ο τανυστής ενέργειας-ορμής, που για να μοντελοποιήσει ένα ομογενές και ισότροπο ρευστό πρέπει να έχει τη μορφή:

$$T_{\mu\nu} = diag(-\rho, p, p, p)$$

όπου ρ η ενεργειακή πυκνότητα του ρευστού και p η πίεσή του. Η παράμετρος Λ είναι η κοσμολογική σταθερά και G: η σταθερά του Νεύτωνα. Οι ανεξάρτητες εξισώσεις για το $a(t)$ που προκύπτουν, ονομάζονται εξισώσεις Friedmann και είναι οι:

$$H^2 = \frac{\rho}{3M_{Pl}^2} + \frac{\Lambda}{3} - \frac{K}{a^2}, \qquad 3\frac{\ddot{a}}{a} = -4\pi G(\rho + 3p) + \Lambda$$

Η παραπάνω περιγραφή αδυνατεί να δώσει πειστική απάντηση σε μια σειρά από παρατηρήσεις, πολλές εκ των οποίων αφορούν στα πρωταρχικά στάδια της ζωής του Σύμπαντος. Ανάμεσά τους, κυρίαρχη θέση έχουν το *πρόβλημα της επιπεδότητας* (flatness problem), το *πρόβλημα του ορίζοντα* (horizon problem) και τα *ανεπιθύμητα παραμένοντα σωματίδια* (unwanted relics).

Το πρώτο από αυτά αφορά στην παρατήρηση ότι το Σύμπαν είναι με πολύ μεγάλη ακρίβεια επίπεδο. Όμως αν αυτό ισχύει για μια στιγμή της ζωής του Σύμπαντος, θα πρέπει να ισχύει για όλη του τη ζωή μέχρι τότε. Αυτό οδηγεί στο συμπέρασμα ότι η σημερινή ενεργειακή πυκνότητα του Σύμπαντος, που έχει τιμή πολύ κοντά στο 1, πρέπει να έχει προέλθει από μια τιμή εξαιρετικά κοντά στο 1, με απόκλιση το πολύ της τάξης του 10^{-64}. Για να έχει συμβεί αυτό ο επιτρεπόμενος φασικός χώρος των αρχικών συνθηκών των παραμέτρων είναι πολύ μικρός και γι'αυτό το αντίστοιχο σενάριο θεωρείται απίθανο να έχει λάβει χώρα.

Αντίστοιχα μπορεί κανείς να αιτιολογήσει τη διατύπωση του προβλήματος του ορίζοντα. Το Σύμπαν είναι με πολύ καλή ακρίβεια ισότροπο, ακόμα και σε μη αιτιακά σχετιζόμενες περιοχές του. Αυτή η αξιοσημείωτη ομοιότητα διαφορετικών περιοχών του ουρανού είναι αδύνατο να αιτιολογηθεί για περιοχές που δεν αλληλεπέδρασαν ποτέ.

Τέλος, ακολουθώντας το Καθιερωμένο Πρότυπο της Φυσικής, αν κανείς θεωρήσει ότι στις αρχικές στιγμές του Σύμπαντος οι 4 θεμελιώδεις αλληλεπιδράσεις ήταν ενοποιημένες, τότε μετά τα διαδοχικά σπασίματα συμμετρίας που έλαβαν χώρα, θα έπρεπε να έχουμε οδηγηθεί σε μια $U(1)$ θεωρία που περιλαμβάνει μαγνητικά μονόπολα, τα οποία όμως μέχρι στιγμής δεν έχουν ανιχνευθεί, όπως επίσης και άλλα σωματίδια που προκύπτουν από άλλες θεμελιώδεις θεωρίες.

Για να λυθούν τα παραπάνω προβλήματα προτάθηκε πως υπήρξε, πρωταρχικά, μια εξαιρετικά γρήγορη εξέλιξη του Σύμπαντος, που έβγαλε από την ακτίνα αιτιακής συσχέτισης, περιοχές που μέχρι τότε ήταν αιτιακά συσχετισμένες και επομένως, μπορεί να δικαιολογήσει την ομοιότητά τους αλλά και να προσφέρει μια πειστική απάντηση στο πρόβλημα του ορίζοντα και των ανεπιθύμητων σωματιδίων. Αυτή η εποχή ονομάστηκε πληθωρισμός και ένας από τους πιθανούς τρόπους που μπορεί να έλαβε χώρα, συνίσταται στην αλληλεπίδραση ενός βαθμωτού πεδίου με τη Βαρύτητα.

Η πιο απλή περίπτωση συμπερίληψης τέτοιου όρου στη θεωρία, περιστρέφεται γύρω από τη δράση:

$$S = \int d^4x\sqrt{-g}\left[\frac{M_{Pl}^2}{2}R - \frac{1}{2}\partial^\mu\phi\partial_\mu\phi - V(\phi)\right]$$

που περιγράφει μια τετριμμένη ζεύξη του βαθμωτού με τη Βαρύτητα. Στασιμοποιώντας αυτή τη δράση προκύπτουν τόσο οι αντίστοιχες εξισώσεις Friedmann όσο και η εξίσωσης κίνησης του βαθμωτού. Καθώς μελετάμε αυτή τη θεωρία σε κοσμολογικό πλαίσιο μπορούμε να κάνουμε χρήση της ομοιογένειας και ισοτροπίας του Σύμπαντος, το οποίο οδηγεί στο συμπέρασμα, μεταξύ άλλων, ότι το βαθμωτό πεδίο έχει εξάρτηση μόνο από το χρόνο.

Για να πάρουμε μια θεωρία που εμπεριέχει ένα πληθωριστικό διάστημα σε αυτό το πλαίσιο, περιορίζόμαστε στην περίπτωση όπου η δυναμική ενέργεια του βαθμωτού υπερτερεί κατά πολύ της κινητικής του ενέργειας, που είναι γνωστή ως Slow Roll. Σε αυτή την περίπτωση φτάνουμε στις απλοποιημένες εξισώσεις:

$$3H\dot{\phi} + V' \approx 0$$

$$H^2 \approx \frac{1}{3M_{Pl}^2} V$$

Η μελέτη αυτής της περιόδου διευκολύνεται ορίζοντας παραμέτρους που την ποσοτικοποιούν (Slow Roll parameters):

$$\epsilon_V \equiv \frac{M_{Pl}^2}{2}\left(\frac{V'}{V}\right)^2 \ll 1, \qquad \eta_V \equiv M_{Pl}^2 \frac{V''}{V} \ll 1$$

Αυτές οι σχέσεις μεταφράζονται σε συγκεκριμένες απαιτήσεις για την κλίση και την καμπυλότητα του δυναμικού μέσα στο οποίο κινείται το βαθμωτό πεδίο, ενώ για να λυθούν τα προβλήματα που αναφέραμε χρειάζεται ο πληθωρισμός να έχει υπάρξει για αρκετό χρόνο. Γι' αυτό, ορίζουμε το μέγεθος:

$$N = ln\frac{a_{end}}{a}$$

που εκφράζει το πόσο πρόκειται να αλλάξει ο παράγοντας κλίμακας μέχρι το τέλος του πληθωρισμού που προβλέπεται από την εκάστοτε θεωρία (*e-folds*). Για να λυθούν τα προβλήματα αυτά, πρέπει η συνκινούμενη ακτίνα Hubble (δηλαδή η ακτίνα των αιτιακά σχετιζόμενων περιοχών), να έχει μικρύνει κατά τη διάρκεια του πληθωρισμού τουλάχιστον τόσο όσο έχει μεγαλώσει μετά το τέλος του. Υπολογίζεται ότι το Σύμπαν πρέπει να έχει προλάβει να μεγαλώσει στο διάστημα του πληθωρισμού, κατά e^{60} φορές. Αυτός είναι και ένας από τους στόχους μιας πληθωριστικής θεωρίας.

Ο πληθωρισμός προσφέρει, επιπλέον, το έδαφος για τη μελέτη των ανομοιογενειών που παρατηρούμε μέχρι κάποια κλίμακα, οι οποίες παίρνουν τη μορφή των δομών που βλέπουμε σήμερα. Λόγω της ελκτικής φύσης της βαρύτητας, οποιαδήποτε ανομοιογένεια παρατηρούμε σήμερα, θα πρέπει να έχει προέλθει από μια πολύ μικρότερη ανομοιογένεια στο παρελθόν. Εικόνα αυτών των ανομοιογενειών είναι το CMBR, στο φάσμα του οποίου να αναζητούμε στοιχεία για τη θεωρία που οδήγησε τη γέννησή τους. Μάλιστα, αφού οι ανομοιογένειες ξεκινούν ως μικροσκοπικές διακυμάνσεις, μπορούμε να μελετήσουμε την εξέλιξή τους ως γραμμικές διαταραχές των δυναμικών ποσοτήτων. Οι διακυμάνσεις αυτές θεωρείται ότι έχουν κβαντική προέλευση, και με την εξέλιξή του Σύμπαντος, μετατράπηκαν σε βαρυτικά ασταθείς σπόρους (Jeans instabilities) που κατέρρευσαν και δημιούργησαν τις μεγάλες δομές. Τα φάσματα των διαταραχών περιέχουν πληροφορίες που μπορούν να χρησιμοποιηθούν για να ξεχωρίσουμε ποια θεωρία Βαρύτητας είναι η σωστή.

Μια διαταραχή του βαθμωτού πεδίου, προκαλεί διαταραχή και της μετρικής και επομένως διαταραχή της καμπυλότητας R. Το μήκος κύματος αυτών των διαταραχών αυξάνει εκθετικά και εξέρχεται από την ακτίνα Hubble όταν τα δύο αυτά μεγέθη γίνουν συγκρίσιμα. Μετά την έξοδο από την ακτίνα Hubble οι διαταραχές αυτές παγώνουν και μπορούν να μελετηθούν κλασσικά. Μετά το τέλος του πληθωρισμού, αυτές οι διαταραχές επανέρχονται εντός του ορίζοντα και αρχίζουν να μεγαλώνουν και να μετατρέπονται σε αντίστοιχες διαταραχές ύλης και θερμοκρασίας που οδηγούν στη δημιουργία μεγάλων δομών. Επομένως, η μελέτη των πρωταρχικών διαταραχών αποκτά κεντρικό ρόλο στο να βοηθήσει στη διατύπωση της σωστής θεωρίας της Βαρύτητας. Στην παρούσα διατριβή, της οποίας μεγάλο μέρος αφιερώνεται στη μελέτη θεωριών ζεύξης βαθμωτού-τανυστή, θα κινηθούμε εντός του πλαισίου που διαμορφώνουν οι θεωρίες Galileon. Οι θεωρίες αυτές είναι ισοδύναμες με τις θεωρίες Horndeski και προκύπτουν από την πιο γενική, μη εκφυλισμένη, Λαγκρανζιανή που περιλαμβάνει μόνο ένα βαθμωτό πεδίο και τη Βαρύτητα. Η επιλογή αυτή γίνεται γιατί οι θεωρίες που προκύπτουν από αυτή τη Λαγκρανζιανή σέβονται το θεώρημα Ostrogradsky και δεν παρουσιάζουν αστάθειες που σχετίζονται με παραγώγους υψηλής τάξης.

Η σύγχρονη μορφή της θεωρίας Horndeski, είναι αυτή της θεωρίας του πεδίου Galileon. Όταν ένα βαθμωτό πεδίο είναι συμμετρικό κάτω από το μετασχηματισμό:

$$\phi \to \phi + b_\mu x^\mu + c$$

ορίζεται ως πεδίο Galileon. Για να αποφύγουμε τις σχετικές με την τάξη των διαφορικών εξισώσεων αστάθειες, περιοριζόμαστε σε θεωρίες που έχουν μέχρι δεύτερης τάξης παραγώγους. Σε ένα υπόβαθρο όπου υπάρχει Βαρύτητα, η Λαγκρανζιανή του συναλλοίωτου Galileon γράφεται:

$$\begin{aligned}\mathcal{L} =& G_2(\phi, X) - G_3(\phi, X)\Box\phi + G_4(\phi, X)R + G_{4X}\left[(\Box\phi)^2 - \phi^{\mu\nu}\phi_{\mu\nu}\right] \\ & G_5(\phi, X)G^{\mu\nu}\phi_{\mu\nu} - \frac{G_{5X}}{6}\left[(\Box\phi)^3 - 3\Box\phi\phi^{\mu\nu}\phi_{\mu\nu} + 2\phi_{\mu\nu}\phi^{\nu\lambda}\phi^{\mu}_{\lambda}\right]\end{aligned}$$

όπου οι συναρτήσεις G_i είναι αυθαίρετες συναρτήσεις των ϕ και X, και οι δείκτες ϕ και X συμβολίζουν παραγώγιση ως προς το αντίστοιχο μέγεθος. Επιλέγοντας κατάλληλα τις συναρτήσεις G_i μπορεί κανείς να παράγει μια πληθώρα Τροποποιημένων Θεωριών Βαρύτητας, όπως επί παραδείγματι τη μη τετριμμένη ζεύξη της μορφής $f(\phi)R$, με την επιλογή $G_4 = f(\phi)$.

Για να βρούμε τις σχέσεις που δίνουν τα παρατηρήσιμα μεγέθη μιας θεωρίας Galileon, ακολουθούμε την τακτική της αποσύνθεσης των διαφόρων όρων της μετρικής, σε μεγέθη που μετασχηματίζονται ως βαθμωτά, διανύσματα ή τανυστές, ενώ παράλληλα θα διατηρήσουμε την παραδοχή ότι $\phi = \phi(t)$. Η πιο κατάλληλη γραφή για αυτή τη διαδικασία είναι η ADM μετρική:

$$ds^2 = -N^2 dt^2 + \gamma_{ij}(dx^i + N^i dt)(dx^j + N^j dt)$$

Εισάγοντας αυτή τη μετρική στην παραπάνω Λαγκρανζιανή έχουμε:

$$S = \int dt d^3x \mathcal{L}(N, \dot{N}, a, \dot{a}, \ddot{s}, \phi, \dot{\phi}, \ddot{\phi})$$

την οποία αν στασιμοποιήσουμε ως προς τις ποσότητες N, a και ϕ παίρνουμε τις δυναμικές εξισώσεις της θεωρίας. Μέσω της πλήρους αποσύνθεσης της μετρικής σε μεγέθη που μετασχηματίζονται με συγκεκριμένο τρόπο (SVT decomposition) κατασκευάζουμε ποσότητες που είναι αναλλοίωτες από βαθμίδα σε βαθμίδα, και επιλέγουμε μια βαθμίδα που θα διευκολύνει στην παραγωγή των υπό εξέταση ποσοτήτων. Διαλέγουμε τη βαθμίδα, όπου η διαταραχή του βαθμωτού πεδίου είναι $\delta\phi = 0$ (unitary gauge). Μπορούμε τότε να γράψουμε

$$N = 1 + \delta N, \quad N_i = \partial_i \psi \quad \text{and } \gamma_{ij} = a^2 e^{2\mathcal{R}} (e^h)_{ij}$$

όπου $(e^h)_{ij} \equiv \delta_{ij} + h_{ij} + \mathcal{O}(h^2)$, και με αντικατάσταση στην παραπάνω δράση και κρατώντας όρους μέχρι δεύτερης τάξης στις διαταραχές έχουμε:

$$S^{(2)} = S^{(2)}_{\text{scalar}} + S^{(2)}_{\text{tensor}}$$

Το βαθμωτό και το τανυστικό μέρος της δράσης έχουν, αντίστοιχα τη μορφή:

$$S^{(2)}_{\text{scalar}} = \int dt d^3x a^3 \left[\frac{\mathcal{F}_T}{a^2}(\partial\mathcal{R})^2 - 3\mathcal{G}_T \dot{\mathcal{R}}^2 + \Sigma \delta N^2 - 2\Theta \delta N \frac{\partial^2 \psi}{a^2} + 2\mathcal{G}_T \dot{\mathcal{R}} \frac{\partial^2 \psi}{a^2} + 6\Theta \delta N \dot{\mathcal{R}} - 2\mathcal{G}_T \delta N \frac{\partial^2 \mathcal{R}}{a^2} \right]$$

και

$$S^{(2)}_{\text{tensor}} = \frac{1}{8} \int dt dx^3 a^3 \left[\mathcal{G}_T \dot{h}^2_{ij} - \frac{\mathcal{F}_T}{a^2} (\partial_k h_{ij})^2 \right]$$

όπου οι ποσότητες $\mathcal{G}_T$, $\mathcal{F}_T$, Θ, Σ είναι συναρτήσεις που εξαρτώνται από τις ποσότητες G_i που αντιστοιχούν στην εκάστοτε θεωρία. Οι ακριβείς μορφές τους παρατίθενται στο Παράρτημα Β. Στασιμοποιώντας ως προς δN και ψ η δράση μπορεί να έρθει στη μορφή:

$$S^{(2)}_{\mathcal{R}} = \int dt d^3x a^3 \left[\mathcal{G}_S \dot{\mathcal{R}}^2 - \frac{\mathcal{F}_S}{a^2} (\partial\mathcal{R})^2 \right]$$

όπου το μέγεθος $\mathcal{R}$ ονομάζεται *διαταραχή καμπυλότητας* (curvature perturbation) και επιπλέον έχουμε ορίσει τις βοηθητικές ποσότητες:

$$\mathcal{G}_S \equiv \frac{\Sigma}{\Theta^2} \mathcal{G}_T^2 + 3\mathcal{G}_T, \qquad \mathcal{F}_S \equiv \frac{1}{a} \frac{d}{dt} \left(\frac{a}{\Theta} \mathcal{G}_T^2 \right) - \mathcal{F}_T \ .$$

Για δοσμένες συναρτήσεις G_i η ταχύτητα διάδοσης των βαθμωτών και τανυστικών διαταραχών είναι:

$$c_s^2 \equiv \frac{\mathcal{F}_S}{\mathcal{G}_S} \ , \qquad c_T^2 \equiv \frac{\mathcal{F}_T}{\mathcal{G}_T} \ .$$

Αυτές οι ποσότητες πρέπει να παραμένουν θετικές, αλλιώς οδηγούμαστε σε διαταραχές που μεγαλώνουν εκθετικά, οπότε και παύει να έχει ισχύ ο συγκεκριμένος τρόπος μελέτης. Ένα άλλο είδος ασταθειών

που πρέπει να αποφεύγεται σχετίζεται με του κινητικούς όρους (ghost instabilities), οι οποίοι πρέπει να είναι θετικοί:

$$\mathcal{G}_S > 0 \ , \quad \mathcal{G}_T > 0 \ ,$$

Συνεχίζοντας, για να μελετήσουμε την εξέλιξη των διαφόρων κυματαριθμών μεγεθών (perturbation modes) χρησιμοποιούμε τους μετασχηματισμούς:

$$dy := \frac{c_s}{a} dt, \quad u := z\mathcal{R}, \quad z := \sqrt{2} a \sqrt[4]{\mathcal{F}_S \mathcal{G}_S}$$

και αντικαθιστώντας στη δράση, τη φέρνουμε στη μορφή Mukhanov-Sasaki:

$$S^{(2)}_{\mathcal{R}} = \frac{1}{2} \int dy d^3x \left[(u')^2 - (\partial u)^2 + \frac{z''}{z} u^2 \right]$$

όπου ο τόνος $'$ αναφέρεται σε παραγώγιση σε σχέση με την καινούργια μεταβλητή y. Μέσω της έκφρασης εντός της αγκύλης, μπορούμε μελετήσουμε την εξέλιξη του φάσματος των διαταραχών. Όμως, αν η εξέλιξη με το χρόνο των διάφορων ποσοτήτων είναι αρκετά αργή, μπορούμε να προσεγγίσουμε τα φάσματα ως:

$$\mathcal{P}_R = \frac{\mathcal{G}_S^{1/2}}{2\mathcal{F}_S^{3/2}} \frac{H^2}{4\pi^2} \ , \qquad \mathcal{P}_{\mathcal{T}} = \frac{8\mathcal{G}_T^{1/2}}{\mathcal{F}_T^{3/2}} \frac{H^2}{4\pi^2} \ ,$$

υπολογισμένων όταν το αντίστοιχο mode εξέρχεται από τον ορίζοντα. Ο λόγος αυτών των δύο ποσοτήτων είναι ένα παρατηρήσιμο μέγεθος και ορίζεται ως:

$$r \equiv \frac{\mathcal{P}_{\mathcal{T}}}{\mathcal{P}_R} \ .$$

Αν αντίθετα υπάρχει γρήγορη εξέλιξη με την πάροδο του χρόνου, πρέπει η αντίστοιχη εξίσωση να λυθεί για το κάθε mode ξεχωριστά.

Ένα άλλο παρατηρίσιμο μέγεθος που εξάγεται από την Κοσμική Ακτινοβολία Υποβάθρου είναι ο βαθμωτός δείκτης φάσματος n_s (scalar spectral index), που εκφράζει την αλλαγή του λογαρίθμου το φάσματος σε σχέση με το λογάριθμο του κυματαριθμού μιας διαταραχής, k:

$$1 - n_s \equiv - \frac{d \ln \mathcal{P}_R}{d \ln k} \Big|_{k=aH} \ ,$$

Με αντίστοιχο τρόπο ορίζουμε και τον τανυστικό δείκτη φάσματος:

$$n_t \equiv - \frac{d \ln \mathcal{P}_{\mathcal{T}}}{d \ln k} \Big|_{k=aH} \ .$$

Μπορούμε τώρα να συσχετίσουμε τα μεγέθη r και n_t με μια συνθήκη, που στην πιο απλή θεωρία ενός βαθμωτού πεδίου παίρνει τη μορφή $r \approx -8 n_t$. Συνοψίζοντας, τα παρατηρήσιμα μεγέθη μιας θεωρίας ενός βαθμωτού που προκαλεί τον πληθωρισμό, είναι τα r, n_s και $\mathcal{P}_R$.

Γενικευμένη μη Τετριμμένη Ζεύξη Κινητικού Όρου: Εφαρμογή στον Πληθωρισμό και στη Δημιουργία Πρωταρχικών Μελανών Οπών

Η προσπάθειά μας εδώ, θα περιστραφεί γύρω από την πιθανή τροποποίηση των θεωριών που προκύπτουν από μη τετριμμένη ζεύξη του κινητικού όρου του πεδίου με τον τανυστή Einstein, στη δράση (Non-Minimal Derivative Coupling-NMDC). Αυτές οι θεωρίες παράγουν μια πολύ πλούσια φαινομενολογία, τόσο σε μικρές όσο και σε μεγάλες κλίμακες. Στην περίπτωση του πληθωρισμού, το πιο ελκυστικό χαρακτηριστικό τους είναι ότι παρουσιάζουν το φαινόμενο της *βαρυτικής τριβής*, δηλαδή της επιβράδυνσης της κίνησης του βαθμωτού πεδίου μέσα στο δυναμικό του, λόγω της αλληλεπίδρασης του κινητικού όρου με τη Βαρύτητα. Επιτρέπουν έτσι σε πληθώρα δυναμικών να παράγουν πληθωρισμό. Ανάμεσά τους βρίσκεται το δυναμικό που αντιστοιχεί στο μοναδικό βαθμωτό πεδίο που έχει ανιχνευθεί μέχρι

τώρα, αυτό του σωματιδίου Higgs. Μάλιστα, στις θεωρίες NMDC τροποποιείται αρκετά και η φαινομενολογία της περιόδου της αναθέρμανσης που ακολουθεί τον πληθωρισμό (reheating). Συγκεκριμένα, στην πιο απλή εφαρμογή του NMDC, το βαθμωτό πεδίο ταλαντώνεται πολύ έντονα και χωρίς απόσβεση, στην περίοδο της αναθέρμανσης, με αποτέλεσμα να επηρεάζεται το κομμάτι της φαινομενολογίας που η Καθιερωμένη Κοσμολογία εξηγεί ικανοποιητικά, όπως η παραγωγή βαρέων σωματιδίων.

Επιπλέον, αυτές οι ταλαντώσεις μεταφράζονται και ως ταλαντώσεις της ταχύτητας διάδοσης των διαταραχών μεταξύ υπέρφωτων και αρνητικών τιμών, που οδηγεί στο συμπέρασμα ότι το σύστημα γίνεται ασταθές, ακυρώνοντας στην πράξη τη διαταρακτική προσέγγιση. Παρόλα αυτά μπορούμε να τροποποιήσουμε κατάλληλα τη θεωρία και να διατηρήσουμε το πλεονεκτήματα της, καταφέρνοντας παράλληλα να μειώσουμε ή και να εξαφανίσουμε τα μειονεκτήματά της. Η θεωρία NMDC προέρχεται από το γενικότερο όρο G_5 της Λαγκρανζιανής Galileon:

$$\mathcal{L}_5 = G_5(\phi, X) G^{\mu\nu} \partial_\mu \phi \partial_\nu \phi$$

αν επιλέξουμε $G_5(\phi, X) = \sigma\tau\alpha\theta$. Αν επιλέξουμε μια πιο γενική μορφή $G_5(\phi, X) = f(\phi)\,\xi(X)$, η φαινομενολογία εμπλουτίζεται τόσο στην περίοδο του πληθωρισμού, όσο και μετά από αυτή. Θα αναφερόμαστε σε αυτού του τύπου τις θεωρίες ως Γενικευμένη μη Τετριμμένη Ζεύξη του Κινητικού Όρου με τον τανυστή Einstein (GNMDC).

Αν επιλέξουμε $f(\phi) \propto \phi$ ο όρος GNMDC θα σβήσει γρήγορα κοντά στον πάτο του δυναμικού του και θα υπάρξει μετάβαση στην κλασσική θεωρία Einstein, ενώ και οι αντίστοιχες ταλαντώσεις θα τροποποιηθούν. Μια GNMDC θεωρία αυτής της μορφής υπακούει στην παρατήρηση ότι τα βαρυτικά κύματα από ύστερα στάδια της εξέλιξης του Σύμπαντος έχουν ταχύτητα ίδια με αυτή του φωτός, κάτι που δεν ισχύει στην απλή θεωρία NMDC.

Ένας τέτοιος όρος τροποποιεί και το φάσμα των διαταραχών, $\mathcal{P}_R(k)$, σε όλες τις κλίμακες, άρα και σε αυτές που είναι μικρότερες από αυτές που παρατηρούνται μέσω της ακτινοβολίας υποβάθρου, καθώς επηρεάζει την ταχύτητα του πεδίου κατά τον πληθωρισμό και, επομένως, το πλάτος των διαταραχών. Αν ο GNMDC όρος είναι τέτοιος ώστε σε κάποιο σημείο της εξέλιξης η ταχύτητα του πεδίου να μικρύνει απότομα, τότε θα ξεκινήσει και παραγωγή Πρωταρχικών Μελανών Οπών (PBH), προσφέροντας έναν καινούργιο μηχανισμό παραγωγής τους, διαφορετικό από τους μηχανισμούς πολλαπλών πεδίων αλλά και των μηχανισμών που περιλαμβάνουν σημείο αλλαγής κλίσης (inflection point) στο δυναμικό.

Υποθέτουμε λοιπόν ότι:

$$\mathcal{L}_5 = G_5(\phi, X)\, G^{\mu\nu} \partial_\mu \phi \partial_\nu \phi \;=\; f(\phi)\, \xi(X)\, G^{\mu\nu} \partial_\mu \phi \partial_\nu \phi \,,$$

όπου για μεγάλο μέρος της παρούσας εργασίας υποθέτουμε τη μορφή $f(\phi) = \alpha \phi^{\alpha-1} G^{\mu\nu} \ll M^{\alpha+1}$, που για $\alpha = 0$ ανακτά τη GR και για $\alpha = 1$ το NMDC, ενώ για $\alpha > 1$, τροποποιεί τα αποτελέσματα όπως συνοπτικά περιγράφηκε παραπάνω. Η δράση είναι λοιπόν, της μορφής:

$$S = \int d^4x \sqrt{-g} \left[\frac{M_{\rm Pl}^2}{2} R - \frac{1}{2} \left(g^{\mu\nu} - f(\phi) G^{\mu\nu} \right) \partial_\mu \phi \partial_\nu \phi - V(\phi) \right] .$$

από όπου παράγονται οι δυναμικές εξισώσεις. Για επίπεδη FLRW γεωμετρία και κοσμολογικό πεδίο ϕ, αυτές είναι:

$$3 M_{\rm Pl}^2 H^2 = V\left(\phi\right) + \frac{1}{2}\dot{\phi}^2 + \frac{9}{2}\, f(\phi)\, \dot{\phi}^2 H^2 \ ,$$

$$M_{\rm Pl}^2 \left(\dot{H} + \frac{3}{2} H^2 \right) \;=\; \frac{V(\phi)}{2} - \frac{\dot{\phi}^2}{4} + f(\phi) \left[\left(\frac{1}{2}\dot{H} + \frac{3}{4} H^2 \right) \dot{\phi}^2 + H \dot{\phi}\, \ddot{\phi} \right] + \frac{1}{2}\, f'(\phi) H \dot{\phi}^3 \ ,$$

και

$$\ddot{\phi} \left(1 + 3 f(\phi) H^2 \right) + 3 H \dot{\phi} \left(1 + 3\, f(\phi)\, H^2 + 2\, f(\phi)\, \dot{H} \right) + \frac{3}{2}\, f'(\phi)\, \dot{\phi}^2 H^2 + \frac{dV}{d\phi} = 0 \ .$$

Και εδώ είναι πολύ χρήσιμο να ορίσουμε παραμέτρους Slow Roll:

$$\epsilon \equiv -\frac{\dot{H}}{H^2} = \frac{3}{2} \frac{\dot{\phi}^2 + 3 f(\phi) \dot{\phi}^2 H^2 - f(\phi) \left(\dot{H} \dot{\phi}^2 + 2 H \dot{\phi}\, \ddot{\phi} \right) - f'(\phi) H \dot{\phi}^3}{\rho_\phi}, \quad \delta \equiv \frac{\ddot{\phi}}{H \dot{\phi}}$$

οπότε για $\epsilon \ll 1$ και $\delta \ll 1$ οδηγούμαστε στις πιο απλές δυναμικές εξισώσεις:

$$3M_{\rm Pl}^2 H^2 \approx V(\phi) \ ,$$

$$3H\dot{\phi}\left(1+3\,f(\phi)H^2+\frac{1}{2}f'(\phi)\,H\,\dot{\phi}\right)+\frac{dV}{d\phi}\approx 0\,.$$

Επιπλέον, έχουμε ότι:

$$\epsilon \simeq \frac{3}{2}\frac{\dot{\phi}^2}{\rho_\phi}\left(1+3H^2 f(\phi)-f'(\phi)H\dot{\phi}\right)\equiv \epsilon_{\rm GR}+\epsilon_D+\epsilon_{\mathcal{B}}\ .$$

όπου έχουμε ορίσει τις βοηθητικές παραμέτρους:

$$\epsilon_{\rm GR}=3\dot{\phi}^2/(2\rho_\phi),\quad \epsilon_{\mathcal{B}}=\frac{\dot{\phi}^2}{M_{Pl}^2H^2}G'(\phi)H\dot{\phi}\ ,\quad \epsilon_D\equiv\frac{3}{2}\frac{f(\phi)\dot{\phi}^2}{M_{\rm Pl}^2}\,.$$

Μπορούμε πλέον να δούμε πιο ξεκάθαρα το αποτέλεσμα ενός όρου GNMDC γιατί η ταχύτητα $\dot{\phi}$ μειώνεται κατά $3H^2f(\phi)$ φορές, μειώνοντας παράλληλα την τιμή του ϵ. Πράγματι:

$$\epsilon \simeq \epsilon_V\,\frac{1+3H^2f(\phi)-f'(\phi)H\dot{\phi}}{\left(1+3H^2f(\phi)+f'(\phi)\,H\dot{\phi}/2\right)^2}\ \equiv\ \epsilon_V\,\frac{\mathcal{A}-\mathcal{B}}{(\mathcal{A}+\mathcal{B}/2)^2}\,,$$

όπου:

$$\epsilon_V=\frac{M_{\rm Pl}^2}{2}\left(\frac{V'}{V}\right)^2,\quad \mathcal{A}\equiv 1+3H^2f(\phi)\ ,\quad \mathcal{B}\equiv f'(\phi)H\dot{\phi}\ .$$

Αντίστοιχα ορίζεται και η παράμετρος $\eta\equiv\eta_V/\mathcal{A}$, όπου $\eta_V=M_{\rm Pl}^2\frac{V''}{V}$.

Η σχέση που δίνει τα e-folds, προκύπτει ότι είναι:

$$N\equiv\int_t^{t_{\rm end}}Hdt=\int_{\phi_{\rm end}}^{\phi}\frac{H}{\dot{\phi}}d\phi\simeq\frac{1}{M_{\rm Pl}}\int_{\phi_{\rm end}}^{\phi}\frac{\mathcal{A}+\mathcal{B}/2}{\sqrt{2\epsilon_V}}d\phi\ ,$$

Το επόμενό μας βήμα είναι να παράγουμε τα παρατηρήσιμα μεγέθη που προβλέπονται από μια θεωρία GNMDC. Η διαταρακτική μελέτη γίνεται πιο εύκολα στη βαθμίδα όπου:

$$\delta\phi=0$$

εφ' όσον ο όρος GNMDC έχει ϕ-εξάρτηση, γιατί οι αντίστοιχοι διαταρακτικοί όροι θα εξαφανιστούν. Τα βοηθητικά μεγέθη που θα χρειαστούμε είναι τα:

$$Q_s\equiv F^2\,G/(f(\phi)H^2),\quad F\equiv\frac{1-\epsilon_D/3}{1-\epsilon_D}\ ,\quad G\equiv\frac{\epsilon_D}{3}\left(1+3H^2f(\phi)\frac{1+\epsilon_D}{1-\epsilon_D/3}\right)\ ,$$

Το τετράγωνο της ταχύτητας διάδοσης των διαταραχών, c_s^2, δίνεται από:

$$c_s^2=\left(1-\frac{\epsilon_D}{3}\right)^{-1}\frac{\epsilon_D}{3G}\left[(1+\epsilon_D)+3H^2f(\phi)\left[(1+\epsilon_D)+\frac{4}{9F}\epsilon_D\right]+6\dot{H}f(\phi)\left(1-\frac{\epsilon_D}{3}\right)\right]\ .$$

όπου αν $f(\phi)\to 0$, επιστρέφουμε στη GR. Το φάσμα των βαθμωτών διαταραχών δίνεται από τον τύπο:

$$\mathcal{P}_{\mathcal{R}}=\frac{H^2}{8\pi^2\,M_{\rm Pl}^2\,\epsilon_V}\left(\mathcal{A}+\mathcal{B}+\mathcal{O}\left(\frac{\mathcal{B}^2}{\mathcal{A}}\right)\right)\ .$$

ενώ ο δείκτης κλίσης των βαθμωτών διαταραχών (tilt) είναι:

$$1 - n_s \equiv -\frac{d\ln\mathcal{P}_\mathcal{R}}{d\ln k}\Big|_{k=aH} \simeq 8\epsilon - 2\eta + \epsilon\, M_{\rm Pl}\frac{f'(\phi)}{f(\phi)}\sqrt{\frac{2}{\epsilon_V}}\ .$$

όπου ο τελευταίος όρος είναι αυτός που ξεχωρίζει την περίπτωση αυτή από το NMDC ($f'(\phi) = 0$). Τέλος, στο όριο όπου το GNMDC κυριαρχεί έναντι της GR (High Friction limit) έχουμε:

$$r = 16\,\frac{\epsilon_V}{\mathcal{A}+\mathcal{B}}\ .$$

Από αυτή τη σχέση βλέπουμε ότι στις GNMDC θεωρίες ο λόγος r ελαττώνεται σε σχέση με τις θεωρίες NMDC αλλά και σε σχέση με τη GR.

Για να είναι ένα τέτοιο μοντέλο συνεπές παράγοντας πληθωρισμό χωρίς αστάθειες και άλλα προβλήματα πρέπει $Q_s > 0$ και $c_s^2 > 0$. Όμως, κατά τη διάρκεια των ταλαντώσεων που ακολουθούν τον πληθωρισμό, η ποσότητα $\dot{H}$ μπορεί να αλλάζει συνεχώς πρόσημο:

$$\dot{H} = -\epsilon\, H^2 = -\frac{p+\rho}{2M_{\rm Pl}^2}\ ,$$

όπου p:

$$p_\phi = \left\{\frac{1}{2}\dot{\phi}^2 - V(\phi)\right\} - \dot{\phi}\, f(\phi)\left\{\left[\left(\dot{H} + \frac{3}{2}H^2\right)\dot{\phi} + 2H\,\ddot{\phi}\right] - f'(\phi)H\dot{\phi}^2\right\}\ .$$

Καθώς λοιπόν η τιμή της παραμέτρου ϵ ταλαντώνεται συμπαρασύρει την τιμή του c_s^2. Για να αντιμετωπίσει κανείς το πρόβλημα αυτό που παρουσιαζόταν στις NMDC θεωρίες, ενδεχόμενα αρκεί να επιλέξει μια συνάρτηση $f(\phi)$ τέτοια ώστε:

$$\dot{\phi} f(\phi) < \dot{\phi}^2$$

Παραδείγματα τέτοιων συναρτήσεων είναι οι:

$$f(\phi) = \frac{\alpha\phi^{\alpha-1}}{M^{\alpha+1}}\ , \qquad \text{or} \qquad f(\phi) = \frac{1}{M^2}e^{\tau\phi/M_{\rm Pl}}\ .$$

Μπορούμε να δείξουμε τα αποτελέσματα αυτής της τροποποίησης με απευθείας σύγκριση των όρων που αντιστοιχούν στη Γενική Σχετικότητα και στο GNMDC. Μπορεί κανείς να παρατηρήσει από την Εικόνα 1.1 (σελ. 9), ότι στο τέλος του πληθωρισμού, ο όρος της GR, μετά από μερικές ταλαντώσεις κυριαρχεί έναντι του όρου GNMDC, κάτι που δε συνέβαινε στην περίπτωση του NMDC. Αντίστοιχα, στην Εικόνα 1.2 (σελ. 10), φαίνεται η διαφορά της εξέλιξης της περίπτωσης NMDC ($\alpha = 1$) με αντίστοιχες περιπτώσεις GNMDC, όπου οι απότομες ταλαντώσεις του c_s^2 σβήνουν με το χρόνο.

Στο όριο όπου $\mathcal{A} \gg 1$ και $\mathcal{B} \sim f'(\phi)/\mathcal{A} \ll \mathcal{A}$ η έκφραση για το φάσμα $\mathcal{P}_\mathcal{R}$ είναι:

$$\mathcal{P}_\mathcal{R}(\phi,\lambda_p,\alpha,M)|_{\phi=\phi_{\rm cmb}} \simeq \frac{H^2}{8\pi^2\, M_{\rm Pl}^2\,\epsilon_V}\mathcal{A} \simeq \frac{V^2(\phi)}{24\pi^2\, M_{\rm Pl}^6\,\epsilon_V(\phi)}f(\phi,\alpha,M)$$

Η παρατηρούμενη τιμή του φάσματος είναι $\mathcal{P}_R \approx 2.2\cdot 10^{-9}$. Με την παραπάνω έκφραση μπορούμε να βρούμε μια κατά προσέγγιση συνθήκη που πρέπει να ισχύει μεταξύ των $f(\phi)$, M σε σχέση με την παράμετρο του δυναμικού, όταν $\phi = \phi_{\rm CMB}$, δηλαδή όταν η διαταραχή με κυματαριθμό $k_{\rm cmb} = 0.05$ Mpc^{-1}, βγήκε από τον ορίζοντα, καθορίζοντας τον επιθυμητό αριθμό e-folds. Για τον δείκτη κλίσης των βαθμωτών διαταραχών έχουμε:

$$1 - n_s \simeq \frac{M_{\rm Pl}^2}{V(\phi,\lambda_p)f(\phi,\alpha,M)}\left(8\epsilon_V - 2\eta_V + M_{\rm Pl}\frac{f'(\phi)}{f(\phi)}\sqrt{2\epsilon_V(\phi,\lambda_p)}\right)\ .$$

Με χρήση αυτών των δύο συνθηκών, μπορούμε να κατασκευάσουμε μοντέλα που ικανοποιούν τις παρατηρησιακές συνθήκες και επιπλέον έχουν καλύτερα χαρακτηριστικά, μετά το τέλος του πληθωρισμού, από τα μοντέλα NMDC. Συγκεκριμένα, ερευνούμε την περίπτωση όπου το δυναμικό είναι μορφής μονωνύμου:

$$V(\phi) = \lambda_p\,\phi^p\,, \qquad f(\phi) = \alpha\frac{\phi^{\alpha-1}}{M^{\alpha+1}}$$

Μπορούμε τώρα να γράψουμε τις διάφορες ποσότητες συναρτήσει της κλίμακας του όρου GNMDC, M, της παραμέτρου α και της παραμέτρου λ_p. Έχουμε:

$$N(\phi) \simeq \frac{\alpha\lambda_p}{p\,(p+a+1)}\,\frac{1}{M_{\rm Pl}^4\,M^{\alpha+1}}\left(\phi^{p+\alpha+1}-\phi_{\rm end}^{p+\alpha+1}\right).$$

και επομένως οι παράμετροι Slow Roll συναρτήσει των e-folds παίρνουν τη μορφή:

$$\epsilon \simeq \frac{p}{2(p+\alpha+1)}\,\frac{1}{N}\,,\quad \eta=\frac{2p-2}{p}\epsilon\,.$$

Αντίστοιχα, για $\alpha \geq 1$ έχουμε:

$$1-n_s \simeq 8\epsilon-2\eta+2\epsilon\frac{\alpha-1}{p}=\frac{2p+\alpha+1}{p+\alpha+1}\,\frac{1}{N}\,,\quad r\simeq\frac{8\,p}{p+\alpha+1}\,\frac{1}{N}\,,$$

Είναι αξιοσημείωτο ότι ούτε ο δείκτης r, ούτε ο δείκτης n_s, εξαρτώνται από την παράμετρο λ του δυναμικού και την κλίμακα M του GNMDC, εξαρτώνται όμως από την τιμή του α. Όσο αυξάνει το α, ο δείκτης n_s αυξάνεται ενώ ο δείκτης r μειώνεται. Επομένως, για $N \lesssim 37$ οι παρατηρησιακοί περιορισμοί από το Planck 2018, $r<0.064$ και $n_s=0.965$, ικανοποιούνται για δυναμικά δευτέρου και τετάρτου βαθμού αν επιλεγεί κατάλληλος όρος GNMDC.

Ένα δεδομένο δυναμικό, για παράδειγμα αυτό που αντιστοιχεί στο μποζόνιο Higgs, μπορεί να γεννήσει πληθωρισμό σε μια GNMDC θεωρία, με κατάλληλες επιλογές M και α, που μπορούν να καθοριστούν από τις παρατηρήσεις.

Αυτές οι συμπεριφορές απεικονίζονται στα διαγράμματα των Εικόνων 1.3 (σελ. 12) και 1.4 (σελ. 13), όπου φαίνονται οι γραφικές παραστάσεις $n_s(N)$ και $r(N)$ για δυναμικά δευτέρου και τετάρτου βαθμού. Αντίστοιχα, στις εικόνες 1.6 (σελ. 18) και 1.8 (σελ. 20), απεικονίζουμε ακριβή αποτελέσματα μοντέλων, που προέκυψαν από αριθμητική ανάλυση για $\alpha=1,3,5,7$ όταν επιλέγονται κατάλληλες παράμετροι για να παράγονται 40, 50 ή 60 e-folds σε δυναμικό δευτέρου βαθμού αλλά και δυναμικό Higgs.

Πέραν της συμπεριφοράς των παρατηρήσιμων μεγεθών, παρατηρεί κανείς το πλεονέκτημα που προσφέρει ένας όρος GNMDC σε σχέση με το NMDC από τα διαγράμματα 1.7 (σελ. 19) και 1.8 (σελ. 20). Για ίδιες τιμές των υπόλοιπων παραμέτρων, πέραν του α, το Slow Roll επιτυγχάνεται πολύ πιο εύκολα από ότι στην περίπτωση του NMDC. Τέλος, στην εικόνα 1.1 (σελ. 9), συγκρίνουμε τον κανονικό κινητικό όρο με τον όρο του GNMDC κοντά στο τέλος του πληθωρισμού. Ο όρος της GR ξεκινά να κυριαρχεί, επιστρέφοντας στη δυναμική της Καθιερωμένης Κοσμολογίας, κάτι που δε συμβαίνει στο NMDC. Αντίστοιχα αποτελέσματα ισχύουν και για εκθετικό όρο GNMDC σε εκθετικό δυναμικό (Εικόνα 1.5, 15).

Αναζητούμε τώρα αντιστοιχία με μοντέλα στο πλαίσιο της GR, για την οποία θα δείξουμε ότι δεν είναι πλήρης, και επομένως μπορεί να υπάρξει διαφοροποίηση μέσα από τις παρατηρήσεις. Στα αρχικά στάδια του Slow Roll, οι δυναμικές εξισώσεις της θεωρίας αυτής προσομοιάζουν αρκετά αυτές της GR, κάτι που υποδεικνύει ότι μπορεί να υπάρχει μετασχηματισμός που φέρνει τις δύο θεωρίες στην ίδια μορφή. Πράγματι, με το μετασχηματισμό:

$$\varphi=g(\phi)\,,\qquad V_m(\varphi)=V[g^{-1}(\varphi)]\,,$$

έχουμε ότι:

$$3H\dot{\phi}\simeq -V'(\phi)/[g'(\phi)]^2$$

όπου η συνάρτηση $g'(\phi)$ εσωκλείει τη σχέση μεταξύ του αρχικού και του μετασχηματισμένου πεδίου:

$$g'(\phi)=d\varphi/d\phi$$

Για $\mathcal{A}\gg\mathcal{B}$ ισχύει ότι $g'(\phi)=(\epsilon_V/\epsilon)^{1/2}\approx\mathcal{A}$ επομένως:

$$\varphi=\int\left(\frac{\epsilon_V}{\epsilon}\right)^{1/2}d\phi=\frac{1}{M_{\rm Pl}}\int\left[\,V(\phi)\,f(\phi)\,\right]^{1/2}\,d\phi\,.$$

Αποδείξαμε δηλαδή, ότι σε πρώτη τάξη στις παραμέτρους Slow Roll, η δυναμική του πεδίου ϕ σε δυναμικό $V(\phi)$ μιας θεωρίας GNMDC κατά το Slow Roll, είναι ισοδύναμη με αυτή ενός κανονικού

πεδίου φ, σε δυναμικό $V_m(\varphi)$, στο πλαίσιο της GR. Παρακάτω δείχνουμε συγκεκριμένα την αντιστοιχία μεταξύ των δύο θεωριών, όταν το GNMDC είναι της μορφής $f(\phi) = \alpha \frac{\phi^{\alpha-1}}{M^{\alpha+1}}$.

Στην περίπτωση των μονώνυμων δυναμικών της μορφής: $V(\phi) = \lambda_p \, \phi^p$ με $f(\phi) = \alpha \frac{\phi^{\alpha-1}}{M^{\alpha+1}}$, έχουμε $\varphi = \int (\epsilon_V/\epsilon)^{1/2} d\phi$. Το πεδίο φ, δίνεται από την έκφραση:

$$\varphi = 2\,\lambda_p^{1/2} \left(\frac{\alpha}{M^{\alpha+1}}\right)^{1/2} \frac{\phi^{\alpha+p+1}}{(\alpha+p+1)/2} \frac{1}{M_{\rm Pl}} \, .$$

και συμπεριφέρεται σαν να έχει τετριμμένη ζεύξη με τη Βαρύτητα. Το αντίστοιχο δυναμικό είναι:

$$V_m(\varphi) = \lambda_p \left[\frac{\alpha+p+1}{2} \frac{M_{\rm Pl}}{\lambda_p^{1/2}} \left(\frac{M^{\alpha+1}}{\alpha}\right)^{1/2} \varphi\right]^{\frac{2p}{\alpha+p+1}} \, ,$$

άρα υπάρχει η αντιστοίχιση: $V \propto \phi^p \quad \longleftrightarrow \quad V_m \propto \varphi^{\frac{2p}{p+\alpha+1}}$.

Επομένως δυναμικά, $V(\phi)$, με εκθέτη $p \gg 1$ θα εμφανίζονται να έχουν δυναμική με ηπιότερη κλίση, από την οπτική της GR. Αντίστοιχα αποτελέσματα προκύπτουν για εκθετικό δυναμικό με εκθετικό GNMDC. Εκμεταλλευόμαστε αυτή την αντιστοίχιση μεταξύ GR και GNMDC ώστε να αναπαράγουμε τις προβλέψεις αυτού του μοντέλου, χρησιμοποιώντας σχέσεις που προκύπτουν από τη GR.

Μετά το τέλος του πληθωρισμού το βαθμωτό πεδίο ταλαντώνεται γύρω από τον πάτο του δυναμικού (περίοδος της αναθέρμανσης-reheating), μετατρέποντας την εναπομένουσα ενέργεια σε άλλους βαθμούς ελευθερίας. Στα μονώνυμα δυναμικά $V(\phi) \propto \phi^p$, η καταστατική εξίσωση ενός βαθμωτού σε υπόβαθρο GR είναι:

$$w \equiv \frac{\langle p \rangle}{\langle \rho \rangle} = \frac{p-2}{p+2} \, .$$

Κατά το reheating το κοσμικό ρευστό θερμοποιείται, και στη συνέχεια ξεκινά η κυριαρχία της ακτινοβολίας. Η θερμοκρασία αυτής της περιόδου δίνεται από τη σχέση:

$$T_{\rm reh} \sim (\Gamma_\phi M_{\rm Pl})^{1/2}$$

όπου Γ_ϕ ο ρυθμός διάσπασης του πεδίου inflaton. Αποδεικνύεται ότι:

$$N \simeq 57.6 + \frac{1}{4} \ln \epsilon_* + \frac{1}{4} \ln \frac{V_*}{\rho_{\rm end}} - \frac{1-3w}{4} \tilde{N}_{\rm rh} \, ,$$

όπου η ποσότητα $\tilde{N}_{\rm rh}$ συμπεριλαμβάνει τα e-folds που λαμβάνουν χώρα κατά το reheating. Επομένως, τα συνολικά e-folds εξαρτώνται και από αυτή την περίοδο.

Τα μοντέλα GR+GNMDC θα έχουν διακριτό reheating, με δύο πιθανές εκφάνσεις, ανάλογα με το ποιος όρος κυριαρχεί. Αν κυριαρχεί το GNMDC, υπάρχει σημαντική τροποποίηση στην παραπάνω καταστατική εξίσωση, με διακριτές τιμές για τον όρο $(1-3w)\tilde{N}_{\rm rh}/4$. Στην αντίθετη περίπτωση, η σχέση αυτή ισχύει ακριβώς.

Ένα άλλο πλεονέκτημα των θεωριών GNMDC είναι ότι προσφέρουν το έδαφος για τη δημιουργία πρωταρχικών μελανών οπών (PBH), χωρίς τη χρήση δυναμικού με μεταβλητή κλίση. Αυτό θα προσέφερε, μεταξύ άλλων, μια πιθανή εξήγηση και για τη Σκοτεινή Ύλη και γι' αυτό η μελέτη τους παρουσιάζει ιδιαίτερο ενδιαφέρον. Στη μελέτη τους, δύο είναι τα βασικά σημεία: το μέγεθος της αλλαγής της τιμής του φάσματος των βαθμωτών διαταραχών, που καθορίζει την αφθονία τους, και το στάδιο στο οποίο συνέβη αυτή η αλλαγή, που καθορίζει τη μάζα τους.

Μια PBH μάζας M, έχει πιθανότητα να δημιουργηθεί όταν καταρρεύσει μια διαταραχή πυκνότητας του κοσμικού ρευστού, αν είναι αρκετά μεγάλη ώστε να κυριαρχήσει έναντι της πίεσης της ακτινοβολίας, όταν επανεισέρχεται στον ορίζοντα. Ο λόγος της αφθονίας των PBH με μάζα M, σε σχέση με τη συνολική αφθονία της Σκοτεινής Ύλης, είναι

$$f_{\rm PBH}(M) \equiv \Omega_{\rm PBH}(M)/\Omega_{\rm DM}$$

Σκοπός μας είναι να υπολογίσουμε την πιθανότητα σχηματισμού μιας PBH και να συνδέσουμε τις αντίστοιχες παραμέτρους με τις τιμές που σχετίζονται με το βαθμωτό φάσμα των διαταραχών. Σε ό,τι

ακολουθεί χρησιμοποιείται ο φορμαλισμός Press-Schechter. Συμβολίζουμε με β το ρυθμό δημιουργίας των PBH, ενώ η πυκνότητα κατωφλίου δημιουργίας μιας οπής συμβολίζεται με δ_c. Αν μια τυχαία διαταραχή έχει πυκνότητα $\delta > \delta_c$, τότε η Βαρύτητα κυριαρχεί και η διαταραχή καταρρέει σε PBH. Ο ρυθμός δημιουργίας εξαρτάται και από την παράμετρο $\sigma(k)$, που ποσοτικοποιεί τη διαφοροποίηση των διαταραχών σε σχέση με τον κυματαριθμό τους k. Αποδεικνύεται ότι το μέγεθος του παράγοντα $\beta(M)$ δίνεται από τη σχέση:

$$\beta(M) \sim \frac{1}{\sqrt{2\pi}} \frac{\sqrt{\mathcal{P}_R}}{\delta_c} e^{-\delta_c^2/2\mathcal{P}_\mathcal{R}} .$$

Στην περίπτωση, λοιπόν, του GNMDC, το φάσμα των διαταραχών έχει ϕ εξάρτηση:

$$\mathcal{P}_R \approx \frac{V}{96\pi^2 M_{\rm Pl}^4 \epsilon_V / \mathcal{A}} .$$

και όταν η παράμετρος ϵ μειώνεται, ο ρυθμός $\beta(M)$ αυξάνεται. Αν κανείς θέλει όλη Σκοτεινή Ύλη να αποτελείται από PBH, τότε: $f_{\rm PBH} \sim 1$, και το φάσμα πρέπει να πάρει την τιμή $\mathcal{P}_\mathcal{R}^{\rm PBH} \sim 10^{-2}$ για $\delta_c \sim 0.5$. Επομένως:

$$\epsilon(\phi_{\rm PBH}) = V(\phi_{\rm PBH})(96\pi^2 M_{\rm Pl}^4)^{-1} \mathcal{P}_\mathcal{R}^{\rm PBH})^{-1}$$

και η παράμετρος $\epsilon_{\rm PBH}$ πρέπει να είναι μικρότερη από μια τιμή $\epsilon_{\rm max}$, που μπορεί να βρεθεί με αντικατάσταση των παρατηρούμενων τιμών του $\mathcal{P}_\mathcal{R}$ και του $r_{\rm max} \simeq 0.64$. Γίνεται τότε:

$$\epsilon_{\rm PBH} \lesssim \frac{10^{-11}}{\mathcal{P}_\mathcal{R}^{\rm PBH}} \sim 10^{-9} .$$

Μια απότομη μείωση στο ϵ συνεπάγεται αύξηση στα δ και η, οπότε η προσέγγιση Slow Roll παύει να ισχύει και πρέπει να λυθεί αναλυτικά η εξίσωση Mukhanov-Sasaki.

Για τη μάζα μιας PBH, έστω μια διαταραχή κλίμακας k^{-1}, που εξέρχεται του ορίζοντα N_k, e-folds πριν το τέλος του πληθωρισμού. Κάνοντας την απλοποίηση $H_{\rm end} \simeq H_k$, που αποδεικνύεται αρκετά ακριβής για κλίμακες που βγαίνουν από τον ορίζοντα, μετά την Ultra Slow Roll φάση, φτάνουμε στη σχέση:

$$N_k = \ln\left(\frac{k_{\rm end}}{k}\right) .$$

Επιπλέον, ορίζουμε την ποσότητα $\tilde{N}_k \equiv \ln(a(t)/a_{\rm end})$, που αντιπροσωπεύει τα e-folds που μεσολαβούν μεταξύ του τέλους του πληθωρισμού και της επανεισόδου μιας διαταραχής κλίμακας k^{-1} στον ορίζοντα. Όταν η καταστατική παράμετρος παίρνει τιμές $w > -1/3$ έχουμε ότι $\tilde{N}_k = 2\,N_k/(1+3w)$. Επομένως, αν δεν έχουμε κυριαρχία της ακτινοβολίας ($w = 1/3$), τότε τα e-folds που απομένουν μέχρι το τέλος του πληθωρισμού όταν μια διαταραχή επανεισέρχεται στον ορίζοντα, θα εξαρτώνται από τη θερμοκρασία κατά την αναθέρμανση. Αντιθέτως, όταν $w = 1/3$, ή όταν λαμβάνουν χώρα οι ταλαντώσεις τύπου ϕ^4, θα ισχύει η σχέση:

$$k(M) = 1.8 \times 10^{18}\,{\rm Mpc}^{-1}\,\gamma^{1/2} \left(\frac{M}{10^{10}\,{\rm g}}\right)^{-1/2} \left(\frac{g_*}{106.75}\right)^{-1/12} .$$

Θα μας απασχολήσουν εδώ δύο πιθανές κλίμακες PBH. Οι PBH με μάζα $M_{\rm PBH} \simeq 10^{21}$ g, αν έχουν κατάλληλη αφθονία, μπορεί να αντιπροσωπεύουν ακόμα και ολόκληρη την πυκνότητα που αντιστοιχεί στη Σκοτεινή Ύλη, και θα μπορούσαν να ανιχνευθούν και μελετηθούν με μελλοντικούς ανιχνευτές βαρ. κυμάτων. Η δεύτερη κατηγορία που μας ενδιαφέρει, είναι οι PBH με μάζα $M_{\rm PBH} \simeq 10^{35}$ g, καθώς μπορούν να προκαλέσουν γεγονότα ανιχνεύσιμα από τους ήδη υπάρχοντες ανιχνευτές. Υπολογίζουμε λοιπόν, ότι αν η επανείσοδος των αντίστοιχων κλιμάκων στον ορίζοντα συνέβη όταν $w = 1/3$ (κυριαρχία της ακτινοβολίας), τότε:

$$k(10^{21}\,{\rm g}) = 10^{14}\,k_{\rm CMB}\,\gamma^{1/2}. \qquad k(10^{35}\,{\rm g}) = 1.1 \times 10^{7}\,k_{\rm CMB}\,\gamma^{1/2}$$

όπου $k_{\rm CMB}$ το pivot scale $k_{\rm CMB} = 0.05\ {\rm Mpc}^{-1}$, ενώ $g_* \simeq \mathcal{O}(100)$.

Πρέπει να υπολογίσουμε τα e-folds $N_{\rm PBH}$, πριν το τέλος του πληθωρισμού, όταν δημιουργήθηκε η κορυφή στο φάσμα των διαταραχών και αυτά που έλαβαν χώρα μετά το τέλος του ($N_{\rm CMB}$). Ισχύει ότι:

$$\ln(\epsilon_* V_*/\rho_{\rm end})^{1/4} = \pm\mathcal{O}(1)\text{άρα}N_{\rm CMB} \lesssim 58$$

Υπολογίζουμε λοιπόν πως:

$$k_{\rm end} = k_{\rm CMB}\, e^{N_{\rm CMB}}\, \frac{H_{\rm end}}{H_{\rm CMB}}\ .$$

και επομένως για πληθωρισμό στα πλαίσια ενός δυναμικού Higgs βρίσκουμε

$$N_{\rm PBH}(M_{\rm PBH} = 10^{21}\,{\rm g}) \sim 27\ , \qquad \text{and} \qquad N_{\rm PBH}(M_{\rm PBH} = 10^{35}\,{\rm g}) \sim 45\ ,$$

οδηγώντας μας στη σχέση: $f_{\rm PBH}(M_{\rm PBH} = 10^{21}\,{\rm g}) \sim 1$ για $\beta(M) \sim 10^{-13}$ and $f_{\rm PBH}(M_{\rm PBH} = 10^{35}\,{\rm g}) \sim 0.1$, όταν $\beta(M) \sim 10^{-7}$. Η πιθανότητα σχηματισμού $\beta(M)$ μπορεί να υπολογιστεί για συγκεκριμένες τιμές του $\epsilon_{\rm PBH}$.

Θα κατασκευάσουμε PBH σε δυναμικό Higgs, στο πλαίσιο μιας θεωρίας GNMDC, με τη χρήση μορφής που σε συγκεκριμένο σημείο της εξέλιξης του συστήματος, οδηγεί σε απότομη αύξηση του φάσματος των διαταραχών, ενώ παράλληλα θα διατηρήσουμε και αποδεκτές από τις παρατηρήσεις, τιμές των παρατηρήσιμων μεγεθών.

Για να αυξηθεί η τιμή του φάσματος σε ένα μοντέλο GNMDC, αρκεί να μειωθεί το μέγεθος $\epsilon_V/\mathcal{A}$, χωρίς παράλληλα να διαταράσσονται οι προβλέψεις για τα παρατηρήσιμα μεγέθη. Επιλέγουμε ζεύξη της μορφής:

$$f(\phi) = f_I(\phi)\,(1 + f_{II}(\phi))\ .$$

Ο όρος $f_I(\phi)$ έχει ισχύ στην αρχή του πληθωρισμού, ενώ ο όρος $f_I(\phi)f_{II}(\phi)$ ενεργοποιείται σε κατάλληλο σημείο, ώστε να έχουμε την παραγωγή PBH που επιθυμούμε. Η συνάρτηση $f_{II}(\phi)$ επιλέγεται ώστε να έχει κορυφή σε σημείο $\phi = \phi_0$, όντας όμως αμελητέα αλλού, όπως για παράδειγμα η συνάρτηση:

$$f_{II}(\phi) = \frac{d}{\sqrt{\left(\frac{\phi-\phi_0}{sM_{\rm Pl}}\right)^2 + 1}}$$

όπου οι παράμετροι d, s και ϕ_0 θα χρησιμοποιηθούν για να καθορίσουμε την αφθονία και τη μάζα των PBH.

Για να τις υπολογίσουμε, έχουμε:

$$\mathcal{P}_R \propto \frac{\mathcal{A}(\phi)}{\epsilon_V} \simeq \frac{3H^2 f_I(\phi) f_{II}(\phi)}{\epsilon_V}\bigg|_{\phi=\phi_{\rm PBH}}\ , \tag{1}$$

όπου $\phi = \phi_{\rm PBH}$ η τιμή όπου το φάσμα γίνεται μέγιστο, την οποία μπορούμε να προσεγγίσουμε ως $\phi_0 = \phi_{\rm PBH}$. Επιπλέον, ζητάμε κορυφή στο φάσμα $N_{\rm PBH}$ e-folds πριν τελειώσει ο πληθωρισμός. Κατά τη φάση II, λαμβάνουν χώρα $= N_{II}$ e-folds και η τιμή του $\dot\phi$ μειώνεται δραματικά. Επιπλέον, πρέπει $N_{II} \lesssim N_{\rm PBH}$. Ο ακριβής αριθμός N_{II}, μπορεί να καθοριστεί από παρατηρησιακές απαιτήσεις σχετικά με την αφθονία των PBH. Αν λοιπόν $f_{II}(\phi) > 1$ ισχύει ότι $\Delta\phi_{II} \simeq 2c(\ln d)^{1/2}$ οπότε:

$$N_{II} = \int_{\phi_0-\Delta\phi_{II}}^{\phi_0+\Delta\phi_{II}} \frac{H}{\dot\phi} d\phi \simeq \frac{1}{M_{\rm Pl}} \int_{\phi_0-\Delta\phi_{II}}^{\phi_0+\Delta\phi_{II}} \frac{\mathcal{A}+\mathcal{B}/2}{\sqrt{2\epsilon_V}}\, d\phi$$

Η φάση II διαρκεί από $\phi_0 + \Delta\phi_{II}$ ως $\phi_0 - \Delta\phi_{II}$, $f_{II}(\phi)$.

Στρεφόμαστε τώρα στην επίλυση της εξίσωσης MS:

$$u_k'' + \left(c_s^2 k^2 - \frac{z''}{z}\right) u_k = 0,$$

για ένα perturbation mode u_k, όπου ο τόνος συμβολίζει παραγώγιση ως προς το σύμμορφο χρόνο, η. Υπολογίζουμε την τιμή ενός mode αφού έχει εξέλθει του ορίζοντα και έχει "παγώσει" και μέσω αυτού βρίσκουμε την ακριβή τιμή του φάσματος:

$$\mathcal{P}_R = \frac{k^3}{2\pi^2}\frac{|u_k|^2}{z^2}\bigg|_{k\ll aH} .$$

Για να θέσουμε αρχικές συνθήκες σε αυτή την εξίσωση, χρησιμοποιούμε το κενό Bunch-Davies. Όταν ένα mode βρίσκεται ακόμα εντός του ορίζοντα ισχύει ότι $k \gg aH$, και ο όρος z''/z είναι αμελητέος. Σε αυτή την περίπτωση:

$$u_k'' + c_s^2 k^2 u_k = 0$$

δίνοντας την αρχική συνθήκη: $u_k = e^{-ik\tau}/\sqrt{2k}$ και κατ' επέκταση:

$$\mathrm{Re}\,[u_k] = \frac{1}{\sqrt{2k}}\,, \quad \mathrm{Im}[u_k] = 0, \quad \mathrm{Re}\left[\frac{du_k}{dt}\right] = 0\,, \quad \mathrm{Im}\left[\frac{du_k}{dt}\right] = \frac{\sqrt{k}}{a(t_i)\sqrt{2}}\,.$$

όπου $a(t_i)$ η τιμή του παράγοντα κλίμακας όταν το mode βρίσκεται μέσα στον ορίζοντα, άρα $a(t_i)H(t_i) \ll k$.

Όταν οι παράμετροι Slow Roll μεταβάλλονται απότομα, μπορούμε να ξαναγράψουμε την εξίσωση ως:

$$\mathcal{R}_k'' + (2+\epsilon_2)aH\mathcal{R}_k' + c_s^2 k^2 \mathcal{R}_k = 0.$$

όπου $\epsilon_2 \equiv \dot{\epsilon}/(H\epsilon)$, εκμεταλλευόμενοι το γεγονός ότι $c_s Q_s \simeq \epsilon$ (αφού $\epsilon_D \ll 1$ και $c_s \simeq 1$). Στο όριο των μεγάλων κλιμάκων, ο τελευταίος όρος είναι αμελητέος και για $(2+\epsilon_2) > 0$ βρίσκουμε ένα σταθερά αποσβεννύμενο mode της διαταραχής. Το αντίθετο συμβαίνει όταν ο όρος εντός της παρένθεσης είναι αρνητικός, οπότε το αντίστοιχο mode αυξάνεται. Στην περίπτωση του GNMDC λοιπόν, όπου το ϵ εξαρτάται από το $f(\phi)$, αν αυτό αλλάξει απότομα, τότε η διαταραχή $\mathcal{R}$ αυξάνεται αντίστοιχα γρήγορα και μπορεί να οδηγήσει στη δημιουργία μιας PBH.

Συγκεκριμένα, θα δούμε τα αποτελέσματα που προκύπτουν σε ένα δυναμικό Higgs στα πλαίσια του GNMDC που παρουσιάστηκε νωρίτερα. Επιλέγουμε λοιπόν:

$$V(\phi) = (\lambda/4)\phi^4, \text{ για } \lambda \simeq 0.1. \quad \text{και } f_I(\phi) = \alpha\phi^{\alpha-1}/M^{\alpha+1}$$

ενώ η συνάρτηση f_{II} είναι όπως παραπάνω. Επιπλέον ορίζουμε $\epsilon_{\rm PBH} \equiv \epsilon_V(\phi_0)/\mathcal{A}(\phi_0)$, που σχετίζεται με την τροποποίηση του φάσματος των διαταραχών, όπου σημειώνουμε ότι $\epsilon(\phi_0) \simeq \epsilon_{\rm PBH}$. Για να υπολογίσουμε την παράμετρο d έχουμε:

$$d \sim \frac{M_{\rm Pl}^2}{V(\phi_0)f_I(\phi_0)}\frac{\epsilon_V}{\epsilon_{\rm PBH}} = \frac{8}{\alpha\lambda}\frac{M_{\rm Pl}^4 M^{\alpha+1}}{\phi_0^{\alpha+5}}\frac{1}{\epsilon_{\rm PBH}}\,.$$

Τέλος, για δεδομένη τιμή e-folds κατά το στάδιο II του πληθωρισμού, μπορεί να καθοριστεί, ποιοτικά, η τιμή και της παραμέτρου s, ενώ η ακριβής τιμή των παραμέτρων αυτών βρίσκεται μόνο αφού λυθεί η εξίσωση MS.

Για μια PBH μάζας $M_{\rm PBH} \sim 10^{21}$ g, από τα παραπάνω βρίσκουμε ότι η κορυφή στο φάσμα πρέπει να δημιουργηθεί περίπου $N_{\rm PBH} \sim 27$ e-folds πριν το τέλος του πληθωρισμού. Για να είναι η παράμετρος $\beta(M)$, αρκετά μεγάλη πρέπει $\beta(M) \approx 10^{-13}$, για αυτή τη μάζα. Βρίσκουμε τότε ότι $\mathcal{P}_R \sim 10^{-2}$. Στα πλαίσια ενός πληθωρισμού Higgs προβλέπεται ότι η κλίμακα $k_{\rm CMB} = 0.05$ Mpc^{-1} βγαίνει από τον ορίζοντα 58 e-folds πριν το τέλος του.

Όταν κυριαρχεί η συνάρτηση f_I λαμβάνουν χώρα $\lesssim N_I$ e-folds, ενώ όταν ξεκινήσει να υπερισχύει η f_{II} συμβαίνουν N_{II} e-folds. Μετά την πάροδο της ισχύος της γίνονται τα υπόλοιπα από τα N_I e-folds, καθώς η f_I ξανακυριαρχεί. Για να καθοριστεί η τιμή των N_I e-folds πρέπει να λάβουμε υπόψη την τιμή του παράγοντα κλίσης n_s, αλλά και την κανονικοποίηση μέσα από την παρατηρούμενη τιμή του φάσματος του CMB όταν $k^{-1} = 0.05 Mpc$.

Σαν εφαρμογή, λύθηκε αριθμητικά η εξίσωση MS, όπου υπολογίστηκε η εξέλιξη 500 modes, $\mathcal{R}_k$, και τα αντίστοιχα αποτελέσματα φαίνονται στην Εικόνα 1.10 (σελ. 29). Πράγματι παράγεται φάσμα με αρκετά υψηλή κορυφή ώστε η αφθονία των PBH να είναι μεγάλη. Οι παράμετροι που επιλέχθηκαν είναι:

$$\alpha = 3, \quad M = 7.1\times10^{-5}M_{\rm Pl}, \quad d = 5.5\times10^{6}, \quad s = 2.1\times10^{-10}$$

που γεννούν 50 e-folds μεταξύ $\phi_{\rm CMB} = 0.0264 \quad M_{\rm Pl}$ και $\phi_{\rm end} = 0.0197 M_{\rm Pl}$. Ο όρος $f_I(\phi) f_{II}(\phi)$ κυριαρχεί για $\phi = 0.02 \quad M_{\rm Pl}$. Με αυτές τις παραμέτρους: $\mathcal{P}_R(k_{\rm peak}) \sim 2 \times 10^{-2}$ (Εικόνες 1.9 και 1.10, σελ. 27, 29).

Όταν η επίδραση του όρου f_{II} τελειώσει, το πεδίο συνεχίζει προς τον πάτο του δυναμικού για μερικά e-folds ακόμα. Οι παράμετροι αυτές, έχουν επιπλέον το χαρακτηριστικό ότι δίνουν αποδεκτές τιμές για τα παρατηρήσιμα μεγέθη. Τέλος, η αφθονία τους υπολογίζεται ότι είναι, (επιλέγοντας $\delta_c \simeq 0.4$) ίση με $f_{\rm PBH} \sim 0.1$, (Εικόνα 1.10).

Σημειώνουμε ότι σε αυτή την Εικόνα παρατηρείται μεγάλη απόκλιση μεταξύ της προσεγγιστικής και της αριθμητικής τιμής του φάσματος, ακόμα και σε περιοχές όπου η παράμετρος ϵ δεν έχει ακόμα αλλάξει σημαντικά. Στην πραγματικότητα όμως, η τιμή του ϵ ταλαντώνεται με πολύ μικρό πλάτος και πολύ υψηλή συχνότητα. Επιπλέον, $\epsilon_2 < -2$, πριν τη δραματική μείωση της τιμής του ϵ. Έτσι, το φάσμα αρχίζει να αυξάνεται από πιο μικρές τιμές του k.

Μέχρι στιγμής λοιπόν, έχουμε δει πως το φαινόμενο της βαρυτικής τριβής, που ήταν γνωστό ότι υπάρχει στις θεωρίες μη Τετριμμένης ζεύξης του κινητικού όρου (NMDC), μπορεί να επεκταθεί και να εμπλουτιστεί, ως όρος GNMDC. Αυτός ο όρος προκαλεί εύκολα μια εποχή Slow Roll και επιπλέον, για κατάλληλη επιλογή του όρου GNMDC, η αντίστοιχη δυναμική αποσυζεύγεται χωρίς κάποιον επιπλέον μηχανισμό, στο τέλος του πληθωρισμού, επιστρέφοντας στην εξέλιξη που προκύπτει από τη GR. Επομένως, δείχνει να διορθώνει την αντίστοιχη συμπεριφορά των θεωριών NMDC που στην εποχή της αναθέρμανσης χαρακτηρίζονταν από αστάθειες.

Πιο συγκεκριμένα, βρήκαμε τις σχέσεις που δίνουν τα παρατηρήσιμα μεγέθη του CMB, όπως ο δείκτης κλίσης των βαθμωτών διαταραχών n_s, ή ο λόγος r. Επιπλέον, στο πλαίσιο του NMDC, το τετράγωνο της ταχύτητας διάδοσης των διαταραχών παρουσίαζε αυξανόμενες ταλαντώσεις μεταξύ θετικών και αρνητικών τιμών, που προκαλούσε εκθετικά εξελισσόμενες διαταραχές και επομένως αστάθειες. Αντίθετα, στον πληθωρισμό που παράγεται μέσω κατάλληλης επιλογής του GNMDC αυτό το πρόβλημα φαίνεται να αποφεύγεται, καθώς οι αντίστοιχες ταλαντώσεις είναι αποσβεννήμενες, χωρίς να χάνονται τα υπόλοιπα πλεονεκτήματα του NMDC.

Εξετάσαμε αριθμητικά, μεταξύ άλλων, τον πληθωρισμό που προκύπτει από δυναμικό Higgs, που είναι το μόνο βαθμωτό σωματίδιο που έχει βρεθεί. Η φαινομενολογία που παράγεται είναι σε καλή συμφωνία με τις παρατηρήσεις του Planck 2018. Αντίστοιχα, μελετήθηκε και εκθετικό δυναμικό με εκθετικό όρο GNMDC, που μάλιστα παρουσιάζει το πλεονέκτημα του φυσικού τέλους του πληθωρισμού, όταν το σύστημα βγαίνει από την περίοδο Slow Roll, ενώ βρήκαμε και μια άμεση αντιστοίχιση με μοντέλα που προκύπτουν από τη GR, διατηρώντας όμως τρόπο να ξεχωρίσουμε, από παρατηρήσεις, ποια είναι η πραγματική θεωρία Βαρύτητας που έχει οδηγήσει σε αυτά τα μεγέθη.

Τέλος, στραφήκαμε στη μελέτη των PBH σε μια θεωρία GNMDC, όπου μπορούν να παραχθούν χωρίς τη συμπερίληψη δυναμικού μεταβλητής κλίσης. Ως παράδειγμα εργαστήκαμε σε δυναμικό Higgs, όπου βρήκαμε κατάλληλες τιμές για τις παραμέτρους ώστε να μπορούν να δημιουργηθούν Οπές διαφόρων μαζών, κάποιες από τις οποίες παρουσιάζουν ιδιαίτερο ενδιαφέρον. Η πιο ενδιαφέρουσα είναι η περίπτωση $M \sim 10^{21}$g, καθώς αν η αφθονία των συγκεκριμένων PBH είναι αρκετά μεγάλη, θα μπορούσε να εξηγήσει πλήρως τη Σκοτεινή Ύλη. Επιπλέον, ελέγξαμε το σενάριο δημιουργίας mini PBH, που θα μπορούσαν να είναι ανιχνεύσιμες μέχρι σήμερα.

Επομένως, μελετήσαμε πληθωριστικά μοντέλα με όρους GNMDC που παράγουν νέα, διακριτά αποτελέσματα ενώ ταυτόχρονα θέτουν ένα πιο αξιόπιστο πλαίσιο μελέτης σε σχέση με τις παρόμοιες θεωρίες NMDC, αφού αποφεύγουν αστάθειες και επιστρέφουν την εξέλιξη στη GR μετά το πέρας του πληθωρισμού. Δείξαμε ότι σε αυτό το πλαίσιο μπορούν να παραχθούν και PBH με ενδιαφέρουσες εφαρμογές σε διάφορα πεδία της Κοσμολογίας, πετυχαίνοντας παράλληλα τα παρατηρήσιμα μεγέθη να είναι όλα σε συμφωνία με τις παρατηρήσεις, ενώ έχουν παραχθεί από το θεωρητικά δικαιολογημένο δυναμικό Higgs.

Επιτυχής Πληθωρισμός Higgs, από συνδυασμό Μη Τετριμμένων Ζεύξεων

Θα επεκτείνουμε τη μελέτη τέτοιου τύπου θεωριών, κρατώντας και άλλον όρο στη Λαγκρανζιανή και μελετώντας τα αποτελέσματα που δίνει η θεωρία που τους συνδυάζει. Σε ό,τι ακολουθεί, μελετάμε το συνδυασμό ενός όρου μη Τετριμμένης ζεύξης (NMC) με τη μη τετριμμένη κινητική ζεύξη που είδαμε μέχρι τώρα. Αποδεικνύεται ότι αυτός ο συνδυασμός έχει θεραπευτικές ιδιότητες σε σχέση με τα αποτελέσματα και των δύο όρων, όταν ο καθένας δρα μόνος του.

Η θεωρία NMC προκύπτει ως υποκατηγορία των Galileons που παρουσιάσαμε νωρίτερα, στην οποία υπάρχει μια απλή ζεύξη του βαθμωτού πεδίου με το βαθμωτό Ricci. Αυτή η τροποποίηση ήταν από τις πρώτες που έγιναν σε σχέση με την απλή θεωρία του πληθωρισμού και εν γένει βελτιώνει την παραγόμενη φαινομενολογία. Με επιλογή NMC της μορφής $\xi\phi^2$, αν η σταθερά ξ είναι αρκετά μεγάλη, τότε ο παραγόμενος πληθωρισμός είναι αρκετά εκτενής και παράγει πολύ χαμηλές τιμές για το λόγο

r. Όμως, για να επιτευχθεί αυτό, στην απλή περίπτωση του NMC, πρέπει να χρησιμοποιηθεί πολύ μεγάλη τιμή για το ξ. Αυτό το γεγονός μπορεί να προκαλέσει πρόβλημα όταν κανείς προσπαθήσει να κβαντώσει τη θεωρία αυτή (unitarity problem).

Από την άλλη πλευρά η θεωρία GNMDC δεν παρουσιάζει αντίστοιχο πρόβλημα, ενώ και αυτή παράγει πλούσια και εντός των παρατηρησιακών ορίων φαινομενολογία, ενώ βελτιώνει, αλλά δε λύνει πλήρως το πρόβλημα των ταλαντώσεων μετά το τέλος του πληθωρισμού, που σχετίζονται με αστάθειες και εκθετική εξέλιξη των μεγεθών του.

Θα μελετήσουμε λοιπόν κάτω από ποιες συνθήκες ένας συνδυασμός τέτοιων όρων μπορεί να λύσει τα προβλήματα της κάθε μιας από τις ξεχωριστές θεωρίες, ενώ παράλληλα διατηρεί τα θετικά της στοιχεία. Θα παρουσιάσουμε πρώτα τα βασικά αποτελέσματα του NMC και στη συνέχεια θα παρουσιάσουμε τα αποτελέσματα του συνδυασμού των δύο όρων καθώς και συγκεκριμένα αριθμητικά αποτελέσματα, όπου θα φανούν πιο καθαρά όλα τα πλεονεκτήματα της συνδυαστικής θεωρίας.

Όταν στη δράση περιλαμβάνεται μόνο η GR και το NMC έχουμε:

$$S = \int d^4x\sqrt{-g}\left[f(\phi)R - \frac{\partial_\mu\phi\partial^\mu\phi}{2} - V(\phi)\right],$$

Το πιο ενδελεχώς μελετημένο σενάριο είναι αυτό στο οποίο: $f(\phi) = \xi\phi^2$, το οποίο σε μονώνυμο (Higgs) δυναμικό, παράγει ένα αξιοσημείωτα χαμηλό r. Επιπλέον, δεν παρουσιάζει αστάθειες που σχετίζονται με το c_s^2 που στην περίπτωσή του είναι ταυτοτικά ίσο με 1, ανεξάρτητα από τη μορφή του NMC. Όμως, για να επιτύχει έναν αξιόλογο πληθωρισμό πρέπει ο συνδυασμός $\xi\phi^2$ να πάρει τιμές μεγαλύτερες από τη μάζα Planck, M_{Pl}, κάτι που είναι προβληματικό από κβαντομηχανικής άποψης.

Μια συνήθης προσέγγιση στη μελέτη του NMC είναι η πραγματοποίηση ενός σύμμορφου μετασχηματισμού που πηγαίνει στο σύστημα Einstein (Einstein frame). Επιλέγοντας $\hat{g}_{\mu\nu} = \Omega^2(x)g_{\mu\nu}$ με $\Omega^2(x) = \frac{16\pi}{M_{Pl}^2}f(\phi)$ και ορίζοντας ένα καινούργιο βαθμωτό πεδίο φ σε δυναμικό U, έχουμε:

$$\frac{d\varphi}{d\phi} \equiv \sqrt{\frac{M_{Pl}^2}{8\pi}\frac{f(\phi)+3f'^2(\phi)}{2f^2(\phi)}}\ , \qquad U(\varphi) \equiv \Omega^{-4}V(\phi)\ ,$$

οπότε η δράση είναι στη μορφή:

$$S = \int d^4x\sqrt{-\hat{g}}\left[\frac{M_{Pl}^2}{2}\hat{R} - \frac{\partial_\mu\varphi\partial^\mu\varphi}{2} - U(\varphi)\right]\ ,$$

Σε πρώτη τάξη, τα παρατηρήσιμα μεγέθη είναι:

$$1 - n_s = 6\epsilon_U - 2\delta_U\ , \qquad r = 16\epsilon_U\ ,$$

όπου έχουμε ορίσει τις παραμέτρους:

$$\epsilon_U = \frac{M_{Pl}^2}{2}\left(\frac{U'}{U}\right)\ , \qquad \delta_U = M_{Pl}^2\frac{U''}{U}\ .$$

Το δυναμικό U έχει πολύ μικρή κλίση για μεγάλες τιμές του όρου NMC ($\xi\phi^2 \gg M_{Pl}$), οπότε οι παράμετροι ϵ_U και δ_U είναι πολύ μικρές, δίνοντας ένα αντίστοιχα μικρό r. Σε πληθωρισμό Higgs με ζεύξη της μορφής $f(\phi) = \xi\phi^2$ το χαμηλό r και ο ικανοποιητικός αριθμός e-folds επιτυγχάνονται μόνο αν $\xi\phi^2 > M_{Pl}$, οδηγώντας σε προβλήματα.

Θα προχωρήσουμε τώρα στην κατασκευή του συνδυασμένου μοντέλου. Θεωρούμε τη δράση:

$$S = \int d^4x\sqrt{-g}\left[\mathcal{L}_{GR} + \mathcal{L}_\phi + \mathcal{L}_{NMC} + \mathcal{L}_{GNMDC}\right],$$

με

$$\mathcal{L}_{GR} = \frac{M_{Pl}^2}{2}R\ , \qquad \mathcal{L}_\phi = -\frac{1}{2}g^{\mu\nu}\partial_\mu\phi\partial_\nu\phi - V(\phi)\ ,$$
$$\mathcal{L}_{NMC} = \xi f(\phi)R\ , \qquad \mathcal{L}_{GNMDC} = G(\phi)G^{\mu\nu}\partial_\mu\phi\partial_\nu\phi\ .$$

Οι εξισώσεις Friedmann και Klein-Gordon αυτού του μοντέλου, θεωρώντας επίπεδη FLRW μετρική και κοσμολογικό πεδίο, είναι:

$$\rho_\phi \equiv 3M_{Pl}^2H^2 = \frac{\dot\phi^2}{2} + V(\phi) + 9G(\phi)H^2\dot\phi^2 - 6\xi\left[f(\phi)H^2 + f'(\phi)\dot\phi H\right],$$

$$\begin{aligned}-p_\phi \equiv M_{Pl}^2\left(3H^2+2\dot H\right) = V(\phi) - \frac{\dot\phi^2}{2} + G(\phi)\left(3H^2\dot\phi^2 + 2\dot H\dot\phi^2 + 4H\dot\phi\ddot\phi\right) + 2G'(\phi)H\dot\phi^3 \\ - 2\xi\left[3f(\phi)H^2 + 2f(\phi)\dot H + 2Hf'(\phi)\dot\phi + \dot\phi^2 f''(\phi) + f'(\phi)\ddot\phi\right],\end{aligned}$$

και

$$\ddot\phi\left(1+6G(\phi)H^2\right) + 3H\dot\phi(1+6G(\phi)H^2 + 4G(\phi)\dot H) + 3H^2G'(\phi)\dot\phi^2 - 6\xi f'(\phi)(\dot H + 2H^2) + V'(\phi) = 0$$

Περιμένει κανείς ότι θα υπάρχουν 3 διαφορετικές περιοχές ενδιαφέροντος, ανάλογα με τη σχετική ισχύ των δύο όρων. Πριν συζητήσουμε κάθε μια από αυτές τις περιοχές, θα αναφερθούμε στο πλαίσιο της προσέγγισης Slow Roll για αυτή τη θεωρία.

Σε αυτή την προσέγγιση, $\dot H \ll H^2$, $\dot\phi \ll H$ και $\ddot\phi \ll 3H\dot\phi$, οπότε κρατάμε μόνο τους κυρίαρχους όρους του NMC και του GNMDC αντίστοιχα:

$$3M_{Pl}^2H^2 = 9G(\phi)H^2\dot\phi^2 - 6\xi f(\phi)H^2 + V(\phi)\ ,$$

και

$$3H\dot\phi\left(1+6G(\phi)H^2\right) - 12H^2\xi f'(\phi) + V'(\phi) = 0\ .$$

Από τις πλήρεις εξισώσεις βρίσκουμε τη μορφή της παραμέτρου $\epsilon = -\frac{\dot H}{H^2}$:

$$\epsilon = \epsilon_{GR} + \epsilon_{G1} + \epsilon_{G2} + \epsilon_{G3} + \epsilon_{G4} + \epsilon_{N1} + \epsilon_{N2} + \epsilon_{N3} + \epsilon_{N4}\ ,$$

όπου έχουμε εισάγει βοηθητικές παραμέτρους που αντιστοιχούν σε κάθε όρο της θεωρίας μας. Για τον όρο της GR έχουμε $\epsilon_{GR} = \frac{\dot\phi^2}{2M_{Pl}^2H^2}$, ενώ για το GNMDC και το NMC:

$$\begin{aligned}\epsilon_{G1} &= \frac{3\dot\phi^2G(\phi)}{M_{Pl}^2}\ , \quad \epsilon_{G2} = -\frac{\dot\phi^2\dot HG(\phi)}{M_{Pl}^2H^2}\ , \quad \epsilon_{G3} = -\frac{2\dot\phi\ddot\phi G(\phi)}{M_{Pl}^2H}\ , \quad \epsilon_{G4} = -\frac{G'(\phi)\dot\phi^3}{M_{Pl}^2H}\ , \\ \epsilon_{N1} &= \frac{2\xi f(\phi)\dot H}{M_{Pl}^2H^2}\ , \quad \epsilon_{N2} = -\frac{\xi f'(\phi)\dot\phi}{M_{Pl}^2H}\ , \quad \epsilon_{N3} = \frac{\dot\phi^2\xi f''(\phi)}{M_{Pl}^2H^2}\ , \quad \epsilon_{N4} = \frac{\xi f'(\phi)\ddot\phi}{M_{Pl}^2H^2}\ .\end{aligned}$$

Οι παράμετροι ϵ_{Gi} σχετίζονται με το GNMDC και οι ϵ_{Ni} με το NMC (ο δείκτης i κινείται από 1 ως 4). Από τα όσα έχουν αναφερθεί μέχρι τώρα, στην προσέγγιση Slow Roll, καταλαβαίνουμε ότι οι κυρίαρχες παράμετροι θα είναι οι ϵ_{G1}, ϵ_{N1} και ϵ_{N2}.

Μπορούμε τώρα να βρούμε τις ποσότητες $\mathcal{G}_T, \mathcal{F}_T, \Sigma, \Theta, \mathcal{G}_s$ και $\mathcal{F}_s$, συναρτήσει αυτών των παραμέτρων. Έτσι, αποκτούμε την παρακάτω μορφή για το τετράγωνου της ταχύτητας διάδοσης των διαταραχών:

$$\begin{aligned}c_s^2 = &\left\{\epsilon\left[\epsilon_{G1}(12\epsilon_{N2} - \epsilon_{GR} + 3) + 3\left(\epsilon_{G1}^2 + \epsilon_{GR} + 3\epsilon_{N2}^2\right)\right] - 3\epsilon_{N1}(\epsilon_{G1} + \epsilon_{GR})\right\}^{-1}\left[\epsilon(\epsilon_{G1} - 3) + 3\epsilon_{N1}\right]^{-1} \\ &\Big\{\epsilon^2\left\{\epsilon_{G1}^2\left[7\epsilon_{N1} + 17\epsilon_{N2} + \epsilon_{N3} - 3\left(\epsilon_{G3} - \epsilon_{G4} - \epsilon_{N4}\right) - 4\right] + 3\epsilon_{G1}\left[5(\epsilon_{N2} - 2)\epsilon_{N2} - 2\epsilon_{G4}(\epsilon_{N2} - 1)\right.\right. \\ &-10\epsilon_{N1} + 2\left(\epsilon_{G3} - \epsilon_{N3} + \epsilon_{N4}\right)\Big] + 4\epsilon_{G1}^3 + 9\left(\epsilon_{G3} + 2\epsilon_{G4}\epsilon_{N2} + \epsilon_{G4} + 3\epsilon_{N1} - 3\epsilon_{N2}^2 + \epsilon_{N2} + \epsilon_{N3}\right. \\ &\left.+\epsilon_{N4}\right)\Big\} + \epsilon\epsilon_{N1}\left\{\epsilon_{G1}\left[6\left(\epsilon_{N3} - \epsilon_{G3} - \epsilon_{G4} - \epsilon_{N4}\right) + 15\epsilon_{N1} + 30\epsilon_{N2}\right] + 4\epsilon_{G1}^2 - 9\left[2\epsilon_{G3} + 3\epsilon_{N1}\right.\right. \\ &\left.\left.+2\epsilon_{G4}(\epsilon_{N2} + 1) + 2(\epsilon_{N2} + \epsilon_{N3} + \epsilon_{N4}) - 3\epsilon_{N2}^2\right]\right\} + \epsilon^3(\epsilon_{G1} - 3)^2(\epsilon_{G1} - 1) + 9\epsilon_{N1}^2(\epsilon_{G3} + \epsilon_{G4} \\ &+ \epsilon_{N1} + \epsilon_{N2} + \epsilon_{N3} + \epsilon_{N4})\Big\}\end{aligned}$$

Με αλγεβρική επεξεργασία της παραπάνω σχέσης μπορούμε, και χρησιμοποιώντας τη μορφή του ϵ συναρτήσει των βοηθητικών παραμέτρων, μπορούμε να φέρουμε αυτή τη σχέση στη μορφή

$$c_s^2 - 1 \approx \frac{\mathcal{O}(\epsilon_{Gi})}{f_\epsilon(\epsilon_{Ni}, \epsilon_{GR}) + \mathcal{O}(\epsilon_{Gi})},$$

όπου f_ϵ μια συνάρτηση που δεν εξαρτάται από τις παραμέτρους ϵ_{Gi}, ενώ στο $\mathcal{O}(\epsilon_{Gi})$ περιέχονται όροι που είναι τουλάχιστον πρώτης τάξης στα ϵ_{Gi}. Ο παρονομαστής είναι μεγαλύτερης τάξης από τον αριθμητή όταν η περίοδος Slow Roll έχει τελειώσει και ο όρος του NMC κυριαρχεί , αρκεί να έχει επιλεγεί GNMDC που σβήνει καθώς πλησιάζουμε τον πάτο του δυναμικού. Αυτό οδηγεί στο συμπέρασμα ότι $c_s^2 \equiv 1$, που είναι και ένα από τα κύρια αποτελέσματα αυτής της δουλειάς: Η συμπερίληψη του NMC και ενός ϕ-εξαρτώμενου GNMDC που ελαττώνει σημαντικά την ισχύ του προς το τέλος του πληθωρισμού, ανεξάρτητα από την ακριβή τους μορφή, θα έχει σαν αποτέλεσμα την πλήρη ίαση της θεωρίας από αστάθειες που σχετίζονται με το c_s^2 (Εικόνα 2.2, σελ. 46).

Αντίστοιχα, στο όριο όπου υπάρχει μόνο το GNMDC, έχουμε:

$$c_s^2 - 1 \approx \frac{\mathcal{O}(\epsilon_{Gi})}{\mathcal{O}(\epsilon_{Gi})}. \tag{2}$$

όπου το κλάσμα είναι προφανώς διάφορο του 0, εν γένει, επιβεβαιώνοντας ότι το GNMDC δε γιατρεύει πλήρως τη θεωρία από τις σχετικές αστάθειες.

Επιστρέφοντας τώρα στη μελέτη των 3 πιθανών περιοχών ισχύος, καταλαβαίνουμε εύκολα ότι η περιοχή όπου NMC $\ll$ GNMDC στερείται ενδιαφέροντος. Στην περιοχή όπου το GNMDC κυριαρχεί κατά το Slow Roll, μέσω των δυναμικών εξισώσεων μπορούμε να εξάγουμε 2 πιθανούς δεσμούς που ποσοτικοποιούν αυτή την κυριαρχία:

$$\xi \ll \frac{G(\phi)}{f'(\phi)} H\dot{\phi} \quad \text{και} \quad \xi \ll \frac{G(\phi)}{f(\phi)} \dot{\phi}^2 \ ,$$

όπου ο δεύτερος είναι ισχυρότερος από τον πρώτο. Όμως, μετά τη φάση Slow Roll, δεν μπορούμε να θεωρήσουμε αμελητέους τους όρους που οφείλονται στο NMC, ακριβώς γιατί επεξεργαζόμαστε GNMDC που σβήνουν, καθώς το πεδίο πλησιάζει το 0. Επομένως, αυτή η περιοχή πρέπει να εξεταστεί με μεγαλύτερη λεπτομέρεια. Όμως, την ίδια απάντηση μπορούμε να αναζητήσουμε μέσω της μελέτης της επόμενης περιοχής, δηλαδή αυτής όπου οι δύο συνεισφέροντες όροι είναι παρόμοιας ισχύος.

Για να βρισκόμαστε στην περιοχή NMC $\approx$ GNMDC, διαλέγουμε τον πιο αδύναμο από τους δύο δεσμούς, που είναι αρκετός για να δείξει τα αποτελέσματα της θεωρίας. Θεωρούμε λοιπόν πως ισχύει:

$$\xi f'(\phi) \approx G(\phi) H\dot{\phi} \ , \quad \xi f(\phi) \gg G(\phi)\dot{\phi}^2 \ ,$$

ενώ για τους όρους λόγω GR θεωρούμε πως είναι αμελητέοι κατά το Slow Roll. Τότε, οι εξισώσεις Klein-Gordon και Friedmann είναι αντίστοιχα:

$$18G(\phi)H^3\dot{\phi} + V'(\phi) = 12H^2\xi f'(\phi) \ , \quad 3M_{Pl}^2 H^2 + 6\xi f(\phi) H^2 = V(\phi) \ .$$

Αναφέραμε ήδη ότι κατά το Slow Roll κυριαρχούν οι ϵ_{G1}, ϵ_{N1} και ϵ_{N2}. Κρατώντας τους όρους πρώτης τάξης σε αυτές τις παραμέτρους, έχουμε:

$$\mathcal{F}_s = \mathcal{G}_s \approx M_{Pl}^2 \epsilon_{G1} \ .$$

Στην περίπτωση του c_s^2 βλέπουμε ότι κρατώντας μόνο αυτούς τους όρους έχουμε το αναμενόμενο αποτέλεσμα $c_s^2 = 1$. Για το φάσμα των βαθμωτών διαταραχών έχουμε

$$\mathcal{P}_R \approx \frac{H^2}{8M_{Pl}^2 \pi^2 \epsilon_{G1}} \ ,$$

Μάλιστα, είναι αξιοσημείωτο το γεγονός ότι σε πρώτη τάξη, οι NMC όροι δεν έχουν επίδραση στην τιμή του φάσματος.

Προχωρώντας, για το λόγο των διαταραχών, r, έχουμε:

$$r \approx 16\epsilon_{G1} + \frac{16\epsilon_{G1}}{\epsilon_{G1}+\epsilon_{N2}}\epsilon_{N1} \ .$$

Κατά τη διάρκεια του Slow Roll έχουμε $\epsilon_{N1} < 0$, οπότε ο όρος NMC μειώνει το αποτέλεσμα $r = 16\epsilon_{G1}$. Επομένως, έχουμε διόρθωση του r σε μικρότερες τιμές, που είναι σε καλύτερη συμφωνία με τις παρατηρήσεις. Τέλος, ο δείκτης κλίσης n_s, παίρνει την πιο πολύπλοκη μορφή:

$$n_s \approx 1 + \frac{-3(\epsilon_{G3}+\epsilon_{G4}) + 2\epsilon_{G1}(\epsilon_{G1}+\epsilon_{N1}+\epsilon_{N2})}{\epsilon_{G1}(\epsilon_{G1}+\epsilon_{N1}+\epsilon_{N2}-1)} \ .$$

όπου σημειώνουμε ότι δε μπορούν να αγνοηθούν οι όροι ϵ_{G3}, ϵ_{G4}, καθώς οι υπόλοιποι όροι είναι δεύτερης τάξης στις παραμέτρους ϵ.

Συνοψίζοντας, όταν ένας ϕ-εξαρτώμενος όρος GNMDC είναι συγκρίσιμης ισχύος με έναν όρο NMC, το παραγόμενο πληθωριστικό μοντέλο είναι δυνατό να ιαθεί πλήρως από τις αστάθειες που σχετίζονται με την τιμή του c_s^2. Ο λόγος r διορθώνεται σε ακόμα καλύτερες τιμές, εντός των ορίων του Planck 2018, και μάλιστα όλο και περισσότερο, όσο πιο σημαντικός είναι ο όρος NMC. Τέλος, το σενάριο αυτό χαμηλώνει τις τιμές των αρχικών συνθηκών και των σταθερών ζεύξης, αποφεύγοντας το πρόβλημα του συνήθους NMC σε σχέση με την αυτοσυνέπεια της θεωρίας. Όλα αυτά τα αποτελέσματα ισχύουν, αρκεί η συνάρτηση $G(\phi)$ να γίνεται αμελητέα πλησιάζοντας τον πάτο του δυναμικού. Με βάση όλα αυτά, καταλαβαίνουμε ότι το συνδυασμένο σενάριο είναι καλύτερο σε σχέση με την κάθε μία θεωρία ξεχωριστά.

Θα παρουσιάσουμε τώρα μια αριθμητική ανάλυση συγκεκριμένων παραδειγμάτων. Για τον NMC όρο επιλέγουμε τη συνάρτηση $f(\phi) = \xi\phi^2$, που έχει μελετηθεί εκτενώς στη βιβλιογραφία, ενώ για τον όρο GNMDC επιλέγουμε πάλι τη μορφή $G(\phi) = \frac{\alpha\phi^{\alpha-1}}{2M^{\alpha+1}}$. Τέλος, επιλέγουμε να εργαστούμε στο πλαίσιο ενός δυναμικού Higgs $V(\phi) = \frac{\lambda\phi^4}{4}$.

Σε ό,τι ακολουθεί έχουμε επιβάλει τον παρατηρησιακό περιορισμό σε σχέση με την τιμή του φάσματος των βαθμωτών διαταραχών για $k = 0.05Mpc^{-1}$: $\mathcal{P}_R = 2.2 \cdot 10^{-9}$, ενώ οι αρχικές συνθήκες επιλέγονται ώστε να παραχθούν μοντέλα με 40, 50 και 60 e-folds.

Στο διάγραμμα 2.1, σελ. 45 φαίνεται η εξέλιξη του βαθμωτού πεδίου σε διάφορες περιπτώσεις. Ενώ στην περίπτωση GR+GNMDC οι ταλαντώσεις είναι πολύ έντονες, στη συνδυασμένη περίπτωση η περίοδός τους αυξάνεται. Αυτή η αύξηση είναι ένας κρίσιμος παράγοντας στο να πάψουν να υπάρχουν οι σχετιζόμενες με το c_s^2, αστάθειες.

Υπολογίσαμε επιπλέον τα παρατηρήσιμα μεγέθη, χρησιμοποιώντας τις σχέσεις που παρατίθενται στο Παράρτημα Β. Στο πάνω διάγραμμα της Εικόνας 2.2 σελ.46, παρατίθενται τα αποτελέσματα των ξεχωριστών θεωριών καθώς και της συνδυασμένης θεωρίας, σε σχέση με τα βεβαιότητας 1σ και 2σ δεδομένα, που προκύπτουν από το Planck 2018. Παρατηρούμε πως και η συνδυασμένη θεωρία παράγει αποδεκτές τιμές για το r.

Στο κάτω διάγραμμα της Εικόνας 2.2 φαίνεται η εξέλιξη του c_s^2 για διάφορες περιπτώσεις. Ενώ στη GNMDC θεωρία χρειάζεται μεγάλος αριθμός ταλαντώσεων μέχρι να σταθεροποιηθεί το c_s^2, όταν υπάρχει και NMC συνεισφορά, έχουμε μια αξιοσημείωτη μείωση των ταλαντώσεων, που μπορούν να περιοριστούν και μόνο σε θετικές τιμές, γιατρεύοντας πλήρως τη θεωρία από το αντίστοιχο πρόβλημα. Ο λόγος για αυτό φαίνεται μέσω της Εικόνας 2.3 σελ. 47, όπου παρουσιάζουμε τη συνεισφορά κάθε ξεχωριστού όρου στις δυναμικές εξισώσεις. Κατά τη διάρκεια του Slow Roll, οι συνεισφορές των NMC και GNMDC είναι παρόμοιες, αλλά όταν ξεκινούν οι ταλαντώσεις, το NMC κυριαρχεί. Η θεωρία NMC οδηγεί στο αποτέλεσμα $c_s^2 = 1$, και επομένως αυτή η κυριαρχία της στο τέλος έχει ευεργετική επίδραση στις αστάθειες λόγω του c_s^2. Αντίστοιχα αποτελέσματα προκύπτουν και αν επιλέξει κανείς ένα πολυώνυμο του ϕ ως GNMDC (Εικόνα 2.4 σελ. 49). Συνοψίζοντας, κατασκευάσαμε μια συνδυασμένη θεωρία NMC και GNMDC, και αποδείξαμε ότι όταν οι δύο όροι είναι συγκρίσιμοι κατά τη διάρκεια του Slow Roll, αυτή διατηρεί τα επιμέρους πλεονεκτήματα, γιατρεύοντας παράλληλα τα επιμέρους προβλήματα. Στη συνδυασμένη θεωρία, μια αρκετά μεγάλη περίοδος πληθωρισμού μπορεί να επιτευχθεί εύκολα, με σχετικά μικρές τιμές του πεδίου και της ζεύξης του, κάτι που αποτελούσε πρόβλημα στην περίπτωση του ξεχωριστού NMC, καθώς οι αναγκαίες τιμές ξεπερνούσαν τη μάζα Planck. Στο τέλος δε αυτής της πληθωριστικής φάσης, ο όρος NMC παραμένει κυρίαρχος επιστρέφοντας τη θεωρία στα αποτελέσματα της Γενικής Σχετικότητας και απομακρύνοντας το πρόβλημα των αστάθειών λόγω ταλαντώσεων του c_s^2 που οφείλεται στο GNMDC, ενώ τα παρατηρήσιμα μεγέθη διατηρούν τιμές εντός των παρατηρήσεων.

Αυτά τα αποτελέσματα ισχύουν τόσο για μονώνυμο όσο και για πολυώνυμο GNMDC, ενώ επιχειρηματολογήσαμε και για το γιατί αυτά τα αποτελέσματα θα είναι ίδια για οποιαδήποτε μορφή GNMDC έχει

το χαρακτηριστικό να εξαφανίζεται στο τέλος του πληθωρισμού (πχ εκθετικό GNMDC). Συμπεραίνει λοιπόν κανείς πως τέτοιου τύπου σενάρια είναι αποδοτικά ως προς τη φαινομενολογία τους και είναι χρήσιμο να μελετηθούν περαιτέρω, σε άλλες εκφάνσεις του πληθωρισμού, όπως για παράδειγμα στην πιθανότητα δημιουργίας PBH.

Αναπαραγωγή της Κοσμολογικής Εξέλιξης Με Παρουσία Επιπλέον Διαστάσεων

Το τελευταίο μέρος της παρούσας διατριβής ασχολείται με μια άλλη τροποποίηση που προτείνεται, αυτή της συμπερίληψης επιπλέον χωρικών διαστάσεων στη μετρική που περιγράφει το χωρόχρονο. Η πρόοδος που έχει σημειωθεί σε θεωρίες που προσπαθούν να ενοποιήσουν όλες τις αλληλεπιδράσεις (όπως η θεωρία χορδών) έχουν φέρει στο προσκήνιο αυτή την ιδέα πέραν της Κοσμολογίας, και στο επίπεδο της σωματιδιακής φυσικής. Αν κανείς κατασκευάσει ένα μοντέλο με παραπάνω διαστάσεις, πρέπει να συμπεριλάβει ένα μηχανισμό με τον οποίο μπορεί να ανακτήσει τον κόσμο, όπως τον αντιλαμβάνεται ένας 4-διάστατος παρατηρητής (μηχανισμός διαστατικής μείωσης - dimensional reduction).

Θα μελετήσουμε λοιπόν την περίπτωση των λεγόμενων Μεγάλων Επιπλέον Διαστάσεων (UED), με βάση το οποίο, αυτές οι διαστάσεις είναι προσβάσιμες σε όλα τα σωματίδια του Καθιερωμένου Μοντέλου. Έτσι, μια διαστατική μείωση οδηγεί σε έναν πύργο από σωματίδια (KK tower), που από 4-διάστατης άποψης, θα γίνονται αντιληπτά ως σωματίδια με μάζα, αλλά παρόμοιες ιδιότητες.

Υπό αυτή τη σκοπιά παρουσιάζεται ιδιαίτερο ενδιαφέρον σε αυτή τη θεωρία καθώς προσφέρει έναν μηχανισμό που ενδεχομένως περιγράφει τη Σκοτεινή Ύλη. Αν ένα σταθερό KK σωματίδιο υπάρχει μέχρι σήμερα και δεν έχει φορτίο και βαρυονική φύση, θα έχει όλες τις αναγκαίες ιδιότητες ενός σωματιδίου που αλληλεπιδρά μόνο με τη βαρύτητα (*weakly interacting massive particle-WIMP*).

Στην ενεργό 3+1-διάστατη εικόνα του σεναρίου αυτού, οι θεμελιώδεις σταθερές ζεύξης έχουν εξάρτηση από το χρόνο, λόγω της εξέλιξης του επιπλέον χώρου. Αυτό έχει σαν αποτέλεσμα, στο σενάριο των UED που μελετάμε εδώ, ο εσωτερικός αυτός χώρος να πρέπει να είναι συμπαγοποιημένος (compactified) και σταθεροποιημένος (stabilized), πριν ακόμα ξεκινήσει η Νουκλεοσύνθεση. Αποδεικνύεται ότι αυτό είναι δυνατό να συμβεί κατά την κυριαρχία της ακτινοβολίας, όχι όμως και κατά την κυριαρχία της ύλης, αν δε συμπεριληφθεί κάποιος επιπλέον μηχανισμός. Ειδικότερα, προκύπτει μια συσχέτιση των καταστατικών εξισώσεων των ρευστών που ζουν στον συνήθη και στον εσωτερικό χώρο, που εν γένει είναι ασύμβατος με το stabilization που προκύπτει απευθείας από τις δυναμικές εξισώσεις.

Η σταθεροποίηση τότε μπορεί να επιτευχθεί είτε από την ύπαρξη άλλων πεδίων (background fields), είτε περιγράφοντας τα κοσμικά ρευστά, μέσω μιας εξωτικής καταστατικής εξίσωσης που προκύπτει ως αποτέλεσμα πιο θεμελιωδών θεωριών (επί παραδείγματι χορδών που είναι τυλιγμένες και συμπαγοποιημένες μαζί με τη διάσταση στην οποία ζουν, με αποτέλεσμα την εμφάνιση αρνητικής πίεσης, η οποία οδηγεί σε επιβράδυνση της εξέλιξης του χώρου).

Παρουσιάζουμε το πλαίσιο της θεωρίας και στη συνέχεια παράγουμε ειδικές αλλά και τη γενική αναλυτική λύση της θεωρίας, η οποία δείχνουμε ότι παρουσιάζει ελκυστή. Στη συνέχεια παρουσιάζουμε τους περιορισμούς που πρέπει να ακολουθηθούν από μια τέτοια θεωρία και τέλος κατασκευάζουμε ένα αριθμητικό παράδειγμα που μπορεί να μιμηθεί τα αποτελέσματα του ΛCDM.

Υποθέτουμε ένα σύμπαν ξεχωριστά ομογενές στο συνήθη και στον εσωτερικό χώρο, με $(3+1+n)$-διαστάσεις. Η μετρική που επιλέγουμε, θα έχει δυο ξεχωριστούς παράγοντες κλίμακας:

$$ds^2 = -dt^2 + a^2(t)\gamma_{ij}dx^i dx^j + b^2(t)\tilde{\gamma}_{pq}dy^p dy^q\,,$$

Οι μετρικές, γ_{ij} και $\tilde{\gamma}_{pq}$ είναι μέγιστα συμμετρικές στις 3 και στις n διαστάσεις αντίστοιχα. Χρησιμοποιούμε αντίστοιχα δύο παραμέτρους καμπυλότητας, $k_a = -1, 0, 1$ και $k_b = -1, 0, 1$. Ο τανυστής ενέργειας ορμής είναι:

$$T^A{}_B = \begin{pmatrix} -\rho & 0 & 0 \\ 0 & \gamma^i{}_j p_a & 0 \\ 0 & 0 & \tilde{\gamma}^p{}_q p_b \end{pmatrix}, \text{ με } p_a = w_a\rho, \quad p_b = w_b\rho$$

και οδηγούμαστε στις δυναμικές εξισώσεις

$$3\left(\frac{\dot{a}}{a}\right)^2+3\frac{k_a}{a^2}+3n\frac{\dot{a}}{a}\frac{\dot{b}}{b}+\frac{n(n-1)}{2}\left[\left(\frac{\dot{b}}{b}\right)^2+\frac{k_b}{b^2}\right]=\kappa^2\rho$$

$$2\frac{\ddot{a}}{a}+\left(\frac{\dot{a}}{a}\right)^2+\frac{k_a}{a^2}+n\frac{\ddot{b}}{b}+2n\frac{\dot{a}}{a}\frac{\dot{b}}{b}+\frac{n(n-1)}{2}\left[\left(\frac{\dot{b}}{b}\right)^2+\frac{k_b}{b^2}\right]=-\kappa^2 w_a\rho$$

$$3\frac{\ddot{a}}{a}+3\left(\frac{\dot{a}}{a}\right)^2+3\frac{k_a}{a^2}+(n-1)\frac{\ddot{b}}{b}+3(n-1)\frac{\dot{a}}{a}\frac{\dot{b}}{b}+\frac{(n-1)(n-2)}{2}\left[\left(\frac{\dot{b}}{b}\right)^2+\frac{k_b}{b^2}\right]=-\kappa^2 w_b\rho$$

Λόγω διατήρησης της ενέργειας, αν οι καταστατικές παράμετροι δεν έχουν χρονοεξάρτηση, φτάνουμε στη σχέση:

$$\rho=\rho_i\left(\frac{a}{a_i}\right)^{-3(1+w_a)}\left(\frac{b}{b_i}\right)^{-n(1+w_b)}.$$

όπου ο δείκτης i αναφέρεται στις αρχικές τιμές, ενώ ο δείκτης 0 στις σημερινές. Εισάγοντας τις παραμέτρους Hubble μπορούμε ισοδύναμα να γράψουμε:

$$3H_a^2+3\frac{k_a}{a^2}+3nH_aH_b+\frac{n(n-1)}{2}\left[H_b^2+\frac{k_b}{b^2}\right]=\kappa^2\rho\,.$$

η οποία είναι η εξίσωση Friedmann για ένα Σύμπαν με ενεργειακή πυκνότητα ρ σε $(3+1+n)$ διαστάσεις, ενώ θα υποθέσουμε ότι η καμπυλότητα και για τους δύο χώρους έχει τιμή 0. Απαλείφοντας τα $\ddot{a}$, $\ddot{b}$, μπορούμε να πάρουμε το ισοδύναμο σύστημα εξισώσεων:

$$\begin{aligned}\dot{H}_a &= \frac{3\big[(n-1)w_a-nw_b-n-1\big]}{2+n}H_a^2+\frac{n\big[(n-1)(3w_a-1)-3nw_b\big]}{2+n}H_aH_b\\ &+ \frac{n(n-1)\big[1+(n-1)w_a-nw_b\big]}{2(2+n)}H_b^2\,, \qquad (4a)\\ \dot{H}_b &= \frac{3\,(2w_b-3w_a+1)}{2+n}H_a^2-\frac{3\,(3nw_a-2nw_b+2)}{2+n}H_aH_b\\ &- \frac{n\big[5+n+3(n-1)w_a-2(n-1)w_b\big]}{2(2+n)}H_b^2\,. \qquad (4b)\end{aligned}$$

Αυτό το σύστημα εξαρτάται μόνο από τις καταστατικές παραμέτρους w_a και w_b. Επιβάλλοντας το δεσμό $H_b(t)=c_iH_a(t)$ παίρνουμε μια ομάδα ειδικών λύσεων, οι οποίες θα δούμε ότι αποτελούν πιθανούς ελκυστές για τη γενική λύση του συστήματος. Πράγματι, έχουμε 3 τιμές c_i όταν $n\geq 2$:

$$\underbrace{c_1=\frac{6}{-3n-\sqrt{3n(2+n)}}}_{\text{K1}}\qquad \underbrace{c_2=\frac{6}{-3n+\sqrt{3n(2+n)}}}_{\text{K2}}\qquad \underbrace{c_3=\frac{1-3w_a+2w_b}{1+(n-1)w_a-nw_b}}_{\text{K3}}$$

ενώ για $n=1$:

$$\underbrace{c_1=-1}_{\text{K1}}\qquad \underbrace{c_3=\frac{-1+3w_a-2w_b}{-1+w_b}}_{\text{K3}}$$

Για $n\geq 2$ υπάρχουν 2 λύσεις τύπου Kasner οι $K1$ και $K2$:

$$\left.\begin{aligned}H_a(t)&=\frac{H_a(0)(n-1)}{n-1+[\sqrt{3n(2+n)}-3]H_a(0)t}\\ H_b(t)&=-\frac{6H_a(0)}{3n+\sqrt{3n(2+n)}+[3n+3\sqrt{3n(2+n)}]H_a(0)t}\end{aligned}\right\}\quad \text{K1}$$

$$\left.\begin{aligned} H_a(t) &= \frac{H_a(0)(n-1)}{n-1-[\sqrt{3n(2+n)}+3]H_a(0)t} \\ H_b(t) &= \frac{6H_a(0)}{-3n+\sqrt{3n(2+n)}+[-3n+3\sqrt{3n(2+n)}]H_a(0)t} \end{aligned}\right\} \quad \text{K2}$$

ενώ για $n=1$ υπάρχει μόνο μια μη τετριμμένη λύση Kasner:

$$\left.\begin{aligned} H_a(t) &= \frac{H_a(0)}{1+2H_a(0)t} \\ H_b(t) &= -\frac{H_a(0)}{1+2H_a(0)t} \end{aligned}\right\} \quad \text{K1 για } n=1$$

Όταν οι παράμετροι w είναι σταθερές, υπάρχει και μια τρίτη ειδική λύση ($K3$):

$$\left.\begin{aligned} H_a(t) = &\quad \frac{2[1+(n-1)w_a-nw_b]H_a(0)}{2+2(n-1)w_a-2nw_b+[3-3w_a^2+n(1+3w_a^2-6w_aw_b+2w_b^2)]H_a(0)t} \\ H_b(t) = &\quad \frac{2(1-3w_a+2w_b)H_a(0)}{2+2(n-1)w_a-2nw_b+[3-3w_a^2+n(1+3w_a^2-6w_aw_b+2w_b^2)]H_a(0)t} \end{aligned}\right\} \quad \text{K3}$$

Αντίθετα με τις $K1$ και $K2$, η λύση $K3$ δεν έχει σταθερή τιμή για την παράμετρο q, η οποία εδώ εξαρτάται από τα w. Για μια θετική τιμή $H_a(0)$ η λύση $K1$ παρουσιάζει τον απειρισμό της για $t<0$ ενώ η $K2$ για $t>0$. Αντιθέτως, ο απειρισμός της $K3$ εξαρτάται από τις παραμέτρους w. Επίσης, για τις $K1$, $K2$ αν ο εσωτερικός χώρος συστέλλεται, ($H_b<0$) ο συνήθης χώρος διαστέλλεται ($H_a>0$), και το αντίστροφο. Δεν ισχύει απαραίτητα κάτι αντίστοιχο για την $K3$.

Απαλείφοντας το χρόνο από τις εξισώσεις των παραμέτρων Hubble, παίρνουμε μια μόνο διαφορική εξίσωση, που είναι πάντα επιλύσιμη αν οι παράμετροι w είναι σταθερές:

$$\begin{aligned} const. = &\Big|\underbrace{H_b}_{H_b \text{ part}}\Big|^{\sqrt{2+n}\left[3(w_a-1)^2+n\left(1-3w_a^2+6w_aw_b-2w_b(1+w_b)\right)\right]} \cdot \\ &\Big|\underbrace{\frac{H_a}{H_b}+\frac{3n+\sqrt{3n}\sqrt{2+n}}{6}}_{K1 \text{ part}}\Big|^{\sqrt{2+n}(3+n-3w_a-nw_b)+\sqrt{3n}(2+n)(w_a-w_b)} \cdot \\ &\Big|\underbrace{\frac{H_a}{H_b}+\frac{3n-\sqrt{3n}\sqrt{2+n}}{6}}_{K2 \text{ part}}\Big|^{\sqrt{2+n}(3+n-3w_a-nw_b)-\sqrt{3n}(2+n)(w_a-w_b)} \cdot \\ &\Big|\underbrace{\frac{(n-1)w_a-nw_b+1}{3w_a-2w_b-1}+\frac{H_a}{H_b}}_{K3 \text{ part}}\Big|^{-\sqrt{2+n}\left(3-3w_a^2+n(1+3w_a^2-6w_aw_b+2w_b^2)\right)} \end{aligned}$$

Κατά την παραγωγή αυτής της γενικής λύσης, οι ειδικές λύσεις $K1$, $K2$, και $K3$ στη μορφή:

$$H_b - c_i H_a = 0$$

εμφανίζονται σε παρονομαστές και επομένως από αυτό προκύπτουν αντίστοιχοι περιορισμοί. Συνεπακόλουθα, στο χώρο των φάσεων H_a, $H_b(H_a)$, οι αντίστοιχες καμπύλες θα εμφανίζονται ως "σύνορα" μιας οποιασδήποτε καμπύλης αντιστοιχεί στη γενική λύση. Οι καμπύλες που αντιστοιχούν στις $K1$, $K2$ δεν εξαρτώνται από τα w και άρα είναι ίδιες για όλες τις περιπτώσεις, αντίθετα με την $K3$, για την οποία θα δείξουμε ότι αποτελεί ρυθμιστή της γενικής λύσης στις κοσμολογικά αξιόλογες περιπτώσεις.

Μελετάμε τώρα ασυμπτωτικά τη γενική λύση. Στην πρώτη περίπτωση: H_a, $|H_b| \to \infty$. Αν $H_a>0$ τότε αντιστοιχεί στην περίπτωση ενός σύμπαντος κοντά στην ανωμαλία του. Αντίστοιχα, η περίπτωση H_a, $|H_b| \to 0$ περιγράφει την ασυμπτωτική συμπεριφορά ενός σύμπαντος που οδεύει προς μια

φάση "ισορροπίας", και μάλιστα αυτή είναι η μόνη περίπτωση που μας χρειάζεται να ταιριάξουμε με την καθιερωμένη κοσμολογική εξέλιξη. Περιπτώσεις όπως η $H_a/H_b \not\to c$ δεν είναι δυνατές. Για παράδειγμα, αν $H_a \gg H_b$, $H_a/H_b \not\to c$, καταλήγουμε στη μορφή $const. = |H_b| \cdots |\frac{H_a}{H_b}| \cdots$, οπότε $|H_b| H_a^x = const.$. Με αντικατάσταση στις δυναμικές εξισώσεις παρατηρούμε ότι μια μη τετριμμένη λύση σε αυτή την περίπτωση είναι αδύνατο να υπάρχει. Επομένως, σε κάθε περίπτωση, κάποια από τις λύσεις $K1$, $K2$ και $K3$ θα έλκουν τη φασική καμπύλη κάθε άλλης λύσης.

Ο παράγοντας που καθορίζει το πως οι παραπάνω ασυμπτωτικές συμπεριφορές επιτυγχάνονται, έχει βεβαίως να κάνει με το πρόσημο των εκθετών των $K1$, $K2$, $K3$ στη γενική λύση καθώς και τη θέσης των αρχικών συνθηκών σε σχέση με τις $K1$, $K2$, $K3$. Με βάση αυτά, το ζεύγος (H_a, H_b) καταλήγει σε κάποιο από τα εξής σενάρια: $(0,0)$, $(\pm\infty, \pm\infty)$ (και $(0, \pm\infty)$ αν $n = 1$).

Ως παράδειγμα, θα εργαστούμε στην περίπτωση $n = 1$, όπου η $K2$ καταλήγει στην τετριμμένη $H_a = 0$:

$$const. = \Big| \underbrace{H_b}_{H_b \text{ part}} \Big|^{2\sqrt{3}(3w_a - w_b - 2)(w_b - 1)} \cdot \Big| \underbrace{\frac{H_a}{H_b} + 1}_{K1 \text{ part}} \Big|^{\sqrt{3}(4 - 3w_a - w_b) + 3\sqrt{3}(w_a - w_b)} \cdot$$

$$\Big| \underbrace{\frac{H_a}{H_b}}_{K2 \text{ part}} \Big|^{\sqrt{3}(4 - 3w_a - w_b) - 3\sqrt{3}(w_a - w_b)} \cdot \Big| \underbrace{\frac{1 - w_b}{3w_a - 2w_b - 1} + \frac{H_a}{H_b}}_{K3 \text{ part}} \Big|^{-\sqrt{3}(4 - 6w_a w_b + 2w_b^2)}$$

Οι περιοχές όπου οι εκθέτες έχουν συγκεκριμένα πρόσημα φαίνονται στο διάγραμμα της Εικόνας 3.1, σελ.58, ως συνάρτηση των w. Η περιοχή με σημασία για την Κοσμολογία είναι η περιοχή 2, που συμπεριλαμβάνει το δεσμό $1 - 3w_a + 2w_b = 0$, που είναι απαραίτητος για να ανακτήσουμε τα αποτελέσματα της Καθιερωμένης Κοσμολογίας. Ας δουλέψουμε για παράδειγμα με την περίπτωση $H_a/H_b \to const$, με H_a, $H_b \to 0$. Επιλέγοντας w στην περιοχή 2 της Εικόνας 3.1, το H_b μέρος της γενικής λύσης για $n = 1$ τείνει στο 0, γιατί υψώνεται σε θετικό εκθέτη. Επομένως, τουλάχιστον ένας από τους υπόλοιπους όρους πρέπει να τείνει στο άπειρο, ώστε το γινόμενο της γενικής λύσης να βγαίνει ίσο με μια σταθερά.

Υποθέτοντας ότι επιλέγουμε κατάλληλες αρχικές συνθήκες, (ανάμεσα στις $K1$ και $K3$ εδώ), αυτό μπορεί να συμβεί ασυμπτωτικά μόνο στην περίπτωση $H_a/H_b \to 1/c_3$. Σε αυτή την περίπτωση η βάση του όρου $K3$ τείνει στο 0, και είναι υψωμένη σε αρνητικό εκθέτη, οπότε αποκλίνει στο άπειρο. Από την άλλη πλευρά, αν $H_a/H_b \to const$ με H_a, $H_b \to \infty$, ο μόνος τρόπος να είναι συνεπής η γενική λύση με w στην περιοχή 2, είναι αν το $K1$ μέρος τείνει στο 0 (γιατί $H_a/H_b \to 1/c_1$), εξουδετερώνοντας το H_b μέρος που τώρα αποκλίνει στο άπειρο.

Άρα για όλα τα ζεύγη αρχικών συνθηκών ανάμεσα στις $K1$ και $K3$, και τιμές των w στην περιοχή 2 η λύση θα καταλήγει ασυμπτωτικά στον ελκυστή $K3$, καθώς H_a, $H_b \to 0$. Αν η αντίστοιχη λύση $K3$ έχει συγκεκριμένες ιδιότητες, τις ίδιες θα έχει, εν καιρώ, και η οποιαδήποτε γενική λύση.

Μια επίδειξη αυτού του γεγονότος γίνεται στην Εικόνα 3.2, σελ. 59, όπου έχουμε επιλέξει w με τα παραπάνω στοιχεία κατά νου. Έχουμε κατασκευάσει τις φασικές καμπύλες για 4 διαφορετικές περιπτώσεις αρχικών συνθηκών, και τις συγκρίνουμε με τις ειδικές λύσεις. Όλες, συγκλίνουν προς την αντίστοιχη $K3$.

Θα μελετήσουμε τους δεσμούς που πρέπει να ισχύουν για να μπορεί να διατυπωθεί ένα κοσμολογικό μοντέλο που είναι βιώσιμο, καθώς πρέπει να διαφυλάσσονται πολλά από τα αποτελέσματα της Καθιερωμένης Κοσμολογίας που είναι συνεπή με τις παρατηρήσεις, όπως η Νουκλεοσύνθεση και η μη παρατήρηση επιπλέον χωρικών διαστάσεων. Οδηγούμαστε λοιπόν σε δύο ιδιότητες που πρέπει να έχουμε κατά νου: μια πρωταρχική σμίκρυνση των επιπλέον διαστάσεων (ή ένα πρωταρχικό ξεδίπλωμα των συνήθων διαστάσεων) έτσι ώστε ο εσωτερικός χώρος να είναι μη παρατηρήσιμος, και μια επακόλουθη σταθεροποίηση της εξέλιξης των εσωτερικών διαστάσεων ($H_b \approx 0$), από τουλάχιστον την εποχή της Νουκλεοσύνθεσης, καθώς οι θεμελιώδεις σταθερές ζεύξης είναι αντιστρόφως ανάλογες του $b(t)$. Σε αντίθετη περίπτωση η αλλαγή στην τιμή τους, θα ήταν ανιχνεύσιμη σε αντικείμενα υψηλής ερυθρομετατόπισης και πειράματα. Μια σχέση που οδηγεί σε μια ακριβή σταθεροποίηση του εσωτερικού χώρου, προκύπτει από τις δυναμικές εξισώσεις, όπου για να μην παρουσιάζει εξέλιξη η εξίσωση του $\dot{H}_b$, πρέπει να ισχύει:

$$1 - 3w_a + 2w_b = 0 \ .$$

Μπορούμε βεβαίως να επιτρέψουμε και μια εξαιρετικά αργή εξέλιξη του εσωτερικού χώρου. Αν οι παράμετροι w_a, w_b είναι τέτοιες ώστε να παράγεται μια αντίστοιχη λύση $K3$ με πολύ μικρό λόγο H_b/H_a, τότε η διαφοροποίηση στις σταθερές ζεύξης θα μπορούσε να είναι μη ανιχνεύσιμη. Οι περιορισμοί που προκύπτουν στη βιβλιογραφία και επιτρέπουν μια πολύ αργή εξέλιξη του εσωτερικού χώρου

ποσοτικοποιούνται ως εξής:

$$|H_b^{(0)}| < \frac{1}{10n} H_a^{(0)} \ , \quad \frac{|b_{BBN} - b_{today}|}{b} \approx 1\% \ .$$

Επιπλέον, θέλουμε η εξέλιξη της παραμέτρου Hubble H_a να συμφωνεί με τις παρατηρήσεις.

Η δράση της λύσης $K3$ ως ελκυστή για όλες τις υπόλοιπες, μας διευκολύνει πολύ στην κατασκευή τέτοιων μοντέλων, ενώ δεν αντιμετωπίζουμε προβλήματα fine-tuning. Θέλουμε να έχουμε έναν πολύ μικρό λόγο H_b/H_a που συσχετίζει και την εξέλιξη των παραμέτρων w:

$$\text{apparent Stabilization} \Rightarrow \Big(\frac{H_b}{H_a}\Big)^{(K3)}_{\text{D. Energy era}} \approx \Big(\frac{H_b}{H_a}\Big)^{(K3)}_{\text{Mat. Dom.}} \approx \Big(\frac{H_b}{H_a}\Big)^{(K3)}_{\text{Rad. Dom.}}$$

Επομένως, καταλαβαίνει κανείς, ότι για να σταθεροποιηθεί ο εσωτερικός χώρος από την εποχή κυριαρχίας της ύλης και έπειτα, πρέπει η παράμετρος w_b να παίρνει "εξωτικές" τιμές, με αρνητική πίεση, οπότε κανείς θα χρειαστεί να καταφύγει σε αντίστοιχα σενάρια (phantom energy) ή πιο θεμελιώδεις θεωρίες (string theory) που εμπεριέχουν τέτοιες περιπτώσεις.

Τέλος, σημειώνουμε ότι αφού οι $K1$, $K2$ και $K3$ λειτουργούν ως ελκυστές, πρέπει να μελετηθούν και διαταρακτικά, ώστε να γνωρίζουμε το αν είναι σταθερές. Για την $K3$, που μας ενδιαφέρει περισσότερο, έχουμε:

$$H_a(t) = H_a^{K3}(t) + H_a^{per}(t), \qquad H_b(t) = H_b^{K3}(t) + H_b^{per}(t)$$

και προκύπτει

$$H_a^{per}, H_b^{per} \propto t^{\frac{-4+3w_a+w_b}{2-3w_a w_b+w_b^2}}$$

οπότε όλες οι κοσμολογικά αξιοσημείωτες περιπτώσεις είναι σταθερές, γιατί στην περιοχή 2, ο εκθέτης του t είναι αρνητικός. Αντίστοιχα για τις $K1$ και $K2$:

$$H_a^{per}, H_b^{per} \propto t^{-w_b}$$

Για να κατασκευάσουμε ένα μοντέλο που περιγράφει όλη την εξέλιξη του Σύμπαντος, θα χρησιμοποιήσουμε μεταβάσεις ανάμεσα στις διάφορες τιμές των w, σε κάθε εποχή, που σέβονται τις παραπάνω απαιτήσεις. Για τα παρατηρησιακά δεδομένα που θέλουμε να ικανοποιήσουμε θα χρησιμοποιήσουμε τις προσεγγιστικές τιμές:

$$H_0 \approx 70 \frac{km/s}{Mpc} \ , \ q_0 \approx -0.6 \ ,$$

ενώ θα διαφυλάξουμε την εξέλιξη του παράγοντα κλίμακας του συνήθους χώρου για την κυριαρχία της ακτινοβολίας και της ύλης ($t^{1/2}$ και $t^{2/3}$ αντίστοιχα). Όμως, οι παρατηρήσεις, πρέπει να ταιριάξουν με τις ενεργές τιμές, από 4-διάστατης σκοπιάς, και όχι με τις τιμές που έχουμε παρουσιάσει παραπάνω. Χρειαζόμαστε λοιπόν, τις ενεργές τιμές, που προκύπτουν μετά τη διαστατική μείωση της δράσης.

Ένας συνήθης τρόπος να γίνει αυτό είναι να έρθει η δράση σε κατάλληλη μορφή μέσω ενός μετασχηματισμού Weyl. Σε αυτή την περίπτωση ο παράγοντας κλίμακας γίνεται αντιληπτός από 4-διάστατης σκοπιάς, σαν ένα βαθμωτό πεδίο σε δυναμικό. Ο μετασχηματισμός Weyl αλλάζει το χρόνο και τον παράγοντα $a(t)$. Ένας τετραδιάστατος παρατηρητής θα αντιλαμβανόταν λοιπόν:

$$t_{eff} = \int b^{n/2}(t)dt + const \equiv g(t) \rightarrow \ t = g^{(-1)}(t_{eff})$$

$$a_{eff}(t_{eff}) = b^{n/2}\big(g^{(-1)}(t_{eff})\big) a\big(g^{(-1)}(t_{eff})\big)$$

Παρατηρεί κανείς ότι αυτές οι διορθώσεις είναι σημαντικές, μόνο αν ο εσωτερικός χώρος δεν είναι σταθεροποιημένος, κάτι που δε μας απασχολεί εδώ.

Κατασκευάζοντας τελικά το μοντέλο μας, θα επιβάλουμε, λοιπόν, τους δεσμούς που αναφέραμε, στη λύση $K3$. Για παράδειγμα, από την Εικόνα 3.3, σελ. 61, βρίσκουμε την περιοχή από την οποία μπορούμε να επιλέξουμε τα w με βάση τους παραπάνω δεσμούς (κόκκινη τριγωνική περιοχή) εν αντιθέσει με το δεσμό για ακριβή σταθεροποίηση (διακεκομμένη γραμμή). Επιπλέον, παρουσιάζουμε 3 περιοχές των παραμέτρων w που αντιστοιχούν σε 3 διαφορετικές τιμές της παραμέτρου q_{K3}. Ο συνδυασμός τους μας αναγκάζει να επιλέξουμε από συγκεκριμένη περιοχή, αφού επιθυμούμε σταθεροποίηση του εσωτερικού χώρου και σημερινή τιμή $q \approx -0.6$. Τέλος, έχουμε ενσωματώσει μια μετάβαση στις τιμές των w

που μοντελοποιεί το πέρασμα από επιβραδυνόμενη σε επιταχυνόμενη διαστολή του Σύμπαντος, όταν η ερυθρομετατόπιση ήταν $z \approx 1-2$, ενώ η εξέλιξη του $b(t)$, είναι αρκετά αργή ώστε να είναι σύμφωνη με τους παραπάνω δεσμούς.

Στην Εικόνα 3.4, σελ. 64, απεικονίζεται η εξέλιξη της παραμέτρου H_a αυτού του μοντέλου, σε σχέση με αυτή που προβλέπεται από το ΛCDM, καθώς και η εξέλιξη του παράγοντα κλίμακας σε σχέση με την αναμενόμενη εξέλιξή του, σε εποχή κυριαρχίας της ύλης. Αν ο παράγοντας κλίμακας $b(t)$ δεν ήταν σταθεροποιημένος, η εξέλιξη αυτή δε θα ήταν ίδια, ανεξάρτητα από την επιλογή της παραμέτρου $w_a = 0$ για την εποχή αυτή. Το ίδιο ισχύει και για την εποχή κυριαρχίας της ακτινοβολίας αλλά και για την εποχή της Σκοτεινής Ενέργειας.

Στην Εικόνα 3.5, 64, βλέπουμε την εξέλιξη των παραγόντων κλίμακας με βάση το μοντέλο, οι οποίοι είναι κανονικοποιημένοι ώστε $a(0) = b(0) = 1$. Τέλος, στην Εικόνα 3.6, σελ. 64, απεικονίζονται η παράμετρος επιβράδυνσης του μοντέλου, αλλά και μια απευθείας σύγκριση με τις παρατηρήσεις, μέσω της καμπύλης $m(z) - M$ σε σχέση με 580 supernova τύπου SNIa.

Τέλος, θα αναφερθούμε σε μια ενδιαφέρουσα ιδιότητα σχετικά με τους παράγοντες κλίμακας $a(t), b(t)$. Οι λύσεις $K1$, $K2$ δεν ικανοποιούν καμία συνθήκη σταθεροποίησης, αλλά δε συμβαίνει το ίδιο και με τη λύση $K3$, όπως για παράδειγμα δείχνουμε εδώ, στην περίπτωση όπου $n = 2$. Οι παράγοντες κλίμακας παίρνουν τη μορφή:

$$\left.\begin{aligned} a(t) &= \tilde{c_1}\left|2(1+w_a-2w_b)+(5+3w_a^2-12w_aw_b+4w_b^2)H_a(0)t\right|^{\frac{2+2w_a-4w_b}{5+3w_a^2-12w_aw_b+4w_b^2}} \\ b(t) &= \tilde{c_2}\left|2(1+w_a-2w_b)+(5+3w_a^2-12w_aw_b+4w_b^2)H_a(0)t\right|^{\frac{2-6w_a+4w_b}{5+3w_a^2-12w_aw_b+4w_b^2}} \end{aligned}\right\} \quad \text{K3}$$

Παρατηρεί, μεταξύ άλλων, κανείς, ότι αν $w_a = -1$ και $w_b = -2$, οι παρονομαστές και των δύο εκθετών, αλλά και ο αριθμητής του παράγοντα $b(t)$ μηδενίζονται. Επιπλέον, ο εκθέτης του $a(t)$ είναι θετικός στις περιοχές 2 και 3 της Εικόνας 3.1, ενώ ο εκθέτης του $b(t)$ είναι θετικός μόνο στο κομμάτι της περιοχής 2 που βρίσκεται αριστερά από τη διακεκομμένη γραμμή. Επομένως, ανάλογα με τον τρόπο προσέγγισης των τιμών παραπάνω, είναι δυνατή μια πολύ θετική τιμή του εκθέτη του $a(t)$ και μια πολύ αρνητική τιμή για τον εκθέτη του $b(t)$. Όμως, από τον τρόπο προσέγγισης εξαρτάται και η σταθερότητα της λύσης σε διαταραχές. Μια μικρή διαταραχή των w, μπορεί να αλλάξει δραστικά τη συμπεριφορά των παραγόντων κλίμακας.

Στην Εικόνα 3.7, σελ. 66, φαίνεται η συμπεριφορά των φασικών καμπυλών για διάφορες τιμές στις περιοχές 1 και 2 του διαγράμματος 3.1, για μια περίπτωση με $n = 1$. Από εκεί μπορεί κανείς να παρατηρήσει τη συμπεριφορά μιας τυχαίας γενικής λύσης, ποιοτικά και πράγματι φαίνεται η μεγάλη διαφορά στις πιθανές εξελίξεις, ανάλογα με την επιλογή των αρχικών συνθηκών ανάμεσα στις ειδικές λύσεις $K1$, $K2$ και $K3$. Ποιοτικά, η συμπεριφορά αυτή είναι ίδια για οποιαδήποτε τιμή του n.

Συνοψίζοντας, προσπαθήσαμε σε αυτή την ενότητα της διατριβής να παρουσιάσουμε το πως η συμπερίληψη ομογενών έξτρα διαστάσεων, θα μπορούσαν να επηρεάσουν την κοσμολογική εξέλιξη. Δείξαμε ότι είναι δυνατό να παραχθεί μια εικόνα παρόμοια με αυτή του ΛCDM, σε αυτό το πλαίσιο, μόνο αν οι επιπλέον διαστάσεις είναι σταθεροποιημένες από πολύ νωρίς στην εξέλιξή του. Επιπλέον, σε ύστερα στάδια αυτής της εξέλιξης είναι απαραίτητο να θεωρήσει κανείς ότι το κοσμικό ρευστό των επιπλέον διαστάσεων, έχει την εξωτική ιδιότητα της αρνητικής πίεσης, που ενδεχομένως προκύπτει από μια πιο θεμελιώδη θεωρία, όπως η Θεωρία Χορδών.

Κατασκευάσαμε ένα τέτοιο μοντέλο, εντός των παρατηρησιακών ορίων, διατηρώντας μια πολύ αργή, μη παρατηρήσιμη εξέλιξη για τον παράγοντα κλίμακας των επιπλέον διαστάσεων. Έχοντας κατορθώσει να βρούμε τις ειδικές και τη γενική λύση του συστήματος σε αναλυτική μορφή, κατορθώσαμε να χτίσουμε αυτό το μοντέλο, αξιοποιώντας το γεγονός ότι, όπως αποδείχθηκε, η λύση $K3$, λειτουργεί ως ελκυστής για όλες τις κοσμολογικά αξιοσημείωτες περιπτώσεις. Επομένως, αναγκάζοντας τη λύση $K3$ να συμπεριφέρεται με συκγκεριμένο τρόπο, εξαναγκάζουμε μια τεράστια ποικιλία από αρχικές συνθήκες να καταλήξουν να συμπεριφέρονται με τον ίδιο, αποδεκτό, τρόπο.

Τέλος, εξετάσαμε πως συμπεριφέρονται οι παράγοντες κλίμακας όταν μια λύση αυτού του συστήματος βρίσκεται κοντά στην ανωμαλία της, σα συνάρτηση των παραμέτρων w. Υπάρχουν συνδυασμοί των καταστατικών παραμέτρων που παράγουν μια πολύ γρήγορη διαστολή του συνήθους χώρου και μια αντίστοιχα γρήγορη συστολή του εσωτερικού χώρου, αν και αυτές οι επιλογές είναι και πάλι εξωτικής φύσης. Επιπλέον, αυτές οι τιμές βρίσκονται στο σύνορο μιας περιοχής του χώρου των w εκατέρωθεν του οποίου οι παραγόμενες εξελίξεις είναι πολύ διαφορετικές. Επομένως, μια μικρή διαταραχή στην τιμή των w θα μπορούσε να πυροδοτήσει μια τόσο διαφορετική εξέλιξη για το συνήθη και τον εσωτερικό χώρο.

Chapter 0

Introduction

0.1 A brief History of General Relativity and Cosmology

Einstein's *General Theory of Relativity* (GR), set the foundation for the study of Gravity and spacetime as we understand it today. According to GR, there exist solutions of the field equations of gravity that describe a universe that expands or contracts. These solutions were first found by Friedmann in 1922, and a few years later, Hubble was the first to prove that the Universe was indeed expanding.

Moreover, nucleosynthesis, studied by Gamow in 1946, demands that the Universe must have started from a very hot and dense initial state, in order to explain current abundances of the various particles and elements. This, in turn, implies that a background microwave radiation would remain as a thermal relic of this initial state. In fact, two decades later, *Cosmic Microwave Background Radiation* (CMBR) was detected by Penzias and Wilson. These successes, lead to what is nowadays called *The Big Bang Theory* (BB), according to which the Universe started from a very hot and dense initial state.

Despite these accomplishments, alternatives have been proposed since the early days of GR, trying to generalize and incorporate it in a broader unified theory. Some notable examples are Weyl's scale independent theory and Kaluza and Klein's theory that included a larger number of dimensions. Another particularly important example of an effort to generalize GR was that of Dirac, who noted that the magnitude of Newton's constant and the ratio of the mass and scale of the Universe are related. This, in turn, sparked the thought that Newton's constant might actually be time-dependent.

Building upon this idea, Brans and Dicke developed, during the 1960s, the first of the theories that are now known as scalar tensor theories, i.e. theories that include a scalar field, and its interactions, in the study of the dynamics of the Universe. Theories including a scalar field coupled to gravity were, since then, thoroughly investigated in various frameworks. A systematic approach to them was performed by Horndeski in 1974, who was able to produce the most general, non-degenerate, Lagrangian, describing the dynamics of a scalar field coupled with gravity, that leads to non-problematic dynamical equations. The Horndeski theory has since then been built upon and stands to be among the most prominent modifications to Standard GR.

There have also been completely different approaches to modifying GR. Sakharov pointed out that the Einstein-Hilbert action is actually only a first approximation to a more elaborate action, that includes higher order terms that can be important in various epochs or aspects of the Universe's life. A prime example among them is Starobinsky's R^2 theory with significant consequences in Cosmology.

However, after more than one century, GR remains completely unchanged and is still our best description of how Gravity works on large scales, even though the model of the Universe's evolution

resulting directly from GR is inadequate in quite a few ways. Observations show that a huge part of the Universe's contents is of dark nature. According to GR, if the only type of gravitationally interacting content of the Universe is the visible baryonic matter, then *Large Scale Structures* (LSS), including galaxies, clusters etc, would not exist as we know them. Hence, these formations are thought to consist not only of visible, but also of *Dark Matter* (DM). This type of matter is thought to interact only gravitationally and thus creates the LSS without being directly observable.

An arguably even more peculiar observation, is that of the accelerated expansion of the Universe. Near the end of the 20th century, observations of high redshift objects have shown that the Universe has transitioned from a period of decelerating expansion to a period of accelerating expansion, a fact that goes far beyond the predictions of GR. This is commonly attributed to yet another exotic content of the Universe that is still of unknown nature and referred to as *Dark Energy* (DE).

Besides these unknown contents of the Universe, there also exist significant problems regarding the birthing states of its life. Indeed, BB theory suffers from a series of problems which require a modification of the dynamics of the very early Universe. These consist of the problem of the horizon, the flatness problem and the problem of the unwanted relics. Hence, the BB theory needs, at the very least, to be accompanied by a theory that solves these issues.

To solve them, it was proposed by Guth in 1981 that there took place an era during which the Universe underwent a dramatic expansion of its size. This scenario is dubbed *inflation*, and it is usually considered that it was realized due to the dynamics of a scalar particle called inflaton. The dynamics of such a modification can, then, be studied within the framework of Horndeski theory, yielding a very rich phenomenology, that can be put to test against observations.

In light of the above, it is understandable that there is a huge variety of theories modifying GR. Hence, testing gravity, in order to distinguish between the various possible modifications has become a centerpiece in modern and future cosmological experiments. This effort is aided by the advances in what is called precision Cosmology experiments. A prime example among them is the Planck collaboration, and perhaps more importantly the recent discovery of Gravitational Waves (GWs) [1]. The prominence of such an observation was shown immediately, since the observation of GW2017 was enough to put a severe constraint on the speed of GWs and thus discard a large number of theories that modified GR [2].

0.2 The Standard Cosmological Model

As a theory of gravity, General Relativity is capable of producing a self-sufficient cosmological scheme within which, one, can further elaborate and test various modifications to it. In this part of the present thesis we present the basic concepts of Cosmology as obtained by unmodified GR.

0.2.1 The Cosmological Principle

In order to build a cosmological model, one has to first describe the geometry of the spacetime under study. While there is no definitive observational or theoretical proof, it is generally accepted that in large enough distances[1], the Universe is homogeneous and isotropic. This assumption, referred to as the *Cosmological Principle*, is backed by a large number of observational results. Arguably, the most prominent observation among them, is the CMBR's temperature, that is nearly the same regardless of the direction observed.

This apparent homogeneity in the CMBR's temperature is of course consistent with a homogeneous and isotropic Universe. The inhomogeneities observed in smaller scales are not in contrast with that, and in fact are expected to exist, emerging when one performs a perturbative study. If

[1] As "large enough distances" in this context, it is usually accepted, and backed by observations, that it is enough to look beyond the radius of average superclusters. This translates to distances of around 100 Mpc.

one, then, wants to study the evolution of a 4-D spacetime of a homogenous and isotropic Universe, a metric that describes a 4-D space-time with a maximally symmetric 3-D subspace is needed.

The homogeneous and isotropic metric[2] can be deduced, then, to be:

$$ds^2 = g_{\mu\nu}dx^\mu dx^\nu = -dt^2 + a^2(t)\left[\frac{dr^2}{1-Kr^2} + r^2(d\theta^2 + sin^2\theta d\phi^2)\right] \tag{1}$$

where t is the cosmic time and $a(t)$ is the scale factor, while K defines the intrinsic curvature of the space under study. This is measured to be significantly close to 0, posing one of the first questions that need to be answered by a theory that modifies Cosmology obtained through GR. Eq. (1) is generally known as the Friedmann-Lemaitre-Robertson-Walker (FLRW) metric.

0.2.2 Cosmological Redshift and Hubble parameter

A measure of whether the Universe expands, contracts or remains unchanged is the scale factor $a(t)$. However, the FLRW metric itself is not enough to indicate which one of these cases is true, and observations need to be carried out. To quantify the evolution of the Universe we define the Hubble parameter:

$$H(t) = \frac{\dot{a}(t)}{a(t)} \tag{2}$$

The sign of the Hubble parameter dictates whether the Universe expands or contracts. We further define a parameter to quantify whether the evolution is accelerating or decelerating. This parameter is, for historic reasons, defined to be negative when the Universe is accelerating, and is given by:

$$q = -\frac{\ddot{a}(t)a(t)}{\dot{a}^2(t)} \tag{3}$$

By calculating the frequency shift in light rays coming to terrestrial and space laboratories we can deduce the behavior of the Universe's evolution. To be able to calculate whether the Universe is expanding or contracting, we need to define a comoving coordinate system. A point is said to belong to this comoving system, when it is moving along with the expansion or contraction of the Universe.

If we suppose that we are at the origin of the said coordinate system in a spacetime described by the FLRW metric, we can carry out the said calculation as follows: A light ray moves on a null geodesic, $dr^2 = 0$, so by use of eq. (1) we obtain

$$dt = \pm a(t)\frac{dr}{\sqrt{1-Kr^2}} \tag{4}$$

Supposing that a light ray is coming towards us, then r should be a decreasing function of cosmic time, t, hence we have to choose the minus sign. If the light starts its journey at the coordinate value r_s, at time t_s, then it will arrive to us ($r = 0$) at a later time, t_0[3]. We have then:

$$\int_{t_s}^{t_0}\frac{dt}{a(t)} = \int_0^{r_s}\frac{dr}{\sqrt{1-Kr^2}} \tag{5}$$

For two consecutive light signals that leave the source with a time difference δt_s and reach the origin with a time difference δt_0, we then reason as follows to define what is called the red shift parameter, z: coordinate r is time independent, and $a(t)$'s change between the two consecutive light signals

[2]The sign convention used throughout is (-,+,+,+).

[3]The usual convention for the subscripts in Cosmology is to denote present time with 0.

is very small. Hence, if we use eq. (5) one time for each light signal and then subtract the two relations, we obtain:

$$\frac{\delta t_0}{R(t_0)} = \frac{\delta t_s}{R(t_s)} \tag{6}$$

Supposing that the two light signals are actually two subsequent wave crests, then the corresponding frequencies are $f_s = 1/\delta t_s$ and $f_0 = 1/\delta t_0$, leading to:

$$\frac{f_s}{f_0} = \frac{a(t_0)}{a(t_s)} \tag{7}$$

We define this fraction as the redshift parameter, which for conventional reasons is expressed as:

$$1 + z = \frac{a(t_0)}{a(t_s)} \tag{8}$$

If $a(t)$ increases then the light signal is redshifted, whereas the opposite happens if it decreases. Hence, if we know the distance between the origin and the light source, we can thus determine whether the proper distance between them increases or decreases with time and, thus, deduce if the Universe is expanding or contracting.

Through the Hubble parameter (2), we can also define a number of other useful quantities. We define the *Hubble time* to be H^{-1} and the *Hubble radius* to be cH^{-1}, where c is the speed of light. The Hubble radius is the radius of a sphere beyond which objects recede with superluminal speed. We also define the *particle horizon* which is the maximum distance that light emitted by a particle can have traveled during the age of the Universe.

The current value of the Hubble parameter was calculated by the Planck 2018 [3] collaboration to be: $67,7\ km \cdot s^{-1} \cdot Mpc^{-1}$. However, there do exist tensions regarding the current value of the Hubble parameter. For example Riess et al. [4] have calculated that $H_0 \approx 73.0\ km \cdot s^{-1} \cdot Mpc^{-1}$.

0.2.3 Cosmology in a FLRW background

Having defined the metric (1), that describes the geometry of the Universe at large scales, we can now proceed to study its dynamical evolution. To do that, we use the Einstein field equations

$$G_{\mu\nu} \equiv R_{\mu\nu} - \frac{1}{2} g_{\mu\nu} R = 8\pi G T_{\mu\nu} - \Lambda g_{\mu\nu} \tag{9}$$

$T_{\mu\nu}$ is the energy momentum tensor. Since we model an isotropic and homogeneous Universe, the energy momentum tensor that would correspond to such an ideal fluid, would be of the form

$$T_{\mu\nu} = diag(-\rho, p, p, p)$$

where ρ is the energy density and p is the pressure of the fluid. Λ is a cosmological constant, G is Newton's constant and $R_{\mu\nu}$ is the Ricci tensor, while R is the Ricci scalar. The continuity equation reads

$$\nabla_\mu T^{\mu\nu} = 0$$

which in our case leads to

$$\dot{\rho} = -3H(\rho + p) \tag{10}$$

Standard cosmological evolution, then, revolves around the nature of the contents of the Universe which are quantified through ρ and p. If radiation is the dominant component of the Universe's contents, then $p = \rho/3$. Plugging this in equation (10) we get $\rho_r \approx a^{-4}$. If however, usual matter is the dominant component, then $p = 0$, leading to $\rho_m \approx a^{-3}$.

To obtain, then, the evolution of the scale factor $a(t)$, we have to solve the dynamical equations resulting from (9). Since the fluid under study is isotropic we only need the 0-0 and 1-1 components. These are usually called the Friedmann equations and read, respectively:

$$H^2 = \frac{\rho}{3M_{Pl}^2} + \frac{\Lambda}{3} - \frac{K}{a^2} \tag{11}$$

and

$$3\frac{\ddot{a}}{a} = -4\pi G(\rho + 3p) + \Lambda \tag{12}$$

As we have already mentioned, according to the observations the Universe has a flat geometry, which means that the K parameter can be set to 0. In this case, in a Universe where there is no cosmological constant and radiation dominates, solving the above equations yields $a(t) \approx t^{1/2}$. If on the other hand, matter dominates, the scale factor is proportional to $a(t) \approx t^{2/3}$.

Moreover, equation (11) implies that for any given moment in cosmic time, there exists a critical value of the energy density that satisfies: $\Lambda, K = 0$. In that case:

$$\rho_c = 3M_{Pl}^2 H_0^2 \tag{13}$$

It is useful to define a density parameter:

$$\Omega \equiv \frac{\rho}{\rho_c} \tag{14}$$

By this definition, then, we can express all the components' contributions to the energy density of the Universe. Then, we can, for example, obtain the cosmological constant's density parameter, as $\Omega_\Lambda = \frac{\Lambda}{3M_{Pl}^2 H^2}$. We can now write down the first Friedmann equation as:

$$\Omega + \Omega_\Lambda - 1 = \frac{K}{a^2 H^2} \tag{15}$$

0.2.4 Shortcomings of Standard Cosmology

As we have already mentioned, despite its great successes, Standard Cosmology, resulting from a completely unmodified version of GR, suffers a few shortcomings. We briefly mention them here, before presenting some of the modifications that are followed to ameliorate these problems.

1. *Flatness Problem*: Equation (15) implies that if the Universe is flat, then $\Omega_{tot} = 1$, where Ω_{tot} includes all the possible contributions in it's density. However, we can deduce that if this is true for one moment during its lifetime, then the Universe will be flat at any given moment after that. If this were not the case, then eq. (15), implies that it evolves with time.

   This can be easily seen since the scale factor is a time-dependent function. The exact form of its time evolution depends on the Universe's contents, but for any plausible case, it can be shown that it is an increasing function of cosmic time. However, the combination aH that appears in eq. (15), is a decreasing function of time.

   According to all observations, today's value of Ω_{tot} is exceptionally close to unity. This in turn means that during the birthing stages of the Universe, this value should be extremely close to unity. In fact, it is calculated that close to the Big Bang should hold that:

   $$\Omega_{tot} - 1 < 10^{-64}$$

   It is clear that such a fine tuning of the initial conditions of the Universe is extremely unlikely, posing a question that Standard Cosmology can not adequately answer.

2. *Horizon Problem*: CMBR observations reveal that the Universe seems to be highly isotropic. This implies that regions that are not causally connected look extremely similar, leading to the so called *Horizon problem*. To show this, we consider the distance a photon, that started its journey at a given time t_i, can travel in a given time interval:

$$d_H(t) = a(t) \int_{t_i}^{t} \frac{dt'}{a(t')} \tag{16}$$

So far, we have seen that both in the radiation and the matter domination era, the scale factor follows a power law, $a(t) \propto t^p$, where $p < 1$. We obtain, then:

$$d_H(t) = a(t) \frac{t^{1-p} - t_i^{1-p}}{1-p} \tag{17}$$

leading to

$$d_H(t) = \frac{p}{1-p} H^{-1} \tag{18}$$

when $t_i = 0$. Thus we have shown that the particle horizon has a finite size, which is of the order of magnitude of the Hubble radius H^{-1}. At the same time, the *comoving* Hubble radius, $a(t)H^{-1}$, which represents the fraction of comoving space in causal contact, grows with time. So Standard Cosmology predicts that the fraction of the Universe in causal contact actually increases with time. But according to the CMBR observations, the Universe was of significant homogeneity at the time of the last scattering, on scales that were causally independent at the time. Thus we are not able to justify, within the Standard Cosmology framework, why regions that are not causally connected look so similar.

3. *Unwanted Relics*: So far the Standard Model of Physics arguably points to the fact that in very high energies the four fundamental interactions of nature are unified. This is the so called Grand Unified Theory (GUT) according to which, its symmetries eventually break one by one, leading to a $U(1)$ theory that includes magnetic monopoles, which have not been detected so far. Different approaches, for example through string theories include similarly undetected spin 0 particles, called moduli. The fact that these particles are not detected poses another problem for the Hot Big Bang scenario resulting from unmodified GR.

4. *Dark Matter*: The formation of galaxies and LSS in general, is of gravitational nature. GR, being the most successful gravitational theory, should be able to model the formation of such structures. However, if one takes into account only the baryonic matter that is visible to us, it is not enough to hold together those structures gravitationally. According to GR, then, LSS should not exist at all, if all the matter of the Universe is of baryonic nature.

   Modern cosmological models include, thus, non-baryonic electromagnetically neutral matter, referred to as *Cold Dark Matter* (CDM). Using ΛCDM's cosmological parameters as a benchmark, DM accounts for roughly 27% of the critical density in the Universe and 84 % of the total matter density. The makeup of DM is, as of yet, still largely of unknown nature, since it has to be interacting only gravitationally and have a negligible pressure, in order to solve the problem of the existence of LSS without affecting the rest of the predictions of cosmological models. Its nature has been speculated to be of spectacularly different origins. It ranges from the possible existence of whole galaxies consisting solely of CDM, *Primordially* created *Black Holes* (PBHs), that may survive until today, existent or exotic particles that only interact gravitationally, or even modifications of GR that come into play at distances that are larger than solar, but still not universal, as that would affect the overall evolution of the Universe.

5. *Dark Energy*: Cosmological models that were constructed in the early days of GR, included a cosmological constant, that offered repulsive gravitational energy, that combined with the attracting nature of usual gravity, offered static solutions. However, the development of dynamic cosmological models and the discovery of cosmic expansion, made this cosmological term appear unnecessary, and for the most part of the 20th century, an expanding, homogeneous and isotropic, spatially flat, matter-dominated Universe was adopted as a default, until observations dictated otherwise. Near the end of the 20th century, supernovae surveys produced evidence for accelerating cosmic expansion [5, 6].

   Moreover, CMB evidence leading to the conclusion that the Universe is spatially flat [7, 8] set the case for an accelerating expanse of the Universe on an even firmer base. The scale factor a(t) of a homogeneous and isotropic Universe as dictated by GR, grows at an accelerating rate only if the pressure $p < -\frac{1}{3}\rho$, which is an effect not possessed by any type of usual matter.

   If one includes a cosmological constant, its energy density is $\rho_\Lambda = const$ and its pressure $p_\Lambda = -\rho_\Lambda$. The cosmological constant, then, will drive acceleration if it dominates the total energy density.

   There also exist alternatives to what could drive an accelerating expansion, however, like a modification of GR that comes into play in cosmological scales and is thus undetectable in solar scale. The different scenarios that are related to the accelerated late time expansion of the Universe are collectively called *Dark Energy* (DE) scenarios, regardless of their nature.

As presented so far, Cosmology resulting directly from GR, can not account for a number of observations both in the very early, and in the late stages of the Universe's life. However, a huge number of modifications can be made to improve or replace some aspects of GR Cosmology.

Among the modifications that hold a prominent position in solving all of the early Universe's problems, is *inflation*. Its main idea is to decouple the causal size from the Hubble radius, so that the size of the horizon in the radiation era obtained from standard Cosmology, is larger than the Hubble radius. Any period in the Universe's evolution where the comoving Hubble radius decreases, is a phase of accelerating expansion, and the corresponding condition is $\ddot{a} > 0$.

As mentioned previously paragraph, the current stage of the Universe's life is also that of an accelerating expansion. However, inflation refers to the primordial exponential expansion of the Universe. Equation (12), when $\Lambda = 0$, implies that $\ddot{a} > 0$ which dictates that $p < -\frac{1}{3}\rho$, a feature not possible for regular matter. On the other hand, a large enough cosmological constant can yield $p = -\rho$. However, that would lead to a permanent exponential inflation which is entirely not consistent with the observations for later stages of the Universe's life.

The previous reasoning has led to a large number of different approaches regarding the driving force of an initial inflationary era that can solve the horizon, flatness and unwanted relics problems, without creating other inconsistencies. Perhaps the most well-studied among them, is the inclusion of a scalar field, whose dynamics offer a simple modification to standard Cosmology with a rich phenomenology. The broad spectrum of theories resulting from this, are collectively called Scalar-Tensor theories.

0.3 Inflationary Cosmology with a single minimally coupled scalar field

The first model of inflation is attributed to Alan Guth [9], who proposed a model based on a first order transition from a false vacuum, with non-zero energy density, to a true vacuum with zero energy density. This is usually referred to as *old inflation*. For this model to produce enough e-folds, the nucleation rate has to be particularly small. However, the true vacuum phase, which appears in the shape of bubbles due to quantum tunneling presents an impassable obstacle for this model.

The space that undergoes inflation and separates them, expands too fast, so they never coalesce. A second type of inflationary models, dubbed *new inflation*, was proposed in the works of [10], [11].

The first effort of including a scalar field's dynamics in order to induce an inflationary phase, came about in the form of a field that is minimally coupled to gravity:

$$S = \int d^4x\sqrt{-g}\left[\frac{M_{Pl}^2}{2}R - \frac{1}{2}\partial^\mu\phi\partial_\mu\phi - V(\phi)\right] \tag{19}$$

By varying with respect to the metric, we obtain the contribution of the scalar field to the energy-momentum tensor as follows:

$$T_{\mu\nu} = \partial_\mu\phi\partial_\nu\phi - g_{\mu\nu}\left(\frac{1}{2}\partial^\rho\phi\partial_\rho\phi + V(\phi)\right) \tag{20}$$

The energy density and pressure, then, are:

$$\rho = -T_0^0 = \frac{df^2}{2}\dot{\phi}^2 + V(\phi), \qquad p = \frac{\dot{\phi}^2}{2} - V(\phi) \tag{21}$$

The Klein-Gordon equation of this field is

$$\nabla^\mu\nabla_\mu\phi = \frac{dV}{d\phi} \tag{22}$$

However, since we study the dynamics of this field in a cosmological context, the homogeneity and isotropy imply that a cosmological scalar field is only time dependent, hence the above equation reduces to

$$\ddot{\phi} + 3H\dot{\phi} + V' = 0 \tag{23}$$

while the Friedmann equation is

$$H^2 = \frac{1}{3M_{Pl}^2}\left(\frac{\dot{\phi}^2}{2} + V(\phi)\right) \tag{24}$$

The two dynamical equations (23), (24) generate an accelerated expansion in the so-called *slow roll* regime. For that to take place, the potential energy of the field has to dominate over its kinetic energy.

This is easily shown within the framework of the slow-roll approximation, where the kinetic terms ($\dot{\phi}^2$ and $\ddot{\phi}$) are omitted, since they are negligible with respect to the rest of the terms. We have then:

$$3H\dot{\phi} + V' \approx 0 \tag{25}$$

$$H^2 \approx \frac{1}{3M_{Pl}^2}V \tag{26}$$

Hence, the velocity is:

$$\dot{\phi} \approx -\frac{V}{3H} \tag{27}$$

But since the slow roll regime demands that $\dot{\phi}^2/2 \ll V$, we obtain that it can be quantified by:

$$\epsilon_V \equiv \frac{M_{Pl}^2}{2}\left(\frac{V'}{V}\right)^2 \ll 1 \tag{28}$$

On the same footing, one can obtain another slow roll parameter. Since slow roll also implies $\ddot{\phi} \ll V'$, using the derivative of eq. (25), and eq. (26) we obtain:

$$\eta_V \equiv M_{Pl}^2 \frac{V''}{V} \ll 1 \tag{29}$$

We understand then, that the slow roll approximation is valid when these two quantities are significantly smaller than unity. This translates to certain conditions for the slope and curvature for the potential V.

However, one can use alternative parameters, referred to as the Hubble slow-roll parameters, defined as follows:

$$\epsilon_1 = -\frac{\dot{H}}{H^2}, \qquad \epsilon_{n+1} = \frac{\dot{\epsilon_n}}{H\epsilon_n}, n \geq 1 \tag{30}$$

To quantify the duration of inflation, it is customary to use the *e-folds* before the end of inflation, defined as

$$N = ln\frac{a_{end}}{a} \tag{31}$$

where a_{end} is the scale factor's value at the end of inflation. If inflation is to solve the problems of the BB as presented earlier, it is roughly estimated that about 60 e-folds are needed.

To show this, let us focus on the scenario that only a single transition in the evolutionary phases of the Universe took place (i.e. from inflation to radiation era). Let us consider a given cosmological scale, characterized by its wavenumber $k = 2\pi/\lambda$. We will suppose that this given scale crossed the Hubble radius at a given instant $t_*(k)$, which is characteristic of this scale. Then, at that moment we have:

$$k = a(t_*)H(t_*) \tag{32}$$

Solving BB's problems, requires that the comoving Hubble radius must have decreased during inflation at least the same amount as it increases after it. But during the radiation phase it increases proportionally to a, while during inflation it roughly behaves as a^{-1}.

The temperature of the Universe is, however, inversely proportionate to the scale factor. Then, the minimum amount of inflation is given by the number of e-folds between inflation and today, i.e.

$$ln(a_0/a_{end}) = ln(T_{end}/T_0) \tag{33}$$

Simple models of inflation usually suggest that radiation era started at around $T \approx 10^{16} GeV$. Plugging this in the above equation, yields roughly 60 e-folds.

0.4 Perturbations and Inflationary Phenomenology

We have so far shown the steps of a direct analysis of single field inflationary models in terms of a direct dynamical approach in a homogeneous and isotropic background. The early universe was very nearly uniform due to this primordial inflationary era. However, the attractive nature of gravity intuitively implies that if an inhomogeneity is born, then it will grow. Considering it reversely in time, it means that any inhomogeneity appearing today would have to be much smaller in the past. A picture of these inhomogeneities is the CMB radiation through which we can probe their properties. Then, since inhomogeneities started as microscopic fluctuations, it is safe to assume that for a large part of their evolution, one can study them as linear perturbations of the dynamical quantities.

Current consensus suggests that exactly these primordial fluctuations are the original seeds of structure in the Universe, which over time grew to become all of the structure we observe. When the universe became matter dominated these seeds started growing due to gravitational instabilities (*Jeans instabilities*) thus forming increasingly larger structures. As already mentioned, the presence of primordial inflation-born seeds is observed and confirmed by detailed measurements of the CMBR's anisotropies; temperature anisotropies at angular scales larger than 1° are caused by inflationary inhomogeneities, since causality prevents microphysical processes to produce anisotropies on angular scales larger than 1°, which corresponds to the angular size of the horizon at the era of last-scattering.

These perturbations are generally thought to be of quantum fluctuations' origin. It is remarkable, that although inflation was originally introduced as a possible solution to some of the cosmological problems presented earlier, it possesses another particularly useful property: that it generates spectra of both density perturbations and gravitational waves.

These perturbations can extend from particularly short scales to cosmological scales, due to the stretching of space during inflation. When inflation ends, the Hubble radius increases faster than the scale factor, so the perturbations will eventually reenter the Hubble radius. Perturbations that exit the horizon around 60 e-folds before reheating, reenter it with wavelengths in the range accessible to cosmological observations. The spectra of cosmological perturbations possess distinctive properties, related to the theory of Gravity that is actually at play, and thus should provide a signature for inflation. Cosmological perturbations are measured in a variety of different ways, the most prominent of which, so far is the analysis of CMBR's anisotropies.

Fluctuations of the inflaton field are related to fluctuations of the metric, giving rise to perturbations of the curvature R. The wavelengths of these perturbations grow exponentially and exit the Hubble radius when their wavelength becomes comparable to its size. Upon exiting, curvature perturbations are frozen and can be studied as classical. When inflation ends and the wavelength of these perturbations reenters the horizon, the curvature perturbations give rise to matter and temperature perturbations, which start to grow, and in turn give rise to the structures we observe today.

Therefore, a large part of inflationary phenomenology revolves around the studying of the perturbations of the inflaton field and take up a crucial role in the construction of such models. A detailed presentation on how perturbations are extracted is included in Appendix A. Moreover, their application to single field inflation, is presented in Appendix B, since perturbations in Modified Gravity theories can be utilized to separate various theories from each other, by means of their observables' predictions, hence their study is a basic prerequisite in what is presented in this thesis. We will now present only a brief summary of what is included in *Galileon theory*, i.e. the most general non-degenerate theory of a single scalar field that does not suffer from the Ostrogradsky instability.

0.5 Galileon Theory - Modifying Gravity with a non-minimally coupled scalar field

During the 19th century, it was shown by M. Ostrogradsky [12] that there is a linear instability in the Hamiltonians that are associated with Lagrangians depending on more than one high time derivatives that can not be integrated away. Ostrogradsky's theorem, when applied to physical phenomena, naturally brought forward the need to work within frameworks that guarantee that no instabilities are produced.

In 1974, ref. [13] showed that the most general non-degenerate Lagrangian of a single scalar field

coupled to gravity, that suffers from no instabilities, has to be of the form (34).

$$\begin{aligned}\mathcal{L} = \delta^{\alpha\beta\gamma}_{\mu\nu\sigma}\Big[&\kappa_1\nabla^\mu\nabla_\alpha\phi R_{\beta\gamma}{}^{\nu\sigma} - \frac{4}{3}\kappa_{1,X}\nabla^\mu\nabla_\alpha\phi\nabla^\nu\nabla_\beta\phi\nabla^\sigma\nabla_\gamma\phi + \kappa_3\nabla_\alpha\phi\nabla^\mu\phi R_{\beta\gamma}{}^{\nu\sigma}\\ &-4\kappa_{3,X}\nabla_\alpha\phi\nabla^\mu\phi\nabla^\nu\nabla_\beta\phi\nabla^\sigma\nabla_\gamma\phi\Big] + \delta^{\alpha\beta}_{\mu\nu}\left[(F+2W)R_{\alpha\beta}{}^{\mu\nu} - 4F_{,X}\nabla^\mu\nabla_\alpha\phi\nabla^\nu\nabla_\beta\phi\right.\\ &\left.+2\kappa_8\nabla_\alpha\phi\nabla^\mu\phi\nabla^\nu\nabla_\beta\phi\right] - 3\left[2(F+2W)_{,\phi} + X\kappa_8\right]\nabla_\mu\nabla^\mu\phi + \kappa_9 \end{aligned} \tag{34}$$

This theory depends on four functions of ϕ and $X = -\nabla^\nu\phi\nabla_\nu\phi/2$, κ_i and function $F = F(\phi, X)$, with the constraint:

$$F_{,X} = \kappa_{1,\phi} - \kappa_3 - 2X\kappa_{3,X}$$

This is known as the *Horndeski* Lagrangian and since then, it has been connected to the Galileon theory [14, 15], which we now present.

When a scalar field is symmetric under the transformation

$$\phi \to \phi + b_\mu x^\mu + c$$

it is defined as a *Galileon*. To avoid ghost instabilities, we demand that ϕ's equation of motion is of second order. Restricting ourselves to a Minkowski four dimensional framework, the most general Lagrangian having these properties is given by [16]:

$$\begin{aligned}\mathcal{L} =&c_1\phi + c_2X - c_3X\Box\phi + \frac{c_4}{2}\left\{X\left(\Box\phi\right)^2 - 2\partial_\mu\partial_\nu\phi\partial^\mu\partial^\nu\phi\right] + \Box\phi\partial^\mu\phi\partial^\nu\phi\partial_\mu\partial_\nu\phi - \partial_\mu X\partial^\mu X\right\}\\ &+ \frac{c_5}{15}\left\{-2X\left[(\Box\phi)^3 - 3\Box\phi\partial_\mu\partial_\nu\phi\partial^\mu\partial^\nu\phi + 2\partial_\mu\partial_\nu\phi\partial^\nu\partial^\lambda\phi\partial_\lambda\partial^\mu\phi\right]\right\}\end{aligned} \tag{35}$$

which can be rewritten in the form

$$\begin{aligned}\mathcal{L} =&c_1\phi + c_2X - c_3X\Box\phi + c_4X\left[(\Box\phi)^2 - \partial_\mu\partial_\nu\phi\partial^\mu\partial^\nu\phi\right]\\ &- \frac{c_5}{3}X\left[(\Box\phi)^3 3\Box\phi\partial_\mu\partial_\nu\phi\partial^\mu\partial^\nu\phi + 2\partial_\mu\partial_\nu\phi\partial^\nu\partial^\lambda\phi\partial_\lambda\partial^\mu\phi\right]\end{aligned} \tag{36}$$

The equivalent form of this Lagrangian when gravity is present, is obtained by adding appropriate curvature dependent terms. If this were not the case, the equations of motion would be of higher order and thus lead to instabilities. We have then

$$\begin{aligned}\mathcal{L} =&c_1\phi + c_2X - c_3X\Box\phi + \frac{c_4}{2}X^2R + c_4X\left[(\Box\phi)^2 - \phi^{\mu\nu}\phi_{\mu\nu}\right]\\ &c_5X^2G^{\mu\nu}\phi_{\mu\nu} - \frac{c_5}{3}X\left[(\Box\phi)^3 - 3\Box\phi\phi^{\mu\nu}\phi_{\mu\nu} + 2\phi_{\mu\nu}\phi^{\nu\lambda}\phi^\mu_\lambda\right]\end{aligned} \tag{37}$$

In the above Lagrangian, R is the Ricci scalar, $G_{\mu\nu}$ is the Einstein tensor and we define $\phi_\mu := \nabla_\mu\phi$, $\phi_{\mu\nu} := \nabla_\mu\nabla_\nu\phi$.

Eq. (37) describes what is called the covariant Galileon, since it breaks the shift symmetry introduced in (35) but maintains the property that the EOMs are of second order. This can be further modified to obtain what is called the *Generalized Galileon*, whose Lagrangian is:

$$\begin{aligned}\mathcal{L} =&G_2(\phi, X) - G_3(\phi, X)\Box\phi + G_4(\phi, X)R + G_{4X}\left[(\Box\phi)^2 - \phi^{\mu\nu}\phi_{\mu\nu}\right]\\ &G_5(\phi, X)G^{\mu\nu}\phi_{\mu\nu} - \frac{G_{5X}}{6}\left[(\Box\phi)^3 - 3\Box\phi\phi^{\mu\nu}\phi_{\mu\nu} + 2\phi_{\mu\nu}\phi^{\nu\lambda}\phi^\mu_\lambda\right]\end{aligned} \tag{38}$$

where G_i are arbitrary functions of ϕ and X, while a subscript ϕ or X denotes a differentiation with respect to them. Eq. (38) can be shown to be completely equivalent to the Horndeski theory in 4 dimensions.

Functions G_i can be selected accordingly in order to yield a great variety of theories of Modified Gravity. For example, the standard non-minimal coupling $f(\phi)R$ can be obtained if one chooses $G_4 = f(\phi)$. Moreover, whole classes of theories like the $f(R)$ gravity can be expressed in an equivalent way as second order scalar tensor theories [17, 18], while models with extra dimensions can also be connected to the Galileon theory [19–24].

0.6 Motivation and contents of this thesis

Despite its successful predictions in short and long-distance experiments, scrutinizing every possible aspect of it, GR still remains an incomplete theory, since it is unable to model a variety of behaviors of the Universe, like the already discussed accelerating expansion phase that it is undergoing.

One of the first approaches to solving this particular problem, was the introduction of an ad hoc cosmological constant, offering a new energy density contribution that accounts for this observation. This, of course immediately poses a new question, regarding the origin of this cosmological constant. Furthermore, the necessary energy density to "solve" the accelerating expansion's problem, severely contradicts the value that would arise from microscopic physics constraints. It can be calculated that the necessary value for the cosmological constant's energy density is approximately $\rho_\lambda \approx 6.7 \cdot 10^{-24} g/m^3$, while the corresponding vacuum energy density is approximately $\rho_{Pl} \approx 5 \cdot 10^{99}\ g/m^3$. This enormous difference of 123 orders of magnitude poses a significant obstacle for GR. This, naturally, leads us to look for theories that modify GR, in order to solve this kind of tensions. At the same time, we possess a robust limit to which a modified gravity theory must reduce to, when looking into phenomena that have already been successfully described by GR.

Among all possible modifications to GR, arguably the simplest one is the inclusion of a scalar field in the action, that describes the gravitational dynamics. We have already presented how the Galileon theory gives rise to the most general, non-degenerate, second order equations for a scalar field that is coupled to gravity (see eq. (38)). This theory provides the framework for both small and large distance modifications to GR. Among them, a prominent position is held by the Scalar-Tensor theories that produce inflation, since as already presented, it plays a crucial role in the very early phases of the Universe's evolution. Motivated by that, we are interested in looking further into the specifics of particular Galileon terms and the effect they produce in cosmological evolution.

There has been an extensive effort in understanding the consequences of the inclusion of what is referred to as *non-minimal derivative coupling* (NMDC) [25–27]. This effort has shown a promising change in dynamics, since it effortlessly offers a lengthening in the inflationary era through the *gravitational friction* effect, i.e. the phenomenon according to which the intertwined dynamics of the scalar field that rolls in its potential and the background dynamics affect each other in such a way that the field remains in slow roll for a very long period of time. This ensures that inflation is achieved, without having to resort to large initial field values, as in the case of a minimal and also a non-minimal, but not derivative, coupling. It also seems that NMDC brings forward the fact that a deviation from the speed of GWs is to be expected in derivative coupling theories. However, the recent observation of GWs has strictly constrained their speed rendering late time deviations from a speed $c_{GW} = 1$ invalid. Moreover, when perturbatively studying such models, it has been shown that the squared sound-speed of the perturbations may oscillate violently between positive and negative values, a fact that is closely related to the appearance of instabilities.

Hence, our basic motivation in setting the framework of the first two chapters of this thesis, is the effort to maintain the positive effects of NMDC, while trying to ameliorate or possibly completely solve its problems. Specifically, in Chapter 1 of this thesis, we will focus our study on the G_5 term of eq. (38) which corresponds to this class of theories (i.e. derivative couplings). When G_5 is chosen to be simply proportional to the scalar field

$$G_5 \propto \phi$$

the class of NMDC theories is obtained, as mentioned above. Our focus then revolves around modifying G_5 to include a different dependence on ϕ, so that a richer phenomenology is obtained. The motivation for this, is as follows: in the simple NMDC case, the coupling of the derivative of the scalar field with gravity is the dynamical reason for the wild oscillations of the squared sound-speed of the perturbations. The fact that the NMDC does not include a mechanism of "graceful exit" to GR dynamics after the end of slow roll is the birthing reason of these instabilities (in fact as we show in an explicit comparison example, the oscillations will enhance as the system evolves). However, if

the G_5 term is richer in its ϕ-dependence this phenomenon can be suppressed. We explicitly show this by producing the expression of every cosmological observable and the squared sound-speed, by the standard inflationary perturbation approach, which is extensively presented in Appendices B. We subsequently move on to construct specific models that yield predictions successfully tested against the observational constraints, while at the same time significantly ameliorating the squared sound-speed shortcoming of the NMDC. Finally, we also highlight another aspect of a richer G_5 term: that of the production of Primordial Black Holes (PBHs), without the inclusion of a potential that has an inflection point which produces a super slow roll, as per usual. Instead, a suitable G_5 term will be used that brings forward such a result.

Moving on to Chapter 2, our intention is to explore the idea of combining two different Galileon terms, specifically G_4 and G_5. While G_5 produces the gravitational friction effect, G_4 is the term that in its simplest form, $G_4 \propto \phi^2$ gives rise to models of *non-minimal coupling* (NMC) inflation. These models are known to produce particularly good observationally tested quantities, but are also known to suffer from unitarity issues, in their generic form, since they employ super Planckian field values to achieve them. However, as we show, the combination of these two terms has, for a not necessarily finely tuned scenario, a healing effect on both of the standalone cases' problems, while maintaining their corresponding advantages. In particular, we produce explicit formulas that yield the observables as well as the squared sound-speed of the scenario. There, we show that the inclusion of the NMC term can immediately solve the corresponding problem, and at the same time produce cosmologically viable observables without having to resort to particularly large field values, due to the gravitational friction effect owed to the G_5 term. This work might hint at the possibility that the inclusion of more Galileon terms can solve the individual theories' problem while it does not necessarily imply that a new fine-tuning problem, between these terms, emerges.

Finally in Chapter 3 we turn our attention to late time cosmology, specifically looking into a scenario of a Universe that contains extra dimensions, within the framework of Kaluza-Klein compactifications [4]. The aim is to explore the idea that the observed transition from an era of decelerating to an era of accelerating expansion could be the result of the dynamics of an "internal" space. Our course of action revolves around producing the special and the general analytic solutions for the system of equations that emerges, in the space of the Hubble parameters H_a, H_b of each space. We show the interesting fact that the special solutions of these differential equations act as attractor solutions to any other possible solution of the Hubble parameters. One of these special solutions depends on the equations of state of the fluid that "lives" in each one of the spaces. Hence, if this special solution is obtained for specific equation of state parameters, then one immediately can infer the phase space of initial conditions that would eventually lead to a Universe that expands at an accelerating manner. Special care is taken so that the internal space remains stabilized, i.e. evolves particularly slowly with respect to the 4-d spacetime. If this were not the case in K-K theories, experiments measuring the Newton constant from various epochs of the Universe's life would show a discrepancy between the measured values. We also test such scenarios versus Supernovae type Ia observations, and see that it does indeed produce a viable evolution. Interestingly, such an acceleration does not take place unless an exotic type of matter with a negative pressure exists, which would be the case in Λ-CDM type scenarios too. However, there do exist models that include strings wound around compactified dimensions that produce an effect of negative pressure, hence

[4] It is an interesting fact that Kaluza-Klein compactification theories do indeed have a connection with the Galileon theory. Higher dimensional theories can, in general, be described by Lagrangians that emerge through a process called dimensional reduction. It can be shown then, that usually the effect of the extra dimensional sector would appear to a 4-D observer as extra particles, like Kaluza-Klein towers, or as a scalar field. It is shown in [23,24], that a Kaluza-Klein compactification of a Lovelock theory with higher dimensions can be reduced into a Horndeski action. Within [23], it is shown that the equations resulting after the compactification are at most of second order, both in terms of the scalar field and also in terms of the metric. It is subsequently shown that some of the classes produced, are equivalent to Galileon theories, showcasing the fact that the dimensional reduction of a Lovelock theory can connect the Lovelock invariants to the Galileons. In [24], a Gauss-Bonnet theory is considered and shown that after a dimensional reduction it uniquely produces an effective 4-D Galileon theory.

such a behavior could be justified, within extra-dimensional theories more easily.

Chapter 1

Generalized Non-Minimal Derivative Coupling: Application to Inflation and Primordial Black Hole Production

1.1 Introduction

We have already seen that if one is to try to model the current observational status of Cosmology, the scenario of a Hot Big Bang offers the context for the most successful theory. However, such a description of the early Universe, dictates that a solution to its problems must be found. These problems, essentially boil down to the fact that the Universe would not be of a proper age to justify our observations. Hence, the description of the early universe revolves around finding a compelling explanation for the initial conditions of the hot big bang, within the context of inflation.

In this scenario, an immense accelerating evolution of the Universe takes place. This evolution has to be studied through the gravitational effects that the dynamics of whatever gives rise to inflation, cause. A usual approach, is the inclusion of a scalar field's dynamics. That field is known as the inflaton. With current precise cosmological tests, that recently entail, among others, gravitational waves, can test the inflationary paradigm and also the laws of gravity that hold at very high-density environments.

There is a variety of ways to modify standard GR. One of them is by including extra, higher-order terms that depend on the Ricci scalar. The most prominent among these theories is the one proposed by Starobinsky [28]. Such kind of corrections to the usual action of GR, arise naturally in the gravitational effective action of String Theory [29].

On the other hand, a particularly fruitful modification comes by the inclusion of scalar fields, that are coupled to gravity. This results in what is generally known as scalar-tensor theory [30]. Arguably the best studied context of Scalar-Tensor theories is the one produced by the Horndeski Lagrangian [13], whose modern version is that of the Galileon theory, which was constructed in such a way that these theories are free of ghost instabilities [12]. Furthermore, a variety of scalar-tensor theories possess a classical Galilean symmetry [31–36].

Within the context of Horndeski theory lie all possible, non-degenerate, scalar tensor theories that are free of instabilities. Among other terms, Horndeski incudes what is referred to as the non-minimal derivative coupling of a scalar field to the Einstein tensor (NMDC). This coupling produces a rich phenomenology both on short and long distances [37], which correspond to black

hole physics [38–41] and inflation [42] respectively.

When inflation is the context of interest, the attractive feature of NMDC is that it acts as a friction mechanism. It thus allows steep potentials to implement a slow-roll era [42, 43], offering the grounds for potentials such as Standard Model Higgs, to be realized [25], whereas that is not the case in standard GR. Moreover, there is a theoretical justification to this kind of theories, since inflationary potentials in the NMDC framework can be described in supergravity [44, 45] via what is known as the gauge kinematic function [46]. Thus, NMDC makes a plethora of inflationary predictions investigated in [27] where the dynamics of both the slow-roll phase, and the subsequent reheating phase, were considered.

In fact, NMDC heavily modifies the standard picture of the reheating phase of inflation. Because of it, the inflaton field oscillates rapidly without any significant damping [47–52], thus affecting heavy particle production [53].

However, such oscillations that happen because the NMDC dominates over the canonical kinetic term, are problematic for the post-inflationary system. They lead to oscillations of the squared sound-speed of the scalar perturbations between superluminal and negative values [51, 54]. This leads to scalar perturbations that are exponentially enhanced. The gravity-inflaton system becomes non-linear, and its dynamics are difficult to study analytically, while at the same time invalidating the inflationary predictions of the perturbative approach.

To avoid this instability, the non-minimal kinetic term must become negligible, when compared to the canonical one, during the post inflationary oscillations. But to satisfy such a constraint, means to effectively reduce the model to just a canonical scalar field with Einstein gravity during the inflationary period, losing the gravitational friction effect's advantages. Hence, the use of the simple NMDC version for inflationary model building must be abandoned.

We can, however, continue on the same footing, since the NMDC studied so far is merely a special case of the Galileon term [34, 35]

$$\mathcal{L}_5 = G_5(\phi, X) G^{\mu\nu} \partial_\mu \phi \partial_\nu \phi \tag{1.1}$$

where $X = -\nabla_\mu \phi \nabla^\mu \phi / 2$. Choosing $G_5(\phi, X)$ to be a constant leads to NMDC. If, instead, one chooses a more general function $G_5(\phi, X) = f(\phi)\, \xi(X)$, the phenomenology can potentially become richer, both during inflation and reheating stages. We will refer to this type of scenarios with the term *Generalized Non-Minimal Derivative Coupling* (GNMDC).

Specifically, for $f(\phi) \propto \phi$ the GNMDC term will quickly vanish when the inflaton field reaches the bottom of the potential and, as we shall demonstrate, the system, will transit to the dynamics of a canonical coupling Einstein gravity. Thanks to such a GNMDC, the resulting models turn to being stable in post-inflationary eras, dominated by GR dynamics during the reheating stage. We will examine the phenomenology resulting from such a case, focusing on the *Higgs potential*, which is known to exist in nature [55] but also on other potentials, possibly motivated by physics beyond the Standard Model.

It is also notable that a GNMDC type of modification also passes the recent tight bounds on the speed of gravitational waves [1, 56], which is not the case for NMDC. If a NMDC term plays the role of dark energy, it has been proven [25, 57] that the speed of the tensor perturbations is different from the speed of light. In fact, this measurement constrains deviations up to order of 10^{-15} from the speed of light. Thus, dark energy models that produce $c_{gw} \neq c$ at late times, put very strong bounds on the parameters of NMDC theories [2, 58].

But a ϕ-dependent form of the GNMDC, as considered here, decouples at the end of inflation and so issues related to the speed of GWs should not pose a significant problem[1].

Also, besides the phenomenology strictly related to the expansion of the Universe, a GNMDC term is expected to generate interesting features on the power spectrum of primordial curvature

[1] Other viable subclasses of Horndeski theory have a conformal action, i.e. a function $f(\phi)$ coupled to curvature [59, 60].

perturbations, $\mathcal{P}_R(k)$, at scales that are smaller than the observed CMB scales. The GNMDC's gravitational friction effect, modifies the velocity of the inflaton, influencing the amplitude of the curvature perturbations. It is known, that if the amplification is strong enough, large density perturbations can be generated, which can in turn trigger the production of primordial black holes (PBH). This feature can be particularly attractive, since it does neither resort to multi-field inflation [61], nor to an inflection point in the inflationary potential, that is usually employed [62].

Therefore, we can utilize specific GNMDC forms to construct single field inflationary models that are also able to generate PBHs (for similar works see [63–65]). We will examine explicit GNMDC functions, that dramatically decelerate the inflaton at specific spots of the inflationary trajectory, thus amplifying $\mathcal{P}_R(k)$. One can then estimate suitable values for the various parameters so that a significant abundance of PBHs is produced at potentially interesting PBH mass windows. The GNMDC dominates during the entire stage of inflation and becomes negligible only at the stage of oscillations.

This chapter of the thesis is organized as follows. In Section 1.2 we present the general context of our theory and derive the field equations. In Section 1.3 the basic observables are calculated, namely the power spectrum, the spectral index and the tensor-to-scalar ratio. In Section 1.4 we study viable inflationary models in the framework of GNMDC, emphasizing on the Standard Model Higgs inflation as well as inflation with exponential potentials. In Section 1.5 we aim to determine the observational signatures of the GNMDC with respect to plain GR models. Then, in Sections 1.6, 1.7 we briefly present the basics of PBH cosmology and construct GNMDC models that produce PBHs within Higgs inflation. Finally, in Section 1.8 we summarize our results.

1.2 The Setup - Derivation of the field equations

It has already been discussed that the general term $G_5(\phi, X)$, appearing in the Galileon Lagrangian, (1.1), is well motivated. More specifically, we will assume that it is of the form:

$$\mathcal{L}_5 = G_5(\phi, X)\, G^{\mu\nu}\partial_\mu\phi\partial_\nu\phi \;=\; f(\phi)\,\xi(X)\, G^{\mu\nu}\partial_\mu\phi\partial_\nu\phi\,, \tag{1.2}$$

where we have taken $\xi(X) = 1$. This term will introduce a field dependent derivative coupling to the Einstein tensor. A well-motivated choice for $f(\phi)$ is $\alpha\phi^{\alpha-1}G^{\mu\nu} \ll M^{\alpha+1}$, since it is a natural generalization of the NMDC: if one chooses $\alpha = 0$ the Einstein gravity is retrieved, while for $\alpha = 1$ the simple NMDC is recovered.

If we choose $\alpha > 1$, then we modify the phenomenology of the NMDC. This choice is well motivated for two reasons. Firstly, the gravitational friction effect is retained for $\alpha\phi^{\alpha-1}G^{\mu\nu} \gg M^{\alpha+1}$, but of course the specific inflationary predictions are expected to change. Secondly, after the end of Slow Roll, GR is expected to take over. $\phi \to 0$ leads to $\alpha\phi^{\alpha-1}G^{\mu\nu} \ll M^{\alpha+1}$ at the bottom of the potential, switching off the GNMDC term. This is in fact what is most desirable, so that the non-minimal kinetic term ceases to source late time instabilities/non-linearities. We will in fact show that (1.2) can produce a reheating period that is essentially described by GR.

1.2.1 The field equations

We now proceed to derive the equations that describe the dynamics of the theory presented here. The action at hand is:

$$S = \int d^4x\sqrt{-g}\left[\frac{M_{\rm Pl}^2}{2}R - \frac{1}{2}\left(g^{\mu\nu} - f(\phi)G^{\mu\nu}\right)\partial_\mu\phi\partial_\nu\phi - V(\phi)\right]. \tag{1.3}$$

By varying with respect to $g_{\mu\nu}$, the field equations are obtained:

$$G_{\mu\nu} = \frac{1}{M_{\rm Pl}^2}\left[T^{(0)}_{\mu\nu} - f(\phi)\,T^{(1)}_{\mu\nu} - \frac{1}{2}f'(\phi)\,T^{(2)}_{\mu\nu}\right], \tag{1.4}$$

where a prime denotes differentiation with respect to ϕ and $G_{\mu\nu}$ is the Einstein tensor. The $T^{(1)}_{\mu\nu}$, $T^{(2)}_{\mu\nu}$ terms correspond to:

$$T^{(0)}_{\mu\nu} = \nabla_\mu\phi\nabla_\nu\phi - g_{\mu\nu}\left[\frac{1}{2}(\nabla\phi)^2 + V(\phi)\right] \ , \tag{1.5}$$

$$\begin{aligned} T^{(1)}_{\mu\nu} =& - G_{\mu\nu}\nabla_\lambda\phi\nabla^\lambda\phi + 4R^\lambda{}_{(\mu}\nabla_{\nu)}\phi\nabla_\lambda\phi - \nabla_\mu\phi\nabla_\nu\phi R + 2[\nabla^\kappa\phi\nabla^\lambda\phi R_{\mu\kappa\nu\lambda} + \nabla_\mu\nabla^\lambda\phi\nabla_\nu\nabla_\lambda\phi \\ & - \nabla_\nu\nabla_\mu\phi\nabla^2\phi] + g_{\mu\nu}[\nabla^2\phi\nabla^2\phi - \nabla_\kappa\nabla_\lambda\phi\nabla^\kappa\nabla^\lambda\phi - 2R_{\kappa\lambda}\nabla^\kappa\phi\nabla^\lambda\phi] \ , \end{aligned} \tag{1.6}$$

$$\begin{aligned} T^{(2)}_{\mu\nu} =& g_{\mu\nu}(\nabla_\lambda\phi\nabla^\lambda\phi\nabla^2\phi - \nabla^\kappa\phi\nabla^\lambda\phi\nabla_\kappa\nabla_\lambda\phi) + 2\nabla^\lambda\phi\nabla_{(\mu}\phi\nabla_{\nu)}\nabla_\lambda\phi - \nabla_\lambda\phi\nabla^\lambda\phi\nabla_\nu\nabla_\mu\phi \\ & - \nabla_\mu\phi\nabla_\nu\phi\nabla^2\phi \ . \end{aligned} \tag{1.7}$$

Parentheses enclosing indices denote a symmetrization on them. Note, that $\alpha = 1$ switches off the term involving $T^{(2)}_{\mu\nu}$ and one retrieves NMDC field equations.

1.2.2 Friedmann Equations and the Klein-Gordon equation for a flat FLRW Universe

To proceed, we will assume the observationally justified flat FLRW geometry. For a cosmological scalar field $\phi = \phi(t)$ we obtain the 0-0 and 1-1 components of the field equations, (1.4):

$$3M_{\rm Pl}^2H^2 = V\left(\phi\right) + \frac{1}{2}\dot{\phi}^2 + \frac{9}{2}\,f(\phi)\,\dot{\phi}^2H^2 \ , \tag{1.8}$$

$$M_{\rm Pl}^2\left(\dot{H} + \frac{3}{2}H^2\right) = \frac{V(\phi)}{2} - \frac{\dot{\phi}^2}{4} + f(\phi)\left[\left(\frac{1}{2}\dot{H} + \frac{3}{4}H^2\right)\dot{\phi}^2 + H\dot{\phi}\,\ddot{\phi}\right] + \frac{1}{2}\,f'(\phi)H\dot{\phi}^3 \ , \tag{1.9}$$

An overdot denotes differentiation with respect to cosmic time, and we define the Hubble parameter:

$$H(t) = \dot{a}(t)/a(t)$$

These equations are of course a modified version of the Einstein equations that one obtains for a minimally coupled field. We can bring them to the familiar form $\rho = 3H^2M^2$, $\rho + 3p = -6M_{\rm Pl}^2(H^2 + \dot{H})$ respectively, by defining the energy density and pressure of the scalar field:

$$\rho_\phi \equiv \frac{1}{2}\dot{\phi}^2 + V(\phi) + \frac{9}{2}f(\phi)\dot{\phi}^2H^2 \ , \tag{1.10}$$

$$p_\phi \equiv \frac{1}{2}\dot{\phi}^2 - V(\phi) - \ f(\phi)\left[\left(\dot{H} + \frac{3}{2}H^2\right)\dot{\phi}^2 + 2H\dot{\phi}\,\ddot{\phi}\right] - f'(\phi)H\dot{\phi}^3 \ . \tag{1.11}$$

Moreover, the Klein-Gordon equation derived is:

$$\begin{aligned} \Big[\Big(\partial_\mu g^{\mu\nu} - & f(\phi)\,\partial_\mu G^{\mu\nu}\Big)\partial_\nu\phi + \Big(g^{\mu\nu} - f(\phi)G^{\mu\nu}\Big)\partial_\mu\partial_\nu\phi - \frac{1}{2}f'(\phi)\,G^{\mu\nu}\partial_\mu\phi\partial_\nu\phi - \frac{dV}{d\phi}\Big]\sqrt{-g} \\ & - \frac{1}{2\sqrt{-g}}\Big[g^{\mu\nu} - f(\phi)G^{\mu\nu}\Big]\partial_\nu\phi\partial_\mu g = 0 \ . \end{aligned} \tag{1.12}$$

which, for a cosmological field $\phi = \phi(t)$, in a flat FLRW geometry, becomes:

$$\ddot{\phi}\left(1 + 3f(\phi)H^2\right) + 3H\dot{\phi}\left(1 + 3\,f(\phi)\,H^2 + 2\,f(\phi)\,\dot{H}\right) + \frac{3}{2}\,f'(\phi)\,\dot{\phi}^2H^2 + \frac{dV}{d\phi} = 0 \ . \tag{1.13}$$

1.2.3 Slow Roll Parameters

We define the first Hubble-flow function (or first slow roll parameter) as:

$$\epsilon \equiv -\frac{\dot{H}}{H^2} = \frac{3}{2}\frac{p+\rho}{\rho} \tag{1.14}$$

$$= \frac{3}{2}\frac{\dot{\phi}^2 + 3f(\phi)\dot{\phi}^2H^2 - f(\phi)\left(\dot{H}\dot{\phi}^2 + 2H\dot{\phi}\,\ddot{\phi}\right) - f'(\phi)H\dot{\phi}^3}{\rho_\phi}\,. \tag{1.15}$$

We additionally define other slow-roll parameters, for instance δ:

$$\delta \equiv \frac{\ddot{\phi}}{H\dot{\phi}}\,. \tag{1.16}$$

These parameters facilitate the implementation of Slow Roll. Specifically, slow-roll inflation is realized if $\epsilon \ll 1$ and $\delta \ll 1$. This of course leads to

$$\dot{H} \ll H^2, \qquad \ddot{\phi} \ll 3H\dot{\phi}$$

We can now approximate the Friedmann and Klein-Gordon equations as:

$$3M_{\rm Pl}^2H^2 \approx V(\phi)\,, \tag{1.17}$$

$$3H\dot{\phi}\left(1 + 3\,f(\phi)H^2 + \frac{1}{2}f'(\phi)\,H\,\dot{\phi}\right) + \frac{dV}{d\phi} \approx 0\,. \tag{1.18}$$

Accordingly, we obtain:

$$\epsilon \simeq \frac{3}{2}\frac{\dot{\phi}^2}{\rho_\phi}\left(1 + 3H^2f(\phi) - f'(\phi)H\dot{\phi}\right) \equiv \epsilon_{\rm GR} + \epsilon_D + \epsilon_{\mathcal{B}}\,. \tag{1.19}$$

where we have defined $\epsilon_{\rm GR} = 3\dot{\phi}^2/(2\rho_\phi)$. It is evident that it corresponds to the GR equivalent of the first slow-roll parameter. We also define $\epsilon_{\mathcal{B}}$, which is a term proportional to $f'(\phi)$, and:

$$\epsilon_D \equiv \frac{3}{2}\frac{f(\phi)\dot{\phi}^2}{M_{\rm Pl}^2}\,. \tag{1.20}$$

GNMDC's effect is now more evident: the velocity $\dot{\phi}$ decreases $3H^2f(\phi)$ times, resulting to a significant decrease in ϵ. Indeed, for slow-roll, eq. (1.19) becomes:

$$\epsilon \simeq \epsilon_V\,\frac{1 + 3H^2f(\phi) - f'(\phi)H\dot{\phi}}{\left(1 + 3H^2f(\phi) + f'(\phi)\,H\dot{\phi}/2\right)^2} \;\equiv\; \epsilon_V\,\frac{\mathcal{A} - \mathcal{B}}{\left(\mathcal{A} + \mathcal{B}/2\right)^2}\,, \tag{1.21}$$

with:

$$\epsilon_V = \frac{M_{\rm Pl}^2}{2}\left(\frac{V'}{V}\right)^2 \tag{1.22}$$

and also:

$$\mathcal{A} \equiv 1 + 3H^2f(\phi)\,, \tag{1.23}$$

$$\mathcal{B} \equiv f'(\phi)H\dot{\phi}\,. \tag{1.24}$$

To recover NMDC, we have $f'(\phi) = 0$ and thus ϵ reads $\epsilon = \epsilon_V/\mathcal{A}$, hence the known result [26] is recovered. Similarly, the second slow roll parameter η is defined as $\eta \equiv \eta_V/\mathcal{A}$, where $\eta_V = M_{\rm Pl}^2\frac{V''}{V}$.

1.2.4 The number of e-folds

A particularly important aspect of inflation is of course its duration. It is generally accepted that if inflation is to solve the problems presented earlier, its duration has to be roughly equal to 60 e-folds. The number of e-folds that take place from initial moment t until the end of inflation $t_{\rm end}$ are:

$$N \equiv \int_t^{t_{\rm end}} H dt = \int_{\phi_{\rm end}}^{\phi} \frac{H}{\dot{\phi}} d\phi \simeq \frac{1}{M_{\rm Pl}} \int_{\phi_{\rm end}}^{\phi} \frac{\mathcal{A}+\mathcal{B}/2}{\sqrt{2\epsilon_V}} d\phi \,, \tag{1.25}$$

where we considered the slow-roll approximation, eq. (1.18):

$$\dot{\phi} = -\frac{V'(\phi)}{3H(\mathcal{A}+\mathcal{B}/2)} \,. \tag{1.26}$$

1.3 Power Spectrum, Spectral Index and the Tensor to Scalar Ratio

A perturbative approach of inflationary models yields a spectrum of both scalar and tensor perturbations. These offer the grounds of testing a given inflationary model against observations. In our case, the GNMDC term's dynamics are expected to affect the evolution of the universe for as long as the inflaton dominates its energy density. An introduction to the perturbative theory of inflation can be found in Appendices A and B. The easiest way to study the perturbations, is to choose the gauge where they are equal to 0:

$$\delta\phi = 0$$

Since the GNMDC is ϕ-dependent, any contributions to the perturbations due to the particular form of $f(\phi)\, G^{\mu\nu}\partial_\mu\phi\partial_\nu\phi$ are thus equal to zero.

The quadratic action for the curvature perturbation $\mathcal{R}$ in the comoving gauge takes the form [26, 51]:

$$S^{(2)}_{\mathcal{R}} \,=\, \frac{M^2_{\rm Pl}}{2} \int dx^4 a^3 Q_s \left[\dot{\mathcal{R}}^2 - \frac{c_s^2}{a^2}(\partial_i \mathcal{R})^2\right] \,, \tag{1.27}$$

where $Q_s \equiv F^2\, G/(f(\phi)H^2)$ with

$$F \equiv \frac{1-\epsilon_D/3}{1-\epsilon_D} \,, \qquad G \equiv \frac{\epsilon_D}{3}\left(1 + 3H^2 f(\phi)\frac{1+\epsilon_D}{1-\epsilon_D/3}\right) \,, \tag{1.28}$$

The squared sound-speed of the scalar perturbations, c_s^2, is given by the expression:

$$c_s^2 = \left(1-\frac{\epsilon_D}{3}\right)^{-1} \frac{\epsilon_D}{3G}\left[(1+\epsilon_D) + 3H^2 f(\phi)\left[(1+\epsilon_D) + \frac{4}{9F}\epsilon_D\right] + 6\dot{H} f(\phi)\left(1-\frac{\epsilon_D}{3}\right)\right] \,. \tag{1.29}$$

We note that $f(\phi) \to 0$, restores the canonical case, since:

$$Q_s = \dot{\phi}^2/(2\, H^2 M^2_{\rm Pl}), \text{ thus } c_s^2 \to 1 \tag{1.30}$$

We have already mentioned that in the NMDC case, c_s^2 wildly oscillates between positive and negative values. We will show that a GNMDC term significantly ameliorates this problem.

The formula giving the power spectrum of the scalar perturbations, in the slow roll case is:

$$\mathcal{P}_{\mathcal{R}} = \frac{H^2}{8\pi^2\, Q_s\, c_s^3} \,. \tag{1.31}$$

During the early stages of the evolution, when we are still in the high friction (HF) limit, it holds that $\epsilon_D \ll 1$. We thus obtain:

$$Q_s \simeq \epsilon\, \mathcal{A}/(\mathcal{A}-\mathcal{B}), \text{and} c_s \simeq 1 \tag{1.32}$$

so the power spectrum's expression becomes:

$$\mathcal{P}_{\mathcal{R}} = \frac{H^2}{8\pi^2\, M_{\rm Pl}^2\, \epsilon_V}\left(\mathcal{A}+\mathcal{B}+\mathcal{O}\left(\frac{\mathcal{B}^2}{\mathcal{A}}\right)\right)\,. \tag{1.33}$$

We moreover define the scalar spectral index (tilt), as the change of the logarithm of the scalar power spectrum per logarithmic interval k:

$$\frac{d\ln\mathcal{P}_{\mathcal{R}}}{d\ln k} \simeq -\left(\mathcal{A}+\frac{\mathcal{B}}{2}\right)^{-1}\left[6\epsilon_V - 2\eta_V + \frac{V'}{V}M_{\rm Pl}^2\frac{d}{d\phi}\ln\left(\mathcal{A}+\mathcal{B}+\mathcal{O}\left(\frac{\mathcal{B}^2}{\mathcal{A}}\right)\right)\right]\,. \tag{1.34}$$

It is safe to assume that $\mathcal{B} \ll \mathcal{A}$ so in the HF limit of the slow-roll period we have:

$$\frac{d\ln\mathcal{P}_{\mathcal{R}}}{d\ln k} \simeq -\frac{1}{\mathcal{A}}\left[8\epsilon_V - 2\eta_V + \frac{V'}{V}M_{\rm Pl}^2\frac{f'(\phi)}{f(\phi)}\right]\,. \tag{1.35}$$

$$\tag{1.36}$$

Now we can write the spectral index as:

$$1-n_s \equiv -\frac{d\ln\mathcal{P}_{\mathcal{R}}}{d\ln k}\Big|_{k=aH} \simeq 8\epsilon - 2\eta + \epsilon\, M_{\rm Pl}\frac{f'(\phi)}{f(\phi)}\sqrt{\frac{2}{\epsilon_V}}\,. \tag{1.37}$$

The last term can turn the spectral index from red to blue. This can be taken advantage of, if one wishes to produce PBHs in the context of GNMDC. If $f'(\phi)=0$, we once again obtain the usual expression $1-n_s = 8\epsilon - 2\eta$.

Regarding the tensor perturbation part, we can decompose it into two independent polarization modes:

$$S_T^{(2)} = \sum_p \int dx^4 a^3 Q_t\left[\dot{h}_p^2 - \frac{c_t^2}{a^2}(\partial h_p)^2\right]\,, \tag{1.38}$$

with

$$Q_t = M_{\rm Pl}^2(1-\epsilon_D/3)/4 \text{ and } c_t^2 \simeq 1+2\epsilon_D/3 \tag{1.39}$$

The power spectrum of the tensor perturbations is given by the expression:

$$\mathcal{P}_T = \frac{H^2}{2\pi^2 Q_t c_t^3} \equiv r\,\mathcal{P}_{\mathcal{R}}\,. \tag{1.40}$$

In the HF limit, we can thus obtain the expression for the tensor-to-scalar ratio as:

$$r = 16\,\frac{\epsilon_V}{\mathcal{A}+\mathcal{B}}\,. \tag{1.41}$$

We see then that r is decreased as compared to the simple NMDC and also the GR case.

1.4 Towards viable inflation with GNMDC

Using eq. (1.8) we can rewrite the 0-0 component of the field equations as:

$$3H^2 M_{\rm Pl}^2 = (V + \dot{\phi}^2/2)(1-\epsilon_D)^{-1}$$

Thus, for a positive definite potential, we have that $\epsilon_D < 1$ and functions F and G are also positive. As we have already mentioned, we wish of course to avoid the appearance of instabilities and scalar ghosts. Thus, it is required that $Q_s > 0$ and $c_s^2 > 0$. During the oscillatory stage, $\dot{H}$ may turn from negative to positive:

$$\dot{H} = -\epsilon\, H^2 = -\frac{p+\rho}{2M_{\rm Pl}^2}\ , \tag{1.42}$$

where p is (see eq. (1.10)):

$$p_\phi = \left\{\frac{1}{2}\dot{\phi}^2 - V(\phi)\right\} - \dot{\phi}\, f(\phi)\left\{\left[\left(\dot{H}+\frac{3}{2}H^2\right)\dot{\phi} + 2H\,\ddot{\phi}\right] - f'(\phi)H\dot{\phi}^2\right\}\ . \tag{1.43}$$

where one sees that the first term in the brackets is due to GR dynamics, while the second one is due to GNMDC's contribution.

Parameter ϵ changes sign during oscillations, which is the reason of the problematic behavior of NMDC models. A possible solution to this problem, then, would be realized if the GNMDC term is smaller than the GR term $\dot{\phi}f(\phi) < \dot{\phi}^2$. Such a constraint is satisfied if $f(\phi) \sim 0$ whenever $\dot{\phi}$ takes the maximum value, which would happen at the bottom of the potential, when $\phi \approx 0$. Thus, we can choose a coupling, $f(\phi)$, that vanishes at the bottom of the potential. Such examples would be:

$$f(\phi) = \frac{\alpha\phi^{\alpha-1}}{M^{\alpha+1}}\ , \qquad \text{or} \qquad f(\phi) = \frac{1}{M^2}e^{\tau\phi/M_{\rm Pl}}\ . \tag{1.44}$$

If $\alpha = 0$ (or $M \to \infty$) the GNMDC term is turned off, retrieving GR, while for $\alpha = 1$ (or equivalently $\tau = 0$ for the exponential case) the NMDC case is restored[2].

To conclude whether GNMDC completely heals gradient and phantom instabilities, one has to perform a full perturbative analysis. However, we present a simpler examination with a direct comparison between the GR and GNMDC terms, that is suggestive of what is obtained through GNMDC. In Fig. 1.1 we compare the canonical and non-canonical kinetic terms, in order to demonstrate the restoration of GR, while in Fig. 1.2 we show the evolution of the squared sound-speed for a variety of choices for the GNMDC parameter α, as compared with the NMDC case ($\alpha = 1$).

1.4.1 Inflationary observables

The main grounds for testing an inflationary scenario come through observable quantities that are extracted via the perturbative approach (see Appendix B). As we have noted before, the main ones are the scalar power spectrum, $\mathcal{P}_R(\phi_{\rm cmb})$, the scalar spectral index n_s, and the tensor-to-scalar ratio of perturbations, r.

It is useful to look at the various observables during the early slow roll era, i.e. in the HF limit. It holds that $\mathcal{A} \gg 1$, which implies $\mathcal{B} \sim f'(\phi)/\mathcal{A} \ll \mathcal{A}$. Thus, the scalar power spectrum can be approximated by:

$$\mathcal{P}_{\mathcal{R}}(\phi,\lambda_p,\alpha,M)|_{\phi=\phi_{\rm cmb}} \simeq \frac{H^2}{8\pi^2\, M_{\rm Pl}^2\,\epsilon_V}\mathcal{A} \simeq \frac{V^2(\phi)}{24\pi^2\, M_{\rm Pl}^6\,\epsilon_V(\phi)} f(\phi,\alpha,M) \,=\, 2.2\times 10^{-9}\,. \tag{1.45}$$

[2]The NMDC is studied in a variety of works (for example [26, 27]), which may prove problematic during the reheating stage . However, there have been reports that are free from such instabilities [54].

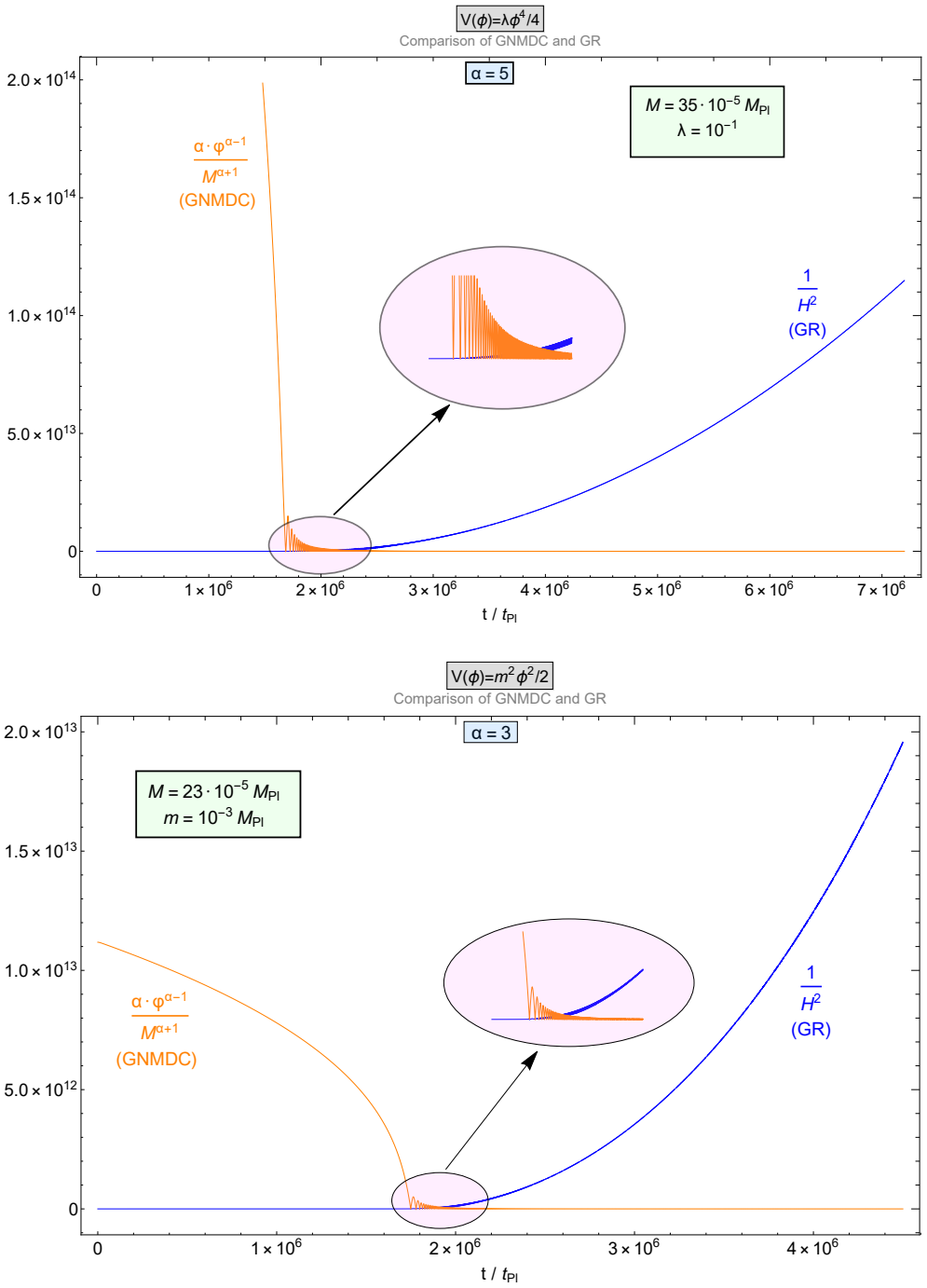

Figure 1.1: *We present the decay of the GNMDC term and the domination of the GR term after the end of inflation. We choose to showcase a Higgs potential with a GNMDC term, with* $\alpha = 5$ **(upper panel)** *and a quadratic potential with a GNMDC term with* $\alpha = 3$ **(lower panel)**. *In both cases, one sees that GR takes over GNMDC after a few oscillations, which in general depends on the value of* α. *This is not the case for* $\alpha = 1$ *(NMDC), where GR is subleading for a vastly longer period, potentially leading to instabilities. The vertical axis has* $1/M_{Pl}^2$ *units.*

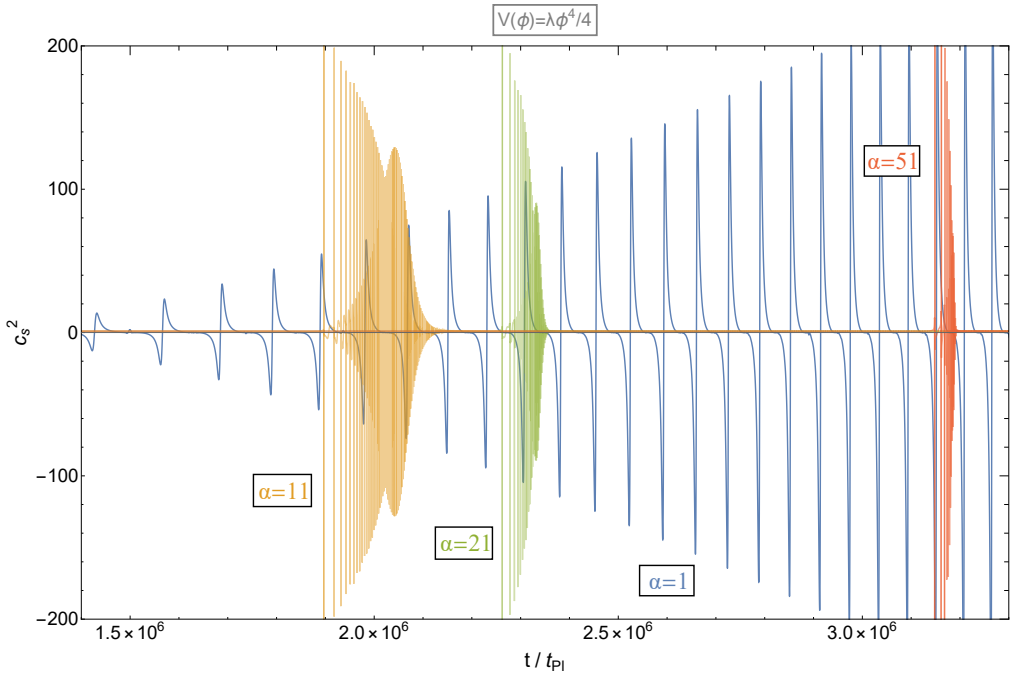

Figure 1.2: *A comparison of the c_s^2 for various values of GNMDC's parameter α, in the context of a Higgs potential. All examples are normalized to yield 60 e-folds, and also $\mathcal{P}_R \approx 2.2 \cdot 10^{-9}$. One observes that for $\alpha = 1$ (NMDC) the oscillations increase, potentially causing post-inflationary instabilities. This is because NMDC remains dominant with respect to GR after inflation. But for $\alpha > 1$, and as α increases, GNMDC decays significantly faster. This leads to $c_s^2 = 1$ after a few oscillations. The fact that GR takes over, ameliorates the problem of post-inflationary instabilities that were present in NMDC models.*

The observed value for $\mathcal{P}_R$ is:

$$\mathcal{P}_R \approx 2.2 \cdot 10^{-9}$$

Expression (1.45) produces an approximate constraint for the parameters of the theory, namely the function $f(\phi)$, M etc, relatively to the potential parameter at $\phi = \phi_{\rm CMB}$. Parameter $\phi_{\rm CMB}$ denotes the field value at the moment that the perturbation of scale $k_{\rm cmb} = 0.05$ Mpc^{-1}, exited the Hubble horizon. To determine its value, one uses the desired number of e-folds:

$$N \simeq \frac{1}{M_P^2} \int_{\phi_{\rm end}}^{\phi} \frac{\epsilon_V}{\epsilon} \frac{V}{V'} \, d\phi \,. \tag{1.46}$$

Moving on, the scalar spectral index (1.37) can be brought to the form:

$$1 - n_s \simeq \frac{M_{\rm Pl}^2}{V(\phi, \lambda_p) f(\phi, \alpha, M)} \left(8\epsilon_V - 2\eta_V + M_{\rm Pl} \frac{f'(\phi)}{f(\phi)} \sqrt{2\epsilon_V(\phi, \lambda_p)} \right) \,. \tag{1.47}$$

We can use what was extracted here to constrain the parameters of a given model. In what follows, we study the dynamics of particular GNMDC terms and inflationary potentials in order to showcase the phenomenology of the GNMDC term by analyzing specific results.

Inflation with monomial potentials and a GNMDC term

We will now attempt to demonstrate the effects of a GNMDC term [3]. We will consider a general class of monomial potentials and a derivative coupling of a similar form:

$$V(\phi) = \lambda_p \, \phi^p \, , \qquad f(\phi) \, = \, \alpha \frac{\phi^{\alpha-1}}{M^{\alpha+1}} \tag{1.48}$$

Parameter λ_p's dimensionality is mass to the power $4-p$. Among the monomial potentials, there is one that holds a particular position since it is known to be realized in nature, namely the Higgs potential. We will later focus on its results within the GNMDC context.

We proceed to examine the parameter space of this GNMDC term. One can obtain a dynamic equation solely for the ϕ field, by eliminating the Hubble parameter. This equation is:

$$\begin{aligned}
&\ddot{\phi} + V'(\phi) + \frac{2\sqrt{3}\alpha\phi^{\alpha}\dot{\phi}V(\phi)\sqrt{\frac{\phi M^{\alpha+1}\left(\dot{\phi}^2+2V(\phi)\right)}{2M_{\rm Pl}^2 M^{\alpha+1}\phi - 3\alpha\phi^{\alpha}\dot{\phi}^2}}}{2M_{\rm Pl}^2 M^{\alpha+1}\phi - \alpha\phi^{\alpha}\dot{\phi}^2} + \sqrt{3}\dot{\phi}\sqrt{\frac{\phi M^{\alpha+1}\left(\dot{\phi}^2+2V(\phi)\right)}{2M_{\rm Pl}^2 M^{\alpha+1}\phi - 3\alpha\phi^{\alpha}\dot{\phi}^2}} \\
&+ \frac{\alpha\left(\dot{\phi}^2+2V(\phi)\right)\left((\alpha-1)\dot{\phi}^2+2\phi\ddot{\phi}\right)}{\alpha\phi\dot{\phi}^2 - 2M_{\rm Pl}^2 M^{\alpha+1}\phi^{2-\alpha}} \\
&= \frac{\sqrt{3}\alpha\phi^{\alpha}\dot{\phi}^3\sqrt{\frac{\phi M^{\alpha+1}\left(\dot{\phi}^2+2V(\phi)\right)}{2M_{\rm Pl}^2 M^{\alpha+1}\phi - 3\alpha\phi^{\alpha}\dot{\phi}^2}}}{2M_{\rm Pl}^2 M^{\alpha+1}\phi - \alpha\phi^{\alpha}\dot{\phi}^2} + \frac{3\alpha\left(\dot{\phi}^2+2V(\phi)\right)\left((\alpha-1)\dot{\phi}^2+2\phi\ddot{\phi}\right)}{6\alpha\phi\dot{\phi}^2 - 4M_{\rm Pl}^2 M^{\alpha+1}\phi^{2-\alpha}} \, .
\end{aligned} \tag{1.49}$$

Thus, to avoid poles and by constraining that the rooted quantities are positive, one obtains a specific part of the phase space of $\{\phi, \dot{\phi}\}$, as well as specific constraints between parameters M and α of the GNMDC.

In the limit $\mathcal{A} \gg \mathcal{B}$ we obtain that:

$$\epsilon(\phi) \simeq \frac{M_{\rm Pl}^2}{2\phi^2}\frac{p^2}{\mathcal{A}(\phi)} = \frac{1}{2}\eta \, . \tag{1.50}$$

Thus, we can infer from eq. (1.46) that the number of e-folds can be found by:

$$N(\phi) \, \simeq \, \frac{\alpha\lambda_p}{p\,(p+a+1)}\,\frac{1}{M_{\rm Pl}^4\, M^{\alpha+1}}\left(\phi^{p+\alpha+1} - \phi_{\rm end}^{p+\alpha+1}\right) \, . \tag{1.51}$$

To roughly determine the end of the inflationary period, we need to solve equation $\epsilon = 1$, i.e.:

$$\epsilon_V \left(\mathcal{A}-\mathcal{B}\right)/\left(\mathcal{A}+\mathcal{B}/2\right)^2 = 1$$

yielding

$$\phi_{\rm end} = \left(\frac{p^2}{2\,\alpha\,\lambda_p}\, M_{\rm Pl}^4\, M^{\alpha+1}\right)^{1/(a+p+1)}$$

For $\phi^{p+\alpha+1} \gg \phi_{\rm end}^{p+\alpha+1}$ we get:

$$\phi^{p+\alpha+1}(N) \, \simeq \, \frac{p(p+\alpha+1)}{\alpha\lambda_p}\, M_{\rm Pl}^4\, M^{\alpha+1}\, N \, . \tag{1.52}$$

We can thus rewrite the slow-roll parameters in terms of the number of the e-folds:

$$\epsilon \simeq \frac{p}{2(p+\alpha+1)}\,\frac{1}{N} \, , \quad \eta = \frac{2p-2}{p}\epsilon \, . \tag{1.53}$$

[3] For a similar work in the context of PBH production see [66].

On the same footing, we obtain the scalar spectral index, for $\alpha \geq 1$:

$$1 - n_s \simeq \frac{p\,(2p+\alpha+1)}{\alpha\lambda_p}\frac{M_{\rm Pl}^4 M^{\alpha+1}}{\phi^{p+\alpha+1}} = \frac{2(2p+\alpha+1)}{p}\,\epsilon\ , \tag{1.54}$$

so in terms of the e-folds we get for $\alpha \geq 1$:

$$1 - n_s \simeq 8\epsilon - 2\eta + 2\epsilon\frac{\alpha-1}{p} = \frac{2p+\alpha+1}{p+\alpha+1}\,\frac{1}{N}\,, \quad r \simeq \frac{8\,p}{p+\alpha+1}\,\frac{1}{N}\ , \tag{1.55}$$

It is notable that neither the spectral index, nor the tensor to scalar ratio depend on the monomial potential's parameter, or the scale of the GNMDC. On the other hand, parameter α affects their behavior. As α grows n_s increases and r decreases. This behavior is depicted in Figs. 1.3, 1.4 as well as an equivalent behavior for the exponential case in Fig. 1.5. The observational constraint that $r < 0.064$ and the spectral index value is approximately $n_s = 0.965$ can be satisfied for $N \lesssim 37$. Thus the quartic or quadratic power-law inflation models can be compatible with the Planck 2018 constraints [67], for a proper GNMDC.

To summarize, when a monomial potential with an exponent p, is considered, the spectral index's observed value constrains N and α, as seen by eq. (1.55). Moreover, we can read the value of the ϕ field that corresponds to the CMB pivot scale, $\phi_{\rm CMB}$, by eq. (1.52). By this value and constraint (1.45), we can determine the scale M of the theory as well as parameter α, by assuming a particular value of N.

We have shown then that a given potential, e.g. the one corresponding to the Higgs boson, can yield viable inflation in the context of the GNMDC case, for appropriate values of M and α, that can be specified by observational constraints. Higgs inflation with a GNMDC is also possible to be weakly coupled on the same footing with the results of [68].

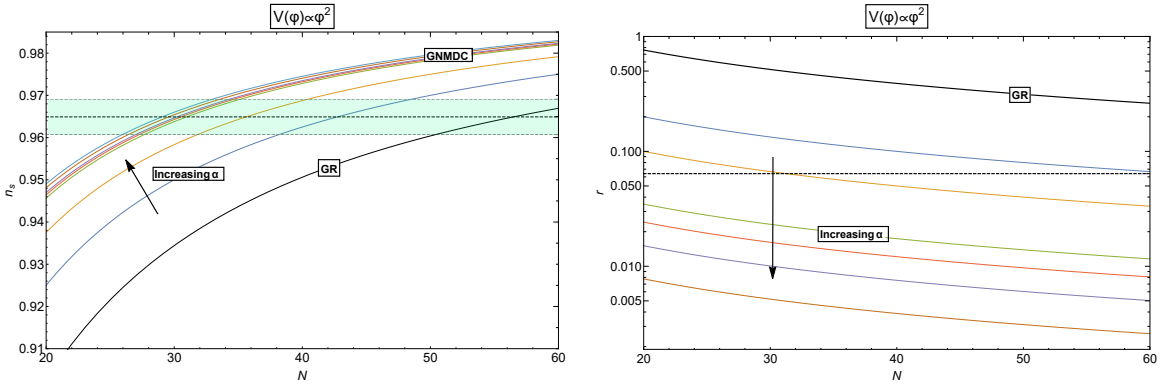

Figure 1.3: *The plots of $n_s(N)$ (**left panel**) and $r(N)$ (**right panel**), for a quadratic potential $V(\phi) = \lambda_2\phi^2$ with GR and with a GNMDC term $f(\phi) = \phi^{\alpha-1}/M^{\alpha+1}$. Colored lines depict models with $\alpha = 1, 5, 20, 30, 50, 100$, while GR is depicted by the thick black line. The spectral index increases as α increases, for a given number of e-folds. The green band within the dashed lines shows the Planck 2018 value for the spectral index at 68% CL. On the contrary, the tensor-to-scalar ratio decreases as α increases. The dashed line depicts the upper limit of r, set by Planck 2018.*

We thus illustrate these results in Figs. 1.3 and 1.4. Therein, the $n_s(N)$ and $r(N)$ graphs are plotted, for a variety of values of parameter α for a quadratic and a quartic potential. One can see the comparison of these models versus GR and NMDC ($\alpha = 1$). Moreover, in Figs. 1.6-1.8 we depict exact results as examples of GNMDC dynamics.

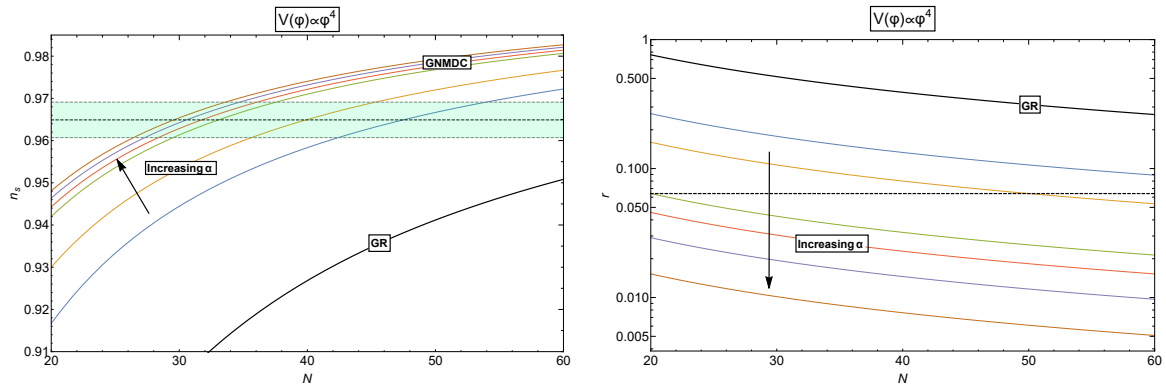

Figure 1.4: *As in Fig. 1.3 the plots of $n_s(N)$ (left panel) and $r(N)$ (right panel), for a quartic potential, $V(\phi) = \lambda_4\phi^4$. We again observe that an increasing α increases the spectral index's value for a given number of produced e-folds, while it decreases the tensor to scalar ratio. The depicted models are for $\alpha = 1, 5, 20, 30, 50, 100$ (colored lines) and GR (thick black line).*

To be more precise, we have performed a full numerical analysis for a variety of cases ($\alpha = 1, 3, 5, 7$) when 40, 50 or 60 e-folds are achieved, in a quadratic and a Higgs potential. The exact results of the observables r and n_s are then depicted in Fig. 1.6, where we also plot the Planck 2018 68% and 95% C.L. regions [67].

For two of these models we also include the evolution of the ϕ field, see Figs. 1.7 and 1.8. The corresponding parameters are included within each one of the graphs. We also include, for reference, the equivalent NMDC ($\alpha = 1$) evolution, for the same parameters, other than α, in order to highlight that GNMDC models achieve a slow-roll stage easier than the simple NMDC case.

Lastly, it is particularly important to examine the post-inflationary evolution of GNMDC models. It has been shown [27, 51, 54] that post-inflation NMDC dynamics are problematic (see also [68]), since the inflaton field oscillates wildly. This in turn leads to instabilities, since the NMDC term does not become subleading, but instead dominates. However, the corresponding behavior of GNMDC theories is more desirable. To show that, we compare the canonical kinetic term versus the GNMDC term at the end, and also after inflation has ended.

Indeed, as one sees in Fig. 1.1, the GNMDC contribution becomes subleading when inflation ends, and GR dynamics take over after a few oscillations (depending on the value of α). This behavior averts the model from having possible instabilities, correcting the corresponding effect in the NMDC case.

Inflation with exponential potentials and GNMDC

Another interesting case to study in the context of GNMDC is that of inflation with exponential potentials. These potentials are interesting for physics beyond the Standard Model due to their connection with the superstring dilaton. A similar study within the NMDC context was performed in [69].

The form of the potential and the GNMDC function, $f(\phi)$ considered here is:

$$V(\phi) = V_0 e^{2\lambda\phi/M_{\rm Pl}}\,, \qquad f(\phi) \,=\, \frac{e^{2\tau\phi/M_{\rm Pl}}}{M^2}\,. \tag{1.56}$$

We thus write the slow-roll parameters as:

$$\epsilon_V = 2\lambda^2, \qquad \text{and } \eta_V = 2\epsilon_V$$

In the limit $\mathcal{A} \gg \mathcal{B}$ we get $\epsilon \simeq \epsilon_V/\mathcal{A}$ and thus:

$$\epsilon(\phi) \simeq \frac{2\lambda^2}{\mathcal{A}(\phi)} = \frac{1}{2}\eta(\phi)\,. \tag{1.57}$$

This is satisfied when

$$\lambda\tau \ll 3H^2 f(\phi) \simeq \mathcal{A}$$

The value of $\mathcal{A}$ is related with the scalar power spectrum's value (1.45). It holds that $\mathcal{A} = 16\epsilon_V/r$. Hence, for $\tau < \lambda/r$ we have $\mathcal{A} \gg \mathcal{B}$. Unlike the GR case, the slow-roll parameters here depend on the field value, implying that exponential models are not eternal in the GNMDC case.

We proceed as usual by calculating the observables. For the scalar spectral index (1.37), we have:

$$1 - n_s \simeq 8\epsilon - 2\eta + \epsilon\, M_{\rm Pl}\frac{f'(\phi)}{f(\phi)}\sqrt{\frac{2}{\epsilon_V}} \simeq 4\epsilon + \epsilon\frac{2\tau}{\lambda} \simeq 2\epsilon\left(2 + \frac{\tau}{\lambda}\right)\ . \tag{1.58}$$

while for the e-folds:

$$N(\phi, \phi_{\rm end}) \simeq \frac{\mathcal{A}(\phi)}{4\lambda(\lambda+\tau)}\Bigg|_{\phi_{\rm end}}^{\phi} \simeq \frac{\lambda}{2(\lambda+\tau)}\frac{1}{\epsilon(\phi)}\ , \tag{1.59}$$

To obtain this equation, we again use that $\mathcal{A}(\phi) \gg \mathcal{A}(\phi_{\rm end}) = 2\lambda^2$ and also suppose that $N(\phi, \phi_{\rm end}) \simeq N(\phi)$. The end of inflation happens when:

$$\phi_{\rm end} = \frac{M_{\rm Pl}}{2(\lambda+\tau)}\ln\left(\frac{2\lambda^2 M^2 M_{\rm Pl}^2}{V_0}\right)\ . \tag{1.60}$$

We are now able to write the spectral index and the tensor to scalar ratio in terms of the potential's parameters and the e-folds:

$$1 - n_s \simeq \frac{2\lambda+\tau}{\lambda+\tau}\frac{1}{N}\,, \quad r \simeq \frac{8\,\lambda}{\lambda+\tau}\frac{1}{N}\ . \tag{1.61}$$

An increase of parameter τ makes $1 - n_s$ converge to $1/N$. At the same time r decreases. For a spectral index value $n_s = 0.965$ [67], λ and τ are both positive, so the GNMDC decreases towards the end of inflation, for $28 \lesssim N \lesssim 57$. Furthermore, constraining r so that $r < 0.064$, produces a constraint in terms of parameters λ, τ:

$$\lambda/\tau < (125/N - 1)$$

In summary, both spectral index and tensor-to scalar ratio constraints, are satisfied when $N < 47$, thus specific values for λ, τ and M can be obtained from the CMB normalization, the value of the spectral index and the number of e-folds. It is indeed interesting that an exponential potential in the context of GNMDC can satisfy the Planck 2018 data. All of the above are demonstrated in Fig. 1.5.

1.5 The observational signatures of the GNMDC

Equations (1.55) and (1.61) entail the predictions of GNMDC models in inflation. We now aim to study whether and how these predictions are different or equivalent with predictions of other types of models. We will, in fact show, that in the SR period, the results are similar to models within the context of GR where the potentials are of the fractional monomial power law form. We will take advantage of this fact, to study in further detail the predictions of the GNMDC scenario. We note that this correspondence is not exact and that it generally breaks down when one wishes to study both inflationary and post inflationary results at the same time.

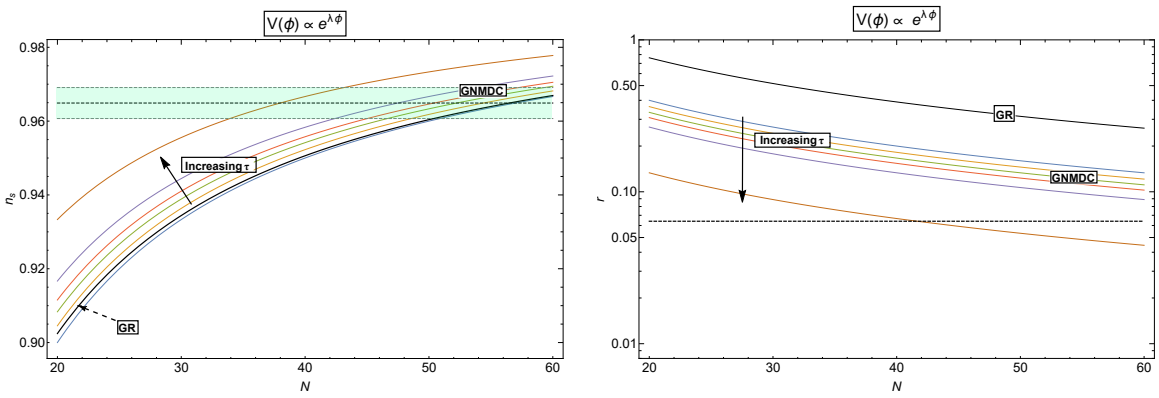

Figure 1.5: *The behavior of $n_s(N)$ and $r(N)$ for an exponential potential $V(\phi) = V_0 e^{2\lambda\phi/M_{Pl}}$ and a GNMDC function of the form $f(\phi) = M^{-2}e^{2\tau\phi/M_{Pl}}$. We have throughout chosen $\lambda = 100$ and $\tau = 0, 10, 20, 30, 50, 200$. The spectral index (left panel) increases as τ increases, for a given produced number of e-folds. while the opposite is true for the tensor to scalar ratio (right panel). We also note that the curves do not depend on λ. These results can be compared with the Planck 2018 68% CL (light green band enclosed by the dashed lines) and GR (thick black line). On the contrary, the tensor-to-scalar ratio, r, decreases as τ increases for a given number of e-folds. Again, we compare the GNMDC results with GR (thick black line) and the upper limit of tensor perturbations by Planck 2018's observations.*

1.5.1 Correspondence between GNMDC and GR models

In the early stages of inflation with GNMDC, we can find a correspondence between GNMDC and GR dynamics. During this period, the approximate Friedmann and Klein-Gordon equations are of the form:

$$H^2 \simeq \frac{V(\phi)}{3M_P^2}\,, \qquad 3H\dot{\phi} \simeq -\frac{\epsilon}{\epsilon_V}V'(\phi)\,, \tag{1.62}$$

Equation (1.21) gives us the ratio ϵ_V/ϵ.

Equations (1.62) are similar to those for the conventional slow roll, which suggests that there possibly exists a redefinition of the field that realizes a transformation between (1.62) and its GR equivalent[4]. For the GNMDC case we see that there is a transformation of the form:

$$\varphi = g(\phi)\ , \qquad V_m(\varphi) = V[g^{-1}(\varphi)]\ , \tag{1.63}$$

that recasts eqs. (1.62) in the form:

$$H^2 \simeq \frac{V_m(\varphi)}{3M_P^2}, \qquad 3H\dot{\varphi} \simeq -V_m'(\varphi)\,, \tag{1.64}$$

We use φ to symbolize the new scalar field that is now minimally coupled to gravity, and $V_m(\varphi)$ is its potential. Then, (1.64) is written with respect to the ϕ field as

$$3H\dot{\phi} \simeq -V'(\phi)/[g'(\phi)]^2$$

and $g'(\phi)$ encompasses the relation between the two fields:

$$g'(\phi) = d\varphi/d\phi$$

[4] A similar treatise has been performed for the simple NMDC case [27, 69].

We can obtain, now, the exact form of the system (1.62), for $\mathcal{A} \gg \mathcal{B}$. It holds that $g'(\phi) = (\epsilon_V/\epsilon)^{1/2} \approx \mathcal{A}$. Therefore, the relation between the two fields is:

$$\varphi \,=\, \int \left(\frac{\epsilon_V}{\epsilon}\right)^{1/2} d\phi \,=\, \frac{1}{M_{\rm Pl}} \int \left[\, V(\phi)\, f(\phi)\,\right]^{1/2}\, d\phi\,. \tag{1.65}$$

We have thus far shown that the dynamics of a field ϕ in a potential $V(\phi)$ and a GNMDC during Slow Roll, can be equivalently described to first order in the SR parameters, by a canonical field φ, in a potential $V_m(\varphi)$, given by eq. (1.63) within GR gravity. We will now proceed to analyze more extensively potentials that were already discussed in the previous sections, when GNMDC takes the forms:

$$f(\phi) \,=\, \alpha \frac{\phi^{\alpha-1}}{M^{\alpha+1}}\ , \quad \text{or} \quad f(\phi) \,=\, \alpha \frac{e^{2\tau\phi/M_{\rm Pl}}}{M^2}\ . \tag{1.66}$$

These GNMDC forms are useful for analytical purposes as well, since the product $V(\phi)\cdot f(\phi)$ appears in equation (1.65).

Correspondence for monomial and exponential potentials

Here we shall consider the class of monomial potentials, with a GNMDC of a similar form, namely:

$$V(\phi) = \lambda_p\, \phi^p\,, \qquad f(\phi) \,=\, \alpha \frac{\phi^{\alpha-1}}{M^{\alpha+1}}\,, \tag{1.67}$$

We mention again that λ_p's dimensionality is $[\text{mass}]^{4-p}$. According to (1.65), we have:

$$\varphi = \int (\epsilon_V/\epsilon)^{1/2} d\phi$$

where

$$\frac{\epsilon_V}{\epsilon} \,=\, \left(3H^2\, \frac{\alpha\, \phi^{\alpha-1}}{M^{\alpha+1}}\right) \,\simeq\, \left(\frac{\alpha V}{M_P^2 M^2}\, \frac{\phi^{\alpha-1}}{M^{\alpha-1}}\right) \gg 1\,, \tag{1.68}$$

Field φ, is given by the expression:

$$\varphi = 2\, \lambda_p^{1/2} \left(\frac{\alpha}{M^{\alpha+1}}\right)^{1/2} \frac{\phi^{\alpha+p+1}}{(\alpha+p+1)/2} \frac{1}{M_{\rm Pl}}\ . \tag{1.69}$$

and it acts as being minimally coupled to gravity, thus in the slow roll regime evolving by equations (1.64).

The corresponding potential can be found, by use of $g^{-1}(\varphi) = \phi$ in Eq. (1.67), to be:

$$V_m(\varphi) = \lambda_p \left[\frac{\alpha+p+1}{2} \frac{M_{\rm Pl}}{\lambda_p^{1/2}} \left(\frac{M^{\alpha+1}}{\alpha}\right)^{1/2} \varphi\right]^{\frac{2p}{\alpha+p+1}}\ , \tag{1.70}$$

There exists, then, a correspondence between $V(\phi)$ of the non-minimally coupled field ϕ and $V_m(\varphi)$ of the minimally coupled:

$$V \propto \phi^p \quad \longleftrightarrow \quad V_m \propto \varphi^{\frac{2p}{p+\alpha+1}}\,. \tag{1.71}$$

Any value of α, with $\alpha \geq 1$ yields a corresponding potential V_m that is less steep than a power of two.

We conclude then that monomial potentials, $V(\phi)$, with a power $p \gg 1$ will effectively appear as potentials with a mild slope that can give viable inflation, from a canonical point of view. Fields ϕ and φ will produce an equal amount of e-folds, as shown by (1.81).

We will now delve into some specific monomial examples in more detail.

Linear potential. We begin with a linear potential. Its correspondence is:

$$V(\phi) = m^3\,\phi \quad \longleftrightarrow \quad V_m(\varphi) = m^3 \left(\frac{\alpha+2}{2\sqrt{\alpha}}\frac{M_{\rm Pl}}{m^{3/2}}M^{\frac{\alpha+1}{2}}\right)^{\frac{2}{\alpha+2}} \varphi^{\frac{2}{\alpha+2}}\ , \tag{1.72}$$

Similar potentials can be found in stringy and supergravity contexts [70], [71].

Quadratic potential. For a GNMDC model with a potential of the form $V = m^2\phi^2/2$ one finds the correspondence:

$$V(\phi) = \frac{1}{2}m^2\,\phi^2 \quad \longleftrightarrow \quad V_m(\varphi) = V[\phi(\varphi)] = \frac{1}{2}m^2 \left(\frac{\alpha+3}{2m}M_{\rm Pl}\sqrt{\frac{2M^{\alpha+1}}{\alpha}}\right)^{\frac{4}{\alpha+3}} \varphi^{\frac{4}{\alpha+3}}\ . \tag{1.73}$$

Thus, the simple case of the quadratic potential corresponds in the equivalent canonical picture to the monomial potential with power $\varphi^{4/(\alpha+3)}$.

Quartic potential. We now look into the more interesting quartic (Higgs-like) potential. We have that:

$$V(\phi) = \lambda\,\phi^4 \quad \longleftrightarrow \quad V_m(\varphi) = \lambda \left(\frac{\alpha+5}{2}\frac{M_{\rm Pl}}{\lambda^{1/2}}\frac{M^{\alpha+1}}{\alpha}\right)^{\frac{8}{\alpha+5}} \varphi^{\frac{8}{\alpha+5}}, \tag{1.74}$$

so the quartic potential in the GNMDC picture, is equivalent to a canonical potential of the form $\varphi^{8/(\alpha+5)}$.

On the same footing, we shall now consider exponential potentials $V(\phi)$, along with an exponential GNMDC function $f(\phi)$:

$$V(\phi) = V_0 e^{2\lambda\phi/M_{\rm Pl}}\,, \qquad f(\phi) \,=\, \frac{e^{2\tau\phi/M_{\rm Pl}}}{M^2}\,. \tag{1.75}$$

As long as $\mathcal{A} > \mathcal{B}$, it holds that $\mathcal{A} > \lambda\tau$. Then, the canonical field φ is expressed in terms of ϕ as:

$$\phi \simeq -\frac{M_{\rm Pl}}{\tau+\lambda}\,\ln\left[(\tau+\lambda)\,\frac{M}{V_0^{1/2}}\,\varphi\right]\,. \tag{1.76}$$

The corresponding effective potential in GR has a notably simple form, namely:

$$V_m(\varphi) \,=\, V[\phi(\varphi)] \,=\, V_0\left[\frac{(\tau+\lambda)}{V_0^{1/2}}M_{\rm Pl}\right]^{\frac{2\lambda}{\lambda+\tau}} \varphi^{\frac{2\lambda}{\lambda+\tau}}\,. \tag{1.77}$$

We also note that if $\lambda^2 > 1/2$, inflation is terminated naturally when GNMDC becomes ineffective, in complete contrast with the GR case, where inflation with an invariant exponential potential is eternal [72, 73]. The termination of inlfation comes about due to the fact that $\mathcal{A} \to 1$ when Hubble scale H and ϕ decrease. After the end of exponential inflation, a (quasi) kination stage takes place.

To summarize, including an exponential potential in an exponential GNMDC scenario gives rise to similar inflationary observables with equivalent GR monomial potentials φ^n with $n < 2$, in agreement with Planck 2018 observational results. Namely:

$$V(\phi) \,=\, V_0\,e^{2\lambda\phi/M_{\rm Pl}} \quad \longleftrightarrow \quad V_m(\varphi) \propto \varphi^{\frac{2\lambda}{\lambda+\tau}}\,. \tag{1.78}$$

For $\tau > 1$ exponential potentials are indeed quite viable models to investigate in the context of GNMDC. In this sense GNMDC revives exponential potentials in inflation, and additionally features a graceful exit.

A final comment is made on the phenomenology resulting from an exponential potential when coupled to a monomial GNMDC:

$$V(\phi) = V_0 e^{2\lambda\phi/M_{\rm Pl}}, \qquad f(\phi) = \alpha\phi^{\alpha-1}/M^{\alpha+1}$$

In this case, the correspondence between the two fields is:

$$\varphi = -2^{\frac{1+\alpha}{2}}\sqrt{a}\,\frac{{V_0}^{1/2}}{M_{\rm Pl}}\left(-\frac{M_{\rm Pl}}{2\lambda\, M}\right)^{\frac{1+\alpha}{2}}\Gamma\left[\frac{1+\alpha}{2}, -\frac{2\lambda\phi}{M_P}\right], \tag{1.79}$$

thus written in terms of the incomplete Gamma function. We note that for $\phi > 0$ odd values for α are necessary. An analytic expression for the effective potential, $V_m(\varphi)$, is possible to find only if $\alpha = 1$, reading $V_m(\varphi) = (\lambda M)^2\,\varphi^2$. For $\alpha > 1$ we can only approximate the equivalent expressions, of which the only viable ones are for odd values of GNMDC's parameter α.

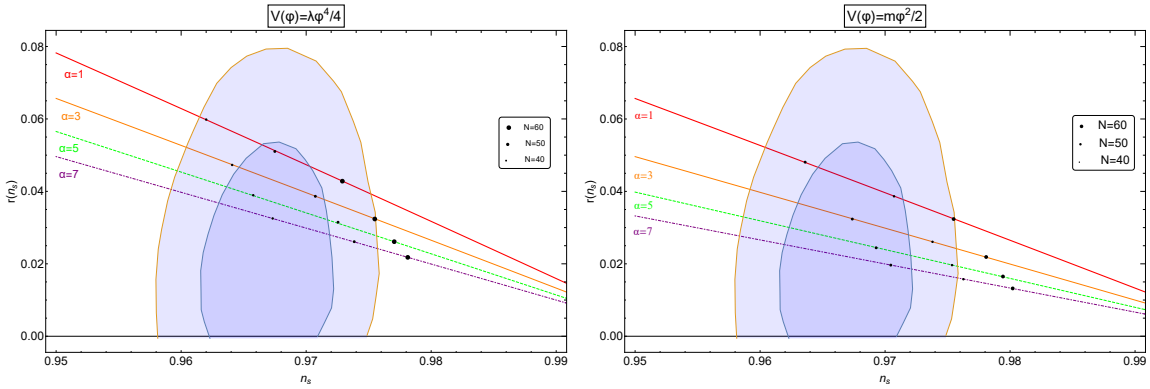

Figure 1.6: *The $r(n_s)$ plots for a Higgs potential (**left panel**) and also a quadratic potential (**right panel**). We show the contours for $\alpha = 1$ (red), $\alpha = 3$ (orange), $\alpha = 5$ (green), $\alpha = 7$ (purple). One can compare these results against the 68% and 95% CL regions of Planck 2018 [67]. Growing bullet points correspond, as shown in the legend, to 40, 50 or 60 e-folds obtained by numerical methods. All models are normalized so that $P_z = 2.2 \cdot 10^{-9}$.*

1.5.2 The expansion history after inflation with GNMDC

We have so far shown that there exists a correspondence between the phenomenologies obtained via GNMDC and GR. For monomial potentials (1.71):

$$p\Big|_{\rm GNMDC} \longleftrightarrow \frac{2p}{p+\alpha+1}\Big|_{\rm GR} \equiv q\,. \tag{1.80}$$

We now take advantage of this, to reproduce basic inflationary predictions using well established GR relations like:

$$1 - n_s \simeq (2q+4)/(4N+q) \text{and} r \simeq 16q/(4N+q).$$

that in the context of GNMDC are derived solely due to its own dynamics, by eqs. (1.55) and (1.61).

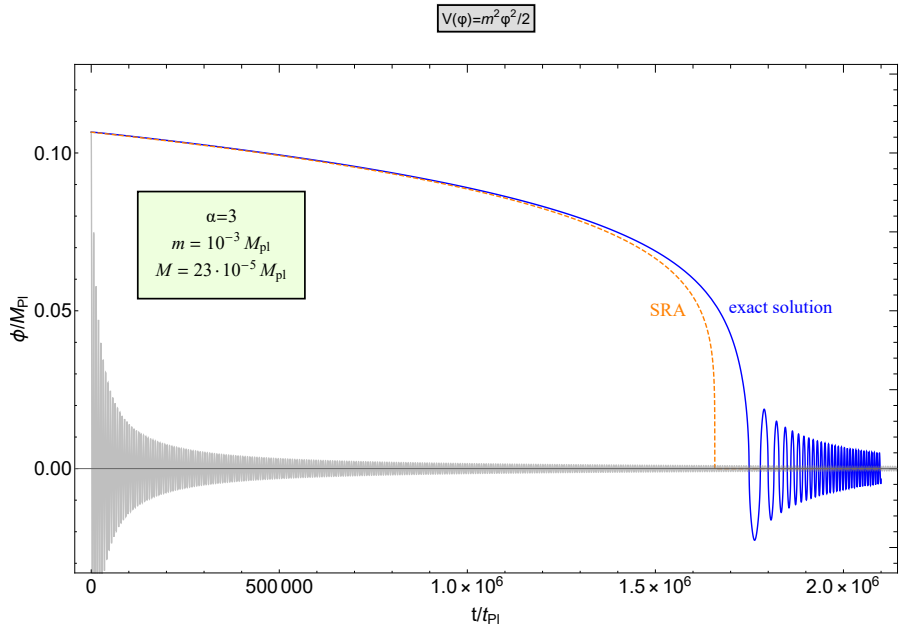

Figure 1.7: *Here we depict the exact and also the SRA evolution of the scalar field $\phi(t)$, for $\alpha = 3$, when a quadratic potential is chosen. The slow-roll approximation is exceptionally accurate in the early stages. This model's parameters have been chosen so that it yields 60 e-folds and is normalized to $\mathcal{P}_\mathcal{R} = 2.2 \cdot 10^{-9}$. At the same time it produces observables in good agreement with Planck 2018, specifically $n_s = 0.978$, $r = 0.022$. For simple reference, we also show the evolution of an NMDC model ($\alpha = 1$), with the same initial conditions and scale M, to emphasize that GNMDC models produce Slow Roll much easier.*

We assume that the number of e-folds in GNMDC and the corresponding GR model are the same. This is justified because in the HF limit, the number of e-folds is:

$$N \simeq \frac{1}{M_{\rm Pl}^2} \int_{\phi_{\rm end}}^{\phi} [g'(\phi)]^2 \frac{V}{V'}\, d\phi = \frac{1}{M_{\rm Pl}^2} \int_{\varphi_{\rm end}}^{\varphi} \frac{V_m}{V_m'}\, d\varphi\,, \tag{1.81}$$

where we use $g'(\phi) = d\varphi/d\phi$ and $(dV/d\phi)(d\phi/d\varphi) = dV_m/d\varphi$.

Having a sufficient amount of e-folds is crucial in inflation or the observables would not match the observed values, see eqs. (1.55) and (1.61). The exact number of e-folds depends on post inflationary evolution for which there are, as of now, not enough cosmic observables. Nevertheless, most models can have a specific range of N-values.

Subsequently, when the end of the acceleration phase happens, the inflaton field is generically expected to oscillate around the bottom of its potential, transforming its leftover energy to other degrees of freedom. Considering specifically power-law potentials, $V(\phi) \propto \phi^p$, the averaged effective equation of state of an oscillating field with GR dynamics is given by [74, 75]:

$$w \equiv \frac{\langle p \rangle}{\langle \rho \rangle} = \frac{p-2}{p+2}\,. \tag{1.82}$$

This period is generally referred to as the reheating period and leads to the thermalization of the

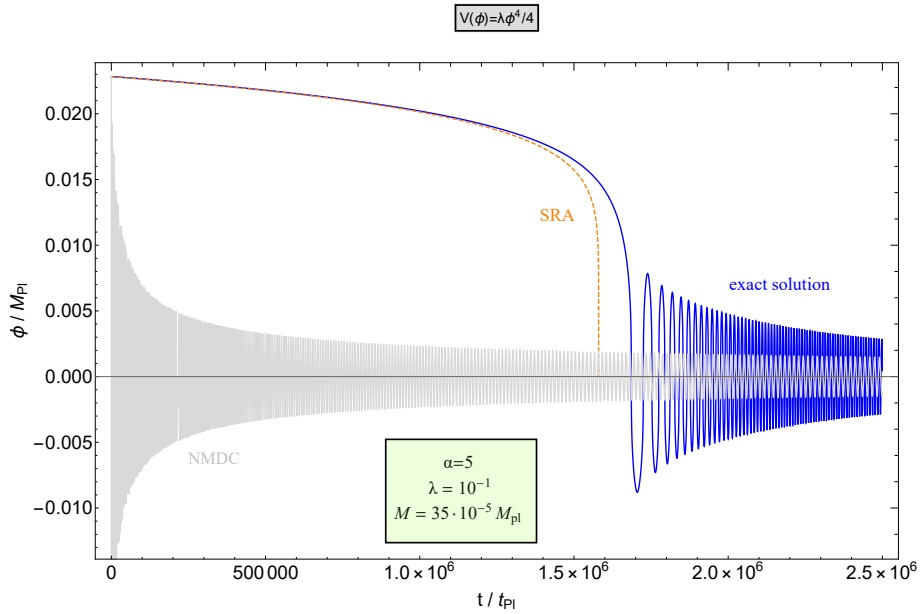

Figure 1.8: *The equivalent to Fig. 1.7 for a Higgs potential. Its parameters again have been chosen so that it yields 60 e-folds and is normalized to* $\mathcal{P}_{\mathcal{R}} = 2.2 \cdot 10^{-9}$. *It yields* $n_s = 0.977$, $r = 0.026$. *We also show the evolution of NMDC* ($\alpha = 1$), *with the same initial conditions and scale* M.

universe and the beginning of radiation domination era, where the temperature is given by:

$$T_{\rm reh} \sim (\Gamma_\phi M_{\rm Pl})^{1/2}$$

where Γ_ϕ denotes the inflaton decay rate. The e-folds of observable inflation can be calculated by:

$$N \simeq 57.6 + \frac{1}{4}\ln\epsilon_* + \frac{1}{4}\ln\frac{V_*}{\rho_{\rm end}} - \frac{1-3w}{4}\tilde{N}_{\rm rh}\,, \tag{1.83}$$

where quantity $\tilde{N}_{\rm rh}$ entails the e-folds that take place during the reheating era. Thus, N also depends on the reheating stage's dynamics, through $\tilde{N}_{\rm rh}$ and the EoS parameter w.

Models that result from GNMDC theories possess a distinct reheating stage, for which there exist two basic cases: i) GNMDC dominates over GR during reheating and, ii) GR takes over GNMDC after the end of inflation. In the first case, GNMDC heavily modifies relation (1.82) [27] that predicts distinct values for the term $(1-3w)\tilde{N}_{\rm rh}/4$. On the other hand, when GNMDC becomes ineffective during reheating, eq. (1.82) applies. There is a clear distinction here when comparing to GR models. While the EoS during reheating is determined by the potential $V(\phi)$, the inflationary dynamics are affected both by the potential $V(\phi)$ and the GNMDC coupling function $f(\phi)$. We now move on to summarize some reheating predictions in the case of a Higgs and an exponential potential in the context of GNMDC, that were presented before [5].

- We first suppose inflation with a Higgs potential, $V(\phi) = \lambda\phi^4/4$, and a GNMDC function of the form: $f(\phi) \propto \phi^{\alpha-1}$. This predicts n_s and r values that are given by eq. (1.55), for $p = 4$. For demonstrative purposes, we will assume here a benchmark value, $\alpha = 11$. According to

[5] An analysis of inflationary and reheating dynamics with NMDC were performed in [27]

Planck 2018, the values of the scalar spectral index and tensor-to-scalar ratio are approximately $n_s = 0.965$ and $r = 0.054$ for $N = 36$. A number of 36 e-folds implies that there has to have taken place an extended non-thermal phase before BBN, whose duration can be specified. As we have shown, after a few oscillations GR takes over and the post inflationary EoS parameter takes the radiational value $w = 1/3$, regardless of the exact reheating temperature, as eq. (1.82) dictates.

On the other hand, the equivalent GR model predicting these n_s and r values for the same e-folds, corresponds to the effective potential $V(\varphi) \propto \varphi^{1/2}$. Hence, eq. (1.82) yields a different EoS after inflation, thus distinguishing the two models. Similar results hold for all monomial potentials with GNMDC.

- Let us now look into the case of inflation with an exponential potential, $V(\phi) = e^{2\lambda\phi/M_{\rm Pl}}$, and a GNMDC of the form $f(\phi) \propto e^{2\tau\phi/M_{\rm Pl}}$. As a demonstration we shall choose the values $\lambda = 100$, $\tau = 320$, for which relations (1.61) hold since $\mathcal{A} \gg \mathcal{B}$. One then finds that when 40 e-folds are achieved, the observables take the values $n_s = 0.969$ and $r = 0.048$. Again, the number of e-folds implies a non-thermal post-inflationary era, in addition to the kination era that generically follows exponential inflation. The equivalent GR model predicting the same n_s and r, for the same amount of e-folds, corresponds to a potential of the form $V(\varphi) \propto \varphi^{10/21}$. Hence, eq. (1.82) hints at a different post-inflationary evolution, again making the two models distinguishable from each other.

1.6 PBH production from the GNMDC

1.6.1 Preliminaries on PBHs

We will now study a different aspect of early Universe cosmology, namely the possible creation of Primordial Black Holes (PBHs). A review and similar works can be found in references [76–79] while attempts in a $f(R)$ context or trapped inflation context, have also been made ([80] and [81] respectively).

In the formation of PBHs, there are two main points to be studied. First, the magnitude of the scalar power spectrum's change, which essentially decides the abundance of PBHs, and then, the stage during which the PBHs were formed, which is related to the mass of the formed PBHs.

The amplitude of the power spectrum peak

A PBH with mass M may form due to a density perturbation that collapses. If the density perturbation is large enough for its gravitational dynamics to dominate over the radiation pressure, it will collapse after the horizon reentry. Then, the mass of the formed PBH will now be equal to

$$\gamma M_{\rm hor}$$

where $M_{\rm hor}$ denotes the horizon mass and γ is a numerical factor related to the particular details of the collapse of the perturbation.

The ratio of the abundance of PBHs with mass M with respect to the total dark matter (DM) abundance,

$$f_{\rm PBH}(M) \equiv \Omega_{\rm PBH}(M)/\Omega_{\rm DM}$$

can be expressed as:

$$f_{\rm PBH}(M) = \left(\frac{\beta(M)}{7.3\times10^{-15}}\right)\left(\frac{\Omega_{\rm DM}h^2}{0.12}\right)^{-1}\left(\frac{\gamma}{0.2}\right)^{\frac{3}{2}}\left(\frac{g(T)}{106.75}\right)^{-\frac{1}{4}}\left(\frac{M}{10^{20}\rm g}\right)^{-1/2}, \tag{1.84}$$

where we approximate that the effective degrees of freedom are equal: $g_* \approx g_s$.

We follow here the Press-Schechter formalism [82] though one could choose a different approach [83]. Firstly, we will assume that curvature perturbations follow canonical (Gaussian) statistics. Our aim is to estimate the probability of formation of a PBH, and subsequently connect the collapse threshold to values of the scalar power spectrum. We will assume that in a spherically symmetric region, PBHs will form with a specific rate, denoted β:

$$\beta(M) = \int_{\delta_c} d\delta \frac{1}{\sqrt{2\pi\sigma^2(M)}} e^{-\frac{\delta^2}{2\sigma^2(M)}} \simeq \frac{1}{2}\mathrm{erfc}\left(\frac{\delta_c}{\sqrt{2}\sigma(M)}\right) \simeq \frac{1}{\sqrt{2\pi}}\frac{\sigma(M)}{\delta_c} e^{-\frac{\delta_c^2}{2\sigma^2(M)}} . \tag{1.85}$$

We quantify the threshold density of the perturbation as δ_c. Function $\mathrm{erfc}(x)$ is the complementary error function. Then, if a given density perturbation has $\delta > \delta_c$, gravity dominates against internal radiational pressure and the perturbation collapses.

The formation rate of PBHs depends on the variance of the density perturbations. We denote this as $\sigma(k)$, which is smoothed on a scale k for radiation domination and is given by the expression [84]:

$$\sigma^2(k) = \left(\frac{4}{9}\right)^2 \int \frac{dq}{q} W^2(qk^{-1})(qk^{-1})^4 \mathcal{P}_R(q) , \tag{1.86}$$

where $\mathcal{P}_R(q)$ denotes the power spectrum of the curvature perturbations. We use the term $W(z)$ to represent the Fourier transformed Gaussian: $W(z) = e^{-z^2/2}$. We can now approximate the magnitude of $\beta(M)$ by use of $\mathcal{P}_R(k) \simeq (9/4)^2\sigma^2(k)$:

$$\beta(M) \sim \frac{1}{\sqrt{2\pi}}\frac{\sqrt{\mathcal{P}_R}}{\delta_c} e^{-\delta_c^2/2\mathcal{P}_\mathcal{R}} . \tag{1.87}$$

Let us now turn our focus to the power spectrum resulting from a GNMDC modification of gravity. It appears to be ϕ-sensitive, since eq. (1.33) is:

$$\mathcal{P}_R \approx \frac{V}{96\pi^2 M_{\rm Pl}^4 \epsilon_V/\mathcal{A}} . \tag{1.88}$$

When the slow roll parameter ϵ decreases, then $\beta(M)$ increases. If we want $f_{\rm PBH} \sim 1$, then the power spectrum has to be:

$$\mathcal{P}_\mathcal{R}^{\rm PBH} \sim 10^{-2}, \qquad \text{for} \qquad \delta_c \sim 0.5.$$

Now eq. (1.88) yields:

$$\epsilon(\phi_{\rm PBH}) = V(\phi_{\rm PBH})(96\pi^2 M_{\rm Pl}^4)^{-1}\mathcal{P}_\mathcal{R}^{\rm PBH})^{-1}$$

It holds that $V(\phi_{\rm PBH}) < V_{\max} = 3\pi^2 A_s r_{\max} M_{\rm Pl}^4/2$. Then, parameter $\epsilon_{\rm PBH}$ has to be less than a specific value, $\epsilon_{\max}$, which is obtained when we substitute the observables' values $A_s \simeq 2.18 \times 10^{-9}$ and $r_{\max} \simeq 0.64$, from Planck 2018 data. Thus, it reads:

$$\epsilon_{\rm PBH} \lesssim \frac{10^{-11}}{\mathcal{P}_\mathcal{R}^{\rm PBH}} \sim 10^{-9} . \tag{1.89}$$

Hence, a significant decrease of the ϵ parameter, implies the increase of δ and η so the SRA does not hold any more. In that case, one has to explicitly solve the Mukhanov-Sasaki equation discussed later.

The PBH mass

Moving on, we shall now consider a perturbation that has a scale k^{-1}, which we suppose exits the Hubble horizon after a number of e-folds before the end of inflation, denoted N_k, which is given by:

$$N_k = \ln\left(\frac{k_{\rm end}}{k}\right) - \ln\left(\frac{H_{\rm end}}{H_k}\right) . \tag{1.90}$$

We now approximate $H_{\rm end} \simeq H_k$. This proves to be a particularly good approximation for perturbation scales k^{-1} that exit the Hubble horizon during, or after, the ultra slow-roll phase of inflation [85, 86]. Thus, we can simplify eq. (1.90) by dropping the second term

When the inflationary evolution of the Universe ends, the Hubble horizon, quantified by H^{-1}, grows faster than the expansion of space and thus the various perturbation scales, that exited due to inflation, gradually reenter it. We then will need to define quantity:

$$\tilde{N}_k \equiv \ln(a(t)/a_{\rm end})$$

which quantifies the e-folds taking place between the end of inflation and the reentry of a given scale [6].

When the EoS parameter takes values $w > -1/3$ we have that:

$$\tilde{N}_k = 2\, N_k/(1+3w)$$

Then, unless $w = 1/3$, the e-folds at which a specific perturbation scale reenters the horizon depends on the temperature during reheating. On the other hand, if a perturbation of scale k^{-1}, reenters during an era of radiation domination, that is $w = 1/3$, or during ϕ^4 oscillating stage, the relation between it and the horizon mass M/γ is:

$$k(M) \,=\, 1.8 \times 10^{18}\, {\rm Mpc}^{-1}\, \gamma^{1/2} \left(\frac{M}{10^{10}\,{\rm g}}\right)^{-1/2} \left(\frac{g_*}{106.75}\right)^{-1/12} . \tag{1.91}$$

Moving on, we shall focus on a few mass scales for the PBHs that are particularly interesting. The first one is a mass $M_{\rm PBH} \simeq 10^{21}$ g. It has been argued that a substantial amount of PBHs with such an approximate mass can actually perform the role of all of the Dark Matter of the Universe. Moreover, this kind of PBHs would be possible to be probed with GW detectors, such as [87–90], as well as other direct observational tests.

Another interesting case comes about if the PBH mass is: $M_{\rm PBH} \simeq 10^{35}$ g. PBHs in this approximate range can explain BH events observed by LIGO [1]. This mass range is not able to constitute all the DM as the previous case, however it can comprise a significant part of it [91]. We will now proceed to calculate the quantities that are essential in the study of PBHs.

We start with the case of PBHs with mass $M_{\rm PBH} = 10^{21}$ g. We suppose that such a PBH reenters the horizon during the radiation domination era, hence, $w = 1/3$. Then, it is

$$k(10^{21}\,{\rm g}) = 5.7 \times 10^{12}\, {\rm Mpc}^{-1} \gamma^{1/2} = 10^{14}\, k_{\rm CMB}\, \gamma^{1/2}.$$

On the other hand, for a PBH with mass $M_{\rm PBH} = 10^{35}$ g, we get:

$$k(10^{35}\,{\rm g}) = 5.7 \times 10^{5}\, {\rm Mpc}^{-1} \gamma^{1/2} = 1.1 \times 10^{7}\, k_{\rm CMB}\, \gamma^{1/2}$$

In the above, we denote $k_{\rm CMB}$ the CMB pivot scale $k_{\rm CMB} = 0.05$ Mpc^{-1}, and use $g_* \simeq \mathcal{O}(100)$.

Our next step will be to calculate the e-folds $N_k = N_{\rm PBH}$ that remain until the end of inflation, when the peak in the power spectrum takes place. We also need $N_{\rm CMB}$, namely the postinflationary e-folds that take place, which is related to cosmic expansion rate through equation (1.83). Here, it holds that:

$$\ln(\epsilon_* V_*/\rho_{\rm end})^{1/4} = \pm\mathcal{O}(1)$$

constraining $N_{\rm CMB} \lesssim 58$ e-folds when the EoS parameter is $w \leq 1/3$. Then, from equation (1.90), we can calculate $k_{\rm end}$:

$$k_{\rm end} = k_{\rm CMB}\, e^{N_{\rm CMB}}\, \frac{H_{\rm end}}{H_{\rm CMB}} \ . \tag{1.92}$$

[6] We use a tilde to signify that these are post-inflationary, so that no confusion arises.

In the context of Higgs inflation, it is $N_{\rm CMB} \simeq 58$ (unless an early non-thermal stage takes place). For our model, then:

$$H_{\rm CMB}/H_{\rm end} \simeq \mathcal{O}(2.6), \text{thus } k_{\rm end} \simeq 4 \times 10^{25}\, k_{\rm CMB}$$

So, from relation:

$$N_{\rm PBH} \simeq \ln\left(k_{\rm end}/k_{\rm PBH}\right)$$

we can find the amount of e-folds before the end of inflation when the peak must have taken place. For PBHs with masses in close range of those presented earlier, we get, respectively:

$$N_{\rm PBH}(M_{\rm PBH} = 10^{21}\,{\rm g}) \sim 27\,, \qquad \text{and} \qquad N_{\rm PBH}(M_{\rm PBH} = 10^{35}\,{\rm g}) \sim 45\,, \tag{1.93}$$

Now using eq. 1.84 we obtain $f_{\rm PBH}(M_{\rm PBH} = 10^{21}\,{\rm g}) \sim 1$ for $\beta(M) \sim 10^{-13}$ and $f_{\rm PBH}(M_{\rm PBH} = 10^{35}\,{\rm g}) \sim 0.1$ for $\beta(M) \sim 10^{-7}$. We can get an estimate of the formation probability, $\beta(M)$, for a given value $\epsilon_{\rm PBH}$.

Having presented the above, it becomes evident that in the context of GNMDC we can produce PBHs, due to its gravitational friction effect. We will now attempt, in the context of a Higgs potential, to construct such a term that abruptly increases at specific scales, much smaller than the CMB scale, thus generating PBHs. Of course, in doing so, we must also preserve the CMB observables.

1.6.2 Power spectrum amplification in the GNMDC theories

We can augment the value of the power spectrum in a GNMDC model by decreasing the value of $\epsilon_V/\mathcal{A}$, eq. (1.33). That, in turn, will bring about large density perturbations that have a probability of collapsing into PBHs. However, we have noted that such a phenomenon must also preserve the CMB observational constraints [92]. To do that in a GNMDC model, we will enforce that $f(\phi)$ gets enhanced in the region of a specific field value. It will be easier to do this by splitting the GNMDC coupling function in two terms:

$$f(\phi) = f_I(\phi)\left(1 + f_{II}(\phi)\right)\,. \tag{1.94}$$

We denote $f_I(\phi)$ as the GNMDC function acting in the beginning of inflation while $f_I(\phi)f_{II}(\phi)$ is activated in the middle or towards the end of it. Function $f_{II}(\phi)$ is a function that peaks at a specific field value $\phi = \phi_0$, while being negligible when the field values is not close to ϕ_0. Thus, inflation is split in two stages. Stage I, where $f_{II}(\phi) \ll 1$ and an amount of N_I e-folds take place, followed by stage II where $f_{II}(\phi) > 1$ and N_{II} e-folds take place. There is of course a freedom in choosing the $f_{II}(\phi)$ function, but we must note that not all function types produce stable models. Among the ones that are stable [66] is:

$$f_{II}(\phi) = \frac{d}{\sqrt{\left(\frac{\phi-\phi_0}{s M_{\rm Pl}}\right)^2 + 1}} \tag{1.95}$$

which we will focus on, from now on. Constants d, s and ϕ_0 are used to parameterize the requirement that the produced PBHs, have a significant abundance.

Specifically, we will estimate these parameters as a function of the power spectrum's amplitude and the e-folds $N_{\rm PBH}$. It is:

$$\mathcal{P}_R \propto \frac{\mathcal{A}(\phi)}{\epsilon_V} \simeq \frac{3H^2 f_I(\phi) f_{II}(\phi)}{\epsilon_V}\bigg|_{\phi=\phi_{\rm PBH}}\,, \tag{1.96}$$

where we denote $\phi = \phi_{\rm PBH}$ as the value of ϕ at which $\mathcal{P}_R$ maximizes, i.e. where $f_I(\phi)f_{II}(\phi) \gg f_I(\phi)$. We can safely approximate $\phi_0 = \phi_{\rm PBH}$. We ask for a peak in the power spectrum $N_{\rm PBH}$ e-folds

before the end of inflation. During stage II, where $f_{II}(\phi) > 1$, $= N_{II}$ e-folds take place and $\dot{\phi}$ decreases significantly. Of course it must hold that $N_{II} \lesssim N_{\rm PBH}$. The exact amount of e-folds N_{II}, can be specified by the observational constraints on the PBH abundance. When $f_{II}(\phi) > 1$ it holds $\Delta\phi_{II} \simeq 2c(\ln d)^{1/2}$ and thus:

$$N_{II} = \int_{\phi_0-\Delta\phi_{II}}^{\phi_0+\Delta\phi_{II}} \frac{H}{\dot{\phi}} d\phi \simeq \frac{1}{M_{\rm Pl}} \int_{\phi_0-\Delta\phi_{II}}^{\phi_0+\Delta\phi_{II}} \frac{\mathcal{A}+\mathcal{B}/2}{\sqrt{2\epsilon_V}}\, d\phi \tag{1.97}$$

We have supposed that stage II begins at $\phi_0+\Delta\phi_{II}$ and ends when $\phi_0-\Delta\phi_{II}$, in order to approximate a sharp $f_{II}(\phi)$.

However, as we mentioned before, when ϵ abruptly decreases, the SR approximation breaks down and (1.31) is no more valid [93]. Hence, in our case we have to solve the Mukhanov-Sasaki (MS) equation.

1.6.3 The Mukhanov-Sasaki equation

To derive the MS equation, we start by the quadratic action for the curvature perturbation $\mathcal{R}$ in the comoving gauge, namely:

$$S_{\mathcal{R}}^{(2)} \;=\; \frac{M_{\rm Pl}^2}{2} \int dx^4 a^3 Q_s \left[\dot{\mathcal{R}}^2 - \frac{c_s^2}{a^2}(\partial_i \mathcal{R})^2\right] \;, \tag{1.98}$$

Quantity c_s^2, (1.29), is the squared sound-speed of the scalar perturbations and Q_s is defined by (1.27). We can introduce a new coordinate [94]:

$$dy = (c_s/a)dt = c_s d\eta \tag{1.99}$$

and redefine:

$$u = z\mathcal{R}, \quad \text{with} \quad z = \sqrt{2}a(c_s Q_s)^{1/2} \equiv a\sqrt{2\tilde{\epsilon}} \tag{1.100}$$

to obtain the transformed action from which the MS equation is obtained[7].

We have then, for a Fourier mode, u_k:

$$u_k'' + \left(c_s^2 k^2 - \frac{z''}{z}\right) u_k = 0, \tag{1.101}$$

where a prime denotes a derivative with respect to the conformal time, η. To obtain the exact power spectrum's values, we have to solve the MS equation. We compute a mode's, u_k, value at super-Hubble scales, well after it has exited the horizon and froze out:

$$\mathcal{P}_R = \frac{k^3}{2\pi^2} \frac{|u_k|^2}{z^2}\bigg|_{k\ll aH} \;. \tag{1.102}$$

To set initial conditions for the modes u_k, we use the Bunch-Davies vacuum. When a mode is well within the horizon, $k \gg aH$, and the evolution of term z''/z is negligible, since $c_s^2 k^2 \gg z''/z$. In this case, all modes have time independent frequencies the MS equation is:

$$u_k'' + c_s^2 k^2 u_k = 0$$

giving the initial condition $u_k = e^{-ik\tau}/\sqrt{2k}$ for the MS equation. We solve separately for the real and imaginary parts of each u_k mode. The Bunch-Davies initial conditions for (1.101) are:

$$\mathrm{Re}\,[u_k] = \frac{1}{\sqrt{2k}}\,, \quad \mathrm{Im}[u_k] = 0, \quad \mathrm{Re}\left[\frac{du_k}{dt}\right] = 0\,, \quad \mathrm{Im}\left[\frac{du_k}{dt}\right] = \frac{\sqrt{k}}{a(t_i)\sqrt{2}}\,. \tag{1.103}$$

[7] One can also obtain the MS equation, written in terms of the slow roll parameters [95].

where $a(t_i)$ is the value of the scale factor when the mode is well inside the horizon, that is, when it holds:

$$a(t_i)H(t_i) \ll k$$

We use these initial conditions to find the evolution of each u_k mode, several e-folds after it exits the horizon and freezes out, where the quantity $|u_k/z|$ converges to a constant value.

In a typical inflationary scenario, we can omit one of the two solutions of the MS equations to estimate the power spectrum. But this is not the case for GNMDC, where the SR parameters change abruptly by a lot. We can see this by writing the MS equation in the form:

$$\mathcal{R}_k'' + (2+\epsilon_2)aH\mathcal{R}_k' + c_s^2 k^2 \mathcal{R}_k = 0. \tag{1.104}$$

where ϵ_2 denotes the second Hubble-flow parameter:

$$\epsilon_2 \equiv \dot{\epsilon}/(H\epsilon)$$

We rewrite (1.101) into (1.104) after observing that $c_s Q_s \simeq \epsilon$. This is obvious if $\epsilon_D \ll 1$, and $c_s \simeq 1$. It is also true when the velocity of the inflaton decreases significantly.

When looking into the large scale limit, the last term is negligible and for $(2+\epsilon_2) > 0$ we find a constant and decaying mode of the curvature perturbation. This is not the case if the term inside the bracket is negative. Then, the second solution corresponds to a growing mode and the omitted solution contributes significantly to the power spectrum. Since in a GNMDC scenario, ϵ depends on $f(\phi)$, if $f(\phi)$ changes abruptly, then the curvature perturbation $\mathcal{R}$ can be significantly enhanced, possibly bringing about the creation of PBHs.

1.7 PBH production from Higgs inflation with GNMDC

We will now be more specific and study inflation with a Higgs potential, that is:

$$V(\phi) = (\lambda/4)\phi^4, \text{ for } \lambda \simeq 0.1.$$

We will remain within the framework of GNMDC presented earlier, by choosing the f_I part of the GNMDC to be of the form (1.67):

$$f_I(\phi) = \alpha\phi^{\alpha-1}/M^{\alpha+1}$$

For later ease, we denote $\epsilon_{\rm PBH} \equiv \epsilon_V(\phi_0)/\mathcal{A}(\phi_0)$, which is the minimum value of the ratio $\epsilon_V/\mathcal{A}$. This quantity is what can modify the power spectrum's amplitude. We also note that $\epsilon(\phi_0) \simeq \epsilon_{\rm PBH}$. Then, for the f_{II} function, we use (1.95). Parameter d, which decides the GNMDC's effectiveness, can be found by:

$$d \sim \frac{M_{\rm Pl}^2}{V(\phi_0)f_I(\phi_0)}\frac{\epsilon_V}{\epsilon_{\rm PBH}} = \frac{8}{\alpha\lambda}\frac{M_{\rm Pl}^4 M^{\alpha+1}}{\phi_0^{\alpha+5}}\frac{1}{\epsilon_{\rm PBH}}\,. \tag{1.105}$$

We finally once again note, that the number of e-folds N_{II}, i.e. the e-folds that take place during stage II (when $f(\phi) \simeq f_I(\phi)f_{II}(\phi)$), must be $N_{II} \leq N_{\rm PBH}$. Given a value of N_{II}, parameter s of (1.95) can also be specified. However, finding exact values of these parameters can only be done after solving the MS equation, while the above approach is mostly of qualitative use. We now proceed to present an explicit example.

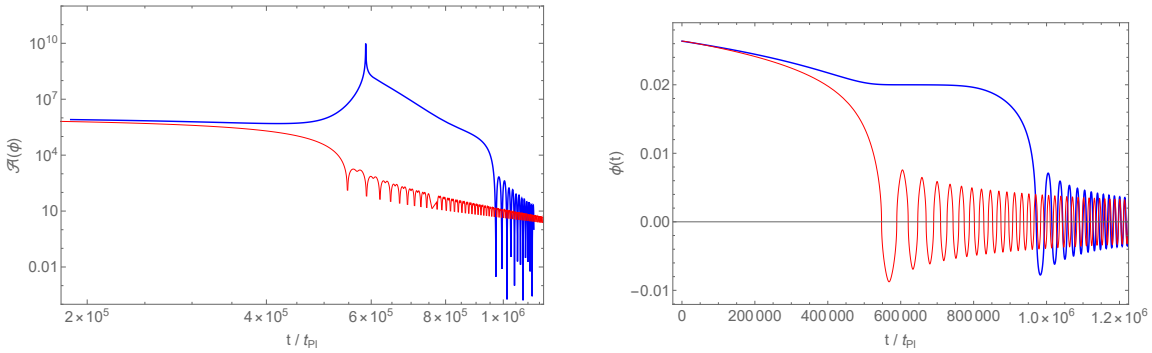

Figure 1.9: ***Left panel****: The evolution of the auxiliary function* $\mathcal{A} = 1 + 3H^2 f(\phi)$ *(thick blue line) with a GNMDC that generates a peak high enough to trigger PBH production with mass about* $10^{21} g$*, while at the same time preserving inflationary observables, in the context of a Higgs potential. For simple reference we include the evolution of the same function (thin, red line), where GNMDC includes only the* f_I *part of GNMDC.* ***Right panel****: The evolution of the field itself (thick blue line), with a GNMDC that creates the aforementioned peak. The plateau in its evolution happens due to the enhanced friction effect that the* $f_{II}(\phi)$ *factor of the GNMDC brings about. Again for simple reference, we include the evolution of the field with the same parameters but only* f_I *being present in GNMDC dynamics. This decrease of the velocity of the field is what enhances the power spectrum at scales around* $k \sim 10^{12}$ Mpc^{-1}*.*

10^{21} grams PBHs as dark matter

For a PBH with an approximate mass $M_{\rm PBH} \sim 10^{21}$ g to be generated, eq. (1.93) shows that the amplitude of the scalar perturbations has to be enhanced at about $N_{\rm PBH} \sim 27$ e-folds before the end of inflation. This is only an approximation, since this number may be modified by various factors, for example the reheating temperature [92, 96]. We work within Higgs inflation, so the background evolution rate should be that of a radiation dominated universe with a large reheating temperature.

We are moreover interested to find the value of $\beta(M)$, i.e. the mass fraction of the universe that has to collapse into PBHs, for them to be cosmologically significant. For this to be the case, $\beta(M)$ must be of order 10^{-13}, when $M_{\rm PBH} \sim 10^{21}$ g. We then can approximate the required amplitude by eq. (1.87), to be $\mathcal{P}_R \sim 10^{-2}$. Finally, eq. (1.45) gives us an approximate value of $\epsilon_V/\mathcal{A} \simeq \epsilon_{\rm PBH}$. Higgs inflation, followed by a thermal era after reheating, predicts that the pivot scale $k_{\rm CMB} = 0.05$ Mpc^{-1} exits the horizon about 58 e-folds before the end of inflation. We have already noted that in a scenario, such as the one studied here, the e-folds are split between two inflationary stages with N_I and N_{II} e-folds respectively.

When f_I function of the GNMDC is at play, a number of $\lesssim N_I$ e-folds. But then f_{II} is chosen so that the GNMDC's friction effect increases abruptly. This slows the inflaton field immensely, and while this is the case, N_{II} e-folds take place. Finally, the effect of f_{II} passes and f_I takes over again for the remaining of the N_I e-folds. The scalar spectral index's value is what ultimately determines the value that N_I has to have to be observationally consistent. This value can actually be decreased when the running of the running is taken into account [67]. Moreover, the scale M of the GNMDC can be fixed, for a given number of N_I by the CMB normalization.

We shall illustrate this GNMDC's dynamics by an explicit example, solving the MS equation numerically. It was solved for approximately 500 modes, $\mathcal{R}_k$, and the results that correspond to the amplitudes are denoted by a red dot in Fig. 1.10. Indeed, we produce a power spectrum with a high enough peak, to generate a significant abundance of PBHs. The GNMDC parameters chosen

for this particular example are

$$\alpha = 3, \quad M = 7.1 \times 10^{-5} M_{\rm Pl}, \quad d = 5.5 \times 10^{6}, \quad s = 2.1 \times 10^{-10}$$

which yield 50 e-folds between the field values $\phi_{\rm CMB} = 0.0264 \quad M_{\rm Pl}$ and $\phi_{\rm end} = 0.0197 M_{\rm Pl}$. It is specified that the $f_I(\phi) f_{II}(\phi)$ term dominates, at $\phi = 0.02 \quad M_{\rm Pl}$. As discussed, and expected, the inflaton's velocity decreases abruptly. This of course coincides with an equally abrupt decrease of the ϵ parameter. That, in turn, is what creates a sharp peak in the power spectrum, which in our case reaches the value $\mathcal{P}_R(k_{\rm peak}) \sim 2 \times 10^{-2}$ (Figs. 1.9 and 1.10).

Gradually the f_{II} term vanishes and the inflaton rolls for a few more e-folds to the bottom of the potential. Choosing parameters that produce viable spectral index values also can produce PBHs with a mass of roughly 10^{21} grams. Moreover, their total fractional abundance is found[8] to be $f_{\rm PBH} \sim 0.1$, (Fig. 1.10).

It is evident by Fig. 1.10 that the numerical solutions of the MS equation are quite different from the approximate analytic curve of the power spectrum. In fact it is so from a much earlier stage than one might naively expect, since the deviation is evident not only close to the peak, but much earlier, at small wavenumbers k. Indeed, there, parameter ϵ does not change significantly, as demonstrated by Fig. 1.10. But there is a feature of ϵ that is not evident from this graph. ϵ's numerical value in fact oscillates with a tiny amplitude and a very large frequency. The second Hubble-flow parameter is negative, $\epsilon_2 < -2$, before the dramatic decrease of ϵ. Hence the power spectrum will in fact increase from small wavenumbers. Moreover, we note that solving numerically the MS equation in such a context is a quite tedious task with many numerical stability subtleties, nevertheless, this example offers a proof of concept that very large values of the power spectrum $\mathcal{P}_R(k)$ are achievable. However, the creation of PBHs is not our only concern, since we wish to fit a given model to the CMB observables.

In principle we can repeat the same procedure for PBHs with mass $M_{\rm PBH} \sim 10^{35}$ g. Then, according to eq. (1.93), such a mass can be generated if the amplitude gets enhanced at about $N_{\rm PBH} \sim 45$ e-folds before the end of inflation. For their abundance to be significant, a mass fraction $\beta(M) \sim 10^{-7}$ has to collapse into such PBHs. Then, eq. (1.87) is used to find that the required amplitude is $\mathcal{P}_R \sim 1.1 \times 10^{-2}$ and finally we can calculate $\epsilon_V / \mathcal{A}$ from eq. (1.45). We can use the CMB observables to determine all parameters' values here too. The parameter space that corresponds to such a large mass of PBHs, however, does not coincide with that of CMB observables. Nevertheless, the concept still stands, and a different f_{II} function could exist that yields good observables and PBHs of such a mass.

A general note to be made, is that it is, in principle, easier to construct a viable PBH creation model, if the peak takes place at the very end of inflation. This is true because a power spectrum with a peak in smaller scales, is, in general, less constrained by data like microlensing, Hawking radiation and CMB observables.

We have already mentioned that PBHs could be a viable DM candidate [98]. That can be the case if the amplitude of the power spectrum has a peak at the smallest scales or if it becomes blue near the ending stages of inflation. If this is the case, the PBHs will be very light, and should evaporate quickly without having an impact on BBN or CMB observables.

However, when the PBHs evaporate, they don't necessarily leave nothing behind. In fact it is argued that they leave behind a stable mass state, called the *PBH remnant*, with a mass $M_{\rm rem} = \kappa M_{\rm Pl}$ [99, 100], where κ is a factor parameterizing the physics at Planck scales. In this scenario, the spectral index can be inside the 68% CL of Planck 2018. It has been shown [101] that if $\mathcal{P}_R \sim 10^{-3} - 10^{-2}$, then a substantial population of PBH remnants can exist, enough to explain the entirety of DM density in the universe for a wide range of values of the κ parameter. For a general background expansion rate, the fractional abundance of the PBH remnants can be found.

[8] We use the Press-Schechter formalism described earlier (section 1.6.1) with a choice for the threshold parameter $\delta_c \simeq 0.4$, similar to the one suggested by [97].

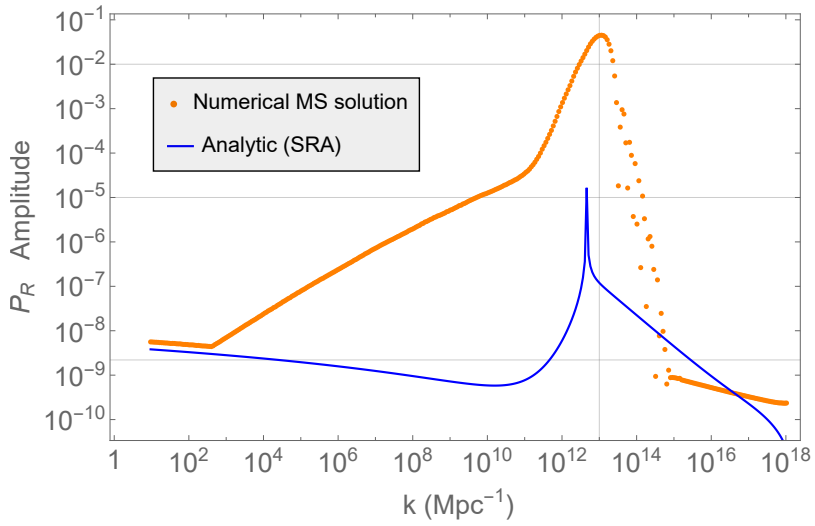

Figure 1.10: *The amplitude of the curvature perturbation $\mathcal{P}_R(k)$. The parameters used are mentioned in the text. The bullet points correspond to numerical results of the Mukhanov-Sasaki equation, while the continuous line corresponds to the approximate results of equation* (1.31)*. It is evident that there is a big deviation between the approximate results and the numerics, a posteriori justifying the use of numerics rather than the approximate analytic approach. For reference we have added grid-lines, to highlight the comparison between the observed value of $\mathcal{P}_\mathcal{R}$ at the pivot scale $k = 0.05 Mpc^{-1}$, and the orders of magnitude that each approach's peak corresponds to (*10^{-5} *and* 10^{-2}*).*

For example, in the case that the remnants are produced during radiation domination, it holds:

$$f_{\rm rem}(M) \simeq \kappa \left(\frac{\beta}{10^{-12}}\right) \left(\frac{\gamma}{0.2}\right)^{\frac{3}{2}} \left(\frac{M}{10^5 {\rm g}}\right)^{-3/2} , \tag{1.106}$$

where M is the original mass of the PBH. Interestingly enough, for large field models, it turns out that small PBHs ($M \sim 10$ g), that correspond to small β values, (10^{-18}) are enough to yield a significant PBH population.

Another way to create mini PBHs is if the power spectrum turns from red to blue, which in our case can be realized simply with a GNMDC term that increases steadily with time, which however poses a problem for reheating, as we discuss below. As an example, we can turn again to the exponential GNMDC considered before, namely,

$$f(\phi) = M^{-2}\, e^{-2\tau\phi}$$

which for specific τ values, could trigger such a generation of PBHs.

Returning to the increasing GNMDC case, we have already discussed that it might be problematic during the reheating stage, (see Section 1.4), where we circumvent the problem by a naturally vanishing $f(\phi)$. But there are other approaches to dealing with reheating instabilities. For example, we can introduce an extra dimension in the field space, so that the system will not end up oscillating around the ϕ direction. This is called *hybrid* inflation [102], and can be visualized as:

$$V_{\rm hyb}(\phi,\chi) = V_0(1-\chi^2/\mu^2)^2 + V(\phi) + \frac{g^2}{2}\chi^2\phi^2 , \tag{1.107}$$

This type of models, can be considered as single field models for the field ϕ. Within this context, inflation can end either due to the end of the slow-roll era, or by the *waterfall* transition of the field χ at a given value $\phi = \phi_c$. These can be realized respectively in the following ways:

$$V(\phi) \gtrsim V_0 \quad \text{and} \quad V(\phi) \ll V_0 \tag{1.108}$$

After the end of inflation, the field that oscillates is χ, which is minimally coupled, and not ϕ which gets stabilized at the value $\phi = 0$. In our case, for an increasing GNMDC, as $\phi \to \phi_c$, the inflaton decelerates and the power spectrum gets enhanced, with the peak existing at ϕ_c where the minimum velocity in the ϕ direction is achieved. When ϕ surpasses value ϕ_c, a (*waterfall*) transition happens for the system which transits in the χ direction and χ is the field that oscillates after inflation.

Another implication that is worth noting is that, the inflationary potential has to be such that the spectral index is in agreement with data, as described before (see Section 1.4). But the PBH remnant scenario can allow potentials without a minimum to be phenomenologically acceptable, since the reheating of the universe can happen due to the evaporation of the PBHs [101].

1.8 Conclusions

Inflation poses as a widely accepted paradigm within which a viable phenomenology can be produced, in light of recent observations. In its context, the initial conditions of a hot BB are provided, and equally importantly, the primordial perturbations described.

Inflation can happen either when a scalar field rolls down a non-steep potential, or alternatively when non canonical kinetic terms are included. Indeed we have concentrated in the study of the $\mathcal{L}_5$ Galileon term, i.e. the term that introduces a non-minimal derivative coupling (NMDC) of the scalar field to gravity, through the Einstein tensor. The simple, field-independent case of $\mathcal{L}_5$ has been studied extensively in many works. It is known to bring about a friction effect, that decelerates the inflaton and thus realizes a slow roll with steeper potentials than what unmodified GR would allow.

Here, we have chosen to study the field dependent case of $\mathcal{L}_5$, that we dubbed GNMDC. This dependence on the field produces a similar in quality, but all around richer, inflationary phenomenology. Interestingly enough, GNMDC inflation can be free from gradient instabilities during the post inflationary oscillations phase, by a suitable choice of the coupling.

Specifically, we derived relations for the CMB observables like the spectral index and the tensor-to-scalar ratio. Moreover, in the context of NMDC, it is known that the squared sound-speed of the scalar perturbations oscillates between positive and negative values. This would create exponentially evolving modes and void the usual analytical results. But within GNMDC inflation this can be alleviated, by suitable forms of the coupling. We have shown that this problem can be significantly ameliorated (Fig. 1.2) or completely avoided during the reheating stage (eq. (1.107)) while at the same time describing inflation with simple, physically motivated potentials.

Indeed, we examined Higgs inflation [25], since the Higgs field is the only scalar discovered in nature [55] so far, as well as an exponential potential, that can successfully drive inflation when GNMDC operates, producing a phenomenology in agreement with the Planck 2018 data [67]. In fact, inflation with an exponential potential and an exponential GNMDC ends naturally, due to the decay of the GNMDC and a kination regime that may follow.

Moreover, we have presented a correspondence between GNMDC and canonical GR inflationary dynamics. It provides a useful, easier, alternative to making predictions of a given GNMDC model, by finding its corresponding canonical model, but also makes model selection and identification through CMB observables possible.

Since GNMDC is affected by the field value, the friction effect can be modified during the course of inflation. An increase of the friction effect, would slow down the inflaton field, at the same

time amplifying the amplitude of the curvature perturbations. But, if the amplitude is sufficiently increased, then the perturbations can collapse producing PBHs. This effect would typically take place due to an inflection point in the potential. However, there can exist specific forms of GNMDC that have this particular effect while the inflaton rolls down a simple potential.

As a demonstration, we carried out PBH production using the Higgs potential. We estimated the abundance of PBHs produced for a couple of benchmark cases, focusing on the interesting case of mass $M \sim 10^{21}$g. A substantial abundance in that mass range can account for all of the DM in the Universe and in order to be more precise, we also presented numerical results.

Another scenario discussed, is that in which the GNMDC demonstrates a steady increase towards the end of inflation. That would trigger the production of mini PBHs and corresponding remnants may be detectable. We aim for suggestive results in order to highlight the richness of phenomenology offered to GNMDC, without going into more complex details (for example non-Gaussian effects).

To summarize, we have studied inflation models with GNMDC, that yield new, distinguishable predictions for inflation, while at the same time posing a more reliable framework than previous similar attempts (NMDC), that also recover GR since the GNMDC vanishes fast after inflation. We elaborated on the implications of an inflaton-affected GNMDC and constructed specific models. Among them, we have shown that there can be cases where the amplitude of the power spectrum of primordial perturbations can be enhanced. If that is the case, at small scales, then the production of PBHs can be triggered. A final attractive feature that we have achieved throughout, is that these models can all happen within the framework of Higgs inflation, and still be completely compatible with current observational results.

Chapter 2

Successful Higgs inflation from combined nonminimal and derivative couplings

2.1 Introduction

A scenario according to which an early exponential expansion of the Universe takes place, offers a particularly good explanation for the initial conditions of a hot Big Bang [103–105]. This description of the very early phases of the Universe (that is generally known as *inflation*) can be studied as the effect of the dynamics of a scalar field that is usually referred to as the *inflaton*. At the same time, observations that are collected through the study of the CMBR offer constraints that become increasingly more accurate, via which we can test the inflationary paradigm, as well as the theory of gravity that operates at such high densities. In the context offered by the inflationary scenario, there has also been a significant effort regarding primordially formed black holes, during a super slow-roll phase, which could be a viable Dark Matter candidate [62–66, 77, 83, 92, 93, 106–109]. Thus, physics surrounding inflation is of great significance to various aspects of our understanding of the birth and formation of the Universe. As such, early-Universe cosmology provides the grounds to test and choose between a rather large number of inflationary models. To identify a viable model, one has to study the dynamics of the full system of the inflaton field and gravity, and compare the results with observations.

To describe the early cosmological evolution according to recent observations, there have been proposed gravity theories that are based on modifications of Einstein's Gravity. A few of the most common ways to modify the General Theory of Relativity, revolve around introducing higher order curvature terms, and/or including scalar fields that are non-minimally coupled to gravity. In fact, higher-order corrections to the Einstein-Hilbert action arise naturally in the gravitational effective action of String Theory [29], that is one of the candidates to become a unifying theory. On the other hand, introducing extra scalar fields, which are, in general, non-minimally coupled to gravity, is a particularly well-studied way to modify GR and results to what is known as scalar-tensor theory [30]. A thoroughly studied scalar-tensor theory is the one obtained via the Horndeski Lagrangian [13]. Theories resulting from this Lagrangian, yield field equations of second order and hence do not produce ghost instabilities [12]. Furthermore, many scalar-tensor theories share a classical Galilean symmetry [31–36, 110].

A simple subclass of Horndeski theories can be obtained with the coupling of a scalar field to the Ricci scalar, which is generally known as Non-Minimal Coupling (NMC). This construction goes beyond the simple case of GR plus a scalar field and can improve the inflationary phenomenology.

In detail, by taking a NMC of the form $\xi\phi^2$, for a large enough scale ξ, the resulting inflationary phase is long enough to satisfy observations [111–115]. In fact, it has been shown that a well-behaved phenomenology is obtained. The tensor to scalar ratio is particularly low, and easily inside the Planck 2018 observational limits. There have also been other works that utilize a different NMC [116]. However, NMC models with large coupling values, albeit very efficient in producing improved inflationary phenomenology, lead to problems related to the unitarity of this theory, exactly due to the large values of their coupling, thus rendering themselves undesirable from a quantum mechanical perspective [117–134], if one considers a single field model. A different picture can be obtained when multi-field theories are taken into account, and it is argued [135, 136] that in such theories these problems do not exist. Moreover, other attempts without unitarity related problems, have been made in a similar context, utilizing a Palatini formulation of gravity [137–139], or by also considering additional interactions [140, 141].

Horndeski theory is, on the other hand, one of the most well-studied frameworks of scalar-tensor theories. A particularly interesting case is the one involving a term corresponding to the non-minimal derivative coupling (NMDC) of the scalar field to the Einstein tensor. This term has notable implications on small scales for black hole physics [38–41, 142–147], as well as dark energy [148, 149] and inflation [37, 42, 150] respectively. Within the inflationary context, the main advantage of NMDC is being free from unitarity problems, leading to the established model of new Higgs inflation [54, 151].

It has been shown, that the NMDC acts as a friction mechanism, therefore allowing for the implementation of a slow-roll phase [42, 43], as well as for inflation with monomial potentials (such as the Standard-Model Higgs) to be realized [25]. In light of the above, it becomes an attractive term within the framework of Horndeski theory. Furthermore, this kind of models can be consistently described within supergravity [44, 45] via the gauge kinematic function [46]. A thorough study of the NMDC predictions was performed in [27], where the dynamics of the inflationary slow-roll phase and the reheating phase were considered. In particular, NMDC oscillations of the inflaton are extremely rapid and remain undamped for a very lengthy period [47–52, 152–154], thus affecting heavy particle production [53]. However, such oscillations, where the NMDC term remains dominant over the GR term, are problematic in terms of the stability of the post-inflationary system, since they lead to oscillations of the squared sound-speed of the perturbations between positive and negative values [51], implying that scalar perturbations are exponentially enhanced.

To avoid this kind of instability, the non-minimal kinetic term has to cease to be dominant or co-leading, when compared to the canonical kinetic term. However, meeting this condition, effectively reduces the model to that of a canonical scalar field in GR, even during the slow-roll period, and the advantages of the NMDC are lost. One can then, generalize the NMDC term in a straightforward manner, since it is a specific case of the Horndeski Lagrangian density, and consider Lagrangians of the form [34, 35, 110]

$$\mathcal{L}_5 = G_5(\phi, X) G^{\mu\nu} \partial_\mu \partial_\nu \phi \ , \tag{2.1}$$

where $X = -\partial_\mu\phi\partial^\mu\phi/2$. By choosing $G_5(\phi, X) = -\phi/(2M^2)$, one obtains the simplest NMDC possible, since after integration by parts the derivative coupling term becomes constant, which as already mentioned, leads to problematic post-inflationary evolution. Instead, in [155] it was shown that by choosing a more general function $G_5(\phi, X) = G(\phi)\,\xi(X)$, the phenomenology of the corresponding terms becomes richer, both during inflation and reheating stages.

If $G(\phi) \propto \phi$ then the Generalized NMDC term (GNMDC) quickly vanishes when the inflaton approaches the minimum of the potential. The system, after a few oscillations, transitions to the dynamics of a canonical kinetic term in GR, leading to a more desirable behavior, dominated by GR dynamics during the reheating stage. It has been shown that with this kind of term, the phenomenology generated in a Higgs potential is in good agreement with observations. Furthermore, tight bounds on the speed of GWs extracted by recent observations [1, 56, 59] and from solar system constraints [156], were dismissive of the NMDC [2, 58]. A NMDC term playing the role of dark

energy can produce superluminal tensor perturbations [25, 57] in FLRW cosmological backgrounds but a GNMDC of the form $G(\phi) \propto \phi$ can heal this problem, since after the end of Slow Roll inflation it decouples from the dynamics of the system. It was also shown that the squared sound-speed was not completely healed of the oscillations between positive and negative values, albeit significantly improved in comparison to NMDC results. One then, is led to seek for further modifications that are able to entirely heal the non-canonical kinetic term theories of this form, from sound-speed related instabilities, and possibly further improve the observable predictions.

The motivation of this work is based on the remarks above, according to which neither NMC nor NMDC scenarios are completely free of disadvantages if a desirable phenomenology is to be achieved. We are, thus, interested in investigating a simple combination of the NMC and GNMDC terms, that could alleviate the problems of both of these standalone modifications. In particular, the GNMDC's gravitational friction effect will be shown to allow for the ξ and ϕ_* to be low enough to not violate unitarity, while the NMC term's domination at late times ensures that no sound-speed related instabilities will occur. Moreover, a lowering of the tensor-to-scalar ratio of this theory is obtained when comparing to the GNMDC case.

This work is organized as follows: In Section 2.2 we analyze basic results of each of the NMC and GNMDC terms as standalone modifications of GR. In Section 2.3, we build the combined scenario of inflation in the presence of both the NMC and GNMDC terms. In Section 2.4 we proceed to a detailed numerical investigation of an inflaton in a Higgs potential, for a variety of interesting cases, through which the advantages of the combined scenario summarized in Section 2.5, become clear.

2.2 Non-minimal coupling and generalized non-minimal derivative coupling as standalone modifications

We now present a synopsis of inflationary models that result from the General Theory of Relativity plus a non-minimal coupling term (GR+NMC), and from general relativity plus a generalized non minimal derivative coupling term (GR+GNMDC).

To successfully build inflationary models it is of great importance to perturbatively study their effects, since each model provides a rich phenomenology related to scalar and tensor perturbations. In order to test their viability, one compares the predictions of a variety of quantities with the corresponding observed values, obtained through CMBR. Observable quantities, include the power spectrum of the scalar perturbations, $\mathcal{P}_{\mathcal{R}}$, the scalar spectral index, or scalar tilt, n_s, and the tensor-to-scalar perturbations ratio r, while a specific amount of e-folds is also required in order for the horizon and flatness problems to be solved. In Appendix B one can find a review of the usual steps taken in this direction. Full single-field perturbations' analysis has been performed in a number of works, e.g. in [26, 51, 94].

2.2.1 Inflation with nonminimal coupling

GR+NMC's action can be written in the form

$$S = \int d^4x\sqrt{-g}\left[f(\phi)R - \frac{\partial_\mu\phi\partial^\mu\phi}{2} - V(\phi)\right], \tag{2.2}$$

The most studied coupling of this form in the literature is $f(\phi) = \xi\phi^2$. NMC as a standalone modification to GR, when taking the form $f(\phi) = \xi\phi^2$ in a monomial (Higgs) potential, has been shown to produce remarkably low r ratio values. It is also notable that it has no post-inflationary instability issues, since c_s^2 is identically equal to 1, regardless of the form of the NMC. However, as already mentioned, it does not preserve unitarity and thus is problematic from a quantum-mechanical point of view, since the term $\xi\phi^2$ takes values larger than M_{Pl} in order to yield a long enough inflation [117–133].

The metric to be considered here is that of a homogeneous and isotropic flat FRW geometry:

$$ds^2 = -dt^2 + a^2(t)\delta_{ij}dx^i dx^j \,, \tag{2.3}$$

where $a(t)$ is the scale factor. The resulting Friedmann equations are:

$$3M_{Pl}^2 H^2 = V(\phi) + \frac{\dot{\phi}^2}{2} - 6\xi\left[f(\phi)H^2 + f'(\phi)\dot{\phi}H\right], \tag{2.4}$$

$$M_{Pl}^2(2\dot{H}+3H^2) = V(\phi) - \xi\left[2\dot{\phi}^2 f''(\phi) + 4H\dot{\phi}f'(\phi) + 2\ddot{\phi}f'(\phi) + 4\,f(\phi)\dot{H} + 6H^2 f(\phi)\right] - \frac{\dot{\phi}^2}{2}, \tag{2.5}$$

and the Klein-Gordon equation reads as:

$$\ddot{\phi} + 3H\dot{\phi} - 6\xi f'(\phi)\left(\dot{H}+2H^2\right) + V'(\phi) = 0 \,. \tag{2.6}$$

In order to calculate the inflationary observables, a usual approach is to perform a conformal transformation, thus passing to the Einstein frame. We choose: $\hat{g}_{\mu\nu} = \Omega^2(x)g_{\mu\nu}$, with:

$$\Omega^2(x) = \frac{16\pi}{M_{Pl}^2}f(\phi) \,,$$

and define a new scalar field φ and potential U such that:

$$\frac{d\varphi}{d\phi} \equiv \sqrt{\frac{M_{Pl}^2}{8\pi}\frac{f(\phi)+3f'^2(\phi)}{2f^2(\phi)}} \,, \qquad U(\varphi) \equiv \Omega^{-4}V(\phi) \,,$$

bringing the action to the Einstein-frame equivalent form:

$$S = \int d^4x\sqrt{-\hat{g}}\left[\frac{M_{Pl}^2}{2}\hat{R} - \frac{\partial_\mu\varphi\partial^\mu\varphi}{2} - U(\varphi)\right] \,, \tag{2.7}$$

The quantities in the Einstein frame are denoted with a hat.

To first order, it has been shown that the spectral index and tensor-to-scalar ratio can be expressed as [105]:

$$1 - n_s = 6\epsilon_U - 2\delta_U \,, \qquad r = 16\epsilon_U \,, \tag{2.8}$$

where we define the slow-roll parameters:

$$\epsilon_U = \frac{M_{Pl}^2}{2}\left(\frac{U'}{U}\right) \,, \qquad \delta_U = M_{Pl}^2\frac{U''}{U} \,. \tag{2.9}$$

It can also be shown that for an arbitrary coupling $f(\phi)$ the c_s^2 of this scenario is identically equal to 1, by simple replacement of the above equations into (B.15).

We note that in the Einstein frame, the potential U is essentially flat for large values of the NMC term ($\xi\phi^2 \gg M_{Pl}$), hence the field rolls slowly and parameters ϵ_U and δ_U are very small, yielding a correspondingly small r.

This conclusion encompasses one of the basic results of single field, NMC, Higgs inflation with the coupling form $f(\phi) = \phi^2$. However, as mentioned above, these attractive features of a very low r and a long inflation, come at the cost of $\xi\phi^2 > M_{Pl}$, leading to non-unitarity. To solve this problem, one should consider other forms of couplings of the scalar field to gravity, like the one described in the next section.

2.2.2 Inflation with non minimal derivative coupling

The scenario according to which the generalized non minimal derivative coupling is a stand-alone modification to GR is presented here. As discussed, within the framework of Horndeski theories non minimal derivative coupling (NMDC) holds a particular position, due to the "gravitational friction", i.e. the phenomenon according to which the inflaton field, when rolling down a potential, stays in slow roll for a significantly lengthier period as compared to GR, resulting in a rich phenomenology, studied extensively in the literature [25, 47–52, 154, 157].

However, it has also been argued that a standalone NMDC modification to GR creates post-inflationary instabilities, because the NMDC term remains dominant after the slow-roll period leading to $c_s^2 < 0$. Then, a further intuitive modification, dubbed generalized non minimal derivative coupling (GNMDC) was proposed in [110, 155]. When the derivative coupling with the Einstein tensor is of the form $G(\phi)\partial_\mu\phi\partial_\nu\phi G^{\mu\nu}$, then this is significantly ameliorated.

Specifically, the corresponding action can be written in the form:

$$S = \int d^4x\sqrt{-g}\left[\frac{M_{Pl}^2}{2}R + G_5(\phi, X)G^{\mu\nu}\partial_\mu\partial_\nu\phi - V(\phi)\right] , \tag{2.10}$$

where $G^{\mu\nu}$ is the Einstein tensor. By considering only a ϕ-dependence of the G_5 function, the Friedmann equations of this scenario take up the form [110, 155]:

$$3M_{Pl}^2H^2 = 9H^2G(\phi)\dot{\phi}^2 + \frac{1}{2}\dot{\phi}^2 + V(\phi) , \tag{2.11}$$

$$M_{Pl}^2(2\dot{H} + 3H^2) = V(\phi) - \frac{\dot{\phi}^2}{2} + 2H\dot{\phi}^3G'(\phi) + G(\phi)\left(2\dot{H}\dot{\phi}^2 + 3H^2\dot{\phi}^2 + 4H\dot{\phi}\ddot{\phi}\right) , \tag{2.12}$$

while the Klein-Gordon equation reads:

$$\ddot{\phi} + V'(\phi) + 3H\dot{\phi} + 3H^2\dot{\phi}^2G'(\phi) + G(\phi)\left(12HH'\dot{\phi} + 6H^2\ddot{\phi} + 18H^3\dot{\phi}\right) = 0 . \tag{2.13}$$

We note that the function $G(\phi)$ results from G_5, by integrating by parts, namely $G(\phi) = -G_5'(\phi)$.

The gravitational friction effect offers the ground for very efficient inflationary predictions, because the slow-roll conditions can be easily satisfied. To investigate inflation in the slow-roll approximation we define the standard slow-roll parameters:

$$\epsilon = -\frac{\dot{H}}{H^2} , \qquad \delta = \frac{\ddot{\phi}}{H\dot{\phi}} , \tag{2.14}$$

as well as the slow roll parameters expressed with respect to the potential:

$$\epsilon_V = \frac{M_{Pl}^2}{2}\left(\frac{V'}{V}\right)^2 , \qquad \eta_V \equiv \frac{M_{Pl}^2}{2}\frac{V''}{V} . \tag{2.15}$$

Slow-roll approximation holds when $\epsilon \ll 1$ and $\delta \ll 1$, thus $\dot{H} \ll H^2$ and $\ddot{\phi} \ll 3H\dot{\phi}$. In this case the Friedmann equations (2.11), (2.13) are simplified to:

$$3M_{Pl}^2H^2 \approx V(\phi) , \tag{2.16}$$

$$3H\dot{\phi}\left[1 + 6G(\phi)H^2 + G'(\phi)H\dot{\phi}\right] + V'(\phi) \approx 0 . \tag{2.17}$$

Under the slow-roll approximation, the first slow-roll parameter, ϵ, can thus be written in the form:

$$\epsilon \approx \epsilon_{\rm GR} + \epsilon_D + \epsilon_{\mathcal{B}} \ , \tag{2.18}$$

where

$$\epsilon_D \equiv \frac{3G(\phi)\dot{\phi}^2}{M_{Pl}^2} \ , \qquad \epsilon_{\mathcal{B}} \equiv \frac{\dot{\phi}^2}{M_{Pl}^2 H^2} G'(\phi) H \dot{\phi} \ , \tag{2.19}$$

These correspond to ϵ_{G1} and ϵ_{G4} of equation (2.44) that we use later. Furthermore:

$$\epsilon_{\rm GR} \equiv \frac{\dot{\phi}^2}{2M_{Pl}^2 H^2} \ , \tag{2.20}$$

where quantity $\epsilon_{\rm GR}$ corresponds to the GR case, while ϵ_D is the leading term during slow-roll.

The GNMDC term decreases the ϵ parameter and hence increases the slow-roll era. In fact, in the slow-roll approximation, equation (2.18) is brought to the form:

$$\epsilon = \epsilon_V \frac{\mathcal{A} - 2\mathcal{B}}{(\mathcal{A} + \mathcal{B})^2} \ , \tag{2.21}$$

with $\mathcal{A} \equiv 1 + 6H^2 G(\phi)$ and $\mathcal{B} \equiv G'(\phi) H \dot{\phi}$.

Regarding the squared sound-speed of scalar perturbations, one can express it in the form [155]:

$$c_s^2 = \left[1 - \frac{\epsilon_D}{3} + 6H^2 G(\phi)(1+\epsilon_D)\right]^{-1} \cdot \left\{ 1 + \epsilon_D + 6H^2 G(\phi) \left[1 + \epsilon_D + \frac{4\epsilon_D(1-\epsilon_D)}{3(3-\epsilon_D)}\right] \right.$$
$$\left. + 12\dot{H} G(\phi) \left(1 - \frac{\epsilon_D}{3}\right) \right\} \tag{2.22}$$

We can also approximate the number of e-folds as [155]:

$$N \approx \frac{1}{M_{Pl}} \int_{\phi_{end}}^{\phi} \frac{\mathcal{A} + \mathcal{B}}{\sqrt{2\epsilon_V}} d\phi \ . \tag{2.23}$$

One sees that for $G(\phi) \to 0$ all above expressions restore the canonical case. Concerning the inflationary observables, the power spectrum of scalar perturbations is of the form [155]:

$$\mathcal{P}_R = \frac{H^2}{8\pi^2 M_{Pl}^2 \epsilon_V} \left[\mathcal{A} + \mathcal{B} + \mathcal{O}\left(\frac{\mathcal{B}^2}{\mathcal{A}}\right)\right] \ , \tag{2.24}$$

while the scalar spectral index becomes:

$$1 - n_s \approx 8\epsilon - 2\eta + \epsilon M_{Pl} \frac{G'(\phi)}{G(\phi)} \sqrt{\frac{2}{\epsilon_V}} \ , \tag{2.25}$$

where $\eta \equiv \frac{\eta_V}{\mathcal{A}}$. The tensor-to-scalar ratio can be written as:

$$r = 16 \frac{\epsilon_V}{\mathcal{A} + \mathcal{B}} \ . \tag{2.26}$$

Considering a specific model of GNMDC, we focus on the case:

$$G(\phi) = \frac{\alpha \phi^{\alpha - 1}}{2M^{\alpha+1}}, \tag{2.27}$$

recovering the simple NMDC for $\alpha = 1$. In the context of this particular term, when α becomes larger, the post-inflationary instabilities related to $c_s^2 < 0$ become remarkably shorter as compared to the $(\alpha = 1)$ case, resulting from the fact that near the bottom of the potential the GNMDC term decouples and GR takes over as the dominant term. This in turn results from the fact that the more the α parameter grows, the more dominant is the gravitational friction effect, allowing the scale of the theory $\frac{1}{M^{\alpha+1}}$ to decrease significantly.

It is also shown that, for a given value of the scalar power spectrum $\mathcal{P}_\mathcal{R}$, while a growing α parameter ameliorates the c_s^2-instability problem, it also affects the values of the spectral index n_s and tensor-to-scalar ratio. While r becomes smaller, n_s increases and tends to the outside of the Planck 2018 likelihood contours, if one seeks to build a 60 e-fold model [155], though, going beyond tree level calculations, can affect the predictions of a given model [158].

2.3 Non minimal coupling and generalized non minimal derivative coupling combined

We previously presented the realization of each of the standalone modifications to GR, namely NMC and GNMDC. NMC leads to observables in good agreement with observations, however it suffers from unitarity problems, while $\alpha = 1$ GNMDC solves the unitarity violation but leads to c_s^2-instabilities. Changing the α parameter, $\alpha > 1$ GNMDC solves the unitarity, but only ameliorates the c_s^2 issues while making observable predictions less attractive, regarding the spectral index.

Keeping the above in mind, we now construct the combination of the scenarios of NMC and GNMDC, intending to maintain their separate advantages while removing the corresponding disadvantages.

2.3.1 The model

We consider the combined action:

$$S = \int d^4x\sqrt{-g}\left[\mathcal{L}_{GR} + \mathcal{L}_\phi + \mathcal{L}_{NMC} + \mathcal{L}_{GNMDC}\right], \tag{2.28}$$

with

$$\begin{aligned} \mathcal{L}_{GR} &= \frac{M_{Pl}^2}{2}R\ , \qquad \mathcal{L}_\phi = -\frac{1}{2}g^{\mu\nu}\partial_\mu\phi\partial_\nu\phi - V(\phi)\ , \\ \mathcal{L}_{NMC} &= \xi f(\phi)R\ , \qquad \mathcal{L}_{GNMDC} = G(\phi)G^{\mu\nu}\partial_\mu\phi\partial_\nu\phi\ . \end{aligned} \tag{2.29}$$

Varying with respect to the metric, gives rise to the field equations as:

$$G_{\mu\nu} = \frac{1}{M_{Pl}^2}\left[T_{\mu\nu}^{(\phi)} + \xi T_{\mu\nu}^{(NMC)} - 2G(\phi)T_{\mu\nu}^{(NMDC1)} - G'(\phi)T_{\mu\nu}^{(NMDC2)}\right]\ , \tag{2.30}$$

while varying with respect to the scalar field leads to:

$$\Box\phi - G_{\mu\nu}\left[2G(\phi)\nabla^\mu\nabla^\nu\phi + G'(\phi)\nabla^\mu\phi\nabla^\nu\phi\right] + \xi f'(\phi)R - V'(\phi) = 0\ , \tag{2.31}$$

where:

$$T_{\mu\nu}^{(\phi)} = \nabla_\mu\phi\nabla_\nu\phi - \frac{1}{2}g_{\mu\nu}\nabla_\lambda\phi\nabla^\lambda\phi - g_{\mu\nu}V(\phi)\ , \tag{2.32}$$

$$T_{\mu\nu}^{(NMC)} = -2f(\phi)\left[R_{\mu\nu} - \frac{1}{2}g_{\mu\nu}R\right] - 2f'(\phi)\left[g_{\mu\nu}\Box\phi - \nabla_\mu\nabla_\nu\phi\right] - 2f''(\phi)\left[g_{\mu\nu}\nabla_\lambda\phi\nabla^\lambda\phi - \nabla_\mu\phi\nabla_\nu\phi\right] \tag{2.33}$$

$$T_{\mu\nu}^{(NMDC1)} = 4R^{\lambda}_{(\mu}\nabla_{\nu)}\phi\nabla_{\lambda}\phi - G_{\mu\nu}\nabla_{\lambda}\phi\nabla^{\lambda}\phi + 2[\nabla^{\kappa}\phi\nabla^{\lambda}\phi R_{\mu\kappa\nu\lambda} + \nabla_{\mu}\nabla^{\lambda}\phi\nabla_{\nu}\nabla_{\lambda}\phi - \nabla_{\nu}\nabla_{\mu}\phi\nabla^{2}\phi] + g_{\mu\nu}[\nabla^{2}\phi\nabla^{2}\phi - \nabla_{\kappa}\nabla_{\lambda}\phi\nabla^{\kappa}\nabla^{\lambda}\phi - 2R_{\kappa\lambda}\nabla^{\kappa}\phi\nabla^{\lambda}\phi] - \nabla_{\mu}\phi\nabla_{\nu}\phi R \ , \tag{2.34}$$

$$T_{\mu\nu}^{(NMDC2)} = g_{\mu\nu}(\nabla_{\lambda}\phi\nabla^{\lambda}\phi\nabla^{2}\phi - \nabla^{\kappa}\phi\nabla^{\lambda}\phi\nabla_{\kappa}\nabla_{\lambda}\phi) + 2\nabla^{\lambda}\phi\nabla_{(\mu}\phi\nabla_{\nu)}\nabla_{\lambda}\phi - \nabla_{\lambda}\phi\nabla^{\lambda}\phi\nabla_{\nu}\nabla_{\mu}\phi - \nabla_{\mu}\phi\nabla_{\nu}\phi\nabla^{2}\phi \ , \tag{2.35}$$

The indices in parentheses denote symmetrization. For $G(\phi) \to 0$ we recover the GR+NMC case, while $f(\phi) \to 0$ recovers the GR+GNMDC case.

For a FLRW metric (2.3) we extract the two Friedmann equations:

$$\rho_{\phi} \equiv 3M_{Pl}^{2}H^{2} = \frac{\dot{\phi}^{2}}{2} + V(\phi) + 9G(\phi)H^{2}\dot{\phi}^{2} - 6\xi\left[f(\phi)H^{2} + f'(\phi)\dot{\phi}H\right], \tag{2.36}$$

and:

$$-p_{\phi} \equiv M_{Pl}^{2}\left(3H^{2} + 2\dot{H}\right) = V(\phi) - \frac{\dot{\phi}^{2}}{2} + G(\phi)\left(3H^{2}\dot{\phi}^{2} + 2\dot{H}\dot{\phi}^{2} + 4H\dot{\phi}\ddot{\phi}\right) + 2G'(\phi)H\dot{\phi}^{3} - 2\xi\left[3f(\phi)H^{2} + 2f(\phi)\dot{H} + 2Hf'(\phi)\dot{\phi} + \dot{\phi}^{2}f''(\phi) + f'(\phi)\ddot{\phi}\right], \tag{2.37}$$

where for convenience the effective energy density (ρ_{ϕ}) and pressure (p_{ϕ}) of the scalar field are introduced. Klein-Gordon equation (2.31) becomes:

$$\ddot{\phi}\left(1 + 6G(\phi)H^{2}\right) + 3H\dot{\phi}(1 + 6G(\phi)H^{2} + 4G(\phi)\dot{H}) + 3H^{2}G'(\phi)\dot{\phi}^{2} - 6\xi f'(\phi)(\dot{H} + 2H^{2}) + V'(\phi) = 0 \tag{2.38}$$

By combining the above equations, one sees that in order for the scalar field to obtain real values, quantity

$$\mathcal{Q} \equiv 6\xi^{2}\dot{\phi}^{2}f'(\phi)^{2} + \xi\left(2f(\phi)\dot{\phi}^{2} + 4f(\phi)V(\phi)\right) + G(\phi)\left(-3\dot{\phi}^{4} - 6\dot{\phi}^{2}V(\phi)\right) + M_{Pl}^{2}\dot{\phi}^{2} + 2M_{Pl}^{2}V(\phi) \ , \tag{2.39}$$

must be positive.

2.3.2 Slow Roll Inflation and the three regimes

From a theoretical point of view, when one investigates a theory combining two different terms, one expects that there will be three different regimes to study, depending on the relative magnitude: one where GNMDC is dominating, one where NMC dominates, and finally a regime where the two terms are approximately of the same order. Before we discuss each one individually, and to facilitate the following discussion, we first provide the slow-roll framework of this theory.

In the slow-roll approach, that is, when $\dot{H} \ll H^{2}$, $\dot{\phi} \ll H$, and $\ddot{\phi} \ll 3H\dot{\phi}$, keeping the leading terms of GNMDC and NMC, the first Friedmann equation (2.36) can be written as:

$$3M_{Pl}^{2}H^{2} = 9G(\phi)H^{2}\dot{\phi}^{2} - 6\xi f(\phi)H^{2} + V(\phi) \ , \tag{2.40}$$

while the scalar field's equation, (2.38), is simplified, taking the form:

$$3H\dot{\phi}\left(1 + 6G(\phi)H^{2}\right) - 12H^{2}\xi f'(\phi) + V'(\phi) = 0 \ . \tag{2.41}$$

Hence for (2.41) we have disregarded the terms coupled to $\ddot{\phi}$, the GNMDC term coupled to $\dot{\phi}^{2}$ and the terms that add $\dot{H}$ to H^{2}, since $\epsilon \ll 1$. Likewise, for (2.40) we have disregarded the $\dot{\phi}^{2}/2$ term as compared to the GNMDC term coupled to $\dot{\phi}^{2}$, as well as the term $f'(\phi)\dot{\phi}H$ as compared to $f(\phi)H^{2}$.

The argument for the latter approximation is as follows: In a SR scenario typically the scale factor changes exponentially while the scalar field rolls very slowly down the potential well. Hence, it is safe to suppose that $\dot{\phi} \ll H$. Regarding $f'(\phi)$ and $f(\phi)$, since the focus here is in monomial forms of $f(\phi)$, which yield $f'(\phi) > f(\phi)$ in the small field scenarios ($\phi < M_{Pl}$), one can see that the difference is less important than the one between $\dot{\phi}$ and H due to the slow-roll. Hence we only keep the $f(\phi)H^2$ term. The numerical analysis that follows will support the above argument, see Fig. 2.3.

Through equations (2.36) and (2.37) one obtains the exact form of the parameter $\epsilon = -\frac{\dot{H}}{H^2}$ as:

$$\epsilon = \epsilon_{GR} + \epsilon_{G1} + \epsilon_{G2} + \epsilon_{G3} + \epsilon_{G4} + \epsilon_{N1} + \epsilon_{N2} + \epsilon_{N3} + \epsilon_{N4} \ , \tag{2.42}$$

where a number of auxiliary slow roll parameters are introduced. For the GR sector we have:

$$\epsilon_{GR} = \frac{\dot{\phi}^2}{2M_{Pl}^2 H^2} \ ,$$

For the GNMDC sector we define:

$$\begin{aligned} \epsilon_{G1} &= \frac{3\dot{\phi}^2 G(\phi)}{M_{Pl}^2} \ , \qquad \epsilon_{G2} = -\frac{\dot{\phi}^2 \dot{H} G(\phi)}{M_{Pl}^2 H^2} \ , \\ \epsilon_{G3} &= -\frac{2\dot{\phi}\ddot{\phi} G(\phi)}{M_{Pl}^2 H} \ , \qquad \epsilon_{G4} = -\frac{G'(\phi)\dot{\phi}^3}{M_{Pl}^2 H} \ , \end{aligned} \tag{2.43}$$

while for the NMC sector we have:

$$\begin{aligned} \epsilon_{N1} &= \frac{2\xi f(\phi)\dot{H}}{M_{Pl}^2 H^2} \ , \qquad \epsilon_{N2} = -\frac{\xi f'(\phi)\dot{\phi}}{M_{Pl}^2 H} \ , \\ \epsilon_{N3} &= \frac{\dot{\phi}^2 \xi f''(\phi)}{M_{Pl}^2 H^2} \ , \qquad \epsilon_{N4} = \frac{\xi f'(\phi)\ddot{\phi}}{M_{Pl}^2 H^2} \ . \end{aligned} \tag{2.44}$$

The above parameters will be used to quantify which term of the theory dominates. In particular the ϵ_{Gi} are related to GNMDC and ϵ_{Ni} are related to the NMC (index i runs from 1 to 4). ϵ_{GR} is the usual slow-roll parameter of the minimally coupled, single-field scenario of inflation. The previous discussion has shown that in the slow-roll era the only important terms should be ϵ_{G1}, ϵ_{N1} and ϵ_{N2}.

Having defined the above, we now move on to calculate the perturbative functions, as functions of the auxiliary parameters. By use of the definitions in Appendix B we find:

$$\mathcal{G}_T = M_{Pl}^2 \left(1 - \frac{\epsilon_{G1}}{3} - \frac{\epsilon_{N1}}{\epsilon}\right), \qquad \mathcal{F}_T = M_{Pl}^2 \left(1 + \frac{\epsilon_{G1}}{3} - \frac{\epsilon_{N1}}{\epsilon}\right) \ , \tag{2.45}$$

$$\Sigma = M_{Pl}^2 H^2 \left(\epsilon_{GR} + 6\epsilon_{G1} + 6\epsilon_{N2} + 3\frac{\epsilon_{N1}}{\epsilon} - 3\right), \qquad \Theta = M_{Pl}^2 H (1 - \epsilon_{G1} - \epsilon_{N2} - \frac{\epsilon_{N1}}{\epsilon}) \ , \tag{2.46}$$

$$\begin{aligned} \mathcal{G}_s = &- \frac{M_{Pl}^2}{9} \left[\epsilon_{N1} + \epsilon(\epsilon_{G1} + \epsilon_{N2} - 1)\right]^{-2} \left[\epsilon(\epsilon_{G1} - 3) + 3\epsilon_{N1}\right] \{-3\epsilon_{N1}(\epsilon_{G1} + \epsilon_{GR}) \\ &+\epsilon \left[3\epsilon_{G1}^2 + 3\epsilon_{GR} + 9\epsilon_{N2}^2 + \epsilon_{G1}(3 - \epsilon_{GR} + 12\epsilon_{N2})\right]\} , \end{aligned} \tag{2.47}$$

$$\begin{aligned} \mathcal{F}_s = &- \frac{M_{Pl}^2}{9[\epsilon(\epsilon_{G1} + \epsilon_{N2} - 1) + \epsilon_{N1}]^2} \Big\{ \epsilon^2 \left\{ \epsilon_{G1}^2 \left[7\epsilon_{N1} + 17\epsilon_{N2} + \epsilon_{N3} - 4 \ -3\left(\epsilon_{G3} + \epsilon_{G4} + \epsilon_{N4}\right) - 4\right] \right. \\ &+ 4\epsilon_{G1}^3 + 3\epsilon_{G1} \left[2\epsilon_{G3} - 2\epsilon_{G4}(\epsilon_{N2} - 1) - 10\epsilon_{N1} \ -2\epsilon_{N3} + 5\epsilon_{N2}(\epsilon_{N2} - 2) + 2\epsilon_{N4}\right] + 9\left(2\epsilon_{G4}\epsilon_{N2}\right. \\ &\left. \left. +\epsilon_{G3} + \epsilon_{G4} + 3\epsilon_{N1} - 3\epsilon_{N2}^2 + \epsilon_{N2} + \epsilon_{N3} + \epsilon_{N4}\right)\right\} + \epsilon\epsilon_{N1} \left[\epsilon_{G1}(-6\epsilon_{G3} - 6\epsilon_{G4} + 15\epsilon_{N1} + 30\epsilon_{N2}\right. \\ &+6\epsilon_{N3} - 6\epsilon_{N4}) - 9\left(2\epsilon_{G3} + 2\epsilon_{G4}(\epsilon_{N2} + 1) + 3\epsilon_{N1} \ \ +2(\epsilon_{N2} + \epsilon_{N3} + \epsilon_{N4}) - 3\epsilon_{N2}^2\right) + 4\epsilon_{G1}^2\Big] \\ &\left. + \epsilon^3(\epsilon_{G1} - 3)^2(\epsilon_{G1} - 1) + 9\epsilon_{N1}^2(\epsilon - \epsilon_{GR} - \epsilon_{G1} - \epsilon_{G2})\right\}. \end{aligned} \tag{2.48}$$

As we argued before, one of the most important quantities to be studied in order to check the viability of a cosmological model, is the squared sound-speed of the perturbations. We insert the above equations into the defining equation of the sound-speed, (B.15), and obtain the exact expression in terms of the *epsilon* parameters:

$$
\begin{aligned}
c_s^2 = &\left\{\epsilon\left[\epsilon_{G1}(12\epsilon_{N2}-\epsilon_{GR}+3)+3\left(\epsilon_{G1}^2+\epsilon_{GR}+3\epsilon_{N2}^2\right)\right]\ -3\epsilon_{N1}(\epsilon_{G1}+\epsilon_{GR})\right\}^{-1}\left[\epsilon(\epsilon_{G1}-3)+3\epsilon_{N1}\right]^{-1}\\
&\Big\{\epsilon^2\left\{\epsilon_{G1}^2\left[7\epsilon_{N1}+17\epsilon_{N2}+\epsilon_{N3}\ -3\left(\epsilon_{G3}-\epsilon_{G4}-\epsilon_{N4}\right)-4\right]+3\epsilon_{G1}\left[5(\epsilon_{N2}-2)\epsilon_{N2}-2\epsilon_{G4}(\epsilon_{N2}-1)\right.\right.\\
&-10\epsilon_{N1}+2\left(\epsilon_{G3}-\epsilon_{N3}+\epsilon_{N4}\right)\Big]+4\epsilon_{G1}^3+9\left(\epsilon_{G3}+2\epsilon_{G4}\epsilon_{N2}+\epsilon_{G4}+3\epsilon_{N1}\ -3\epsilon_{N2}^2+\epsilon_{N2}+\epsilon_{N3}\right.\\
&\left.+\epsilon_{N4}\right)\Big\}+\epsilon\epsilon_{N1}\left\{\epsilon_{G1}\left[6\left(\epsilon_{N3}-\epsilon_{G3}-\epsilon_{G4}-\epsilon_{N4}\right)\ +15\epsilon_{N1}+30\epsilon_{N2}\right]+4\epsilon_{G1}^2-9\left[2\epsilon_{G3}+3\epsilon_{N1}\right.\right.\\
&\left.\left.+2\epsilon_{G4}(\epsilon_{N2}+1)+2(\epsilon_{N2}+\epsilon_{N3}+\epsilon_{N4})-3\epsilon_{N2}^2\right]\right\}+\epsilon^3(\epsilon_{G1}-3)^2(\epsilon_{G1}-1)+9\epsilon_{N1}^2(\epsilon_{G3}+\epsilon_{G4}\\
&\left.+\epsilon_{N1}+\epsilon_{N2}+\epsilon_{N3}+\epsilon_{N4})\right\}
\end{aligned}
\tag{2.49}
$$

It is interesting to check its various limits. We begin with the GR limit, where $\epsilon_{Gi},\ \epsilon_{Ni}\to 0$, and see that c_s^2 becomes identically equal to 1 as expected. The same result is obtained in the NMC limit, where $\epsilon_{Gi}\to 0$, again as we expected. Lastly, in the GNMDC limit, where $\epsilon_{Ni}\to 0$, we get:

$$
\begin{aligned}
c_s^2 = &\frac{1}{(\epsilon_{G1}-3)(3\epsilon_{G1}(\epsilon_{G1}+1)-(\epsilon_{G1}-3)\epsilon_{GR})}\cdot\\
&\cdot\left\{\epsilon(\epsilon_{G1}-1)(\epsilon_{G1}-3)^2+9(\epsilon_{G3}+\epsilon_{G4})\ +\ \epsilon_{G1}\left[\epsilon_{G1}(4\epsilon_{G1}-3\epsilon_{G3}-3\epsilon_{G4}-4)+6(\epsilon_{G3}+\epsilon_{G4})\right]\right\},
\end{aligned}
\tag{2.50}
$$

which by use of the definitions (2.44) gives expression (2.22).

In general, we want to extract more information about the behavior of the full equation (2.49). By a tedious manipulation of this equation there is a clear note that one can make. Using equation (2.42), to substitute ϵ with the auxiliary ϵ functions, one ends up with the following expression:

$$
c_s^2-1\approx\frac{\mathcal{O}(\epsilon_{Gi})}{f_\epsilon(\epsilon_{Ni},\epsilon_{GR})+\mathcal{O}(\epsilon_{Gi})},
\tag{2.51}
$$

where f_ϵ is a function that does not depend on the ϵ_{Gi} parameters, while $\mathcal{O}(\epsilon_{Gi})$ is a function at least of first order in ϵ_{Gi}. Hence, the denominator of the fraction is of greater order when compared to the numerator, when Slow Roll has ended and the NMC terms take over, as long as the derivative coupling chosen, vanishes towards the bottom of the potential. This leads to $c_s^2\equiv 1$, which is one of the main results of this work: Including NMC and a vanishing ϕ-dependent GNMDC, regardless of its exact form, can have the effect of completely healing the c_s^2 instabilities of derivative coupling (see Fig. 2.2 for the corresponding numerical results). This is to be expected since the NMC term has a sound speed equal to 1 and it remains dominant after the end of the slow roll, unlike GNMDC.

On the same footing, using the same reasoning with equation (2.50), one can show that in the GNMDC limit one acquires:

$$
c_s^2-1\approx\frac{\mathcal{O}(\epsilon_{Gi})}{\mathcal{O}(\epsilon_{Gi})}.
\tag{2.52}
$$

In this case, the fraction, is clearly non-zero in general, and can actually be both larger or smaller than 1. This reconfirms the results of [155], regarding the squared sound-speed oscillations between negative and superluminal values.

Regime 1: NMC $\gg$ GNMDC

We now turn to a detailed study of the three regimes. We start with the case where the GNMDC term is negligible compared to the NMC term during the slow-roll era. Observing equations (2.40),

(2.41), we deduce two requirements that should be satisfied, namely:

$$\xi \gg \frac{G(\phi)}{f'(\phi)} H\dot{\phi} \ , \tag{2.53}$$

and

$$\xi \gg \frac{G(\phi)}{f(\phi)} \dot{\phi}^2 \ , \tag{2.54}$$

Based on our previous discussion, the former is actually stronger than the latter. Nevertheless, the GNMDC form (2.27) on which we focus in this work, decouples at the end of inflation. Hence, enforcing the above constraints, makes the GNMDC unimportant throughout the field's evolution, bearing no particular effect in both the early and late stages of the Universe's evolution. This renders it irrelevant in terms of phenomenology and we do not study it further.

Regime 2: GNMDC $\gg$ NMC

To bring about this regime of GNMDC domination, using equations (2.40) and (2.41), we can extract relations:

$$\xi \ll \frac{G(\phi)}{f'(\phi)} H\dot{\phi} \ , \tag{2.55}$$

and

$$\xi \ll \frac{G(\phi)}{f(\phi)} \dot{\phi}^2 \ , \tag{2.56}$$

where the latter is stronger than the former, if NMC dynamics are to be negligible in the slow-roll era. But unlike the case where GNMDC $\ll$ NMC, the post-slow-roll dynamics cannot be studied without terms owed to the NMC. This is owed to the fact that a ϕ-dependent GNMDC term, quickly becomes subdominant near the bottom of the potential, in the post-slow-roll phase. Thus, this case ought to be studied in greater detail, specifically in order to examine the sound-speed, due to the corresponding GNMDC instabilities.

As discussed and shown with eq. (2.51), our aim is to investigate whether the inclusion of the NMC term corrects the c_s^2 values towards 1, compared to the standalone GNMDC modification. An indication towards this direction comes from the fact that the NMC sound speed is identically equal to 1. Since the NMC takes over (or is at least comparable) with GNMDC in the post-slow-roll period, one expects that the sound speed will be corrected. Instead, of providing explicit results here, we do it in the analysis of the next regime, namely where NMC $\approx$ GNMDC, which also showcases what we have discussed here.

Regime 3: NMC $\approx$ GNMDC

We shall start with the slow-roll equations presented before. To enforce the regime NMC $\approx$ GNMDC, we choose between the two requirements presented earlier, one of which is stronger. It is easier to choose the weaker constraint which nevertheless is enough to showcase the results of our model. In particular, we will enforce:

$$\xi f'(\phi) \approx G(\phi) H\dot{\phi} \ , \tag{2.57}$$

while still

$$\xi f(\phi) \gg G(\phi)\dot{\phi}^2 \ , \tag{2.58}$$

and additionally suppose that the GR terms are negligible when compared to the GNMDC and NMC ones during slow-roll. Then, equation (2.41) becomes:

$$18G(\phi)H^3\dot{\phi} + V'(\phi) = 12H^2\xi f'(\phi) \ , \tag{2.59}$$

while equation (2.40) is particularly simplified:

$$3M_{Pl}^2H^2 + 6\xi f(\phi)H^2 = V(\phi) \ . \tag{2.60}$$

By the discussion following equations (2.40) and (2.41) one understands that the dominant parameters during the slow-roll period are ϵ_{G1}, ϵ_{N1} and ϵ_{N2}. Hence, if one is interested in the early phases' predictions, we can keep only the first-order contributions with regards to these ϵ parameters. We get then:

$$\mathcal{F}_s = \mathcal{G}_s \approx M_{Pl}^2\epsilon_{G1} \ . \tag{2.61}$$

From (B.15) we now obtain $c_s^2 = 1$ during the slow-roll period (equivalently maintaining only parameters ϵ_{G1}, ϵ_{N1} and ϵ_{N2} in expression (2.49) gives $c_s^2 = 1$).

Using expression (B.19), for the scalar power spectrum at first order we obtain:

$$\mathcal{P}_R \approx \frac{H^2}{8M_{Pl}^2\pi^2\epsilon_{G1}} \ , \tag{2.62}$$

coinciding with (2.24), if we only keep the first order contribution. It is notable that up to first order, the NMC term does not have an effect on the power spectrum's value, since the only ϵ parameter that appears is ϵ_{G1}.

For the tensor-to-scalar ratio r, using (B.19), (B.20) we get:

$$r \approx 16\epsilon_{G1} + \frac{16\epsilon_{G1}}{\epsilon_{G1} + \epsilon_{N2}}\epsilon_{N1} \ . \tag{2.63}$$

Unlike the power spectrum, this result emphatically shows the effect of the combined theory. In particular, during slow-roll we have $\epsilon_{N1} < 0$, implying that the NMC term lowers the standard result $r = 16\epsilon_{G1}$. Thus, it corrects the tensor-to-scalar ratio to better agreement with the observations. The low tensor-to-scalar ratio, which is a characteristic result of the standalone NMC term, is maintained in the combined theory.

Turning to the scalar spectral index, n_s, using (B.19), (B.21) we obtain:

$$n_s \approx 1 + \frac{-3(\epsilon_{G3} + \epsilon_{G4}) + 2\epsilon_{G1}(\epsilon_{G1} + \epsilon_{N1} + \epsilon_{N2})}{\epsilon_{G1}(\epsilon_{G1} + \epsilon_{N1} + \epsilon_{N2} - 1)} \ . \tag{2.64}$$

Note that terms ϵ_{G3}, ϵ_{G4} can not be ignored here, because the rest of the terms are of second order in ϵ parameters. As expected, when NMC parameters go to zero we recover (2.25).

To summarize, when a ϕ-dependent GNMDC and the NMC terms are of comparable magnitude, the inflationary model can be completely healed from the $c_s^2 < 0$ unstable region. Moreover, the tensor-to-scalar ratio remains inside the Planck 2018's contour plots, increasingly improving as the NMC term becomes more significant. Finally, the scenario can be healed from the unitarity problem, because if GNMDC becomes more significant during the slow-roll period, the magnitude of $\xi\phi_*^2$ decreases drastically. All of the above results hold as long as function $G(\phi)$ is ϕ-dependent, and at the bottom of the potential becomes negligible. These features make the combined scenario better than its individual counterparts.

2.4 Numerical investigation

In this Section we will perform a numerical study to demonstrate the general results of our theory by use of specific examples. The main results of the previous section are equations (2.51) and (2.63). In order to satisfy the necessary ansatz for these results to hold, namely that GNMDC becomes negligible at the end of inflation, we will choose a monomial/polynomial form for $G(\phi)$[1].

We consider, then, specific forms for the NMC and GNMDC. For the coupling function $f(\phi)$ we choose the well-documented case of the standalone NMC, namely $f(\phi) = \xi\phi^2$. For the latter, we consider monomial form (2.27), namely $G(\phi) = \frac{\alpha\phi^{\alpha-1}}{2M^{\alpha+1}}$. We will also discuss an example with a polynomial form $G(\phi) = \sum_i \frac{\alpha_i\phi^{\alpha_i-1}}{2M_i^{\alpha_i+1}}$. Furthermore, to increase our theoretical justification, and to compare with the literature, we shall consider the inflaton to be the Higgs boson, making the corresponding choice in terms of the potential [25, 151]:

$$V(\phi) = \frac{\lambda\phi^4}{4}. \tag{2.65}$$

Finally, in what follows, we impose a normalization constraint obtained through observations, that the scalar power spectrum value at $k = 0.05Mpc^{-1}$ is $\mathcal{P}_R = 2.2 \cdot 10^{-9}$ [67]. Initial conditions are chosen in order for the produced models to yield 40, 50 and 60 e-folds.

For the monomial GNMDC case, in Fig. 2.1 we show the evolution of the scalar field for various cases. The main observation to be made from this graph is that even though in the standalone GNMDC case the oscillations of ϕ and $\dot{\phi}$ are wild, in the scenario at hand, the period of the field oscillations increases. This plays a crucial role in the analysis that follows, since it is the healing factor for the c_s^2-instabilities.

We move on to calculate the inflationary observables. In particular we focus on the scalar spectral index and tensor to scalar ratio, using expressions of Appendix B. In the upper panel of Fig. 2.2, one can see the obtained results for the single scenarios of NMC and GNMDC, as well as for the combined theory at hand. In the same figure we provide the 1σ and 2σ contours of the Planck 2018 data [67]. It can be seen that NMC yields very satisfactory predictions, however due to unitarity violation this model has to be modified or abandoned. Single GNMDC scenario solves the unitarity issue, but leads to quite large r values and instabilities related to c_s^2. We can see that, in the combined NMC+GNMDC scenario we ameliorate the unitarity issue, and at the same time improve the obtained r values, in agreement with Planck 2018 contours. An increasing α improves the results further. In more detail, one observes that for the same value of α (dashed lines for $\alpha = 3$, dotted lines for $\alpha = 5$), as parameter ξ grows, r lowers. For the same value of ξ (blue lines for $\xi = 1500$, red lines for $\xi = 2000$), increasing α lowers r. This result was expected as it is known to be one of the main results of single GNMDC [155].

In summary, monomial GNMDC models with larger α are more desirable in the context of the combined theory proposed in this work, due to the enhancement of the gravitational friction effect that α quantifies. But a polynomial GNMDC can bring about the same effect, since inflation can be carried by two or more "frictious" terms present in it. We will demonstrate such a model later.

We shall now examine the evolution of c_s^2 in order to demonstrate that the combined scenario heals the c_s^2-instabilities of the standalone GNMDC. In the lower panel of Fig. 2.2 the evolution of c_s^2 is depicted, for a variety of cases. While in the standalone GNMDC (i.e. for $\xi = 0$) the squared sound-speed wildly oscillates between positive and negative values, when the NMC is switched on, we obtain a remarkable decrease of the oscillatory behavior and a stabilization to positive values. We note that in the combined scenario, near the end of inflation, the GNMDC contribution smooths out, while the NMC term remains co-leading alongside standard GR terms (i.e. of the minimally coupled scalar field). Since the standalone NMC as well as the GR terms have no instability issues, the $c_s^2 < 0$ related instabilities are healed.

[1] Other similar forms still produce viable results.

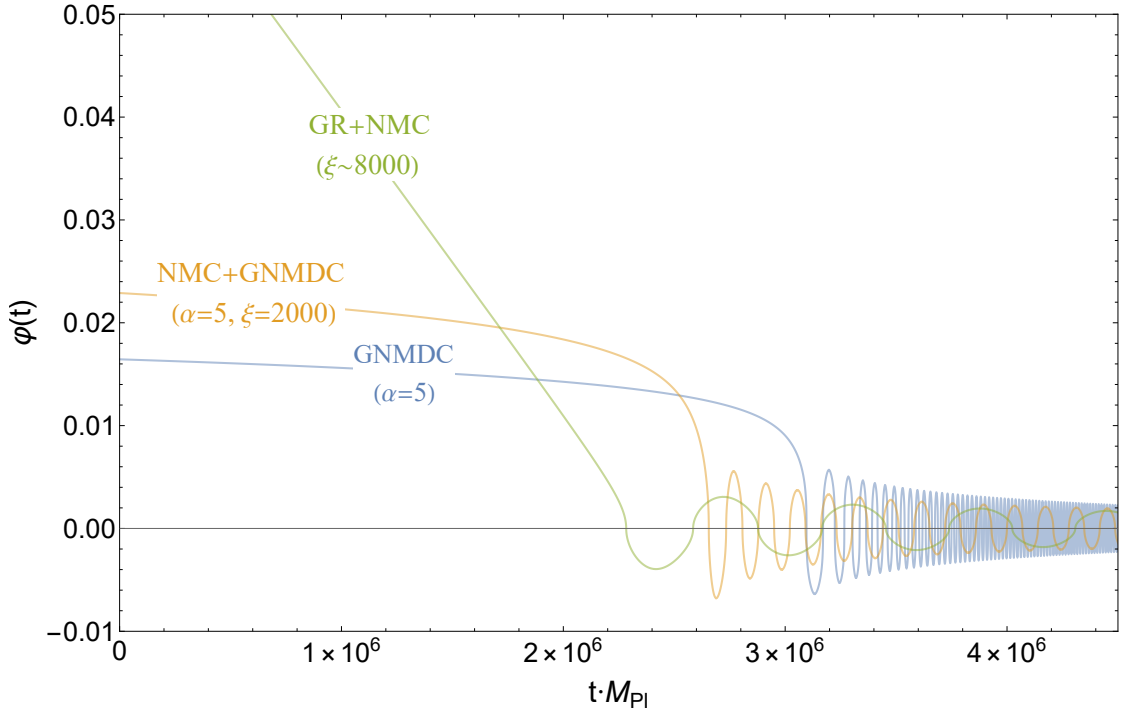

Figure 2.1: *The evolution of the inflaton in three different scenarios: GNMDC with* $\alpha = 5$*, NMC with* $\xi \approx 8000$ *and combined NMC+GNMDC with* $\alpha = 5$ *and* $\xi = 2000$*, respectively. All models produce 60 e-folds and* $\mathcal{P}_R = 2.2 \cdot 10^{-9}$*. The period of oscillations increases. Also the initial value of the field, in the case where NMC becomes more important (equivalently as* ξ *grows). Note that when the two theories are combined,* $\xi\phi_*^2$ *remains less than* M_{Pl}*.*

To clarify the picture painted with the above discussion, the relative effect of the GNMDC and the NMC contributions can be seen in Fig. 2.3, where we present the contribution of each term in the dynamic equations. It becomes clear that even though during slow-roll, the contributions from NMC and GNMDC are comparable, when the oscillations start, the NMC sector dominates completely. Since NMC alone leads to $c_s^2 = 1$, its dominance in the combined model is adequate to bring c_s^2 away from the unstable region of the standalone GNMDC. Thus, the GNMDC contribution to the c_s^2 near the end of inflation is dominated by the NMC and the wild oscillations of the sound speed are damped much earlier. This damping of oscillations is more efficient for larger α values. This also leads to better r values, thus, larger α values would be more desirable.

One then may wonder whether this is a realistic scenario, since quantum corrections should bring about terms that might be of lower order, thus one should check the resulting phenomenology. In fact, if one chooses a polynomial form for function $G(\phi)$, a very similar phenomenology is produced. This happens because, unless the various terms of the polynomial are extremely finely tuned, there will still be one monomial term that drives the slow roll and thus produce essentially the same results.

But even in the case that two, or more, terms of the polynomial are actually of the same order of magnitude, the resulting phenomenology is still the same, since the results of Section 2.3 are independent of the exact form of the GNMDC chosen. They hold as long as the GNMDC is such that becomes negligible at the end of inflation. Nevertheless, we will provide a numerical example

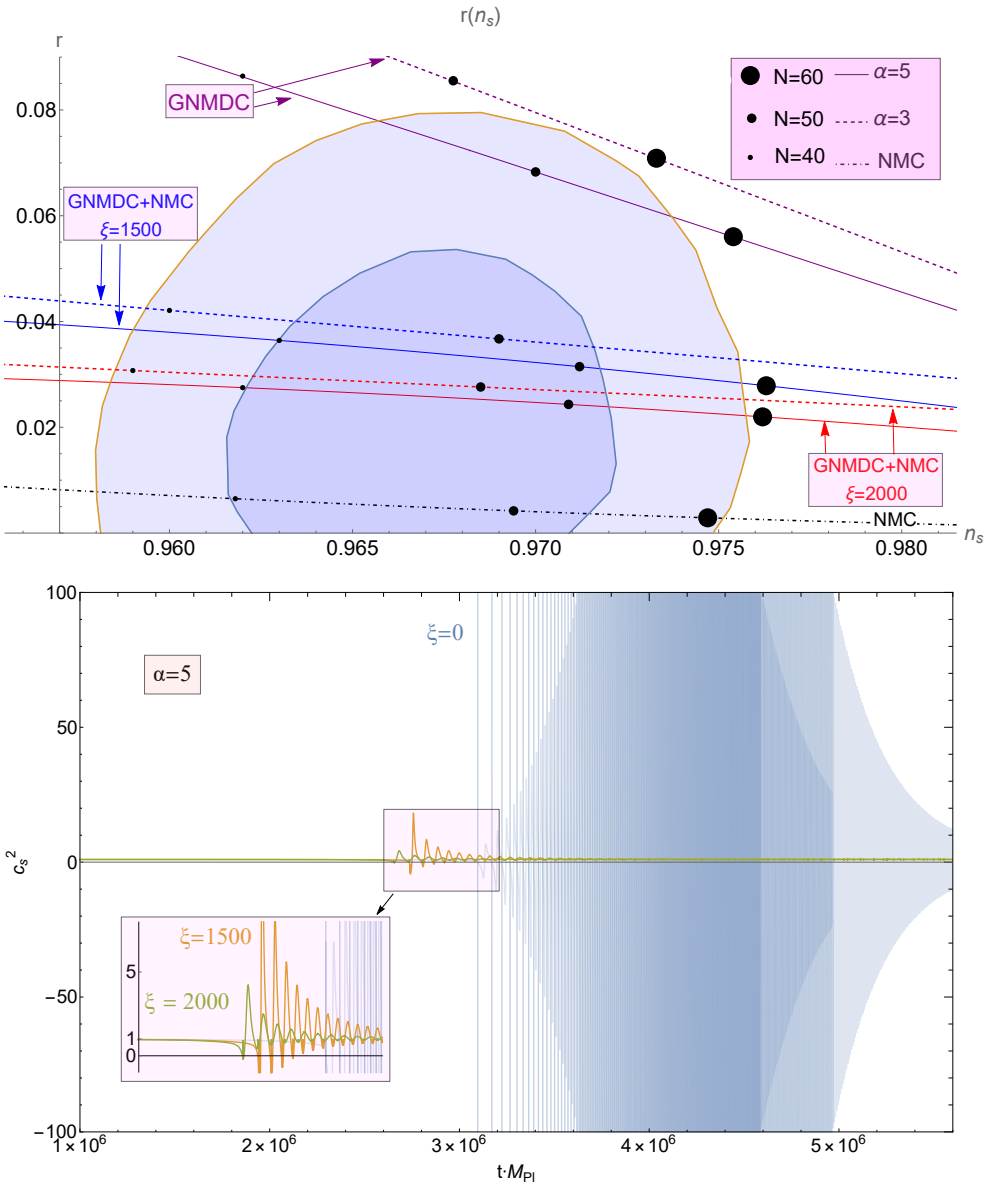

Figure 2.2: *Upper panel: Comparison of the predictions of the scenarios at hand versus the 1σ (purple) and 2σ (light purple) contours for Planck 2018 results (Planck $+TT+lowP$) [67]. NMC corresponds to the dot-dashed line. GNMDC (purple lines) has been shown here for two cases, one with $\alpha = 3$ (dashed line) and one with $\alpha = 5$ (dotted line). We use the same convention for the combined NMC+GNMDC scenario in terms of α. We use the colour code of blue lines for $\xi = 1500$ and red lines for $\xi = 2000$. It is clear that NMC lowers the r value as it becomes more significant, when compared to the standalone GNMDC. Low r-values are a signature feature of NMC of the form ϕ^2. Furthermore, one can see that for the same value of ξ, as α increases, r is also lowered [155]. Growing dots represent 40, 50 and 60 e-folds respectively. Lower panel: The c_s^2 evolution for the scenario at hand, for $\alpha = 5$, with $\xi = 0, 1500$ and 2000. As the NMC contribution becomes more significant (ξ increases), oscillations in its value are damped and the squared sound-speed is corrected towards 1.*

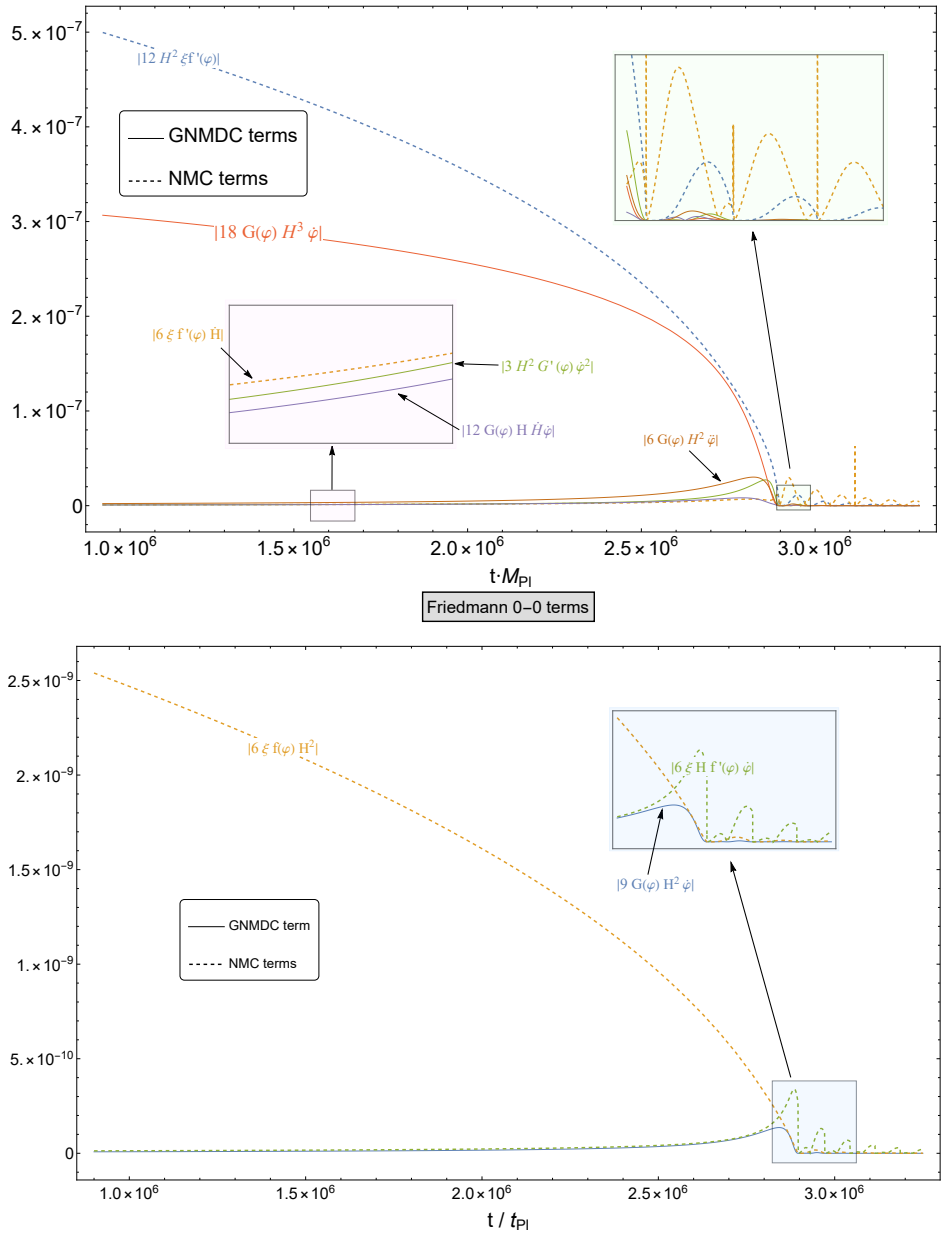

Figure 2.3: *Upper panel: Contributions of GNMDC related terms (continuous lines) and NMC related terms (dashed lines) in the Klein-Gordon equation* (2.38)*, for* $\alpha = 5$ *and* $\xi = 2000$*. We observe that when the oscillations start, NMC terms dominate and hence the GNMDC effects are negligible, while during the slow-roll era they are comparable. Standard GR terms are intentionally omitted to simplify the graph. Lower panel: Contributions of GNMDC related term (continuous line) and NMC terms (dashed lines) in the 0-0 field equation* (2.38)*, for* $\alpha = 7$ *and* $\xi = 2000$*. We observe that during slow roll, the NMC is dominant in the field equation. A similar picture as in the upper panel is also obtained: when oscillations start, NMC is the largest contributing term.*

of such a scenario as a further demonstration.

To summarize our results so far, we see that in the combined scenario studied here, when inflation starts, the gravitational friction effect due to the GNMDC term is what causes the model to produce enough e-folds without resorting to $\xi\phi_*^2 > M_{Pl}$ values as in the standalone NMC case, alleviating the unitarity issue. The NMC term causes, at the same time, the tensor to scalar ratio of the model to be low, and in good agreement with observations, especially when compared to the standalone GNMDC case. When inflation ends and the oscillations start, NMC terms remain more significant than GNMDC terms, leading to a fast damping of the oscillations in the c_s^2 value, saving the theory of instabilities. These advantages of the combined scenario are the main results of the present work.

A final note is to be made, regarding the role of the GNMDC parameter α on the results. In the combined scenario even α values still lead to viable models. This is not the case when GNMDC is considered alone because of the constraint (2.39), which disqualifies the area of the phase space corresponding to desirable values for the inflationary observables. The fact that in the combined theory all α values can be used, is another advance in the richness of the resulting models.

This obviously holds for a polynomial GNMDC form too. If an even-valued α term is dominant, the polynomial GNMDC numerics become unstable due to (2.39). This is healed, when polynomial GNMDC is combined with NMC.

A further demonstration of the effects of the theory proposed here, will be performed by including numerical results of a polynomial GNMDC term. Specifically, we will suppose that:

$$G(\phi) = \sum_i \frac{\alpha_i \phi^{\alpha_i - 1}}{2M_i^{\alpha_i + 1}},$$

where i defines which and how many corresponding polynomial terms are taken into consideration. Here, we will pick:

$$\frac{\alpha\phi^{\alpha-1}}{2M_1^{\alpha+1}} + \frac{(\alpha-1)\phi^{\alpha-2}}{2M_2^{\alpha}}, \tag{2.66}$$

with $\alpha = 4$, while the scale of the NMC is $\xi \approx 2000$. The values of the coupling coefficients should be such that these two monomials are of comparable magnitude. If that is not the case, then one of them would dominate during the slow roll period, reducing the model to the monomial GNMDC case already studied. But such a scenario ($\alpha = 4$) is not viable in the sole GNMDC case.

We note that a polynomial GNMDC form clearly falls within the ansatz needed for the results presented in Section 2.3 to hold, namely that the GNMDC decouples near the end of inflation. The results produced therein, still hold. A polynomial GNMDC only affects the exact form of the ϵ_{G_i} parameters but not their overall behavior.

Constructing the phase space from which we obtain initial conditions and scales for the combined theory, with a polynomial GNMDC, is a tedious task when compared to the monomial case. However, if one imposes the ansatz discussed earlier, regarding the magnitude of the monomials of the GNMDC, one can straightforwardly obtain results well within observational bounds. The overall outcome is similar to the monomial GNMDC case, as one observes in Fig. 2.4. This was, of course, expected since the ϵ_{G_i} show similar behavior between the two cases.

2.5 Conclusions

It is a widely accepted fact, that if modern Cosmology is to explain the hot big bang and the resulting primordial perturbations observed through the CMBR it has to be modified, by including an initial inflationary period. Among the variety of ways to achieve that, arguably the most well-studied is the inclusion of a scalar field. Its dynamics affect the evolution of the early Universe's expansion, perhaps leading to a solution of the corresponding problems. However, the only scalar field observed so far is the Higgs field, hence it would be the best candidate for such a scenario.

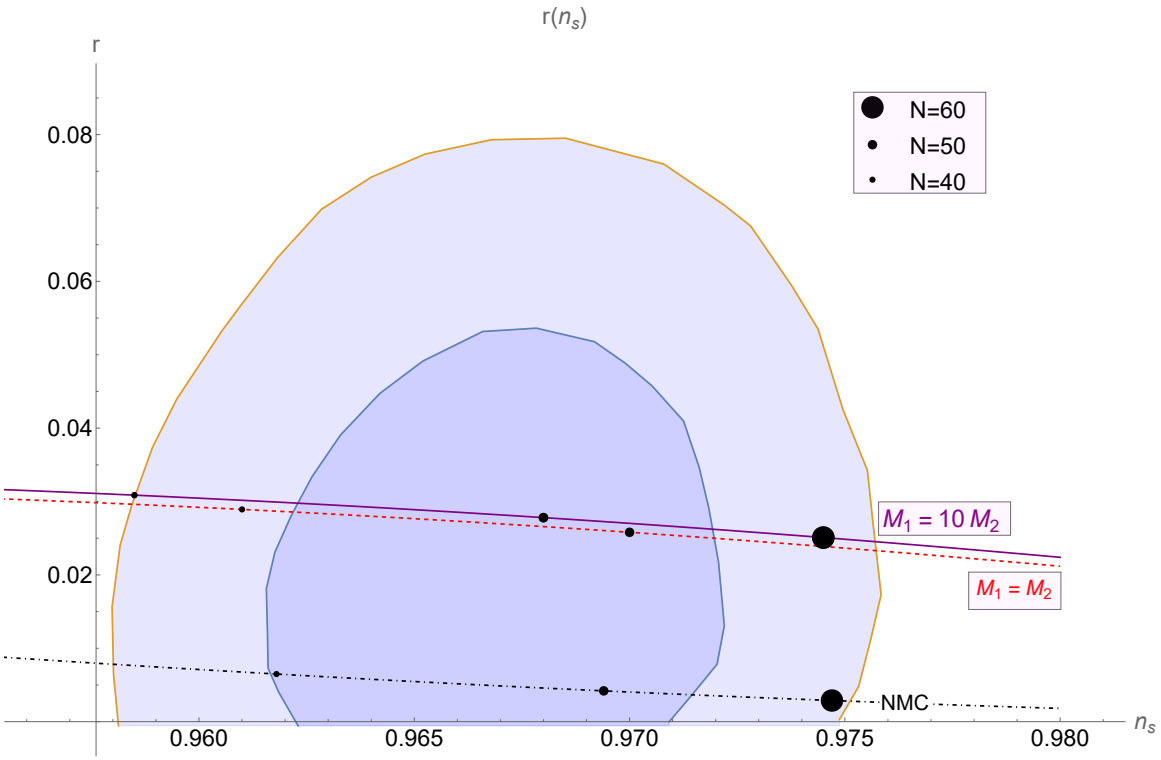

Figure 2.4: *Planck 2018 1σ (purple) and 2σ (light purple) contours (Planck $+TT+lowP$) [67], on the $r-n_s$ space. The predictions of the polynomial GNMDC+NMC scenario are also presented. The resulting phenomenology is very similar to the monomial case of Fig. 2.2. We present two cases, quantified by the scale of each term, M_i, one with $M_1 = M_2$ (red dashed line) and one with $M_1 = 10M_2$ (purple continuous line). Growing dots represent 40, 50 and 60 e-folds as before. When NMC is not included, polynomial GNMDC are not as stable due to constraint* (2.39).

Theories in which the Higgs field is only minimally coupled to gravity have been excluded from Planck observations [67]. The next step is to allow the field to couple non minimally with the gravitational sector (NMC). Indeed, Higgs inflation, with a quadratic NMC coupling ($f(\phi) = \phi^2$), has been shown to yield particularly good results, in terms of the comparison with the observations, namely a low tensor-to-scalar ratio, while it is free of instabilities related to the sound-speed of perturbations. However, it is also known to lead to unitarity violation - a rather significant problem if one wishes to quantize the theory.

Considering non minimal derivative couplings of the scalar field to gravity has been shown to avoid the unitarity issue, while still leading to satisfactory observables for inflation, due to the "gravitational friction" phenomenon, that lowers the initial values producing a long enough slow-roll period. Thus, a significant amount of e-folds can be obtained. On the other hand, these models are plagued by perturbative instabilities, in particular when $c_s^2 < 0$. One can construct generalized versions of non-minimal derivative couplings (GNMDC) that improve but don't completely solve the instability issue, considering for instance a coupling function of the form: $\frac{\alpha\phi^{\alpha-1}}{M^{\alpha+1}}$. But the potential problematic behavior is still existent.

Here we constructed a scenario that combines NMC and GNMDC, maintaining the advantages of the individual models, and removing their individual disadvantages. In the combined theory

considered, a long inflationary phase is easily achieved, while the initial value of the scalar field and the scale of the NMC term are sub-Planckian. This feature is not possible in the single field NMC scenario, because they are achieved due to the GNMDC term, bringing about the gravitational friction effect. That is what extends the slow-roll phase, allowing for lower initial values of ϕ_*, alleviating the problem. Additionally, at the end of inflation, when the field reaches the bottom of the potential, a suitable GNMDC term can be decoupled leaving the NMC term to dominate completely.

To show this behavior, we chose to include two examples, one with a monomial GNMDC form and one with a polynomial form, both satisfying the above ansatz (other GNMDC forms should also be viable, if they become negligible at the end of inflation). In both cases we can see that a desirable phenomenology is produced. Due to this setup, when inflation ends, canonical gravity is restored, and therefore, the theory does not suffer from c_s^2-instabilities due to wild oscillations, neither from superluminal scalar perturbations that are related to the $\alpha = 1$ NMDC case. Finally, the present construction passes the recent LIGO-VIRGO contstraints on the gravitational wave speed [159,160], since the non-minimal derivative coupling terms are among the ones leading to a gravitational wave speed different than one.

In conclusion, the combined theory proposed here, leads to inflationary observables in agreement with observations, and is free from c_s^2-instabilities. At the same time, it alleviates the unitarity issue, because it does not require as high values for the scales and initial conditions of the theory, as NMC. We therefore understand that it maintains the advantages of the individual scenarios while healing their disadvantages.

We thus conclude that inflationary scenarios with combined non minimal and derivative couplings to gravity, may provide successful grounds for the description of inflationary dynamics, as well as other mechanisms related to inflation, like the formation of Primordial Black Holes, and deserve further investigation.

Chapter 3

Reconstruction of cosmological evolution in the presence of extra dimensions

3.1 Introduction

Advances in string theory have brought forward the idea that unifying all physical interactions might require the study of models with more than three spatial dimensions. When building a model with extra dimensions, a mechanism has to exist, to recover the four-dimensional spacetime. This is generally known as a *dimensional reduction* mechanism. One way to perform such an act, comes about by the use of the Kaluza-Klein (KK) dimensional reduction formalism [161, 162]. One usual way of working in this direction, is by building models in the so-called brane-world scenario [163], according to which the Standard Model of Physics, with its matter and gauge interactions, is localized on a three-dimensional hypersurface, the *brane*, that is itself embedded in a higher-dimensional spacetime. Gravity propagates in all spacetime, which is referred to as *bulk*, and thus connects the Standard Model sector with the space dynamics [164].

Cosmology resulting from theories with branes embedded in extra spatial dimensions has been extensively studied. A particularly detailed analysis has been done for brane-world models in five-dimensional (4+1) spacetime. The dynamics of the extra dimension have an effect both at early and late times during the Universe's evolution, depending on the model. The dynamics of this and similar models with one, transverse to the brane, extra dimension (codimension-1 brane models) is in fact well understood. The cosmological generalization of the early-time (high energy limit) evolution [163] is modified by the squared value of the matter density living on the brane. The bulk's imprint on the brane, is realized through the *dark radiation* term. It leads to the presence of a bulk cosmological constant, thus recreating conventional late time cosmology (low energy limit) [165].

A different approach has been proposed [166], based on the existence of *large* extra dimensions, with a size of a few TeV, leading to new mechanisms for supersymmetry breaking as one of its primary results. One particular case within this context, is the case referred to as *Universal Extra Dimensions* [167]. According to this scenario, the extra dimensions are accessible to all Standard Model particles. Then, a dimensional reduction of the full Lagrangian of any Standard Model particle will lead to a tower of Kaluza Klein states that will be perceived, from a 4-D perspective, as massive particles (see [168], [169]).

Hence, this setup is particularly interesting in a cosmological context, because it incorporates naturally possible candidates for dark matter, which is one of the main shortcomings of the cosmological Standard Model. A stable KK Particle (LKP) could still exist today as a thermal relic and

if not charged and of baryonic nature, it possesses all essential properties of what is referred to as a *weakly interacting massive particle* (WIMP) [170], [171].

In the effective 3+1-dimensional picture of the UED scenario, the fundamental coupling constants can be shown to vary with the volume of the internal space, due to the dimensional reduction. However, strong cosmological constraints are imposed on the allowed variation of these constants. These require the extra space to not only be compactified, but also stabilized (i.e. neither increasing nor decreasing in volume), before Big Bang Nucleosynthesis (BBN) takes place. Therefore, one has to find a compelling explanation for the stabilization of the extra dimension(s), in order to produce a viable cosmological model in the context of UED.

It has been shown [172] that this is possible to achieve during the radiation domination era with no explicit mechanism, but this is not the case for matter domination [173, 174]. Using the typical definition of momentum flux for both the usual and extra spatial sectors, it was shown that if dark matter consists of a significant amount of KK particles, a constraint regarding the equations of state of the usual and extra spatial fluids is obtained. This constraint is in general incompatible with the stabilization constraint, coming directly from the field equations. Thus a mechanism that circumvents this problem has to be proposed, for example stabilizing the extra dimensions by use of background fields [175].

We will now reproduce a cosmological evolution similar to that predicted by the ΛCDM, without imposing any constraint regarding KK dark matter. To be consistent, then, we have to either suppose that KK modes are not a substantial fraction of the dark matter, or abolish the typical connection between momentum flux and pressure for the extra spatial fluid, instead assuming that matter is described by a more fundamental theory in the microscopic level.

Examples include [176, 177], where a case with strings wound around the compactified extra dimensions was proposed, and explored. Such a setup would result in a negative pressure effect, holding the compactified dimensions in place. Note that this is unlike the usual picture of non-compactified dimensions where negative pressure drives their accelerated expansion ([178], but also [179]). Regardless, our effort will revolve around recovering a picture equivalent to that of the ΛCDM, in the context of UED, while imposing stabilization constraints that are solely quantified by related phenomenology/observations.

In Section 3.2 we present the setup of this scenario, generally following the setup of [172]. In Section 3.3 the solutions of this setup are presented, showing the existence of an attractor solution. This solutions attracts a huge variety of initial conditions. In Sections 3.4 and 3.5 the constraints that have to be followed are discussed, and thus we construct such a model with the sole purpose of recovering late time results of the ΛCDM. In Section 3.6 an interesting case of the equations of state is presented, before we conclude in Section 3.7.

3.2 A Homogeneous Universe in $(3+1+n)$-dimensions

A first assumption made is that the Universe is homogeneous in $(3+1+n)$-dimensions, but also we assume that it is not isotropic as a whole, but is instead isotropic in the usual 3 dimensions and extra n dimensions separately. To describe then this Universe, we allow for different scale factors in 3-D and n dimensions of the FRW metric:

$$ds^2 = -dt^2 + a^2(t)\gamma_{ij}dx^i dx^j + b^2(t)\tilde{\gamma}_{pq}dy^p dy^q\,, \tag{3.1}$$

Naturally, γ_{ij} and $\tilde{\gamma}_{pq}$ are maximally symmetric metrics in three and n dimensions, respectively according to what we specified above. Thus, to parametrize spatial curvature in the usual way, we will use two separate parameters, $k_a = -1, 0, 1$ in ordinary space, and $k_b = -1, 0, 1$ in the extra dimensions.

Choosing this metric, the energy-momentum tensor takes the form:

$$T^A{}_B = \begin{pmatrix} -\rho & 0 & 0 \\ 0 & \gamma^i{}_j p_a & 0 \\ 0 & 0 & \tilde{\gamma}^p{}_q p_b \end{pmatrix}, \tag{3.2}$$

describing a homogeneous fluid that is, in general, anisotropic, in its rest frame. The pressure and energy density in the ordinary and in the extra space are related by the respective equations of state:

$$p_a = w_a \rho, \qquad p_b = w_b \rho \tag{3.3}$$

We can now recover the nonzero components of the field equations, by use of the background metric (3.1), which read as:

$$3\left(\frac{\dot{a}}{a}\right)^2 + 3\frac{k_a}{a^2} + 3n\frac{\dot{a}}{a}\frac{\dot{b}}{b} + \frac{n(n-1)}{2}\left[\left(\frac{\dot{b}}{b}\right)^2 + \frac{k_b}{b^2}\right] = \kappa^2\rho\,, \tag{3.4a}$$

$$2\frac{\ddot{a}}{a} + \left(\frac{\dot{a}}{a}\right)^2 + \frac{k_a}{a^2} + n\frac{\ddot{b}}{b} + 2n\frac{\dot{a}}{a}\frac{\dot{b}}{b} + \frac{n(n-1)}{2}\left[\left(\frac{\dot{b}}{b}\right)^2 + \frac{k_b}{b^2}\right] = -\kappa^2 w_a \rho\,, \tag{3.4b}$$

$$3\frac{\ddot{a}}{a} + 3\left(\frac{\dot{a}}{a}\right)^2 + 3\frac{k_a}{a^2} + (n-1)\frac{\ddot{b}}{b} + 3(n-1)\frac{\dot{a}}{a}\frac{\dot{b}}{b} + \frac{(n-1)(n-2)}{2}\left[\left(\frac{\dot{b}}{b}\right)^2 + \frac{k_b}{b^2}\right] = -\kappa^2 w_b \rho\,, \tag{3.4c}$$

An overdot is used to denote differentiation with respect to cosmic time, t. Because of the conservation of energy:

$$T^A{}_{0;A} = 0 \tag{3.5}$$

we obtain relation:

$$\frac{\dot{\rho}}{\rho} = -3(1+w_a)\frac{\dot{a}}{a} - n(1+w_b)\frac{\dot{b}}{b}\,. \tag{3.6}$$

If the equations of state are non-dynamical, this can be integrated to give

$$\rho = \rho_i \left(\frac{a}{a_i}\right)^{-3(1+w_a)} \left(\frac{b}{b_i}\right)^{-n(1+w_b)}. \tag{3.7}$$

Note that a subscript i indicates arbitrary initial values, and subscript 0 indicates today's values throughout this chapter.

We can rewrite eq. (3.4a) in a more familiar form, by introducing the Hubble parameters $H_a = \frac{\dot{a}}{a}$ and $H_b = \frac{\dot{b}}{b}$ for the ordinary and the extra space respectively:

$$3H_a^2 + 3\frac{k_a}{a^2} + 3nH_aH_b + \frac{n(n-1)}{2}\left[H_b^2 + \frac{k_b}{b^2}\right] = \kappa^2\rho\,. \tag{3.8}$$

Equation (3.8), then, is the Friedmann equation of a homogeneous Universe with energy density ρ in $(3+1+n)$-dimensions. A further assumption that we make henceforth is that the curvature of the three-dimensional space and that of the extra dimensional-space are zero. Then, the above relation yields a simple algebraic connection of the Hubble parameters H_a and H_b through ρ, while equations (3.4b) and (3.4c), yield the codependent accelerations of the two scale factors, $a(t)$ and $b(t)$. These equations result in a constraint between the equations of state if one aims to achieve exact stabilization of the internal space.

3.3 Evolution of the Hubble parameters

We now study how a $(3+1+n)$-dimensional cosmological model could evolve to an effective $(3+1)$-dimensional one. The extra n-dimensions have to eventually follow a compactification and stabilization mechanism. We will show that a natural way of stabilization for the extra dimensions can be achieved for certain values of the parameters of the equations of state, w_a, w_b. Moreover, the field equations have Kasner-type solutions [180] which are known to act as compactifying mechanisms [181].

As already mentioned, we will use $k_a = 0$, which is the accepted value according to observations. Regarding the extra dimensions, we will only consider toroidal compactifications, hence also $k_b = 0$[1].

Using:

$$\frac{\ddot{a}}{a} = \dot{H}_a + H_a^2 \, , \; \frac{\ddot{b}}{b} = \dot{H}_b + H_b^2 \, , \tag{3.9}$$

and eliminating ρ by use of (3.8), we get an equivalent system of differential equations:

$$\begin{aligned} \dot{H}_a &= \frac{3\big[(n-1)w_a - nw_b - n - 1\big]}{2+n} H_a^2 + \frac{n\big[(n-1)(3w_a-1) - 3nw_b\big]}{2+n} H_a H_b \\ &+ \frac{n(n-1)\big[1 + (n-1)w_a - nw_b\big]}{2(2+n)} H_b^2 \, , \end{aligned} \tag{3.10a}$$

$$\begin{aligned} \dot{H}_b &= \frac{3\,(2w_b - 3w_a + 1)}{2+n} H_a^2 - \frac{3\,(3nw_a - 2nw_b + 2)}{2+n} H_a H_b \\ &- \frac{n\big[5 + n + 3(n-1)w_a - 2(n-1)w_b\big]}{2(2+n)} H_b^2 \, . \end{aligned} \tag{3.10b}$$

This system depends only on the Equation of State (EoS) parameters w_a and w_b. In order to look for particular solutions, that play a very important role, as we will later see, we impose the ansatz $H_b(t) = c_i H_a(t)$. Substituting this in (3.10) we get two equations for $\dot{H}_a$. Demanding that these equations provide the same solution, gives 3 values for c_i when $n \geq 2$. They read:

$$\underbrace{c_1 = \frac{6}{-3n - \sqrt{3n(2+n)}}}_{\text{K1}} \qquad \underbrace{c_2 = \frac{6}{-3n + \sqrt{3n(2+n)}}}_{\text{K2}} \qquad \underbrace{c_3 = \frac{1 - 3w_a + 2w_b}{1 + (n-1)w_a - nw_b}}_{\text{K3}} \tag{3.11}$$

while for $n = 1$

$$\underbrace{c_1 = -1}_{\text{K1}} \qquad \underbrace{c_3 = \frac{-1 + 3w_a - 2w_b}{-1 + w_b}}_{\text{K3}} \tag{3.12}$$

For $n \geq 2$ there are two Kasner-type solutions, $K1$ and $K2$:

$$\left.\begin{aligned} H_a(t) &= \frac{H_a(0)(n-1)}{n - 1 + [\sqrt{3n(2+n)} - 3]H_a(0)t} \\ H_b(t) &= -\frac{6H_a(0)}{3n + \sqrt{3n(2+n)} + [3n + 3\sqrt{3n(2+n)}]H_a(0)t} \end{aligned}\right\} \quad \text{K1} \tag{3.13}$$

$$\left.\begin{aligned} H_a(t) &= \frac{H_a(0)(n-1)}{n - 1 - [\sqrt{3n(2+n)} + 3]H_a(0)t} \\ H_b(t) &= \frac{6H_a(0)}{-3n + \sqrt{3n(2+n)} + [-3n + 3\sqrt{3n(2+n)}]H_a(0)t} \end{aligned}\right\} \quad \text{K2} \tag{3.14}$$

[1] One can see from the equivalent of equation (3.10b), that for $k_b \neq 0$, a stabilized extra space is only compatible with $H_a = const.$, which through equation (3.8) implies $\rho = const.$. That is particularly hard to match with Standard Cosmology.

while for $n = 1$ there is only one Kasner-type solution, since one of them reduces to $H_a = 0$:

$$\left.\begin{aligned} H_a(t) &= \frac{H_a(0)}{1+2H_a(0)t} \\ H_b(t) &= -\frac{H_a(0)}{1+2H_a(0)t} \end{aligned}\right\} \qquad \text{K1 for } n=1 \tag{3.15}$$

It might seem peculiar that (3.10), with an explicit dependence on the EoS parameters, has any solution that does not depend on them. We note that, originally, Kasner solutions were vacuum solutions of the Einstein equations [180]. Returning to the system (3.4), from which (3.10) is produced through algebraic manipulation, and using $\rho = 0$, one can see that all w-dependences are switched off. Moreover, Kasner solutions can be generalized in the presence of matter [181].

When the EoS parameters are constant, eq. (3.10) has another *Kasner-type* solution (hinted at in [182]), that we refer to as $K3$ solution:

$$\left.\begin{aligned} H_a(t) = &\quad \frac{2[1+(n-1)w_a - nw_b]H_a(0)}{2+2(n-1)w_a - 2nw_b + [3-3w_a^2+n(1+3w_a^2-6w_aw_b+2w_b^2)]H_a(0)t} \\ H_b(t) = &\quad \frac{2(1-3w_a+2w_b)H_a(0)}{2+2(n-1)w_a - 2nw_b + [3-3w_a^2+n(1+3w_a^2-6w_aw_b+2w_b^2)]H_a(0)t} \end{aligned}\right\} \qquad \text{K3} \tag{3.16}$$

All these particular solutions have a constant H_b/H_a ratio, throughout their evolution. Their role is central in studying the behavior of the general solution of this problem, which will be shown to be a product of these, when written in the phase space H_a, $H_b(H_a)$. Their form $(1/t)$, implies that these solutions have a singularity and some more interesting properties. Kasner solutions ($K1$, $K2$) have a constant deceleration parameter throughout. Specifically, for $n = 1$ we have $q_{K1} = 1$ while for $n \geq 2$:

$$q = -1 - \frac{\dot{H}_a}{H_a^2} = \begin{cases} \frac{2+n-\sqrt{3n(2+n)}}{1-n} > 0 \;\forall\; n \;\geq\; 2 & (K1) \\ \frac{2+n+\sqrt{3n(2+n)}}{1-n} < 0 \;\forall\; n \;\geq\; 2 & (K2) \end{cases}$$

However, in the case of $K3$, the sign of q depends also on the values of the w parameters:

$$q = \frac{1+n+(2-2n)w_a - 6nw_aw_b + 2nw_b + (3n-3)w_a^2 + 2nw_b^2}{2+2(n-1)w_a - 2nw_b}$$

Moreover, for a positive value of H_a for $t = 0$, $K1$ solution has its singularity for $t < 0$ and $K2$ for $t > 0$, while $K3$'s singularity again depends on the w parameters. Finally, it is notable that for the $K1$, $K2$ solutions a contraction of the extra space ($H_b < 0$) guarantees the growing ($H_a > 0$) of the 3-d space and vice versa, while that is not necessarily true for $K3$ because of the w parameters.

We proceed to obtain the general solution, (i.e. without imposing any ansatzes between H_a, H_b). Eliminating time in (3.10), we get a single differential equation. This is always integrable when the EoS parameters, w, are constant.

$$\begin{aligned} \frac{dH_a}{dH_b} = &\frac{6\big(1+w_a+n(1-w_a+w_b)\big)H_a^2 + 2n(-1+n+3w_a-3nw_a+3nw_b)H_aH_b}{6(3w_a-2w_b-1)H_a^2 + 6\big(2+n(3w_a-2w_b)\big)H_aH_b + n\big(5+n+(n-1)(3w_a-2w_b)\big)H_b^2} \\ &+ \frac{-n(n-1)\big(1+(n-1)w_a-nw_b\big)H_b^2}{6(3w_a-2w_b-1)H_a^2 + 6\big(2+n(3w_a-2w_b)\big)H_aH_b + n\big(5+n+(n-1)(3w_a-2w_b)\big)H_b^2} \end{aligned} \tag{3.17}$$

Integrating this, we get a solution that, after some algebraic manipulation, is written as a product of the above particular solutions:

$$
\begin{aligned}
const. = & \Big| \underbrace{H_b}_{H_b \text{ part}} \Big|^{\sqrt{2+n}\left[3(w_a-1)^2+n\left(1-3w_a^2+6w_aw_b-2w_b(1+w_b)\right)\right]} \cdot \\
& \Big| \underbrace{\frac{H_a}{H_b}+\frac{3n+\sqrt{3n}\sqrt{2+n}}{6}}_{K1 \text{ part}} \Big|^{\sqrt{2+n}(3+n-3w_a-nw_b)+\sqrt{3n}(2+n)(w_a-w_b)} \cdot \\
& \Big| \underbrace{\frac{H_a}{H_b}+\frac{3n-\sqrt{3n}\sqrt{2+n}}{6}}_{K2 \text{ part}} \Big|^{\sqrt{2+n}(3+n-3w_a-nw_b)-\sqrt{3n}(2+n)(w_a-w_b)} \cdot \\
& \Big| \underbrace{\frac{(n-1)w_a-nw_b+1}{3w_a-2w_b-1}+\frac{H_a}{H_b}}_{K3 \text{ part}} \Big|^{-\sqrt{2+n}\left(3-3w_a^2+n(1+3w_a^2-6w_aw_b+2w_b^2)\right)}
\end{aligned}
\tag{3.18}
$$

The general solution's taking of this form, as a product of special solutions of the system, ought to be expected. This is due to the similarity of the resulting differential equation, with the Darboux equation (see [183], §2.21). We also note that during the derivation of the general solution, $K1$, $K2$, and $K3$ in the form:

$$H_b - c_i H_a = 0$$

become forbidden constraints, due to their appearance in denominators of partial fractions.

Hence, the curves that correspond to them in the phase space of H_a, $H_b(H_a)$, will appear as *limiting curves* of every other possible solution curve in the phase space. We of course limit our study only to solutions that are cosmologically viable (so for example we exclude solutions with contracting 3-space: $H_a < 0$). However, a more general picture is presented at the end of Section 3.6, in the form of flow diagrams. Finally, we note that the Kasner-type curves are straight lines in this space, which in the case of $K1$ and $K2$ depend only on n (see eq. (3.11)), and thus are the same regardless of the w parameters chosen. For the $K3$ case the ratio H_b/H_a depends also on the w parameters.

We can now use (3.18) to study the solution asymptotically, distinguishing two main cases. The first case would be H_a, $|H_b| \to \infty$ uniformly. The case $H_a > 0$ would, then, correspond to the behavior of a universe close to a singularity. The case H_a, $|H_b| \to 0$ would equivalently describe the asymptotic behavior of a universe heading towards an "equilibrium" state and is, in fact, the only case needed to match this setup with standard cosmological evolution[2].

The exact form of the exponents to which $K1$, $K2$, $K3$ solutions are raised, in (3.18), are the deciding factors of how the above asymptotic behaviors can be reached. The dependence on the powers' signs and the position of the initial values $\big(H_a(0), H_b(0)\big)$ with respect to the $K1$, $K2$, $K3$ curves in the phase space is what determines towards which of the (H_a, H_b) pairs: $(0,0)$, $(\pm\infty, \pm\infty)$ (and $(0, \pm\infty)$ if $n = 1$) the solution goes asymptotically[3].

To illustrate the above, we will work, without any loss of generality, with the solution for $n = 1$. We can incidentally see that the $K2$ part reduces to the trivial solution $H_a = 0$, mentioned before:

[2]We can directly see from (3.18) that asymptotic cases like $H_a/H_b \not\to c$ are not actually possible. As an example, consider a case where asymptotically $H_a \gg H_b$, $H_a/H_b \not\to c$. Ignoring the non-important constants, we end up with an equation of the form $const. = |H_b|^{\cdots} |\frac{H_a}{H_b}|^{\cdots}$, yielding $|H_b| H_a^x = const.$. By substitution of this constraint in (3.10), we can see that a non-trivial solution of this type is impossible. Thus, one sees that asymptotically it is possible only for one of the $K1$, $K2$, $K3$ solutions to end up attracting the phase curve of any other solution.

[3]This is only incidentally true in the cases that are of cosmological interest. The deciding factors for the attractors are the combination of the signs of the factors of eq. (3.10), along with the position of the initial conditions in the phase space compared to the $K1$, $K2$, $K3$ curves.

$$const. = \Big| \underbrace{H_b}_{H_b \text{ part}} \Big|^{2\sqrt{3}(3w_a - w_b - 2)(w_b - 1)} \cdot \Big| \underbrace{\frac{H_a}{H_b} + 1}_{K1 \text{ part}} \Big|^{\sqrt{3}(4 - 3w_a - w_b) + 3\sqrt{3}(w_a - w_b)} \cdot$$
$$\Big| \underbrace{\frac{H_a}{H_b}}_{K2 \text{ part}} \Big|^{\sqrt{3}(4 - 3w_a - w_b) - 3\sqrt{3}(w_a - w_b)} \cdot \Big| \underbrace{\frac{1 - w_b}{3w_a - 2w_b - 1} + \frac{H_a}{H_b}}_{K3 \text{ part}} \Big|^{-\sqrt{3}(4 - 6w_a w_b + 2w_b^2)} \tag{3.19}$$

The regions where the exponents of (3.19) have specific signs, are shown in Figure 3.1, as functions of the w parameters. We note that the region relevant to cosmologically viable models is region 2. This area includes the constraint $1 - 3w_a + 2w_b = 0$, which as shown in Section 3.4, is necessary to recover many results of Standard Cosmology.

Let us work, as an example, in the case $H_a/H_b \to const$, with $H_a,\, H_b \to 0$. We see that choosing EoS parameters in region 2 of Fig. 3.1, the H_b part of (3.19) will go to 0, because it is raised to a positive exponent. We have seen that (3.19) is a product of various factors, so at least one of them needs to go to infinity, in order to nullify the H_b part going to 0, and thus be consistent with the constant value of (3.19) on the $l.h.s$.

Assuming one chooses appropriate initial values[4], this can only be achieved asymptotically in the case $H_a/H_b \to 1/c_3$. This makes the $K3$ part's base go to zero raised to a negative exponent, so in total it diverges to infinity. On the other hand, if $H_a/H_b \to const$ with $H_a,\, H_b \to \infty$, the only way to be consistent in (3.19) with EoS parameters in region 2, is if the $K1$ part goes to 0 (because $H_a/H_b \to 1/c_1$), to nullify the H_b part that now diverges to infinity.

We can make use of this mathematical result to construct cosmological models with desirable properties, since region 2 of Figure 3.1 contains, all the cosmologically relevant values that we will need in terms of the EoS parameters. For any initial values that are contained between the $K1$ and $K3$ curves, and EoS parameters in region 2, we know exactly the asymptotic behavior of the corresponding solution: it will converge on the $K3$ special solution as $H_a,\, H_b \to 0$. Making the $K3$ solution have specific properties by means of fixing the w parameters (for example $q < 0$ and $|H_b| \ll H_a$), we force the general solution (3.18) to eventually behave like that.

We illustrate this in Fig. 3.2, where we have chosen a specific pair of w parameters, with the above in mind. We numerically construct the phase curves for 4 different choices of initial conditions, to show the behaviors of their phase curves as compared to the curves of the Kasner-type solutions.

Before concluding this section, it is quite interesting to note that the asymptotically attracting behavior of the Kasner-type solutions implies the existence of an attractor for the energy density, ρ, through eq. (3.8) (for $k_a = k_b = 0$). The energy density of these scenarios will ultimately be attracted to either empty universe scenarios ($\rho = 0$) through $K1$ and $K2$ solutions, or to the value predicted by the $K3$ solution:

$$k^2\rho = -\frac{2(2+n)\big[-3(w_a-1)^2 + n\big(3w_a^2 - 6w_a w_b + 2w_b(1+w_b) - 1\big)\big]H_a(0)^2}{\big[2 + 2(n-1)w_a - 2nw_b + t\big(3 - 3w_a^2 + n(1 + 3w_a^2 - 6w_a w_b + 2w_b^2)\big)H_a(0)\big]^2}. \tag{3.20}$$

[4]Meaning initial values that correspond to a phase curve limited by the $K1$ and $K3$ curves in this example.

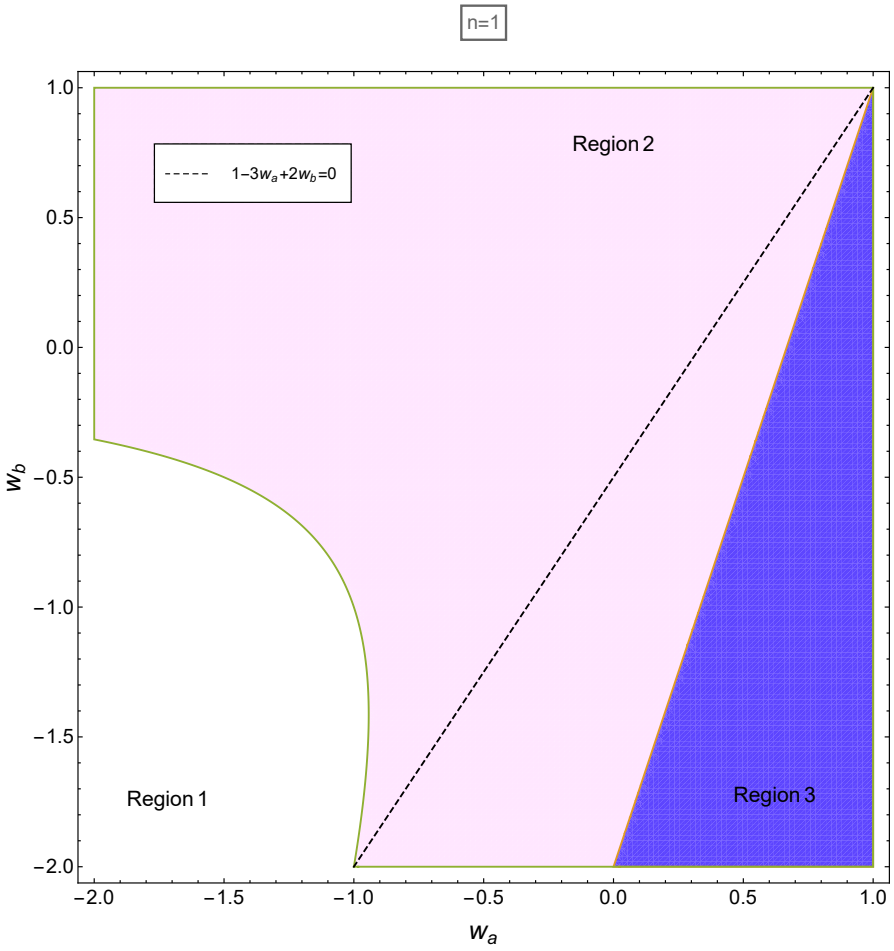

Figure 3.1: *For $n = 1$, the term containing only H_b in (3.19) is raised to an exponent that is everywhere positive, except for region 3. $K3$'s exponent is negative in regions 2 and 3. $K1$ is raised to a positive exponent everywhere, while $K2$ part is positive only in regions 1 and 2. As an example, in the case $\frac{H_a}{H_b} \to const$ with H_a, $H_b \to 0$ the general solution is consistent in region 2 where the H_b part converges to 0, but is canceled out by the $K3$ part that diverges to infinity. On the other hand, when H_a, $H_b \to \infty$, the roles are reversed. The $K1$ part is canceling out the H_b part in region 2. Similar results are obtained for any n, although the various regions are different in size and shape.*

3.4 Constraints to obtain a Cosmologically Viable Model

We proceed to discuss the constraints to be imposed on the parameters in order to produce a viable cosmological model. First and foremost, many results of Standard Cosmology that are consistent with observations need to be safeguarded, like the Big Bang Nucleosynthesis (BBN), and of course the non-detection of any extra dimensions so far. This leads us to two main properties to keep in mind, when it comes to the extra dimensions' evolution: a primordial super-contraction[5] of their size, rendering the extra space unobservable, followed by an (apparent) stabilization of their evolution ($H_b \approx 0$), from at least as early as BBN. Stabilizing the extra space is extremely important in this setup, since the fundamental coupling constants like Newton's G_N, are inversely proportionate to

[5]Or according to [176], an initial decompactification and super-expansion of the usual dimensions.

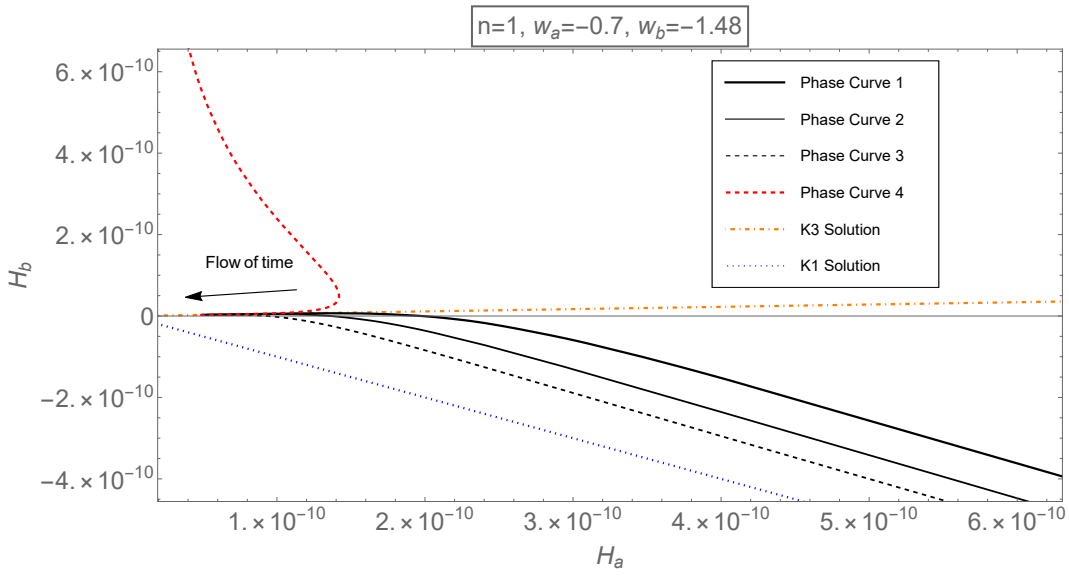

Figure 3.2: *The phase curves for 4 different choices of current values of H_a, H_b are presented. Curves $1-3$, are produced with current H values increasingly further from the $K3$ solution. Thus, the general solution is dominated by $K3$ for a smaller region (that in general would also imply a smaller time period). Curve #4 corresponds to a current ratio between the Hubble parameters, H_b/H_a, that is bigger than that of the $K3$ solution. Thus it corresponds to a different family than the first 3 curves. Going backwards in time one observes that the $K1$ solution dominates for curves $1-3$, while $K2$ dominates for the fourth curve, which for $n=1$ degenerates to the curve $H_a=0$.*

the extra dimensions' scale factor, $b(t)$:

$$G_N \propto b^{-n}$$

If that were not the case, then we would be able to measure a change in G_N by observations of high redshift objects, which so far is not the case.

The first of these properties is somewhat vague, since the minimum detection energy of the extra dimensions obviously depends on the compactification radius of a given theory. However, the second is very specific. Experiments and observations have been carried out, studying the values of the fundamental constants of all theories [184]. There exists no evidence that fundamental constants are not, indeed, constant throughout the evolution. As already mentioned, this would not be the case if extra dimensions, in the context of UED, evolved quickly, though a very slow evolution is not excluded.

Furthermore, we can follow a straightforward process to obtain a constraint for an exact stabilization, with regards to the EoS parameters [172]. By simple inspection of the equation of H_b, (3.10b), if we switch off all terms containing it, leaves as the only non-trivial solution the equation[6]:

$$1-3w_a+2w_b=0\ . \tag{3.21}$$

[6]The combination of the w parameters is affected only by the dimensionality of the usual space, not that of the extra space. For example, if $a(t)$ corresponded to m instead of 3 dimensions, the corresponding constraint would be $1-mw_a+(m-1)w_b=0$. The c_i factors would be different too. For example $c_3=\frac{1-mw_a+(m-1)w_b}{1-(n-1)w_a-nw_b}$

However, we do not impose this particular constraint. We will instead allow for a slow evolution of the extra dimensions, which, obviously, leads to a looser version of (3.21). It is easy to see that: by observing (3.21), we see that it is actually a special case of the $K3$ solution - the one in which we demand that $c_3 = 0$. In the phase space of the Hubble parameters, this corresponds to the $H_b = 0$ axis. So enforcing a looser version of (3.21) simply demands that w_a, w_b are such as to produce a $K3$ curve with a very small ratio H_b/H_a.

Moving on, in order to build a viable model, there are two specific constraints to be used to quantify an apparent stabilization to an effective 3-dimensional observer, namely:

$$|H_b^{(0)}| < \frac{1}{10n} H_a^{(0)} \ , \tag{3.22}$$

and

$$\frac{|b_{BBN} - b_{today}|}{b} \approx 1\% \ . \tag{3.23}$$

The first one is derived in [185] by a comparison of the experimental/observational results for $\frac{\dot{G_N}}{G_N}$ with the currently accepted value of the Hubble parameter, H_0, and utilizing the fact that in the UED scenario, it holds that $G_N \propto b^{-n}$. On the other hand, constraint (3.23) is inferred by a variety of works that take into account a plethora of tests, like element abundancies to check the electroweak coupling for various redshifts [184].

We could of course apply stricter constraints and still obtain solutions. But a much stricter constraint would effectively lead to an exact stabilization of the extra dimensions, which we already saw that is merely a special case of the $K3$ solution. Moreover, we will fit H_a results with observations, and also other observationally studied parameters, like the deceleration parameter, q:

$$q = -1 - \frac{\dot{H}}{H^2} \ ,$$

These will lead to a picture that is similar to that of the ΛCDM.

Combining specific observational results with stabilization constraints would, in general, be a tedious task. However, the $K3$ solution acts as an attractor for all possible pairs of initial conditions with a positive H_a that are between the $K1$ and $K3$ solution [7]. So, by making $K3$ consistent with these constraints, we create a significant in size class of phase curves, that correspond to a model compatible with imposed constraints. This completely removes any possible fine-tuning problems in terms of the initial values of H_a, H_b. Essentially, the study of any cosmologically viable solution for a given pair of w_a, w_b of the system, reduces to the study of its corresponding $K3$ solution.

We want to create a model that is stabilized from an early epoch. The $K3$ solutions for the various w parameters in its evolution (i.e. $w_a^{RD} = 1/3$, $w_a^{MD} = 0$ and their w_b counterparts) will be required to have a very small H_b/H_a ratio. This implies a closely correlated evolution of the EoS parameters themselves:

$$\text{apparent Stabilization} \Rightarrow \left(\frac{H_b}{H_a}\right)^{(K3)}_{\text{D. Energy era}} \approx \left(\frac{H_b}{H_a}\right)^{(K3)}_{\text{Mat. Dom.}} \approx \left(\frac{H_b}{H_a}\right)^{(K3)}_{\text{Rad. Dom.}}$$

We note that this comes at the cost of having to motivate a mechanism leading to w parameters evolving in the manner outlined above. This incidentally implies that w_b behaves in an exotic manner, if the stabilization holds from matter domination and on (for example through phantom energy scenarios [187], [188], or through string theory [176]).

Since, K-type solutions attract all other phase curves, it is important to know whether their perturbations decay with time. For solution $K3$, setting:

$$H_a(t) = H_a^{K3}(t) + H_a^{per}(t), \qquad H_b(t) = H_b^{K3}(t) + H_b^{per}(t)$$

[7] That is also true between $K2$ and $K3$. However , they are less desirable since they correspond to an expanding extra space

in equations (3.10), if we disregard all the non-linear perturbative terms, we obtain:

$$\dot{H}_a^{per} = \frac{2H_a^{(0)}\left[\left(3(w_a^2-1)+n(w_b-3w_a^2+3w_aw_b-1)\right)H_a^{per}+nw_b(w_a-nw_a+nw_b-1)H_b^{per}\right]}{2+2(n-1)w_a-2nw_b+\left(3-3w_a^2+n(1+3w_a^2-6w_aw_b+2w_b^2)\right)tH_a^{(0)}} \tag{3.24a}$$

$$\dot{H}_b^{per} = \frac{2H_a^{(0)}\left[3w_a(3w_a-2w_b-1)H_a^{per}+\left(3(w_a-1)+n(3w_aw_b-2w_b^2-1)\right)H_b^{per}\right]}{2+2(n-1)w_a-2nw_b+\left(3-3w_a^2+n(1+3w_a^2-6w_aw_b+2w_b^2)\right)tH_a^{(0)}} \tag{3.24b}$$

which is integrable for any value of n and constant w parameters. We now present the behavior of the perturbations as a function of t for $n=1$, which for both Hubble parameters is:

$$H_a^{per}, H_b^{per} \propto t^{\frac{-4+3w_a+w_b}{2-3w_aw_b+w_b^2}}$$

For all interesting values of the w parameters (and in particular for those that guarantee a stabilized extra space), the perturbations are decaying with time. This is because the exponent of t is negative in regions 2 and 3 of Fig. 3.1, so one obtains the convergence on $K3$ of all cosmologically relevant, in terms of the w parameters, solutions, that are close to it.

If the same procedure is followed for $K1$ and $K2$ solutions, for $n=1$ (meaning solution (3.15) and $H_a=0$), it can be shown that the perturbations' evolution is:

$$H_a^{per}, H_b^{per} \propto t^{-w_b}$$

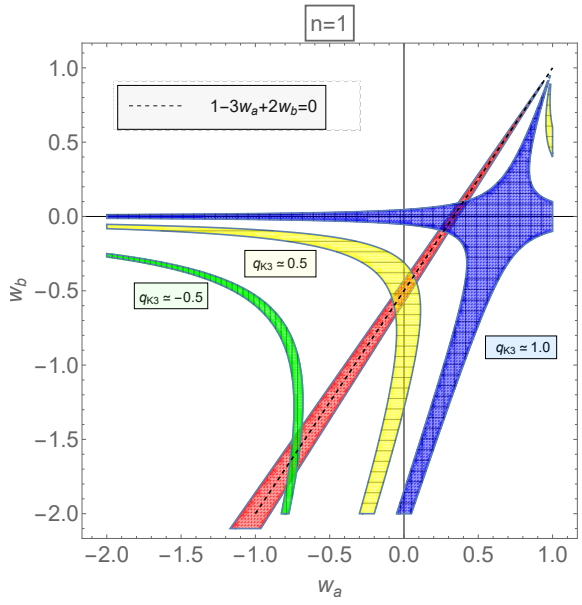

Figure 3.3: *The red triangular area includes the values of the w parameters making $K3$ solution satisfy the stabilization constraint for today. The blue, yellow and green areas of the graph, represent values for these parameters that produce an increasing (as we go towards $(1,1)$) value for q. The dashed line represents the exact stabilization constraint. We observe that as the values of the w parameters become more exotic, the constraint becomes less stringent.*

3.5 A reconstruction from today until the era of Radiation Domination

In order to model the behavior for the EoS parameters as outlined above, we will use transitions between values of w_a that are consistent with the Standard Model of Cosmology and the observations. The same will be done for w_b, while demanding that the stabilization constraints are satisfied. As long as the reasoning presented earlier is satisfied, any transition between these values, like a generalized Chaplygin gas [186], should be a viable option.

To build our model then, we will make appropriate choices to satisfy observational results for the current values of some cosmological parameters:

$$H_0 \approx 70 \frac{km/s}{Mpc} \ , \ q_0 \approx -0.6 \ ,$$

while at the same time preserving the theoretical results of Standard Cosmology, with regards to the evolution of the scale factor during radiation and matter domination ($t^{1/2}$ and $t^{2/3}$ respectively).

We will utilize our earlier result, that any solution will converge on a $K3$ solution, that satisfies any constraint that we want to impose. Since we analytically know the behavior of all $K3$-type solutions, it will be straightforward to quantify the various constraints. For example, in Fig. 3.3 one reads the region from which the EoS parameters can take values that satisfy constraint (3.22) (red triangular area), by using (3.16), in comparison with the constraint for an exact stabilization, (3.21) (dashed line). We also show 3 regions of the w parameters that correspond to 3 different current values of q_{K3}. Combining these compels us to choose from a specific region if we desire an apparent stabilization and $q \approx -0.6$ that corresponds to the observations. Finally, the transitions of the w parameters, will be such to also take into account the generally accepted transition from a decelerating to an accelerating expansion of the Universe at a redshift $z \approx 1-2$, as well as a particularly slow total evolution of $b(t)$, quantified by constraint (3.23).

Before presenting, the results of the above process, we make a final note: the observational results have to be matched with the effective values of the dimensionally reduced action, that typically corresponds to a Gravity plus Radion-field action, and not directly to those of the full $3+n+1$ action. Starting from the action of the full theory:

$$S \propto \int d^{4+n}x\sqrt{-g}(R - \mathcal{L}_{matter}) \tag{3.25}$$

and using the metric:

$$g_{AB}dx^A dx^B = g^{(4)}_{\mu\nu}dx^\mu dx^\nu + b^2(t)\gamma^{(n)}_{pq}dx^p dx^q$$

it is straightforward to go to the Gravity + Radion action [175]:

$$S \propto \int d^4x\sqrt{-\hat{g}}\big(R - \frac{1}{2}\partial_\mu\phi\partial^\mu\phi + V_{eff}(\phi)\big) \tag{3.26}$$

This is done by first integrating out the extra dimensional terms, followed by a Weyl transformation:

$$\hat{g}_{\mu\nu} = b^n(t)g^{(4)}_{\mu\nu} \tag{3.27}$$

This leads to the extra dimensions' scale factor, $b(t)$ being realized, from a 4-D point of view, as a scalar field in a potential:

$$\phi \propto lnb \qquad V_{eff}(\phi) = f(\mathcal{L}_{matter}, \phi)$$

The Weyl transformation changes the time and the 3-D scale factor that an effective 4-D observer would perceive in the following manner:

$$t_{eff} = \int b^{n/2}(t)dt + const \equiv g(t) \rightarrow \ t = g^{(-1)}(t_{eff}) \tag{3.28}$$

$$a_{eff}(t_{eff}) = b^{n/2}\big(g^{(-1)}(t_{eff})\big)a\big(g^{(-1)}(t_{eff})\big) \tag{3.29}$$

This leads to:

$$H_a^{(eff)} = \Big[\frac{n}{2}H_b\big(g^{(-1)}(t_{eff})\big) + H_a\big(g^{(-1)}(t_{eff})\big)\Big]\frac{dg^{(-1)}(t_{eff})}{dt_{eff}} \tag{3.30}$$

$$q_{eff}(t_{eff}) = -1 - \frac{dH_a^{(eff)}/dt_{eff}}{H_a^{(eff)2}} \tag{3.31}$$

But one sees from (3.28)-(3.31) that these corrections, with the exception of a scaling $b_0 \approx const$, are only important if the extra space is not stabilized. Hence it is necessary to take them into account only in primordial times, which are not studied here.

In Fig. 3.4 we show the evolution of H_a as predicted by this model, in comparison with the evolution predicted by the ΛCDM. The evolution of the 3-D scale factor compared with the expected evolution for a matter dominated universe is also presented. If scale factor $b(t)$ were not stabilized, the evolution of the scale factor would not be the same, regardless of the choice $w_a = 0$ for matter domination. This is because of (3.29). The same is true for the radiation domination and Dark Energy era.

In Fig. 3.5 we see the evolution of the scale factors whose today values are normalized as $a(0) = b(0) = 1$. Finally, in Fig. 3.6 we present the deceleration parameter of the model, as well as a direct comparison of the $m(z) - M$ curve that it predicts, with 580 SNIa observational points [189].

3.6 K - type scale factors and their effective picture

We now demonstrate the evolution of the scale factors of the K-type solutions and also that of their effective counterparts $a_{eff}(t_{eff})$, which proves to be quite different from $a(t)$ when the extra space is not stabilized. It is evident that the two Kasner solutions, $K1$ and $K2$, do not satisfy any stabilization condition[8], hence we expect a discrepancy between their evolution.

For demonstrative purposes, we will work in a scenario with $n = 2$. Integrating (3.13) and (3.14) we obtain the scale factors that read:

$$\left.\begin{aligned} a(t) &= \tilde{c_1}\big|-\sqrt{3} + 3(\sqrt{3} - 2\sqrt{2})H_a(0)t\big|^{\frac{1}{-3+2\sqrt{6}}} \\ b(t) &= \tilde{c_2}\big|2\sqrt{2} + 2\sqrt{3} + (6\sqrt{2} + 2\sqrt{3})H_a(0)t\big|^{-\frac{2}{2+2\sqrt{6}}} \end{aligned}\right\} \quad \text{K1} \tag{3.32}$$

$$\left.\begin{aligned} a(t) &= \tilde{c_1}\big|-\sqrt{3} + 3(\sqrt{3} + 2\sqrt{2})H_a(0)t\big|^{\frac{1}{-3-2\sqrt{6}}} \\ b(t) &= \tilde{c_2}\big|-2\sqrt{2} + 2\sqrt{3} + (2\sqrt{3} - 6\sqrt{2})H_a(0)t\big|^{-\frac{2}{2-2\sqrt{6}}} \end{aligned}\right\} \quad \text{K2} \tag{3.33}$$

where $\tilde{c_1}$, $\tilde{c_2}$ are constants of integration. According to (3.28) and (3.29) we could, in principle, get the time coordinate as a function of the effective time: $t = t(t_{eff})$ and thus $a_{eff} = a_{eff}(t_{eff})$. But that is a tedious task, even though we have the explicit forms of the scale factors, so instead we continue qualitatively.

From (3.32) we can see for the $K1$ solution, that if $t \gg t_{sing}$, then $b(t) \propto t^{-\frac{2}{2+2\sqrt{6}}}$. Thus, from eq. (3.28), one can deduce that $t \propto t_{eff}^{\frac{6-\sqrt{6}}{5}} \approx t_{eff}^{7/10}$. Then, eq. (3.29) leads to $t \gg t_{sing}$, $a_{eff} \propto t_{eff}^{1/3}$, as opposed to $a \propto t^{1/2}$.

When however, one contains one's study to the primordial stages, immediately after the singularity, the dimensionally reduced metric would not necessarily be the physical one. Nevertheless, if one naively looked for an "inflationary"-like evolution of solution $K1$, one would conclude that neither $a(t)$, nor the effective scale factor, a_{eff}, have a satisfactory evolution. We can follow the

[8] If, however, an infinite dimensionality n is considered, it can be shown that vacuum solutions can be stabilized [190].

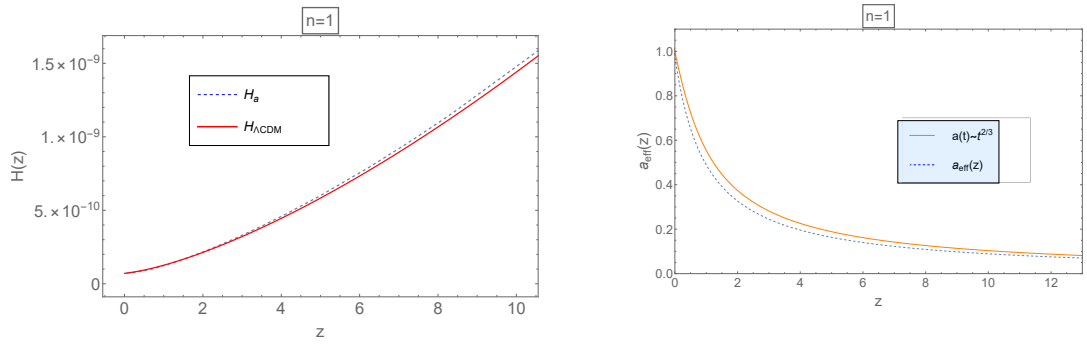

Figure 3.4: *The comparison of the evolution of H_a and $a(t)$ for a universe with stabilized extra space and their Standard Cosmology counterparts.*

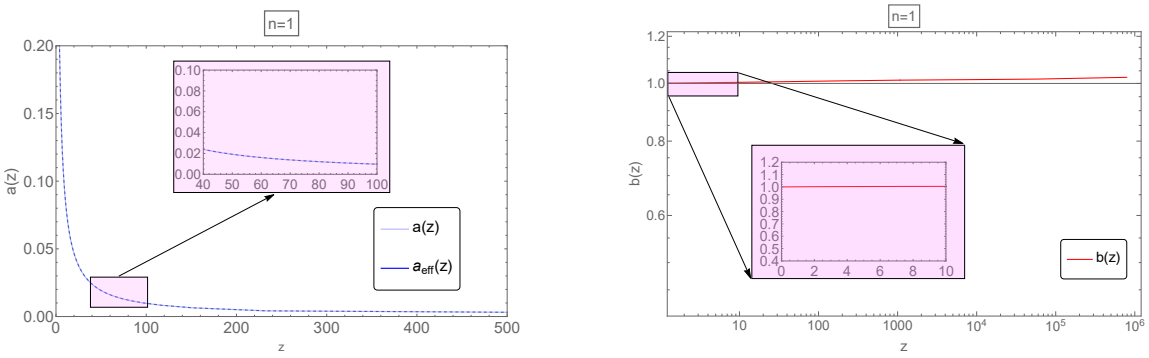

Figure 3.5: *The evolution of the scale factors.*

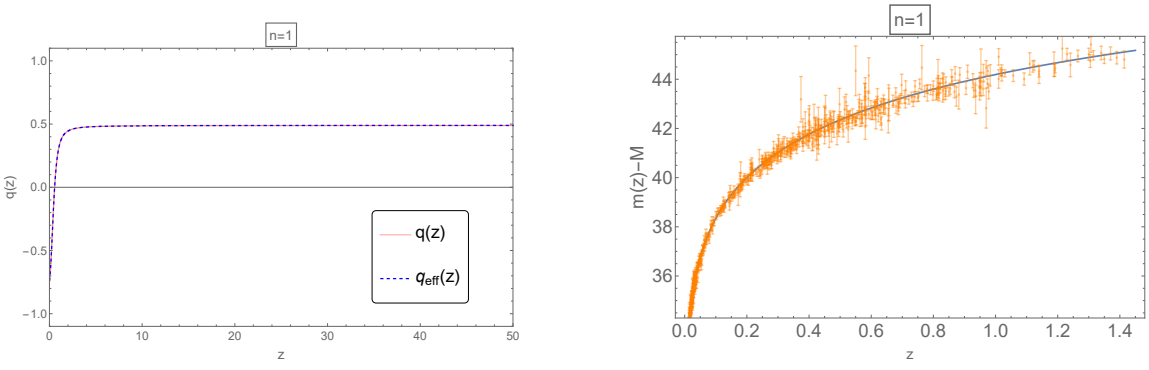

Figure 3.6: *The deceleration parameter and a comparison of the predicted $m(z) - M$ curve with 580 SNIa points [189].*

exact same reasoning for the $K2$ solution. However, we also note that this solution has a singularity in the future and not in the past.

The situation, however, is not the same for $K3$. To demonstrate this, we choose an example for $n = 2$. The corresponding scale factors are:

$$\left.\begin{aligned} a(t) &= \tilde{c_1}\left|2(1+w_a-2w_b)+(5+3w_a^2-12w_aw_b+4w_b^2)H_a(0)t\right|^{\frac{2+2w_a-4w_b}{5+3w_a^2-12w_aw_b+4w_b^2}} \\ b(t) &= \tilde{c_2}\left|2(1+w_a-2w_b)+(5+3w_a^2-12w_aw_b+4w_b^2)H_a(0)t\right|^{\frac{2-6w_a+4w_b}{5+3w_a^2-12w_aw_b+4w_b^2}} \end{aligned}\right\} \quad \text{K3} \quad (3.34)$$

It is easy to observe that there of course exist suitable values for the w parameters, namely $w_a = -1$, $w_b = -2$, that make the denominators of both the exponents, as well as the numerator of scale factor $b(t)$, equal to zero. Scale factor's $a(t)$ exponent is positive in regions 2 and 3 of Fig. 3.1, while the exponent of $b(t)$, is positive only in the area of region 2 appearing to the left of the dashed line (which represents the exact stabilization condition $1 - 3w_a + 2w_b = 0$). Thus, if one properly approaches the above values of the EoS parameters, then one can achieve a significant positive value for $a(t)$'s exponent, while at the same time a small negative value for $b(t)$'s exponent.

We note, however, that both the stability of the solution and the value of the exponent of $b(t)$ depend on the approaching of the aforementioned values. The necessary values lie on the boundary of regions 1 and 2 of Fig. 3.1 (a result that holds for every n), so a fluctuation of the EoS parameters, drastically changes the behavior of the solution. In the two panels of Fig. 3.7, the behaviors of the phase curves for values in regions 1 and 2 of Figure 3.1 respectively, for $n = 1$, can be seen. These examples are chosen to illustrate the behavior of the general solution qualitatively, without necessarily trying to match them with realistic cosmological results. In section 3.3, we mentioned that the evolution of a system of this type depends on the values of the EoS parameters and the initial values of the Hubble parameters, $H_a^{(i)}$, $H_b^{(i)}$. Depending on their relative position to the curves of the Kasner type solutions $K1$, $K2$, $K3$ in the phase space, the evolutions are quite different. But $K1$ and $K2$ (which for $n = 1$ reduces to the axis $H_a = 0$) have constant ratios of the Hubble parameters. Then, the deciding factor of where the phase curve is with regard to the $K1$, $K2$ curves and how it evolves, is the value of the $K3$ solution's ratio, which of course depends on the EoS values. That, in turn, in combination with the initial values of the Hubble parameters, and the signs of the $r.h.s$ factors of (3.10), decides which one of the special K-type solutions will be the attractor-curve in each case. We note that the dimensionality of the extra space bears no significance in the behaviors of the phase curves, which are qualitatively the same for any n.

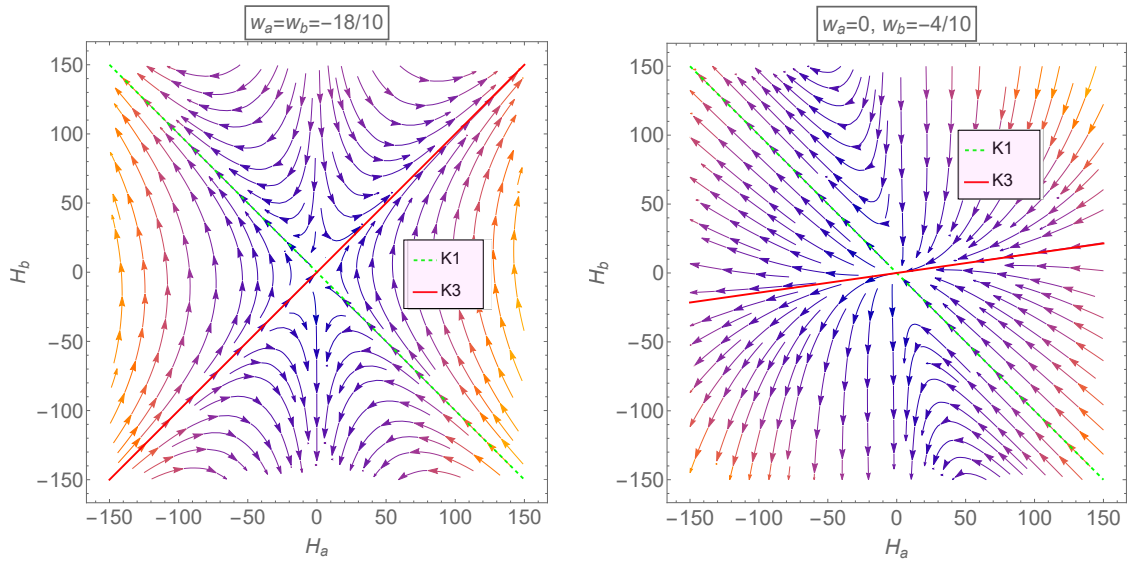

Figure 3.7: *Two examples for w parameters that correspond to values in Regions 1 and 2 of Fig. 3.1 respectively. Qualitatively the behaviors of the curves are independent of the exact value of n.*

3.7 Conclusions

To conclude this section, we reiterate that we have tried to present a concise view of how flat, homogeneous Universal Extra Dimensions would affect standard cosmological evolution. We have shown how one can recreate a picture similar to that of the ΛCDM. We have argued, that in the framework of UED, this can only be achieved if the extra dimensions are stabilized (i.e. evolve very slowly, or not at all) from a very early epoch. If that were not the case, then we would be able to measure a significant fluctuation in the values of fundamental coupling constants, as well as observe a variety of different phenomena. For example, one would expect a significant deviation from models of very high redshift events, like BBN, which of course is one of the best described eras within the Standard Cosmological Model. Thus, one understands that the stabilization of the extra dimensions must be settled, if such models are to be built, and produce viable phenomenology.

Taking that into account, we have managed to build such a model within the given observational limits. We do so for non-exactly static, but very slowly evolving extra dimensions. To do that, we use a special case solution for constant EoS parameters that acts as an attractor solution for a large variety of possible cosmologically relevant initial conditions of the Hubble parameters H_a, H_b (i.e. yielding an expanding 3-D space and a contracting extra space). This special case Kasner-type solution, is an exact solution of the Friedmann equations. Since it is analytically known we can manipulate it to yield the desired cosmological evolution, that is compatible with phenomenology, through its dependence on the EoS parameters. A large variety of initial conditions, that would otherwise correspond to a random general solution, will converge rapidly on this phenomenologically correct attractor-solution. However, we note that to achieve the stabilization of the extra dimensions without the use of any explicit mechanism, a larger, more exotic range of values has to be allowed for the EoS parameters, for both the usual and the extra spatial fluid. One could, possibly, expect this range of EoS parameters to arise from string theory, since it is, for example, known that strings, when wound around compactified dimensions, give similar effects.

Finally, we have studied, in terms of the EoS parameters, how the scale factors corresponding to this special Kasner-type solution would behave, close to its singularity. There exists a pair of the EoS parameters that can, produce a very fast expansion of the usual space's scale factor. At the same time, it yields a very slow, contracting, extra spatial scale factor. This, again, is achieved for exotic values of the EoS parameters, that one would have to justify via more fundamental theories. Moreover, these EoS parameters lay on the border of two regions that in general produce very different evolution patterns. Thus, a small fluctuation in the w's values could trigger a significant change in the evolution of the usual and extra space. One would have to perform a perturbative study not only for the scale factors but also for the w parameters' evolution themselves, in order to completely investigate this case.

Appendices

Appendix A

Cosmological Perturbations

A.1 Introduction

We now present the framework of studying primordial perturbations, mainly following [191–193]. As mentioned throughout the text, we are interested in studying the evolution of perturbations in cosmological fields, since they are thought to be the seeds of structure in the Universe. For an arbitrary cosmological field $\mathcal{F}$, we may write:

$$\mathcal{F}(x^\alpha) = \bar{\mathcal{F}}(\eta) + \delta\mathcal{F}(x^\alpha) \tag{A.1}$$

where η: the conformal time and $\delta\mathcal{F}$: the perturbation from the background value of the field, $\bar{\mathcal{F}}$. The fact that the field is cosmological means that the background value is only a function of time, due to isotropy and homogeneity, hence $\bar{\mathcal{F}} = \bar{\mathcal{F}}(\eta)$.

By definition, the spatial average of the perturbation of a field is 0:

$$\frac{\int \delta\mathcal{F} dV}{V} = 0 \tag{A.2}$$

implying that the spatial average of a perturbed field is, thus, equal to its background value:

$$\frac{\int \mathcal{F} dV}{V} = \bar{\mathcal{F}} \tag{A.3}$$

To produce the basic formulas needed in perturbation theory we will utilize three gauges, the background gauge and two perturbed gauges denoted with a caret ”” and a tilde ”” respectively. When referring to a specific physical point in spacetime, P, to transform from one gauge to another we have:

$$\begin{aligned} \hat{x}^\alpha\big|_P &= x^\alpha\big|_P + \kappa^\alpha\big|_P \\ \tilde{x}^\alpha\big|_P &= x^\alpha\big|_P + \lambda^\alpha\big|_P \end{aligned} \tag{A.4}$$

leading to the transformation between the two perturbed gauges:

$$\tilde{x}^\alpha\big|_P = \hat{x}^\alpha\big|_P + \xi^\alpha\big|_P \tag{A.5}$$

where: $\xi^\alpha = \lambda^\alpha - \kappa^\alpha$ is the transformation vector. We note that a specific physical point P, corresponds to 3 different sets of coordinates in the three gauges. On the contrary, a specific set of coordinate values corresponds, in general, in the three different gauges, to 3 different physical points in spacetime, that is:

$$\tilde{x}^\alpha\big|_{\tilde{P}} = \hat{x}^\alpha\big|_{\hat{P}} = x^\alpha\big|_P \tag{A.6}$$

Thus, we can rewrite eq. (A.1) in the perturbed gauges in terms of the background coordinates, rather than the perturbed ones:

$$\begin{aligned}\hat{\mathcal{F}}(x^\alpha) &= \bar{\mathcal{F}}(\eta) + \delta\hat{\mathcal{F}}(x^\alpha)\\ \tilde{\mathcal{F}}(x^\alpha) &= \bar{\mathcal{F}}(\eta) + \delta\tilde{\mathcal{F}}(x^\alpha)\end{aligned} \tag{A.7}$$

A.2 Transformations at a specific point

We have already mentioned that when referring to a specific physical point, in general, it holds that $x^\alpha(P) \neq \hat{x}^\alpha(P) \neq \tilde{x}^\alpha(P)$. Regarding the fields that we will use, we know, however, that scalar fields do not change their value in different gauges, when referring to the same point. On the other hand, the same set of coordinate values will yield different values for all fields, even scalars, in different gauges. Hence, for a scalar field f:

$$f\big|_P = \hat{f}\big|_P = \tilde{f}\big|_P \tag{A.8}$$

This is not the case for vector and tensor fields. For a vector field f^α we have:

$$\tilde{f}^\alpha\big|_P = X^{\tilde{\alpha}}_{\hat{\beta}}\big|_P \hat{f}^\beta\big|_P \tag{A.9}$$

where we have defined the transformation matrix

$$X^{\tilde{\alpha}}_{\hat{\beta}} = \frac{\partial\tilde{x}^\alpha}{\partial\hat{x}^\beta} \tag{A.10}$$

However, to first order we can approximate that, at a specific point, when a derivative acts on a quantity that is to be perturbed, it holds that:

$$\frac{\partial}{\partial\tilde{x}^\alpha} \approx \frac{\partial}{\partial\hat{x}^\alpha} \approx \frac{\partial}{\partial x^\alpha} \tag{A.11}$$

since to first order, we have:

$$\frac{\partial}{\partial x^\alpha} = \frac{\partial\hat{x}^\beta}{\partial x^\alpha}\frac{\partial}{\partial\hat{x}^\beta} = \frac{\partial}{\partial x^\alpha}\left(x^\beta + \kappa^\beta\right)\frac{\partial}{\partial\hat{x}^\beta} = \left(\delta^\beta_\alpha + \kappa^\beta_{,\alpha}\right)\frac{\partial}{\partial\hat{x}^\beta} \approx \frac{\partial}{\partial\hat{x}^\beta} \tag{A.12}$$

Returning to (A.10), we get:

$$X^{\tilde{\alpha}}_{\hat{\beta}} = \frac{\partial\tilde{x}^\alpha}{\partial\hat{x}^\beta} = \frac{\partial\left(\hat{x}^\alpha + \xi^\alpha\right)}{\partial\hat{x}^\beta} = \delta^\alpha_\beta + \xi^\alpha_{,\hat{\beta}} \overset{(A.12)}{\approx} \delta^\alpha_\beta + \xi^\alpha_{,\beta} \tag{A.13}$$

We can now obtain a relation for the transformation of a vector in terms of the transformation vector ξ, at a specific point from one gauge to another:

$$\tilde{f}^\alpha = \left(\delta^\alpha_\beta + \xi^\alpha_{,\beta}\right)\hat{f}^\beta = \hat{f}^\alpha + \xi^\alpha_{,\beta}\left(\bar{f}^\beta + \delta\tilde{f}^\beta\right) \approx \hat{f}^\alpha + \xi^\alpha_{,\beta}\bar{f}^\beta \tag{A.14}$$

but since $\bar{f} = \bar{f}(\eta)$ we get[1]:

$$\tilde{f}^\alpha\big|_P = \hat{f}^\alpha\big|_P + \xi^\alpha_{,0}\big|_P\bar{f}^0 \tag{A.15}$$

In a similar manner we may obtain the transformation relations at one point P for tensor quantities, at first order. For a 2-0, 1-1 and 0-2 tensor we have then, respectively:

$$\tilde{f}^{\alpha\beta}\big|_P = \hat{f}^{\alpha\beta}\big|_P + \xi^\alpha_{,\mu}\big|_P\hat{f}^{\mu\beta}\big|_P + \xi^\beta_\nu\big|_P\hat{f}^{\nu\alpha}\big|_P \tag{A.16}$$

$$\tilde{f}^\alpha_\beta\big|_P = \hat{f}^\alpha_\beta\big|_P + \xi^\alpha_{,\mu}\big|_P\hat{f}^\mu_\beta\big|_P - \xi^\nu_\beta\big|_P\hat{f}^\alpha_\nu\big|_P \tag{A.17}$$

$$\tilde{f}_{\alpha\beta}\big|_P = \hat{f}_{\alpha\beta}\big|_P - \xi^\mu_{,\alpha}\big|_P\hat{f}_{\beta\mu}\big|_P - \xi^\nu_\beta\big|_P\hat{f}_{\alpha\nu}\big|_P \tag{A.18}$$

[1] A background vector is of the form $\bar{f}^\alpha(\eta) = (\bar{f}^0(\eta), \bar{f}^i(\eta))$. But due to isotropy the spatial average of $f^i(\eta, x^j)$ is 0, hence $\int f^i(\eta, x^j) = \bar{f}^i(\eta) = 0$.

A.3 Gauge transformation of a perturbation

We are now interested in producing the gauge transformation of the perturbation of a field, that is, the transformation of the perturbation between gauges at a specific point. To proceed, we need two more approximations regarding the transformation vector and the perturbation of a field in different gauges. Regarding the transformation vector, it can be proven that to first order it is the same for two neighboring points:

$$\xi^\alpha\big|_{\tilde{P}} \approx \xi^\alpha\big|_{\hat{P}} \approx \xi^\alpha\big|_P \tag{A.19}$$

To prove this we work as follows:

$$\begin{aligned}
\xi^\alpha\big|_{\hat{P}} &= \xi^\alpha\big|_P + \left(\frac{\partial \xi^\alpha}{\partial x^\beta}\right)_P \left(x^\beta\big|_{\hat{P}} - x^\beta\big|_P\right) \\
&\overset{(A.6)}{=} \xi^\alpha\big|_P + \left(\frac{\partial \xi^\alpha}{\partial x^\beta}\right)_P \left(x^\beta\big|_{\hat{P}} - \hat{x}^\beta\big|_{\hat{P}}\right) \\
&= \xi^\alpha\big|_P + \left(\frac{\partial \xi^\alpha}{\partial x^\beta}\right)_P \kappa^\beta\big|_{\hat{P}} \\
&\approx \xi^\alpha\big|_P
\end{aligned} \tag{A.20}$$

where the second term is dropped since it is of higher order. We thus see that the transformation vector ξ^α can, and will unless otherwise noted, be associated with the background point P when working in first order approximation. In a similar manner, we can prove that the perturbation of an arbitrary field is the same for two neighboring physical points, that is:

$$\delta\mathcal{F}\big|_{\tilde{P}} \approx \delta\mathcal{F}\big|_{\hat{P}} \approx \delta\mathcal{F}\big|_P \tag{A.21}$$

Moving on, we are interested in knowing the change between the values of an arbitrary field $\mathcal{F}$ in a single gauge, for two points that correspond to the same set of coordinate values in different gauges, i.e.: $\mathcal{F}\big|_{\tilde{P}} - \mathcal{F}\big|_{\hat{P}}$. We have then:

$$\begin{aligned}
\hat{\mathcal{F}}\big|_{\tilde{P}} &= \hat{\mathcal{F}}\big|_{\hat{P}} + \frac{\partial \hat{\mathcal{F}}\big|_{\hat{P}}}{\partial \hat{x}^\beta}\left(\hat{x}^\beta\big|_{\tilde{P}} - \hat{x}^\beta\big|_{\hat{P}}\right) \\
&\overset{(A.11)}{\approx} \hat{\mathcal{F}}\big|_{\hat{P}} + \frac{\partial \hat{\mathcal{F}}\big|_{\hat{P}}}{\partial x^\beta}\left(\hat{x}^\beta\big|_{\tilde{P}} - \tilde{x}^\beta\big|_{\tilde{P}}\right) \\
&\overset{(A.7)}{=} \hat{\mathcal{F}}\big|_{\hat{P}} + \left(\frac{\partial \bar{\mathcal{F}}\big|_P}{\partial x^\beta} + \frac{\partial\left(\delta\hat{\mathcal{F}}\big|_P\right)}{\partial x^\beta}\right)\left(-\xi^\beta\big|_{\tilde{P}}\right) \\
&\overset{(A.20)}{\approx} \hat{\mathcal{F}}\big|_{\hat{P}} + \frac{\partial \bar{\mathcal{F}}\big|_P}{\partial x^\beta}\left(-\xi^\beta\big|_P\right)
\end{aligned} \tag{A.22}$$

so finally

$$\hat{\mathcal{F}}\big|_{\tilde{P}} = \hat{\mathcal{F}}\big|_{\hat{P}} - \frac{\partial \bar{\mathcal{F}}\big|_P}{\partial x^0}\xi^0\big|_P \tag{A.23}$$

We are now ready to find the transformation rules for perturbations between the two gauges when referring to the same physical point.

A.3.1 Gauge Transformation of Scalar Perturbations

Let us now consider the perturbation of a scalar field f. When eq. (A.23) refers to a scalar field we get:

$$f\big|_{\tilde{P}} = f\big|_{\hat{P}} - \bar{f}'(\eta)\xi^0\big|_P \tag{A.24}$$

where a prime denotes differentiation with respect to conformal time, η. But eqs. (A.6) and (A.7) lead to:

$$\tilde{\mathcal{F}}\big|_{\tilde{P}} = \bar{\mathcal{F}}(\eta) + \delta\tilde{\mathcal{F}}\big|_{P} \tag{A.25}$$

hence, when referring to a scalar:

$$\begin{aligned} f\big|_{\tilde{P}} &= \bar{f}(\eta) + \delta\tilde{f}\big|_{P} \\ f|_{\hat{P}} &= \bar{f}(\eta) + \delta\hat{f}|_{P} \end{aligned} \tag{A.26}$$

Substituting in (A.24) we then obtain:

$$\delta\tilde{f} = \delta\hat{f} - \bar{f}'\xi^0 \tag{A.27}$$

where we have stopped denoting the point to which we refer, since all the above quantities are expressed with respect to the coordinates of this particular point, in the background gauge.

A.3.2 Gauge Transformation of Vector Perturbations

Moving on, we now consider the perturbation of a vector field. Equation (A.23) reads, in the case of vectors:

$$\tilde{f}^{\alpha}\big|_{\tilde{P}} = \tilde{f}^{\alpha}\big|_{\hat{P}} - \bar{f}'^{\alpha}(\eta)\xi^0 \tag{A.28}$$

But for a vector we have proven (A.15):

$$\tilde{f}^{\alpha}\big|_{\hat{P}} = \hat{f}^{\alpha}\big|_{\hat{P}} + \xi^{\alpha}_{,0}\bar{f}^0$$

Thus, we get

$$\tilde{f}^{\alpha}\big|_{\tilde{P}} = \hat{f}^{\alpha}\big|_{\hat{P}} + \xi^{\alpha}_{,0}\bar{f}^0(\eta) - \bar{f}'^{\alpha}(\eta)\xi^0 \tag{A.29}$$

and along with (A.25) in the case of a vector, we can obtain the following equation, where we again have dropped P since all quantities refer to the same point:

$$\delta\tilde{f}^{\alpha} = \delta\hat{f}^{\alpha} + \xi^{\alpha}_{,0}\bar{f}^0 - \bar{f}'^{\alpha}\xi^0 \tag{A.30}$$

A.3.3 Gauge Transformation of Tensor Perturbations

Along the same lines, we can obtain the transformation of tensor perturbations between gauges. Once again, we start from (A.23) which for a 1-1 tensor is of the form:

$$\tilde{f}^{\alpha}_{\beta}\big|_{\tilde{P}} = \tilde{f}^{\alpha}_{\beta}\big|_{\hat{P}} - \bar{f}^{\alpha}_{\beta}(\eta)\xi^0 \tag{A.31}$$

But using eq. (A.17) we obtain:

$$\tilde{f}^{\alpha}_{\beta}\big|_{\tilde{P}} = \hat{f}^{\alpha}_{\beta}\big|_{\hat{P}} + \xi^{\alpha}_{,\mu}\hat{f}^{\mu}_{\beta}|_{\hat{P}} - \xi^{\nu}_{,\beta}\hat{f}^{\alpha}_{\nu}|_{\hat{P}} - \bar{f}'^{\alpha}_{\beta}(\eta)\xi^0 \tag{A.32}$$

Once again, using eq. (A.25), we get, for a tensor quantity:

$$\begin{aligned} \tilde{f}^{\alpha}_{\beta}\big|_{\tilde{P}} &= \bar{f}^{\alpha}_{\beta}(\eta) + \delta\tilde{f}^{\alpha}_{\beta}\big|_{P} \\ \hat{f}^{\alpha}_{\beta}\big|_{\hat{P}} &= \bar{f}^{\alpha}_{\beta}(\eta) + \delta\hat{f}^{\alpha}_{\beta}\big|_{P} \end{aligned} \tag{A.33}$$

Thus, we finally obtain the relation for the gauge transformation of a 1-1 tensor perturbation, at a specific physical point:

$$\delta\tilde{f}^{\alpha}_{\beta} = \delta\hat{f}^{\alpha}_{\beta} + \xi^{\alpha}_{,\mu}\bar{f}^{\mu}_{\beta} - \xi^{\nu}_{,\beta}\bar{f}^{\alpha}_{\nu} - \bar{f}'^{\alpha}_{\beta}\xi^0 \tag{A.34}$$

A.4 Decomposition of Perturbations

A.4.1 Fourier Decomposition of a Scalar Perturbation

As already mentioned, only Scalar Perturbations are responsible for the structure formation of the Universe. Scalar fields can however be extracted also from vectors and tensors. Hence, it is easier to study the scalar perturbations by first linearly decomposing all perturbation modes.

We start by the Fourier decomposition of a scalar perturbation, namely:

$$\delta f(\eta, \vec{x}) = \sum_{\vec{k}} \delta f_{\vec{k}}(\eta) e^{i\vec{k}\cdot\vec{x}} \tag{A.35}$$

Then, each mode $\delta f_{\vec{k}}(\eta) e^{i\vec{k}\cdot\vec{x}}$ is a wave that corresponds to the comoving wave vector $\vec{k}$

A.4.2 Fourier Decomposition of a Vector Perturbation

However, we can extract other scalar modes from vector and tensor perturbations as well, through Helmholtz decomposition. In the case of vector perturbations, we obtain a longitudinal part (which is called the *scalar potential*) and a transverse part which is a *pure* vector.

We can always decompose a vector field into a curl free and a divergence free component. Hence, for a vector perturbation we can write:

$$\delta\vec{f} = \vec{S} + \vec{V}, \qquad \nabla \times \vec{S} = 0, \qquad \nabla \cdot \vec{V} = 0 \tag{A.36}$$

But the curl of a divergence is equal to 0, so we can express $\vec{S}$ as the divergence of a scalar $\mathcal{S}$:

$$\vec{S} = -\nabla\mathcal{S} \tag{A.37}$$

Rewriting the above in index notation we have:

$$\delta f_i = S_i + V_i, \qquad S_i = -\mathcal{S}_{,i} \qquad \textit{and} \qquad \delta^{ij} V_{i,j} = V_{i,i} = 0 \tag{A.38}$$

It is interesting to see that $\vec{S}$ and $\vec{V}$ are decoupled, because in the Fourier space, $\vec{S}_{\vec{k}}$ is parallel to $\vec{k}$ while $\vec{V}_{\vec{k}}$ is orthogonal to $\vec{k}$. Decomposing $\vec{S}$ and $\mathcal{S}$ in the Fourier space, we get:

$$\begin{aligned} \vec{S}(x^\alpha) &= \sum_{\vec{k}} \vec{S}_{\vec{k}}(\eta) e^{i\vec{k}\cdot\vec{x}} \\ \mathcal{S} &= \sum_{\vec{k}} Q_{\vec{k}}(\eta) e^{i\vec{k}\cdot\vec{x}} \end{aligned} \tag{A.39}$$

Using (A.37) we then obtain that

$$\vec{S}_{\vec{k}}(\eta) = -i\vec{k} Q_{\vec{k}}(\eta) \tag{A.40}$$

and hence we have proven that $\vec{S}_{\vec{k}}$ is parallel to $\vec{k}$. As a convention, we define from now on that $\mathcal{S}_{\vec{k}} = kQ_{\vec{k}}$, where $k = |\vec{k}|$. So finally, we can write:

$$\vec{S}(x^\alpha) = \sum_{\vec{k}} \vec{S}_{\vec{k}} e^{i\vec{k}\cdot\vec{x}}, \qquad \text{where} \qquad \vec{S}_{\vec{k}} = -i\frac{\vec{k}}{k}\mathcal{S}_{\vec{k}} \tag{A.41}$$

Dropping the $\vec{k}$ index we can relate the modes, in index notation, as:

$$S_j = -i\frac{k_j}{k}\mathcal{S} \tag{A.42}$$

Regarding the transverse part, we rotate the coordinate system in such a way that the z- axis is parallel to $\vec{k} : \vec{k} - k\hat{z}$. Since $V_{i,i} = 0$, we obtain $k_i V_i = 0$, since

$$\vec{V} = \sum_{\vec{k}} \vec{V}_{\vec{k}}(\eta) e^{i\vec{k}\cdot\vec{x}} \tag{A.43}$$

and

$$\nabla \cdot \vec{V} = \sum_{\vec{k}} \vec{V}_{\vec{k}}(\eta) \nabla e^{i\vec{k}\vec{x}} = \sum_{\vec{k}} i\vec{V}_{\vec{k}}(\eta)\vec{k} e^{i\vec{k}\cdot\vec{x}} = 0 \tag{A.44}$$

so, it follows that:

$$\vec{k} \cdot \vec{V}_{\vec{k}} = 0$$

But since the axes are rotated as mentioned above, we obtain $k_3 V_3 = 0$, therefore it follows that $V_3 = 0$.

Moreover, from (A.42) and the fact that $\vec{k} = k\hat{z}$, we obtain that $S_z = -i\mathcal{S}$, while $S_x = S_y = 0$. Thus, we can write that

$$\delta\vec{f} = \vec{S} + \vec{V} = (V_1, V_2, -i\mathcal{S}) \tag{A.45}$$

A.4.3 SVT Decomposition of Tensor Perturbations

Our next step is to decompose a tensor perturbation. As a working example we will work with a $(0, 2)$ tensor, which we will suppose to be symmetric ($\delta f_{i0} = \delta f_{0i}$):

$$\delta f_{\alpha\beta}(x^\alpha) = \begin{pmatrix} \delta f_{00}(x^\alpha) & \delta f_{i0}(x^\alpha) \\ \delta f_{0i}(x^\alpha) & \delta f_{ij}(x^\alpha) \end{pmatrix} = \begin{pmatrix} A & B_i \\ B_i & C_{ij} \end{pmatrix} \tag{A.46}$$

Scalar A and vector B_i can be decomposed as before. However, matrix C_{ij} is a 3×3 matrix that can be decomposed into scalar, vector and tensor quantities. This is referred to as the *SVT decomposition*.

For a random tensor C_{ij} we can use the trace $C_{\alpha\alpha}$ to write it as:

$$C_{ij} = C_{ij} - \frac{1}{3}\delta_{ij}C_{\alpha\alpha} + \frac{1}{3}\delta_{ij}C_{\alpha\alpha}, \qquad C_{\alpha\alpha} = C_{11} + C_{22} + C_{33} \tag{A.47}$$

and by defining $D = \frac{1}{3}C_{\alpha\alpha}$, $E_{ij} = C_{ij} - \delta_{ij}D$ we obtain:

$$\delta f_{\alpha\beta}(x^\alpha) = \begin{pmatrix} A & B_i \\ B_i & \delta_{ij}D + E_{ij} \end{pmatrix} \tag{A.48}$$

E_{ij} is traceless ($E_{ii} = 0$) and symmetric. It splits into three parts, that correspond to a scalar, a vector and a tensor quantity[2]. We show that as follows:

$$E_{ij} = S_{ij} + V_{ij} + \tau_{ij} \tag{A.49}$$

Each one of S_{ij}, V_{ij} and τ_{ij} is symmetric and traceless and are decoupled from each other in linear perturbation theory.

First, we want to construct a symmetric and traceless S_{ij} matrix. Thus, we define a new scalar potential, $\mathtt{S}$, and write S_{ij} as:

$$S_{ij} = (\partial_i\partial_j - \frac{1}{3}\delta_{ij}\nabla^2)\mathtt{S} = \mathtt{S}_{,ij} - \frac{1}{3}\delta_{ij}\delta^{ab}\mathtt{S}_{,ab} = \mathtt{S}_{,ij} - \frac{1}{3}\delta_{ij}\mathtt{S}_{,aa} \tag{A.50}$$

[2]The names "scalar, vector" and "tensor" are used to refer to their transformation properties under rotations in the background gauge. This can be easily seen since, for example, scalar perturbations are *not* gauge invariant.

It is easy to confirm that the above construction is both symmetric and traceless.

Next, we can extract a tensor that encompasses the vector part of $\delta f_{\alpha\beta}$. We define V_{ij} as:

$$V_{ij} = \frac{1}{2}\left(\mathcal{V}_{i,j} + \mathcal{V}_{j,i}\right) \tag{A.51}$$

which is symmetric by construction. We have also defined the above decomposition in such a way that $\mathcal{V}_i$ is a pure vector, thus divergence free. This translates to:

$$\nabla \cdot \vec{\mathcal{V}} = \delta^{ij}\mathcal{V}_{i,j} = \mathcal{V}_{i,i} = 0 \tag{A.52}$$

which also makes V_{ij} a traceless matrix, since $V_{ii} = \frac{1}{2}(2V_{i,i}) = 0$

The tensor component, then, must also be symmetric and traceless, since it can be expressed as

$$\tau_{ij} = E_{ij} - S_{ij} - V_{ij} \tag{A.53}$$

Thus

$$\tau_{ij} = \tau_{ji}, \qquad \delta^{ij}\tau_{ij} = \tau_{ii} = 0 \tag{A.54}$$

A.4.4 Fourier Decompositions of SVT quantities

For the 00 scalar of $\delta f_{\alpha\beta}$ we have in the Fourier space that

$$A(x^\alpha) = \sum_{\vec{k}} A_{\vec{k}} e^{i\vec{k}\vec{x}} \tag{A.55}$$

The vector part, B_i, can be decomposed in a similar manner as before, and be written as:

$$B_i = \beta_i + b_i \tag{A.56}$$

where b_i is such that $b_i = -\nabla\mathcal{B}$, and $\mathcal{B}$ is written in the Fourier space as:

$$\mathcal{B}(x^\alpha) = \sum_{\vec{k}} \frac{\mathcal{B}_{\vec{k}}(\eta)}{k} e^{i\vec{k}\vec{x}} \tag{A.57}$$

while β_i is:

$$\beta_i(x^\alpha) = \sum_{\vec{k}} \beta_{i_{\vec{k}}}(\eta) e^{i\vec{k}\vec{x}} \tag{A.58}$$

Moving on to the 3×3 part of $\delta f_{\alpha\beta}$, $C_{ij} = \delta_{ij}D + E_{ij}$, scalar D in the Fourier space, is expressed as:

$$D(x^\alpha) = \sum_{\vec{k}} D_{\vec{k}}(\eta) e^{i\vec{k}\vec{x}} \tag{A.59}$$

We now turn to the E_{ij} part that we further decompose into three parts. Scalar $\mathtt{S}$ is decomposed as:

$$\mathtt{S} = \sum_{\vec{k}} Q_{\vec{k}}(\eta) e^{i\vec{k}\vec{x}} \tag{A.60}$$

In order for S_{ij} and $\mathtt{S}$ to have the same dimensions we get according to (A.50):

$$\begin{aligned} S_{ij_{\vec{k}}} &= \left(-k_i k_j + \frac{1}{3}\delta_{ij}k^2\right) Q_{\vec{k}} \\ &= \left(-\frac{k_i k_j}{k^2} + \frac{1}{3}\delta_{ij}\right) k^2 Q_{\vec{k}} \\ &= \left(-\frac{k_i k_j}{k^2} + \frac{1}{3}\delta_{ij}\right) k^2 \mathtt{S}_{\vec{k}} \end{aligned} \tag{A.61}$$

where we have defined $Q_{\vec{k}} = \mathtt{S}_{\vec{k}}$, leading to the more convenient definition for $\mathtt{S}$:

$$\mathtt{S}(x^\alpha) = \sum_{\vec{k}} \frac{\mathtt{S}_{\vec{k}}}{k^2} e^{i\vec{k}\vec{x}} \tag{A.62}$$

On the same footing, in the case of the vector part, we have

$$V_{ij} = \frac{1}{2}\left(\mathcal{V}_{i,j} + \mathcal{V}_{j,i}\right) \tag{A.63}$$

Decomposing $\vec{\mathcal{V}}$, we have that

$$\vec{\mathcal{V}}(x^\alpha) = \sum_{\vec{k}} \vec{Q}_{\vec{k}} e^{i\vec{k}\vec{x}} \tag{A.64}$$

so, in the Fourier space:

$$V_{ij} = \frac{i}{2}\left(k_i Q_j + k_j Q_i\right) \tag{A.65}$$

and

$$\delta^{ij} k_j Q_i = 0 \tag{A.66}$$

To obtain coefficients with the same dimensionality, we rewrite as:

$$V_{ij} = \frac{i}{2k}\left(k_i k Q_j + k_j k Q_i\right) = \frac{i}{2k}\left(k_i \mathcal{V}_j + k_j \mathcal{V}_i\right) \tag{A.67}$$

where we have defined $\mathcal{V}_i = kQ_i$ and it follows that:

$$\delta^{ij} k_j \mathcal{V}_i = 0 \tag{A.68}$$

Therefore, it is more useful to define the components of vector $\vec{\mathcal{V}}$ as:

$$\mathcal{V}_i(x^\alpha) = \sum_{\vec{k}} \frac{\mathcal{V}_{i_{\vec{k}}}(\eta)}{k} e^{i\vec{k}\vec{x}} \tag{A.69}$$

Finally, we decompose the tensor part in Fourier modes:

$$\tau_{ij}(x^\alpha) = \sum_{\vec{k}} \tau_{ij_{\vec{k}}}(\eta) e^{i\vec{k}\vec{x}} \tag{A.70}$$

We will now focus on showing the independence of the various sectors of the SVT decomposed components. We rotate the z-axis in such a way that it is parallel to $\vec{k}$. We begin with B_i, which as

before, will be shown to be decomposed as a divergence-free plus a curl free component. The curl free component is defined as b_i and the divergence free component is defined as β_i. We have:

$$B_i = b_i + \beta_i, \qquad \text{where} \qquad b_i = -\mathcal{B}_{,i} \qquad \text{and} \qquad \beta_{i,i} = 0 \tag{A.71}$$

It is straightforward to prove that in the Fourier space we have

$$B_i = (\beta_1, \beta_2, -i\mathcal{B}) \tag{A.72}$$

We express $\mathbf{b}$ and $\mathcal{B}$ in the Fourier space as

$$\vec{b} = \sum_{\vec{k}} \vec{Q}_{\vec{k}} e^{i\vec{k}\vec{x}}, \qquad \mathcal{B} = \sum_{\vec{k}} \Phi_{\vec{k}} e^{i\vec{k}\vec{x}} \tag{A.73}$$

But $\vec{b} = -\nabla\mathcal{B}$ so we obtain $\vec{Q}_{\vec{k}} = -i\vec{k}\Phi_{\vec{k}}$. We see then that $\vec{b}$ is the longitudinal part, parallel to $\vec{k}$ in the Fourier space, hence

$$\vec{b} = (0, 0, -i\mathcal{B}) \tag{A.74}$$

Moreover:

$$\vec{\beta} = \sum_{\vec{k}} \vec{\beta}_{\vec{k}} e^{i\vec{k}\vec{x}} \tag{A.75}$$

representing the curl free part. Hence,

$$\nabla\vec{\beta} = \sum_{\vec{k}} i\vec{k} \cdot \vec{\beta}_{\vec{k}} e^{i\vec{k}\vec{x}} = 0 \tag{A.76}$$

leading to $\vec{k} \cdot \vec{\beta}_{\vec{k}} = 0$. But $\vec{k} = (0, 0, k)$, thus $\beta_{3_{\vec{k}}} = 0$. So in total:

$$B_i = (\beta_1, \beta_2, -i\mathcal{B}) \tag{A.77}$$

We now turn to the 3×3 part. As already mentioned, it can be split into 3 different matrices, each containing a pure scalar, vector or tensor part. We begin by the scalar part S_{ij}, which we already have written as:

$$S_{ij} = (\partial_i\partial_j - \frac{1}{3}\delta_{ij}\nabla^2)\mathtt{S}, \qquad \text{with} \qquad \mathtt{S} = \sum_{\vec{k}} Q_{\vec{k}} e^{i\vec{k}\vec{x}} \tag{A.78}$$

Decomposing S_{ij} in the Fourier space, we have $S_{ij} = \sum_{\vec{k}} S_{ij_{\vec{k}}} e^{i\vec{k}\vec{x}}$. We thus obtain:

$$S_{ij} = \left(-k_i k_j + \frac{1}{3}\delta_{ij}k^2\right) Q_{\vec{k}} = \left(-\frac{k_i k_j}{k^2} + \frac{1}{3}\delta_{ij}\right) k^2 Q_{\vec{k}} \tag{A.79}$$

so it is helpful to define:

$$\mathtt{S}_{\vec{k}} = k^2 Q_{\vec{k}} \tag{A.80}$$

Hence,

$$S_{ij} = \left(-\frac{k_i k_j}{k^2} + \frac{1}{3}\delta_{ij}\right) \mathtt{S} \tag{A.81}$$

All non diagonal terms are equal to 0, since $\vec{k} = (0, 0, k)$ while for the diagonal terms it holds that:

$$S_{11} = \frac{1}{3}\mathtt{S}, \qquad S_{22} = \frac{1}{3}\mathtt{S}, \qquad S_{33} = -\frac{2}{3}\mathtt{S} \tag{A.82}$$

thus

$$S_{ij} = \begin{pmatrix} \frac{1}{3}\mathtt{S} & 0 & 0 \\ 0 & \frac{1}{3}\mathtt{S} & 0 \\ 0 & 0 & -\frac{2}{3}\mathtt{S} \end{pmatrix} \tag{A.83}$$

We continue by proving that in the Fourier space the pure vector part is of the form:

$$V_{ij} = \frac{i}{2}\begin{pmatrix} 0 & 0 & \mathcal{V}_1 \\ 0 & 0 & \mathcal{V}_2 \\ \mathcal{V}_1 & \mathcal{V}_2 & 0 \end{pmatrix} \tag{A.84}$$

V_{ij} is defined as $V_{ij} = \frac{1}{2}\left(\mathcal{V}_{i,j} + \mathcal{V}_{j,i}\right)$. In the Fourier space we have:

$$V_{ij} = \sum_{\vec{k}} V_{ij_{\vec{k}}} e^{i\vec{k}\vec{x}}, \qquad \mathcal{V}_i = \sum_{\vec{k}} Q_{i_{\vec{k}}} e^{i\vec{k}\vec{x}} \tag{A.85}$$

But

$$\mathcal{V}_{i,j} = \sum_{\vec{k}} ik_j Q_{i_{\vec{k}}} e^{i\vec{k}\vec{x}} \tag{A.86}$$

so then

$$V_{ij_{\vec{k}}} = \frac{1}{2}\left(ik_j Q_{i_{\vec{k}}} + ik_i Q_{j_{\vec{k}}}\right) \tag{A.87}$$

so to obtain the same dimensionality between V_{ij} and $\mathcal{V}_\rangle$ we define $\mathcal{V}_{i_{\vec{k}}} = \frac{Q_{i_{\vec{k}}}}{k}$, and thus:

$$V_{ij_{\vec{k}}} = \frac{i}{2k}\left(k_j \mathcal{V}_i + k_i \mathcal{V}_j\right) \tag{A.88}$$

Moreover, by construction, $\nabla\vec{\mathcal{V}} = 0$, and since $\vec{k} = (0, 0, k)$, it follows that $\mathcal{V}_3 = 0$. Thus, equation (A.84) is obtained.

Our next step is to show that $\tau_{ij,i} = \tau_{ij,j} = 0$. We introduce an auxiliary quantity, L_j as $L_j = \tau_{ij,i}$. Tensor τ_{ij} is symmetric and traceless, and in the Fourier space can be written as:

$$\tau_{ij} = \sum_{\vec{k}} \tau_{ij_{\vec{k}}} e^{i\vec{k}\vec{x}} \tag{A.89}$$

thus

$$L_j = \sum_{\vec{k}} ik_i \tau_{ij_{\vec{k}}} e^{i\vec{k}\vec{x}} \tag{A.90}$$

So by the standard expansion in the Fourier space of L_j, we obtain the Fourier modes:

$$L_{j_{\vec{k}}} = ik_i \tau_{ij_{\vec{k}}} = ik_3 \tau_{3j_{\vec{k}}} \tag{A.91}$$

We now define $L_{ij} = L_{i,j} = \sum_{\vec{k}} ik_i L_{j_{\vec{k}}} e^{i\vec{k}\vec{x}}$, from which we obtain that the Fourier modes of quantity L_{ij} will be

$$L_{ij_{\vec{k}}} = ik_i L_{j_{\vec{k}}} = ik_3 L_{j_{\vec{k}}} = -k^2 \tau_{3j} \tag{A.92}$$

Thus

$$\begin{aligned}\tau_{ij_{\vec{k}}} &= \begin{pmatrix}\tau_{11} & \tau_{12} & 0\\ \tau_{12} & \tau_{22} & 0\\ 0 & 0 & 0\end{pmatrix} + \begin{pmatrix}0 & 0 & \tau_{13}\\ 0 & 0 & \tau_{23}\\ \tau_{13} & \tau_{23} & \tau_{33}\end{pmatrix}\\ &= \begin{pmatrix}\tau_{11} & \tau_{12} & 0\\ \tau_{12} & \tau_{22} & 0\\ 0 & 0 & 0\end{pmatrix} - \frac{i}{k}\begin{pmatrix}0 & 0 & L_1\\ 0 & 0 & L_2\\ L_1 & L_2 & L_3\end{pmatrix}\\ &= \begin{pmatrix}\tau_{11} & \tau_{12} & 0\\ \tau_{12} & \tau_{22} & 0\\ 0 & 0 & 0\end{pmatrix} - \frac{1}{k^2}\begin{pmatrix}0 & 0 & L_{13}\\ 0 & 0 & L_{23}\\ L_{12} & L_{23} & L_{33}\end{pmatrix}\\ &= a_{ij} - \frac{1}{k^2}L_{ij}\\ &= a_{ij} - \frac{1}{k^2}L_{j,i}\end{aligned} \tag{A.93}$$

But we know that τ_{ij} must be a pure tensor, thus $L_{ji} = 0$, since it corresponds to a "vector" part. Thus $L_i = 0 = \tau_{ij,j}$.

From this last equation we can also deduce:

$$\tau_{ij,j} = k_i\tau_{ij} = 0, \text{ thus } \tau_{3j} = \tau_{j3} = 0 \tag{A.94}$$

Moreover, since τ is traceless it follows that

$$\tau_{ij} = \begin{pmatrix}\tau_{11} & \tau_{12} & 0\\ \tau_{12} & -\tau_{11} & 0\\ 0 & 0 & 0\end{pmatrix} \tag{A.95}$$

Thus, we finally obtain:

$$C_{ij} = \begin{pmatrix}D + \frac{1}{3}\mathtt{S} + \tau_{11} & \tau_{12} & \frac{i}{2}\mathcal{V}_1\\ \tau_{12} & D + \frac{1}{3}\mathtt{S} - \tau_{11} & \frac{i}{2}\mathcal{V}_2\\ \frac{i}{2}\mathcal{V}_1 & \frac{i}{2}\mathcal{V}_2 & D - \frac{2}{3}\mathtt{S}\end{pmatrix} \tag{A.96}$$

We are now ready to expand the SVT 3×3 matrices to 4×4 versions by including all scalar, vector and tensor sectors in different 4×4 matrices. A tensor perturbation $\delta f_{\alpha\beta}$ can be written then, as:

$$\delta f_{\alpha\beta} = S_{\alpha\beta} + V_{\alpha\beta} + \tau_{\alpha\beta} \tag{A.97}$$

where

$$S_{\alpha\beta} = \begin{pmatrix}A & -\mathcal{B}_{,i}\\ -\mathcal{B}_{,i} & \delta_{ij}D + \mathcal{S}_{ij}\end{pmatrix}, \qquad V_{\alpha\beta} = \begin{pmatrix}0 & \beta_i\\ \beta_i & \frac{1}{2}(\mathcal{V}_{i,j} + \mathcal{V}_{j,i})\end{pmatrix}, \qquad \tau_{\alpha\beta} = \begin{pmatrix}0 & 0\\ 0 & \tau_{ij}\end{pmatrix} \tag{A.98}$$

A.4.5 Gauge transformations of Linear Decompositions

We have already shown that a tensor's $f_{\alpha\beta}$ perturbation transforms as:

$$\delta\tilde{f}_{\alpha\beta} = \delta f_{\alpha\beta} - \xi^{\mu}_{,\alpha}\bar{f}_{\mu\beta} - \xi^{\nu}_{,\beta}\bar{f}_{\alpha\nu} - \bar{f}'_{\alpha\beta}\xi^0 \tag{A.99}$$

We shall now see in more detail what this transformation implies for each type of component. We start with the $0-0$ component, $\delta\tilde{f}_{00}$, which in our case corresponds to field A of equation (A.98). Then, from eq (A.99) we obtain:

$$\delta\tilde{f}_{00} = \delta f_{00} - 2\xi^0_{,0}\bar{f}_{00} - \bar{f}'_{00}\xi^0 \tag{A.100}$$

thus:

$$\tilde{A} = A - 2\xi^0_{,0}\bar{f}_{00} - \bar{f}'_{00}\xi^0 \tag{A.101}$$

which in Fourier space remains the same. This brings to our attention a very important fact. Even though A represents a "scalar" perturbation, it does not transform as a scalar, as equation (A.27) would suggest, but according to eq. (A.101). So for example a density perturbation, which is a component of the energy-momentum tensor should be transformed according to (A.100) and not (A.27).

We now move on to the $0-i$ component. Due to homogeneity and isotropy one can infer that $\bar{f}_{0i} = 0$ and $\bar{f}_{11} = \bar{f}_{22} = \bar{f}_{33} = \frac{1}{3}\bar{f}_{kk}$. Then, eq. (A.99), yields:

$$\delta\tilde{f}_{0i} = \delta f_{0i} - \frac{1}{3}\xi_{i,0}\bar{f}_{kk} - \xi^0_{,i}\bar{f}_0 0 \tag{A.102}$$

In our case,

$$\begin{aligned}\tilde{B}_i &= B_i - \frac{1}{3}\xi_{i,0}\bar{f}_{kk} - \xi^0_{,i}\bar{f}_{00} \\ &= B_i - \frac{1}{3}\xi_{i,0}\bar{f}_{kk} - ik_i\xi^0\bar{f}_{00} \quad \text{(in Fourier space)}\end{aligned} \tag{A.103}$$

This relation can be further analyzed, if we Helmholtz decompose B_i and ξ_i into their pure "scalar" and "vector" parts. Using:

$$B_i = -\mathcal{B}_{,i} + \beta_i \qquad \text{and } \xi_i = -\Xi_{,i} + \mathtt{x}_i \tag{A.104}$$

By substituting (A.104) in (A.103) we obtain:

$$-\tilde{\mathcal{B}}_{,i} + \tilde{\beta}_i = -\mathcal{B}_i + \beta_i - \frac{1}{3}(-\Xi_i + \mathtt{x}_i)_{,0}\bar{f}_{kk} - \xi^0_{,i}\bar{f}_{00} \tag{A.105}$$

This equation can be decomposed even more, since it contains a longitudinal and a transverse part that are independent:

$$-\tilde{\mathcal{B}}_{,i} = -\mathcal{B}_i + \frac{1}{3}\Xi_{,i,0}\bar{f}_{kk} - \xi^0_{,i}\bar{f}_{00} \tag{A.106}$$

$$\tilde{\beta} = \beta_i - \frac{1}{3}\mathtt{x}_{i,0}\bar{f}_{kk} \tag{A.107}$$

The equality of the gradient of perturbations implies the equality of the perturbations themselves, and because the background field is only a function of η, we obtain:

$$\tilde{\mathcal{B}} = \mathcal{B} - \frac{1}{3}\Xi_{,0}\bar{f}_{kk} + \xi^0\bar{f}_{00} \tag{A.108}$$

which in Fourier space leads to:

$$\tilde{\mathcal{B}} = \mathcal{B} - \Xi_{,0}\frac{\bar{f}_{kk}}{3} + k\xi^0\bar{f}_{00} \tag{A.109}$$

We finally turn to the ij component of a tensor perturbation. It holds that:

$$\begin{aligned}\delta\tilde{f}_{ij} &= \delta f_{ij} - \xi^\kappa_{,i}\bar{f}_{\kappa j} - \xi^\kappa_{,j}\bar{f}_{i\kappa} - \bar{f}'_{ij}\xi^0 \\ &= \delta f_{ij} - \frac{1}{3}(\xi_{j,i} + \xi_{i,j})\bar{f}_{ll} - \frac{1}{3}\delta_{ij}\bar{f}'_{ll}\xi^0\end{aligned} \tag{A.110}$$

which in our case translates to:

$$\delta_{ij}\tilde{D} + \tilde{E}_{ij} = \delta_{ij}D + E_{ij} - \frac{1}{3}(\xi_{i,j} + \xi_{j,i})\bar{f}_{ll} - \frac{1}{3}\delta_{ij}\bar{f}'_{ll}\xi^0 \tag{A.111}$$

We are now in a position to split the trace and traceless parts and then perform an SVT decomposition. We begin with $\xi_{i,j} + \xi_{j,i}$:

$$\begin{aligned}\xi_{i,j} + \xi_{j,i} &= \frac{1}{3}\delta_{ij}(\xi_{k,k} + \xi_{k,k}) + \xi_{i,j} + \xi_{j,i} - \frac{1}{3}\delta_{ij}(\xi_{k,k} + \xi_{k,k}) \\ &= \frac{2}{3}\delta_{ij}\xi_{k,k} + \xi_{i,j} + \xi_{j,i} - \frac{2}{3}\delta_{ij}\xi_{k,k}\end{aligned} \tag{A.112}$$

and returning to (A.111) we get:

$$\delta_{ij}\tilde{D} + \tilde{E}_{ij} = \delta_{ij}D - \frac{2}{9}\delta_{ij}\xi_{l,l}\bar{f}_{kk} - \frac{1}{3}\delta_{ij}\bar{f}'_{kk}\xi^0 + E_{ij} - \frac{\bar{f}_{kk}}{3}(\xi_{i,j} + \xi_{j,i} - \frac{2}{3}\delta_{ij}\xi_{l,l}) \tag{A.113}$$

The trace and traceless parts can now be equated. We will use the fact that $\xi_i = -\Xi_{,i} + \mathtt{x}_i$, where $\mathtt{x}_i$ is divergence free. We have then, that:

$$\tilde{D} = D + \frac{2}{9}\bar{f}_{kk}\Xi_{,ll} - \frac{1}{3}\bar{f}'_{kk}\xi^0 \tag{A.114}$$

$$\tilde{E}_{ij} = E_{ij} + \frac{\bar{f}_{kk}}{3}\left(2\Xi_{,ji} - \mathtt{x}_{i,j} - \mathtt{x}_{j,i} - \frac{2}{3}\delta ij\Xi_{,ll}\right) \tag{A.115}$$

Part E_{ij} can be SVT decomposed. We get:

$$\tilde{S}_{ij} + \tilde{V}_{ij} + \tilde{\tau}_{ij} = S_{ij} + V_{ij} + \tau_{ij} + \frac{\bar{f}_{kk}}{3}\left(2\Xi_{,ji} - \frac{2}{3}\delta ij\Xi_{,ll} - \mathtt{x}_{i,j} - \mathtt{x}_{j,i}\right) \tag{A.116}$$

It is noteworthy that the parentheses enclose a tensor quantity that can be further decomposed. The first two terms within it form the "scalar" part while the other two comprise the divergence-free "vector" part. Equating then the S, V and T components we finally obtain, for the scalar part:

$$\tilde{S}_{ij} = S_{ij} + \frac{2}{3}\bar{f}_{kk}\left(\Xi_{,ij} - \frac{1}{3}\delta_{ij}\Xi_{,ll}\right) \tag{A.117}$$

and for the vector and tensor parts:

$$\tilde{V}_{ij} = V_{ij} - (\mathtt{x}_{j,i} + \mathtt{x}_{i,j}) \qquad \tilde{\tau}_{ij} = \tau_{ij} \tag{A.118}$$

We can see from the last relation that the pure tensor part of perturbation $\delta f_{\alpha,\beta}$ is gauge invariant. Recalling that $V_{ij} = \frac{1}{3}(\mathcal{V}_{i,j} + \mathcal{V}_{j,i})$, we can also rewrite the vector part as:

$$\tilde{\mathcal{V}}_{i,j} + \tilde{\mathcal{V}}_{j,i} = \mathcal{V}_{i,j} + \mathcal{V}_{j,i} - 2(\mathtt{x}_{j,i} + \mathtt{x}_{i,j}) \tag{A.119}$$

Regarding the scalar part, we can write $S_{ij} = (\partial_i\partial_j - \frac{1}{3}\delta_{ij}\nabla^2)\mathtt{S}$, so (A.117) becomes:

$$(\partial_i\partial_j - \frac{1}{3}\delta_{ij}\nabla^2)\tilde{\mathtt{S}} = (\partial_i\partial_j - \frac{1}{3}\delta_{ij}\nabla^2)\mathtt{S} + \frac{2}{3}\bar{f}_{kk}\left(\Xi_{,ij} - \frac{1}{3}\delta_{ij}\Xi_{,ll}\right) \tag{A.120}$$

leading to:

$$(\partial_i\partial_j - \frac{1}{3}\delta_{ij}\nabla^2)(\tilde{\mathtt{S}} - \mathtt{S} - \frac{2}{3}\bar{f}_{kk}\Xi) = 0 \tag{A.121}$$

This relation holds for all i, j, hence also for $i \neq j$. Since the equality of the gradient of perturbations implies the equality of the perturbations themselves, we get then:

$$\tilde{\mathtt{S}} = \mathtt{S} + \frac{2}{3}\bar{f}_{kk}\Xi \tag{A.122}$$

which remains the same when written in the Fourier space.

A.5 Gauge Freedom and Gauge independent Scalar Potentials

So far it has been shown that all scalar perturbations' transformations depend on two variables: Ξ and ξ^0 (see eqs. (A.101), (A.109), (A.114) and (A.122)). We can choose these two quantities in such a way that two of these four quantities are equal to 0, hence only 2 "scalar" components are real, while the others are gauge induced.

In the case of the vector parts, β_i and $\mathcal{V}_i$, out of the 6 possible components, only 4 are non-zero, since they are divergenceless ($\beta_{i,i} = \mathcal{V}_{i,i} = 0$). Moreover, their gauge transformations depend on the three components of $\mathtt{x}_i$ (see eqs. (A.107) and (A.119)), for which it also holds that $\mathtt{x}_{i,i} = 0$. Thus, the actual degrees of freedom in this case are reduced to 2, while the others are gauge-induced.

Finally, the pure tensor perturbation, τ_{ij}, has 9 components but it is symmetric, reducing the free components to 6. Moreover, it is a "pure" tensor, meaning $\tau_{ii} = 0$, and finally $\tau_{ij,i} = 0$. This last relation holds for each value of j separately, thus it takes away 3 more degrees of freedom. Lastly, τ_{ij} is gauge invariant so there are no components of a transformation vector to deduct, hence τ_{ij} has, in fact, 2 components, none of which are gauge induced.

In total, we deduce that fixing a gauge yields:

$$2S \ d.o.f. + 2V \ d.o.f. + 2T \ d.o.f.$$

We will use the above to define gauge independent scalar potentials. Solving (A.122) with respect to Ξ and differentiating with respect to conformal time η, we get:

$$\Xi' = \frac{3}{2}\left[\left(\frac{\tilde{\mathtt{S}}}{\bar{f}_{kk}}\right)' - \left(\frac{\mathtt{S}}{\bar{f}_{kk}}\right)'\right] = \tilde{M}' - M', \quad \text{with } M = \frac{3}{2}\frac{\mathtt{S}}{\bar{f}_{kk}} \tag{A.123}$$

Substituting this in (A.109) we get:

$$\xi^0 = \frac{1}{\bar{f}_{00}}\left[\tilde{\mathcal{B}} + \frac{\bar{f}_{kk}}{2}\left(\frac{\tilde{\mathtt{S}}}{\bar{f}_{kk}}\right)'\right] - \frac{1}{\bar{f}_{00}}\left[\mathcal{B} + \frac{\bar{f}_{kk}}{2}\left(\frac{\mathtt{S}}{\bar{f}_{kk}}\right)'\right] = \tilde{P} - P \tag{A.124}$$

where we have defined $P = \frac{1}{\bar{f}_{00}}\left[\mathcal{B} + \frac{\bar{f}_{kk}}{2}\left(\frac{\mathtt{S}}{\bar{f}_{kk}}\right)'\right]$. Using (A.5) in eqs. (A.101) and (A.114) we can obtain two gauge independent quantities. The first one leads to:

$$\tilde{A} + 2\tilde{P}'\bar{f}_{00} + \bar{f}'_{00}\tilde{P} = A + 2P'\bar{f}_{00} + \bar{f}'_{00}P \tag{A.125}$$

so the first scalar gauge invariant quantity is defined as:

$$\mathcal{X} = A + 2P'\bar{f}_{00} + \bar{f}'_{00}P \tag{A.126}$$

The second one yields:

$$\tilde{D} - \frac{2}{9}\bar{f}_{kk}\nabla^2\tilde{M} + \frac{1}{3}\bar{f}'_{kk}\tilde{P} = D - \frac{2}{9}\bar{f}_{kk}\nabla^2 M + \frac{1}{3}\bar{f}'_{kk}P \tag{A.127}$$

so the second scalar gauge invariant quantity is:

$$\mathcal{Y} = D - \frac{2}{9}\bar{f}_{kk}\nabla^2 M + \frac{1}{3}\bar{f}'_{kk}P \tag{A.128}$$

A.6 Perturbing the metric tensor - Bardeen Potentials

Finally, we are ready to apply what was presented so far to the metric tensor. The background metric tensor of an expanding universe that is homogeneous and isotropic is symbolized as $\bar{g}_{\mu\nu}$, and is of the form:

$$\bar{g}_{\mu\nu} = a^2 \begin{pmatrix} -1 & 0 \\ 0 & \mathbb{1} \end{pmatrix} = a^2 \eta_{\mu\nu} \tag{A.129}$$

in conformal time[3], and $\eta_{\mu\nu}$ is the Minkowski metric. When the Minkowski metric is perturbed, the expanding universe's metric can be written in the form:

$$g_{\mu\nu} = \eta_{\mu\nu} + h_{\mu\nu} \tag{A.130}$$

so in fact the perturbation of the metric is $\delta g_{\mu\nu} = a^2 h_{\mu\nu}$. We will apply what was presented so far to $h_{\mu\nu}$. In matrix form we have that:

$$h_{\mu\nu} = \begin{pmatrix} -2A & -B_i \\ -B_i & h_{ij} \end{pmatrix}, \quad B_i = -\mathcal{B}_i + \beta_i, \quad h_{ij} = -2D\delta_{ij} + 2E_{ij} \tag{A.131}$$

E_{ij} is the traceless part of h_{ij}, which we will proceed to SVT decompose. We write $E_{ij} = E_{ij}^{(S)} + E_{ij}^{(V)} + E_{ij}^{(T)}$, where:

$$E_{ij}^{(S)} = \left(\partial_i\partial_j - \frac{1}{3}\delta_{ij}\nabla^2\right)\mathcal{S} = \mathcal{S}_{,ij} \tag{A.132}$$

$$E_{ij}^{(V)} = \frac{1}{2}(\mathcal{V}_{i,j} + \mathcal{V}_{j,i}), \quad \mathcal{V}_{i,i} \tag{A.133}$$

$$E_{ij}^{(T)} = \tau_{ij}, \quad \tau_{ij,i} = \tau_{ij,j} = 0 \tag{A.134}$$

Thus, we can separate the scalar part and have: $h_{ij} = S_{ij} + V_{ij} + 2\tau_{ij}$, with $S_{ij} = -2D\delta_{ij} + 2\left(\partial_i\partial_j - \frac{1}{3}\delta_{ij}\nabla^2\right)$ and $V_{ij} = \mathcal{V}_{i,j} + \mathcal{V}_{j,i}$. The full perturbation matrix will finally be of the form:

$$\delta g_{\alpha\beta} = a^2 \begin{pmatrix} -2A & \mathcal{B}_{,i} + \beta_i \\ \mathcal{B}_{,i} + \beta_i & -2\delta_{ij}D + 2\mathcal{S}_{,ij} + \mathcal{V}_{i,j} + \mathcal{V}_{j,i} + 2\tau_{ij} \end{pmatrix} \tag{A.135}$$

of which only 6 components are physical.

Since we are mainly interested in scalar perturbations in Cosmology, we will need their gauge transformations. Combining eqs. (A.101), (A.109), (A.114), (A.122), which refer to a perturbation:

$$\delta f_{\alpha\beta} = \begin{pmatrix} A & B_i \\ B_i & \delta_{ij}D + E_{ij} \end{pmatrix}$$

and the scalar part of the perturbed metric:

$$\delta g_{\alpha\beta} = a^2 \begin{pmatrix} -2A & \mathcal{B}_{,i} \\ \mathcal{B}_{,i} & -2\delta_{ij}D + 2\mathcal{S}_{,ij} \end{pmatrix} \tag{A.136}$$

we obtain:

$$\tilde{A} = A - \xi^{0\prime} - \mathcal{H}\xi^0, \quad \tilde{D} = D + \frac{1}{3}k\Xi + \mathcal{H}\xi^0, \quad \tilde{B} = B + \Xi' + k\xi^0, \quad \tilde{\mathcal{S}} = \mathcal{S} + k\Xi \tag{A.137}$$

[3]Conformal time η is defined through $d\eta = \frac{dt}{a(t)}$. Through that, we also define the conformal Hubble parameter $\mathcal{H} = \frac{a(\eta)'}{a(\eta)}$, where a prime denotes differentiation with respect to η.

Finally, with these correspondences in mind, we are led to define the equivalent to eqs. (A.126) and (A.128):

$$\Phi = A + (\mathcal{B} - \mathcal{S}')' + \mathcal{H}(\mathcal{B} - \mathcal{S}') \tag{A.138}$$

$$\Psi = D + \frac{1}{3}\nabla^2\mathcal{S} - \mathcal{H}(\mathcal{B} - \mathcal{S}') \tag{A.139}$$

These two quantities are known as the *Bardeen* potentials.

We can proceed to find the connection coefficients that correspond to the background and the full metric, since through them we calculate most GR related quantities. For simple reference we include the corresponding values here. The affine connection is given by:

$$\Gamma^{\alpha}_{\beta\gamma} = \frac{1}{2}g^{\alpha\mu}(g_{\mu\beta,\gamma} + g_{\mu\gamma,\beta} - g_{\beta\gamma,\mu}) \tag{A.140}$$

leading to:

$$\Gamma^0_{00} = \mathcal{H} + A', \quad \Gamma^0_{0i} = \mathcal{H}\mathcal{B}_{,i} + A_{,i},$$

$$\Gamma^i_{00} = \mathcal{H}\mathcal{B}_{,i} + \mathcal{B}'_{,i} + A_{,i}, \quad \Gamma^i_{0j} = \mathcal{H}\delta_{ij} - \psi'\delta_{ij} + E'_{,ij},$$

$$\Gamma^0_{ij} = \mathcal{H}\left[(1 - 2A - 2\psi)\delta_{ij} + 2E_{,ij}\right] - \delta_{ij}\psi' + E'_{,ij},$$

$$\Gamma^i_{jk} = E_{,ijk} - \mathcal{H}\delta_{jk}\mathcal{B}_{,i} + \delta_{jk}\psi_{,i} - \delta^i_j\psi_{,k} - \delta^i_k\psi_{,j} \tag{A.141}$$

A.7 Threading-Slicing and Worldlines

It is known from GR that the time measured along a trajectory is called the proper time, and is given by:

$$d\tau = \sqrt{-ds^2} \Rightarrow \frac{ds^2}{d\tau^2} = -1$$

and since $ds^2 = g_{\mu\nu}dx^\mu dx^\nu$, we have:

$$g_{\mu\nu}\frac{dx^\mu}{d\tau}\frac{dx^\nu}{d\tau} = -1 \tag{A.142}$$

The 3-velocity and 4-velocity of a fluid are given, respectively, by:

$$v^i = \frac{dx^i}{d\eta}, \quad u^\mu = (u^0, u^i) = \frac{dx^\mu}{d\tau} \tag{A.143}$$

We are interested to study whether the perturbation in the metric carries over to the 4-velocity of a given fluid. In order to do that we need the relation between u^i and v^i:

$$u^i = u^0 v^i \tag{A.144}$$

Hence, for the background -homogeneous and isotropic- universe, we have $\bar{u}^i = (0, 0, 0)$, leading to $\bar{v}^i = (0, 0, 0)$. We can then deduce that

$$\bar{u}^0 = \frac{1}{a}$$

by using the above relations. So in total, $\bar{u}^\mu = a(-1, 0, 0, 0)$

We are now ready to proceed to a perturbed universe. We write down the perturbations as:

$$u^0 = \bar{u}^0 + \delta u^0 = \frac{1}{a} + \delta u^0 \tag{A.145}$$

$$u^i = \bar{u}^i + \delta u^i = \delta u^i \tag{A.146}$$

$$v^i = \bar{v}^i + \delta v^i = \delta v^i \tag{A.147}$$

and from (A.144), we get to first order that $\delta u^i = \frac{1}{a}\delta v^i$. Using relation (A.142) and working to 1st order in the perturbations, we are led to $\delta u^0 = -\frac{A}{a}$, so that:

$$u^\mu = \frac{1}{a}(1 - A, v^i) \tag{A.148}$$

and since $u_\mu = g_{\mu\nu}u^\nu$ we also obtain:

$$u_\mu = \bar{u}_\mu + \delta u_\mu = a(-1 - A, v_i - B_i) \tag{A.149}$$

We can show now that a perturbation in the metric carries over to the worldline of an observer. Let us suppose that we have a timelike curve with:

$$x^i = constant, \quad dx^i = 0, \quad \text{and} \quad dx^\mu = (d\eta, 0, 0, 0) \tag{A.150}$$

This type of curve is called a *thread*, and a fluid's 3-velocity along a thread is 0: $\frac{dx^i}{d\eta} = 0$. On the same footing, a spacelike curve with:

$$\eta = constant, \quad d\eta = 0, \quad dx^\mu = (0, dx^i) \tag{A.151}$$

is called a *slice*. It can be immediately seen, that to 0th order in perturbations, a thread, dx^μ, and a slice, dy_μ, are orthogonal. However, to first order:

$$dx^\mu dy_\mu = g_{\mu\nu}dx^\mu dy^\mu = g_{0i}dx^0 dy^i = -a^2 B_i d\eta dy^i \tag{A.152}$$

so a perturbation makes slices and threads non-orthogonal. To first order, the worldline that is orthogonal to slices is $dx^\mu = dx^0(1, X_i)$, with $X_i = B_i$, since:

$$g_{\mu\nu}dx^\mu dy^\nu = g_{\mu i}dx^\mu dy^i = a^2 dx^0 dy^i \left(-B_i + X_i + 2(D\delta_{ij} + E_{ij})X_j\right)$$

So the 3-velocity of a thread is 0 but it is shifted to B_i, for a worldline of the above type, hence B_i is known as the *shift* vector.

Along the same lines, quantity A is the *lapse* function, which relates the proper time with the actual time via:

$$d\tau \approx a(1 + A)d\eta = (1 + A)dt$$

hence if there is no perturbation (no lapse), it holds that $d\tau = dt$.

A.8 Conformal-Newtonian Gauge

We can utilize gauge freedom to reduce the free quantities that appear during the perturbative analysis. A commonly used gauge is the *Conformal Newtonian gauge*, where we set:

$$\begin{aligned} \Xi &= -E \\ \xi^0 &= -\mathcal{B} + E' \end{aligned} \tag{A.153}$$

We see then that in this gauge:

$$\begin{aligned} A^N &= \Phi \\ D^N &= \psi^N = \Psi \end{aligned} \tag{A.154}$$

so that the Bardeen potentials are now equal to the only nonzero metric perturbations. The metric is now reduced to:

$$ds^2 = a^2(\eta)\left[-(1+2\Phi)d\eta^2 + (1-2\Psi)\delta_{ij}dx^i dx^j\right] \tag{A.155}$$

A.9 Perturbations of $R_{\mu\nu}$ and $T_{\mu\nu}$

By use of (A.155), and working to 0th and 1st order in perturbations, we obtain the following values for the Christoffel symbols:

$$\bar{\Gamma}^0_{00} = \mathcal{H}, \quad \bar{\Gamma}^0_{0k} = \bar{\Gamma}^i_{00} = \bar{\Gamma}^i_{jk} = 0, \quad \bar{\Gamma}^0_{ij} = \mathcal{H}\delta_{ij}, \quad \bar{\Gamma}^i_{0j} = \mathcal{H}\delta^i_j \tag{A.156}$$

and

$$\begin{aligned} \delta\Gamma^0_{00} = \Phi', \quad \delta\Gamma^0_{0k} = \Phi_{,k}, \quad \delta\Gamma^i_{00} = \Phi_{,i}, \quad \delta\Gamma^i_{0j} = -\Psi'\delta^i_j \\ \delta\Gamma^0_{ij} = -\left[2\mathcal{H}(\Phi+\Psi) + \Psi'\right]\delta_{ij}, \quad \delta\Gamma^i_{kl} = -\left(\Psi_{,l}\delta^i_k + \Psi_{,k}\delta^i_l\right) + \Psi_{,i}\delta_{kl} \end{aligned} \tag{A.157}$$

The Ricci tensor can now be obtained, since:

$$R_{\mu\nu} = \Gamma^\alpha_{\nu\mu,\alpha} - \Gamma^\alpha_{\alpha\mu,\nu} + \Gamma^\alpha_{\alpha\beta}\Gamma^\beta_{\nu\mu} - \Gamma^\alpha_{\nu\beta}\Gamma^\beta_{\alpha\mu} \tag{A.158}$$

yielding:

$$\begin{aligned} R_{00} &= -3\mathcal{H}' + 3\Psi'' + \nabla^2\Phi + 3\mathcal{H}(\Phi' + \Psi') \\ R_{0i} &= 2(\Psi + \mathcal{H}\Phi)_{,i} \\ R_{ij} &= (\mathcal{H}' + 2\mathcal{H}^2)\delta_{ij} + \left[\nabla^2\Psi - \Psi'' - \mathcal{H}(\Phi' + 5\Psi') - (2\mathcal{H}' + 4\mathcal{H}^2)(\Phi+\Psi)\right]\delta_{ij} + (\Psi - \Phi)_{,ij} \end{aligned} \tag{A.159}$$

Then, we can raise the index with the full metric and obtain the Ricci scalar by contracting the indices:

$$R = \frac{1}{a^2}\left[6(\mathcal{H} + H^2) + 2\nabla^2(2\Psi - \Phi) - 6\Psi'' - 6\mathcal{H}(\Phi' + 3\Psi') - 12(\mathcal{H}' + H^2)\Phi\right] \tag{A.160}$$

We now proceed to study the perturbation in the energy-momentum tensor. The energy-momentum tensor can be SVT decomposed like the metric tensor, and also has 10 degrees of freedom, of which only 6 are physical, while 4 are gauge related. Moreover, we can decompose the perturbation of T^μ_ν into perfect+imperfect fluid, having 10 dofs, 5 of which are related to the perfect fluid and the rest to the imperfect fluid. Taking into account the perfect fluid degrees of freedom, the energy-momentum tensor can be written in the perfect fluid form, i.e.:

$$T^\mu_\nu = (\rho + p)u^\mu u_\nu + p\delta^\mu_\nu \tag{A.161}$$

The perturbations of the quantities appearing are:

$$\rho = \bar{\rho} + \delta\rho, \quad p = \bar{p} + \delta p, \quad u^\mu = \frac{1}{a}(1 - A, v_i), \quad u_\mu = a(-1 - A, v_i - B_i) \tag{A.162}$$

and inserting them in (A.161), we can write T^{μ}_{ν}

$$\begin{aligned} T^{\mu}_{\nu} &= \bar{T}^{\mu}_{\nu} + \delta T^{\mu}_{\nu} \\ &= \begin{pmatrix} -\bar{\rho} & 0 \\ 0 & \bar{p}\delta_{ij} \end{pmatrix} + \begin{pmatrix} -\delta\rho & (\bar{\rho}+\bar{p})(v_i + B_i) \\ -(\bar{\rho}+\bar{p})v_i & \delta p \delta^i_j \end{pmatrix} \end{aligned} \tag{A.163}$$

Moving on, there are 5 degrees of freedom that remain in the δT^i_j part, which correspond to perturbations that deviate from the perfect fluid form. This anisotropic pressure can be sourced by various phenomena, for example the neutrino background and the CMBR during and after decoupling. We can, then, write the space part as:

$$\delta T^i_j = \delta p \delta^i_j + \Sigma_{ij} \equiv \bar{p}\left(\frac{\delta p}{\bar{p}} + \Pi_{ij}\right) \tag{A.164}$$

where Σ_{ij} and Π_{ij} are symmetric and traceless. So the trace and the traceless part of δT^i_j are unique:

$$\delta p \equiv \frac{1}{3} T^i_i \frac{\delta p}{\bar{p}}, \quad \Sigma_{ij} \equiv \delta T^i_j - \frac{1}{3}\delta^i_j \frac{\delta p}{\bar{p}} T^i_i \tag{A.165}$$

Quantity Π_{ij} is the dimensionless version of Σ_{ij}, which encompasses the anisotropic pressure of a fluid.

It is straightforward to decompose $\delta T_{\mu\nu}$ as in the case of the metric tensor. We extract a scalar perturbation from v_i and a scalar and a vector perturbation from Π_{ij}. It holds that:

$$v_i = v^S_i + v^V_i, \quad \text{with } v^S_i = -v_{,i} \quad \text{and } \nabla \cdot \vec{v}^V = 0 \tag{A.166}$$

$$\Pi_{ij} = \Pi^S_{ij} + \Pi^V_{ij} + \Pi^T_{ij} \tag{A.167}$$

where

$$\Pi^S_{ij} = (\partial_i\partial_j - \frac{1}{3}\delta_{ij}\nabla^2)\Pi, \quad \Pi^V_{ij} = -\frac{1}{2}(\Pi_{i,j} + \Pi_{j,i}) \quad \text{and} \quad \delta^{ik}\Pi^T_{ij,k} = 0 \tag{A.168}$$

Following the corresponding steps as in the case of the metric tensor, we have that for the perturbations of the energy density, pressure, 3-velocity and anisotropic stress it holds:

$$\delta\tilde{\rho} = \delta\rho - \bar{\rho}'\xi^0 \tag{A.169}$$

$$\delta\tilde{p} = \delta p - \bar{p}'\xi^0 \tag{A.170}$$

$$\tilde{v}_i = v_i + \xi^i_{,0} \tag{A.171}$$

$$\tilde{\Pi}_{ij} = \Pi_{ij} \tag{A.172}$$

For the scalar perturbations, we have that

$$v_i = -v_{,i} \quad \text{and } \xi^i = -\xi_{,i}$$

so

$$\tilde{v} = v + \xi', \quad \tilde{\Pi} = \Pi$$

So in the conformal Newtonian Gauge, where $\xi^0 = -\mathcal{B} + E'$, $\xi = -E$, $\mathcal{B} = 0$ and considering only scalar perturbations (that $v_i = -v_{,i}$ and $B_i = \mathcal{B}_{,i}$) we finally obtain the form of the perturbations of the energy momentum tensor:

$$\delta T^{\mu}_{\nu} = \begin{pmatrix} -\delta\rho^N & -(\bar{\rho}+\bar{p})v^N_{,i} \\ (\bar{\rho}+\bar{p})v^N_{,i} & \delta p^N \delta^i_j + \bar{p}(\Pi_{,ij} - \frac{1}{3}\delta_{ij}\nabla^2\Pi) \end{pmatrix} \tag{A.173}$$

The natural next step is to express the field equations that the perturbations follow.

A.10 Field Equations of Scalar Perturbations

The perturbed version of the field equations, for scalar perturbations in the Newtonian gauge is:

$$\delta G^{\mu}_{\nu} = 8\pi G \delta T^{\mu}_{\nu} \tag{A.174}$$

and using the equations of the previous section, we can obtain, by separating δG^{i}_{j} into its trace and traceless parts, that:

$$4\pi G a^2 \delta\rho^N = \nabla^2\Psi - 2\mathcal{H}(\Psi' + \mathcal{H}\Phi) \tag{A.175a}$$

$$4\pi G a^2 (\bar{\rho} + \bar{p}) v^N_{,i} = (\Psi' + \mathcal{H}\Phi)_{,i} \tag{A.175b}$$

$$4\pi G a^2 \delta p^N = \Psi'' + \mathcal{H}(\Phi' + 2\Psi') + (2\mathcal{H}' + \mathcal{H}^2)\Phi + \frac{1}{3}\nabla^2(\Phi - \Psi) \tag{A.175c}$$

$$8\pi G a^2 \bar{p}(\partial_i\partial_j - \frac{1}{3}\delta^i_j\nabla^2)\Pi = (\partial_i\partial_j - \frac{1}{3}\delta^i_j\nabla^2)(\Psi - \Phi) \tag{A.175d}$$

The off-diagonal constraint from the last equation of (A.175):

$$(\Psi - \Phi)_{,ij} = 8\pi G a^2 \bar{p}\Pi_{,ij} \quad \text{so that } \Psi - \Phi = 8\pi G a^2 \bar{p}\Pi \tag{A.176}$$

Similarly, from the second equation of (A.175) we get:

$$\Psi' + \mathcal{H}\Phi = 4\pi G a^2 (\bar{\rho} + \bar{p}) v^N \tag{A.177}$$

so inserting this in the first equation we get:

$$\nabla^2\Psi = 4\pi G a^2 \bar{\rho}(\frac{\delta\rho}{\bar{\rho}} + 3\mathcal{H}(1+w)v^N) \tag{A.178}$$

Finally, by using the background relation:

$$4\pi G a^2 \bar{\rho} = \frac{3}{2}\mathcal{H}^2$$

we get a concise form of the field equations of the perturbations Ψ and Φ:

$$\nabla^2\Psi = \frac{3}{2}\mathcal{H}^2\left[\frac{\delta\rho}{\bar{\rho}}^N + 3\mathcal{H}(1+w)v^N\right] \tag{A.179}$$

$$\Psi - \Phi = 3\mathcal{H}^2 w\Pi \tag{A.180}$$

$$\Psi' + \mathcal{H}\Phi = \frac{3}{2}\mathcal{H}^2(1+w)v^N \tag{A.181}$$

$$\Psi'' + \mathcal{H}(\Phi' + 2\Psi') + (2\mathcal{H}' + \mathcal{H}^2)\Phi + \frac{1}{3}\nabla^2(\Phi - \Psi) = \frac{3}{2}\mathcal{H}^2(\frac{\delta p}{\bar{\rho}})^N \tag{A.182}$$

Appendix B

Perturbative Analysis of Single Field Inflation

Having presented the general framework of cosmological perturbations, we now turn to applying it to the case of single field inflation. We will first obtain the field equations starting from an ADM decomposition, and then proceed on the same footing to analyze perturbatively the single field inflation scenario.

B.1 Background Field Equations

A usual approach to expressing the metric in order to obtain the field equations, is by writing it down in the ADM form [194]:

$$ds^2 = -N^2 dt^2 + \gamma_{ij}(dx^i + N^i dt)(dx^j + N^j dt) \tag{B.1}$$

We will further suppose that the field is cosmological, (or equivalently that there is a gauge where $\phi = \phi(t)$).

Then, plugging metric (B.1) in equation (38):

$$\begin{aligned}\mathcal{L} =& G_2(\phi, X) - G_3(\phi, X)\Box\phi + G_4(\phi, X)R + G_{4X}\left[(\Box\phi)^2 - \phi^{\mu\nu}\phi_{\mu\nu}\right] \\ & G_5(\phi, X)G^{\mu\nu}\phi_{\mu\nu} - \frac{G_{5X}}{6}\left[(\Box\phi)^3 - 3\Box\phi\phi^{\mu\nu}\phi_{\mu\nu} + 2\phi_{\mu\nu}\phi^{\nu\lambda}\phi^{\mu}_{\lambda}\right]\end{aligned} \tag{B.2}$$

we obtain, for a universe that is only filled with a scalar field $\phi(t)$, that the action is of the form:

$$S = \int dt d^3x \mathcal{L}(N, \dot{N}, a, \dot{a}, \ddot{s}, \phi, \dot{\phi}, \ddot{\phi}) \tag{B.3}$$

Varying this action with respect to quantities N and a, yields the field equations, while varying with respect to ϕ yields the Klein-Gordon equation [35].

B.2 Perturbations in Single Field Inflation

It has already been presented how linear perturbations around a FLRW background are SVT decomposed, and that it is possible to use a gauge transformation to remove some of the perturbation modes. For example, a time transformation of the form

$$t \to t - T(t, \vec{x})$$

will transform the field's perturbation as:

$$\delta\phi \to \delta\phi + \dot{\phi}T$$

and by a suitable choice of T, we can switch off the field's perturbation: $\delta\phi = 0$. This is referred to as the unitary gauge. The perturbations in this gauge are all within the metric tensor, so we can write them in the form [26, 35, 51, 94]:

$$N = 1 + \delta N, \quad N_i = \partial_i \psi \quad \text{and } \gamma_{ij} = a^2 e^{2\mathcal{R}} (e^h)_{ij} \tag{B.4}$$

where $(e^h)_{ij} \equiv \delta_{ij} + h_{ij} + \mathcal{O}(h^2)$. Then,by substituting metric (B.1) in (B.3) and keeping up to second order perturbations, we have:

$$S^{(2)} = S^{(2)}_{\text{scalar}} + S^{(2)}_{\text{tensor}} \tag{B.5}$$

These two parts can concisely be written by use of auxiliary quantities. In particular:

$$S^{(2)}_{\text{scalar}} = \int dt d^3x a^3 \left[\frac{\mathcal{F}_T}{a^2} (\partial\mathcal{R})^2 - 3\mathcal{G}_T \dot{\mathcal{R}}^2 + \Sigma \delta N^2 - 2\Theta \delta N \frac{\partial^2 \psi}{a^2} + 2\mathcal{G}_T \dot{\mathcal{R}} \frac{\partial^2 \psi}{a^2} + 6\Theta \delta N \dot{\mathcal{R}} - 2\mathcal{G}_T \delta N \frac{\partial^2 \mathcal{R}}{a^2} \right] \tag{B.6}$$

where we have defined:

$$\mathcal{G}_T \equiv 2\left[G_4 - 2XG_{4X} - X\left(H\dot{\phi} G_{5X} - G_{5\phi} \right) \right] , \qquad \mathcal{F}_T \equiv 2\left[G_4 - X\left(\ddot{\phi} G_{5X} + G_{5\phi} \right) \right] , \tag{B.7}$$

$$\begin{aligned} \Theta \equiv & -\dot{\phi} X G_{3X} + 2H\left(G_4 - 4XG_{4X} - 4X^2 G_{4XX} \right) + \dot{\phi}\left(G_{4\phi} + 2XG_{4\phi X} \right) \\ & - H^2 \dot{\phi}\left(5XG_{5X} + 2X^2 G_{5XX} \right) + 2HX\left(3G_{5\phi} + 2XG_{5\phi X} \right) , \end{aligned} \tag{B.8}$$

and

$$\begin{aligned} \Sigma \equiv & X\left(G_{2X} + 2XG_{2XX} \right) + 6H\dot{\phi} X\left(2G_{3X} + XG_{3XX} \right) - 2X\left(G_{3\phi} + XG_{3\phi X} \right) - 6H^2 G_4 \\ & + 6\left[H^2\left(7XG_{4X} + 16X^2 G_{4XX} + 4X^3 G_{4XXX} \right) - H\dot{\phi}\left(G_{4\phi} + 5XG_{4\phi X} + 2X^2 G_{4\phi XX} \right) \right] \\ & + H^3 \dot{\phi} X\left(30G_{5X} + 26XG_{5XX} + 4X^2 G_{5XXX} \right) - 6H^2 X\left(6G_{5\phi} + 9XG_{5\phi X} + 2X^2 G_{5\phi XX} \right) . \end{aligned} \tag{B.9}$$

where all auxiliary quantities depend on the Galileon functions and the field derivatives. Similarly, the tensor part is of the form:

$$S^{(2)} = \frac{1}{8} \int dt dx^3 a^3 \left[\mathcal{G}_T \dot{h}_{ij}^2 - \frac{\mathcal{F}_T}{a^2} (\partial_k h_{ij})^2 \right] \tag{B.10}$$

Varying with respect to δN and ψ yields:

$$0 = \Sigma \delta N - \Theta \frac{\partial^2 \psi}{a^2} + 3\Theta \dot{\mathcal{R}} - \mathcal{G}_T \frac{\partial^2 \mathcal{R}}{a^2} \tag{B.11}$$

$$0 = \Theta \delta N - \mathcal{G}_T \dot{\mathcal{R}} \tag{B.12}$$

and using these equations we can obtain a simpler form for the 2nd order action:

$$S^{(2)}_{\mathcal{R}} = \int dt d^3x a^3 \left[\mathcal{G}_S \dot{\mathcal{R}}^2 - \frac{\mathcal{F}_S}{a^2} (\partial\mathcal{R})^2 \right] \tag{B.13}$$

where $\mathcal{R}$ is referred to as the curvature perturbation and we further have defined the auxiliary quantities:

$$\mathcal{G}_S \equiv \frac{\Sigma}{\Theta^2}\mathcal{G}_T^2 + 3\mathcal{G}_T, \qquad \mathcal{F}_S \equiv \frac{1}{a}\frac{d}{dt}\left(\frac{a}{\Theta}\mathcal{G}_T^2\right) - \mathcal{F}_T \ . \tag{B.14}$$

One can specify the Galileon functions that lead to a given theory, and then calculate the squared sound-speed of scalar and tensor perturbations by use of:

$$c_s^2 \equiv \frac{\mathcal{F}_S}{\mathcal{G}_S} \ , \qquad c_T^2 \equiv \frac{\mathcal{F}_T}{\mathcal{G}_T} \ . \tag{B.15}$$

If these quantities turn negative, the theory has gradient instabilities[1], like the exponential growth of perturbation modes. Moreover, one has to ensure that the kinetic terms are positive, to avoid ghost instabilities. Thus it should also hold that:

$$\mathcal{G}_S > 0 \ , \quad \mathcal{G}_T > 0 \ , \tag{B.16}$$

B.3 Mukhanov-Sasaki Equation and the Observable Quantities

Within this framework we can study the evolution of the perturbations. It is very convenient to use the transformation of the time coordinate:

$$dy := \frac{c_s}{a}dt$$

and redefine the $\mathcal{R}$ variable as:

$$u := z\mathcal{R}, \quad z := \sqrt{2}a\sqrt[4]{\mathcal{F}_S\mathcal{G}_S} \tag{B.17}$$

in equation (B.13), leading to the *Mukhanov-Sasaki* form:

$$S_{\mathcal{R}}^{(2)} = \frac{1}{2}\int dy d^3x \left[(u')^2 - (\partial u)^2 + \frac{z''}{z}u^2\right] \tag{B.18}$$

where a prime denotes differentiation with respect to the new time coordinate y. We can now find the spectrum of the scalar and tensor perturbations. In the case that the time dependent terms have a very slow evolution with respect to time, the power spectrums are evaluated by [191]:

$$\mathcal{P}_R = \frac{\mathcal{G}_S^{1/2}}{2\mathcal{F}_S^{3/2}}\frac{H^2}{4\pi^2} \ , \qquad \mathcal{P}_\mathcal{T} = \frac{8\mathcal{G}_T^{1/2}}{\mathcal{F}_T^{3/2}}\frac{H^2}{4\pi^2} \ , \tag{B.19}$$

at the horizon crossing. The quotient of these two is the tensor-to-scalar ratio r:

$$r \equiv \frac{\mathcal{P}_\mathcal{T}}{\mathcal{P}_R} \ . \tag{B.20}$$

However, in the case of not slowly varying quantities, one has to explicitly solve the full Mukhanov-Sasaki differential equation corresponding to each perturbative mode, to predict its evolution. This is the case in models where there is a significant shift in the evolution pattern of the inflaton field, like the one introduced in Section 2.

[1] For example, in the NMC scenario, briefly presented in Section 2, we can prove through equations (2.4),(2.5) and (2.6), that $c_s^2 = 1$, hence there are no corresponding instabilities.

Another observable that we can obtain through CMBR is the scalar spectral index, n_s, that expresses the change of the logarithm of the power spectrum of the scalar perturbations, per logarithmic interval k:

$$1 - n_s \equiv -\frac{d \ln \mathcal{P}_R}{d \ln k}\Big|_{k=aH} , \tag{B.21}$$

Similarly, we define the tensor spectral index:

$$n_t \equiv -\frac{d \ln \mathcal{P}_\mathcal{T}}{d \ln k}\Big|_{k=aH} . \tag{B.22}$$

Parameters r and n_t are related by what is referred to as *the consistency condition*. In standard single-field inflation it is of the form

$$r \approx -8 n_t$$

However, in modified theories of inflation, its form is generally non-standard. So in summary, the observables of a single field inflationary model are r, n_s and $\mathcal{P}_R$.

Bibliography

[1] The LIGO Scientific Collaboration and the VIRGO Collaboration, *Observation of Gravitational Waves from a Binary Black Hole Merger*, Phys. Rev. Lett. **116**, 061102 (2016)

[2] J. M. Ezquiaga and M. Zumalacárregui, *Dark Energy After GW170817: Dead Ends and the Road Ahead*, Phys. Rev. Lett. **119**, no. 25, 251304 (2017) [arXiv:1710.05901 [astro-ph.CO]].

[3] The Planck Collaboration, *Planck 2018 results. I. Overview and the cosmological legacy of Planck*, A&A **641**, A1 (2020), [arXiv:1807.06205 [astro-ph.CO]]

[4] A. G. Riess et al., *A 2.4 Determination of the Local Value of the Hubble Constant*, Astrophys. J. **826**, no.1, 56 (2016), [arXiv:1604.01424 [astro-ph.CO]].

[5] A. G. Riess et al. (Supernova Search Team), *Observational Evidence from Supernovae for an Accelerating Universe and a Cosmological Constant*, Astron. J. **116**, 1009 (1998), [arXiv:astro-ph/9805201].

[6] S. Perlmutter et al. (Supernova Cosmology Project), *Measurements of Omega and Lambda from 42 High-Redshift Supernovae*, Astrophys. J. **517**, 565 (1999), [arXiv:astro-ph/9812133]

[7] P. de Bernardis et al. (Boomerang), *A Flat Universe from High-Resolution Maps of the Cosmic Microwave Background Radiation*, Nature **404**, 955 (2000), [arXiv:astro-ph/0004404]

[8] S. Hanany et al., *MAXIMA-1: A Measurement of the Cosmic Microwave Background Anisotropy on angular scales of 10 arcminutes to 5 degrees* Astrophys. J. **545**, L5 (2000), [arXiv:astro-ph/0005123].

[9] A. H. Guth, *Inflationary universe: A possible solution to the horizon and flatness problems*, Phys. Rev. D **23**, 347 (1981)

[10] A. D. Linde, *A new inflationary universe scenario: A possible solution of the horizon, flatness, homogeneity, isotropy and primordial monopole problems*, Phys. Lett. B **108**, 389 (1982)

[11] A. Albrecht and P. J. Steinhardt, *Cosmology for Grand Unified Theories with Radiatively Induced Symmetry Breaking* Phys. Rev. Lett. **48**, 1220 (1982)

[12] M. Ostrogradsky, *Memoires sur les equations differentielles, relatives au probleme des isoperimetres*, Mem. Acad. St. Petersbourg **6**, no. 4, 385 (1850).

[13] G. W. Horndeski, *Second-order scalar-tensor field equations in a four-dimensional space*, Int. J. Theor. Phys. **10** (1974) 363.

[14] C. Deffayet and D. A. Steer, *A formal introduction to Horndeski and Galileon theories and their generalizations*, Class. Quant. Grav **30** (2013) 214006 [1307.2450]

[15] C. Charmousis, C. E. J., P. Antonia and P. M. Saffin *General second order scalar tensor theory, self tuning and the fab four*, Phys. Rev. Lett. **108** (2012) 051101 [1106.2000]

[16] A. Nicolis, R. Rattazzi and E. Trincherini, *The Galileon as a Local Modification of Gravity*, Phys. Rev. **D79**, 064036 (2009), [arXiv:0811.2197]

[17] T. P. Sotiriou and V. Faraoni, *f(R) Theories Of Gravity*, Rev. Mod. Phys. **82** (2010) 451 [0805.1726].

[18] A. De Felice and S. Tsujikawa, *f(R) theories*, Living Rev. Rel. **13** (2010) 3 [1002.4928].

[19] C. de Rham and A. J. Tolley, *DBI and the Galileon reunited*, JCAP **1005** (2010) 015 [1003.5917].

[20] G. Goon, K. Hinterbichler and M. Trodden, *Symmetries for Galileons and DBI scalars on curved space*, JCAP **1107** (2011) 017 [1103.5745].

[21] G. Goon, K. Hinterbichler and M. Trodden, *A New Class of Effective Field Theories from Embedded Branes*, Phys. Rev. Lett. **106** (2011) 231102 [1103.6029].

[22] M. Trodden and K. Hinterbichler, *Generalizing Galileons*, Class. Quant. Grav. **28** (2011) 204003 [1104.2088].

[23] K. Van Acoleyen and J. Van Doorsselaere, *Galileons from Lovelock actions*, Phys. Rev. **D83** (2011) 084025 [1102.0487].

[24] C. van de Bruck and C. Longden, *Einstein-Gauss-Bonnet gravity with extra dimensions*, [1809.00920 [gr-qc]].

[25] C. Germani and A. Kehagias, *New Model of Inflation with Non-minimal Derivative Coupling of Standard Model Higgs Boson to Gravity*, Phys. Rev. Lett. **105** (2010) 011302, [arXiv:1003.2635 [hep-ph]].

[26] S. Tsujikawa, *Observational tests of inflation with a field derivative coupling to gravity*, Phys. Rev. D **85** (2012) 083518 [arXiv:1201.5926 [astro-ph.CO]].

[27] I. Dalianis, G. Koutsoumbas, K. Ntrekis and E. Papantonopoulos, *Reheating predictions in Gravity Theories with Derivative Coupling*, JCAP **1702**, no. 02, 027 (2017) [arXiv:1608.04543 [gr-qc]].

[28] A.A. Starobinsky, *A new type of isotropic cosmological models without singularity*, Phys. Lett. B **91**, 99 (1980).

[29] D. J. Gross and J. H. Sloan, *The Quartic Effective Action for the Heterotic String*, Nucl. Phys. B **291**, 41 (1987).

[30] Y. Fujii and K. Maeda, *The scalar-tensor theory of gravitation*, Cambridge University Press, Cambridge (2003).

[31] A. Nicolis, R. Rattazzi, E. Trincherini, *The Galileon as a local modification of gravity*, Phys. Rev. **D79** (2009) 064036. [arXiv:0811.2197 [hep-th]].

[32] C. Deffayet, G. Esposito-Farese, A. Vikman, *Covariant Galileon*, Phys. Rev. **D79** (2009) 084003. [arXiv:0901.1314 [hep-th]].

[33] C. Deffayet, S. Deser and G. Esposito-Farese, *Generalized Galileons: All scalar models whose curved background extensions maintain second-order field equations and stress-tensors*, Phys. Rev. D **80**, 064015 (2009). [arXiv:0906.1967].

[34] C. Deffayet, X. Gao, D. A. Steer and G. Zahariade, *From k-essence to generalised Galileons*, Phys. Rev. D **84**, 064039 (2011). [arXiv:1103.3260 [hep-th]].

[35] T. Kobayashi, M. Yamaguchi and J. Yokoyama, *Generalized G-inflation: Inflation with the most general second-order field equations*, Prog. Theor. Phys. **126** (2011) 511 [arXiv:1105.5723 [hep-th]].

[36] K. Kamada, T. Kobayashi, M. Yamaguchi and J. Yokoyama, *Higgs G-inflation*, Phys. Rev. D **83** (2011) 083515 [arXiv:1012.4238 [astro-ph.CO]].

[37] E. Papantonopoulos, *Effects of the kinetic coupling of matter to curvature*, Int. J. Mod. Phys. D **28**, no. 05, 1942007 (2019).

[38] T. Kolyvaris, G. Koutsoumbas, E. Papantonopoulos and G. Siopsis, *Scalar Hair from a Derivative Coupling of a Scalar Field to the Einstein Tensor*, Class. Quant. Grav. **29**, 205011 (2012), [arXiv:1111.0263 [gr-qc]].

[39] M. Rinaldi, *Black holes with non-minimal derivative coupling*, Phys. Rev. D **86**, 084048 (2012) [arXiv:1208.0103 [gr-qc]].

[40] T. Kolyvaris, G. Koutsoumbas, E. Papantonopoulos and G. Siopsis, *Phase Transition to a Hairy Black Hole in Asymptotically Flat Spacetime*, JHEP **1311**, 133 (2013), [arXiv:1308.5280 [hep-th]].

[41] G. Koutsoumbas, K. Ntrekis, E. Papantonopoulos and M. Tsoukalas, *Gravitational Collapse in Horndeski Theory*, [arXiv:1512.05934 [gr-qc]].

[42] L. Amendola, *Cosmology with nonminimal derivative couplings*, Phys. Lett. B **301**, 175 (1993) [arXiv:gr-qc/9302010].

[43] S. V. Sushkov, *Exact cosmological solutions with nonminimal derivative coupling*, Phys. Rev. D **80**, 103505 (2009) [arXiv:0910.0980 [gr-qc]].

[44] F. Farakos, C. Germani, A. Kehagias and E. N. Saridakis, *A New Class of Four-Dimensional N=1 Supergravity with Non-minimal Derivative Couplings*, JHEP **1205** (2012) 050 [arXiv:1202.3780 [hep-th]].

[45] F. Farakos, C. Germani and A. Kehagias, *On ghost-free supersymmetric galileons*, JHEP **1311** (2013) 045 [arXiv:1306.2961 [hep-th]].

[46] I. Dalianis and F. Farakos, *Higher Derivative D-term Inflation in New-minimal Supergravity*, Phys. Lett. B **736** (2014) 299 [arXiv:1403.3053 [hep-th]].

[47] H. M. Sadjadi and P. Goodarzi, *Reheating in nonminimal derivative coupling model*, JCAP **1302** (2013) 038, [arXiv:1203.1580 [gr-qc]].

[48] A. Ghalee, *A new phase of scalar field with a kinetic term non-minimally coupled to gravity*, Phys. Lett. B **724** (2013) 198, [arXiv:1303.0532 [astro-ph.CO]].

[49] B. Gumjudpai and P. Rangdee, *Non-minimal derivative coupling gravity in cosmology*, Gen. Rel. Grav. **47**, no. 11, 140 (2015), [arXiv:1511.00491 [gr-qc]].

[50] Y. S. Myung and T. Moon, *Inflaton decay and reheating in nonminimal derivative coupling*, JCAP **1607**, 014 (2016) [arXiv:1601.03148 [gr-qc]].

[51] Y. Ema, R. Jinno, K. Mukaida and K. Nakayama, *Particle Production after Inflation with Non-minimal Derivative Coupling to Gravity*, JCAP **1510**, no. 10, 020 (2015), [arXiv:1504.07119 [gr-qc]].

[52] Y. Ema, R. Jinno, K. Mukaida and K. Nakayama, *Gravitational particle production in oscillating backgrounds and its cosmological implications*, Phys. Rev. D **94** (2016) no.6, 063517 [arXiv:1604.08898 [hep-ph]].

[53] G. Koutsoumbas, K. Ntrekis and E. Papantonopoulos, *Gravitational Particle Production in Gravity Theories with Non-minimal Derivative Couplings*, JCAP **1308**, 027 (2013), [arXiv:1305.5741 [gr-qc]].

[54] C. Germani, N. Kudryashova and Y. Watanabe, *On post-inflation validity of perturbation theory in Horndeski scalar-tensor models*, JCAP **1608** (2016) 015 [arXiv:1512.06344 [astro-ph.CO]].

[55] S. Chatrchyan *et al.* [CMS Collaboration], *Observation of a New Boson at a Mass of 125 GeV with the CMS Experiment at the LHC*, Phys. Lett. B **716** (2012) 30 [arXiv:1207.7235 [hep-ex]].

[56] B. P. Abbott *et al.* [LIGO Scientific and Virgo Collaborations], *GW151226: Observation of Gravitational Waves from a 22-Solar-Mass Binary Black Hole Coalescence*, Phys. Rev. Lett. **116**, no. 24, 241103 (2016) [arXiv:1606.04855 [gr-qc]].

[57] C. Germani and Y. Watanabe, *UV-protected (Natural) Inflation: Primordial Fluctuations and non-Gaussian Features*, JCAP **1107**, 031 (2011) Addendum: [JCAP **1107**, A01 (2011)] [arXiv:1106.0502 [astro-ph.CO]].

[58] Y. Gong, E. Papantonopoulos and Z. Yi, *Constraints on scalar-tensor theory of gravity by the recent observational results on gravitational waves*, Eur. Phys. J. C **78**, no. 9, 738 (2018) [arXiv:1711.04102 [gr-qc]].

[59] T. Baker, E. Bellini, P. G. Ferreira, M. Lagos, J. Noller and I. Sawicki, *Strong constraints on cosmological gravity from GW170817 and GRB 170817A*, Phys. Rev. Lett. **119**, no. 25, 251301 (2017) [arXiv:1710.06394 [astro-ph.CO]].

[60] P. Creminelli and F. Vernizzi, *Dark Energy after GW170817 and GRB170817A*, Phys. Rev. Lett. **119**, no. 25, 251302 (2017) [arXiv:1710.05877 [astro-ph.CO]].

[61] M. Kawasaki, N. Sugiyama and T. Yanagida, *Primordial black hole formation in a double inflation model in supergravity*, Phys. Rev. D **57** (1998) 6050 [hep-ph/9710259].

[62] J. Garcia-Bellido and E. Ruiz Morales, *Primordial black holes from single field models of inflation*, Phys. Dark Univ. **18** (2017) 47 [arXiv:1702.03901 [astro-ph.CO]].

[63] G. Ballesteros, J. Beltran Jimenez and M. Pieroni, *Black hole formation from a general quadratic action for inflationary primordial fluctuations*, JCAP **1906** (2019) 016 [arXiv:1811.03065 [astro-ph.CO]].

[64] Y. F. Cai, X. Tong, D. G. Wang and S. F. Yan, *Primordial Black Holes from Sound Speed Resonance during Inflation*, Phys. Rev. Lett. **121** (2018) no.8, 081306 [arXiv 1805.03639 [astro-ph.CO]].

[65] C. Chen and Y. F. Cai, *Primordial black holes from sound speed resonance in the inflaton-curvaton mixed scenario*, [arXiv:1908.03942 [astro-ph.CO]].

[66] C. Fu, P. Wu and H. Yu, *Primordial Black Holes from Inflation with Nonminimal Derivative Coupling*, Phys. Rev. D **100**, no. 6, 063532 (2019) [arXiv:1907.05042 [astro-ph.CO]].

[67] Y. Akrami *et al.* [Planck Collaboration], *Planck 2018 results. X. Constraints on inflation*, [arXiv:1807.06211 [astro-ph.CO]].

[68] C. Germani, Y. Watanabe and N. Wintergerst, *Self-unitarization of New Higgs Inflation and compatibility with Planck and BICEP2 data*, JCAP **1412** (2014) 009 [arXiv:1403.5766 [hep-ph]].

[69] I. Dalianis and F. Farakos, *Exponential potential for an inflaton with nonminimal kinetic coupling and its supergravity embedding*, Phys. Rev. D **90** (2014) no.8, 083512 [arXiv:1405.7684 [hep-th]].

[70] L. McAllister, E. Silverstein, A. Westphal and T. Wrase, *The Powers of Monodromy*, JHEP **1409** (2014) 123 [arXiv:1405.3652 [hep-th]].

[71] S. Ferrara, A. Kehagias and A. Riotto, *The Imaginary Starobinsky Model and Higher Curvature Corrections*, Fortsch. Phys. **63** (2015) 2 [arXiv:1405.2353 [hep-th]].

[72] F. Lucchin and S. Matarrese, *Power Law Inflation*, Phys. Rev. D **32** (1985) 1316.

[73] J. Yokoyama and K. i. Maeda, *On the Dynamics of the Power Law Inflation Due to an Exponential Potential*, Phys. Lett. B **207** (1988) 31.

[74] M. Turner, *Coherent scalar-field oscillations in an expanding universe*, Phys. Rev. D 28, 1243.

[75] Y. Shtanov, J. H. Traschen and R. H. Brandenberger, *Universe reheating after inflation*, Phys. Rev. D **51** (1995) 5438 [arXiv:hep-ph/9407247].

[76] M. Sasaki, T. Suyama, T. Tanaka and S. Yokoyama, *Primordial black holes perspectives in gravitational wave astronomy*, Class. Quant. Grav. **35** (2018) no.6, 063001 [arXiv:1801.05235 [astro-ph.CO]].

[77] M. Yu. Khlopov, *Primordial Black Holes*, Res.Astron.Astrophys. **10** 495-528, 2010 [arXiv:0801.0116 [astro-ph]].

[78] B. Carr, M. Raidal, T. Tenkanen, V. Vaskonen and H. Veermäe, *Primordial black hole constraints for extended mass functions*, Phys. Rev. D **96** (2017) no.2, 023514 [arXiv:1705.05567 [astro-ph.CO]].

[79] M. Raidal, C. Spethmann, V. Vaskonen and H. Veermäe, *Formation and Evolution of Primordial Black Hole Binaries in the Early Universe*, JCAP **1902** (2019) 018 [arXiv:1812.01930 [astro-ph.CO]].

[80] S. Pi, Y. l. Zhang, Q. G. Huang and M. Sasaki, *Scalaron from R^2-gravity as a heavy field*, JCAP **1805** (2018) 042 [arXiv:1712.09896 [astro-ph.CO]].

[81] S. L. Cheng, W. Lee and K. W. Ng, *Production of high stellar-mass primordial black holes in trapped inflation*, JHEP **1702** (2017) 008 [arXiv:1606.00206 [astro-ph.CO]].

[82] W. H. Press and P. Schechter, *Formation of galaxies and clusters of galaxies by selfsimilar gravitational condensation*, Astrophys. J. **187**, 425 (1974).

[83] C. Germani and I. Musco, *Abundance of Primordial Black Holes Depends on the Shape of the Inflationary Power Spectrum*, Phys. Rev. Lett. **122** (2019) no.14, 141302 [arXiv:1805.04087 [astro-ph.CO]].

[84] S. Young, C. T. Byrnes and M. Sasaki, *Calculating the mass fraction of primordial black holes*, JCAP **1407** (2014) 045 [arXiv:1405.7023 [gr-qc]].

[85] W. H. Kinney, *Horizon crossing and inflation with large eta*, Phys. Rev. D **72** (2005) 023515 [arXiv:0503017 [gr-qc]].

[86] H. Motohashi and W. Hu, *Primordial Black Holes and Slow-Roll Violation*, Phys. Rev. D **96** (2017) no.6, 063503 [arXiv:1706.06784 [astro-ph.CO]].

[87] R. g. Cai, S. Pi and M. Sasaki, *Gravitational Waves Induced by non-Gaussian Scalar Perturbations*, Phys. Rev. Lett. **122**, no. 20, 201101 (2019) [arXiv:1810.11000 [astro-ph.CO]].

[88] N. Bartolo, V. De Luca, G. Franciolini, M. Peloso, D. Racco and A. Riotto, *Testing primordial black holes as dark matter with LISA*, Phys. Rev. D **99**, no. 10, 103521 (2019) [arXiv:1810.12224 [astro-ph.CO]].

[89] J. Garcia-Bellido, M. Peloso and C. Unal, *Gravitational Wave signatures of inflationary models from Primordial Black Hole Dark Matter*, JCAP **1709** (2017) no.09, 013 [arXiv 1707.02441 [astro-ph.CO]].

[90] Y. F. Cai, C. Chen, X. Tong, D. G. Wang and S. F. Yan, *When Primordial Black Holes from Sound Speed Resonance Meet a Stochastic Background of Gravitational Waves*, Phys. Rev. D **100** (2019) no.4, 043518 [arXiv:1902.08187 [astro-ph.CO]].

[91] B. Carr, F. Kuhnel and M. Sandstad, *Primordial Black Holes as Dark Matter*, Phys. Rev. D **94** (2016) no.8, 083504 [arXiv:1607.06077 [astro-ph.CO]].

[92] I. Dalianis, *Constraints on the curvature power spectrum from primordial black hole evaporation*, JCAP **2019** (2019) no.08, 032 [arXiv:1812.09807 [astro-ph.CO]].

[93] S. Chongchitnan and G. Efstathiou, *Accuracy of slow-roll formulae for inflationary perturbations: implications for primordial black hole formation*, JCAP **0701** (2007) 011 [arXiv:0611818 [astro-ph].

[94] T. Kobayashi, *Horndeski theory and beyond: a review*, Rept.Prog.Phys. 82 (2019) no.8, 086901 [arXiv:1901.07183 [gr-qc]].

[95] R. Saito, J, Yokoyama and R. Nagata, *Single-field inflation, anomalous enhancement of superhorizon fluctuations, and non-Gaussianity in primordial black hole formation*, JCAP 0806:024,2008 [arXiv:0804.3470 [astro-ph]].

[96] I. Dalianis, A. Kehagias and G. Tringas, *Primordial black holes from α-attractors*, JCAP **1901** (2019) 037 [arXiv:1805.09483 [astro-ph.CO]].

[97] T. Harada, C. M. Yoo and K. Kohri, *Threshold of primordial black hole formation*, Phys. Rev. D **88** (2013) no.8, 084051 Erratum: [Phys. Rev. D **89** (2014) no.2, 029903] [arXiv:1309.4201 [astro-ph.CO]].

[98] K. M. Belotsky, A. D. Dmitriev, E. A. Esipova, V. A. Gani, A. V. Grobov, M. Yu. Khlopov, A. A. Kirillov, S. G. Rubin and I. V. Svadkovsky, *Signatures of primordial black hole dark matter*, Mod. Phys. Lett. A 29 (2014) 1440005 [arXiv:1410.0203 [astro-ph.CO]].

[99] B. J. Carr, J. H. Gilbert and J. E. Lidsey, *Black hole relics and inflation: Limits on blue perturbation spectra*, Phys. Rev. D **50**, 4853 (1994) [astro-ph/9405027].

[100] J. D. Barrow, E. J. Copeland and A. R. Liddle, *The Cosmology of black hole relics*, Phys. Rev. D **46**, 645 (1992).

[101] I. Dalianis and G. Tringas, *Primordial black hole remnants as dark matter produced in thermal, matter, and runaway-quintessence postinflationary scenarios*, Phys. Rev. D **100** (2019) no.8, 083512 [arXiv:1905.01741 [astro-ph.CO]].

[102] A. D. Linde, *Hybrid inflation*, Phys. Rev. D **49** (1994) 748 [astro-ph/9307002].

[103] K. A. Olive, *Inflation*, Phys. Rept. **190**, 307 (1990).

[104] D. H. Lyth and A. Riotto, *Particle physics models of inflation and the cosmological density perturbation*, Phys. Rept. **314**, 1-146 (1999) [arXiv:hep-ph/9807278].

[105] J. Martin, C. Ringeval and V. Vennin, *Encyclopædia Inflationaris*, Phys. Dark Univ. **5-6**, 75-235 (2014) [arXiv:1303.3787 [astro-ph.CO]].

[106] Y. Lu, Y. Gong, Z. Yi and F. Zhang, *Constraints on primordial curvature perturbations from primordial black hole dark matter and secondary gravitational waves*, JCAP **12**, 031 (2019) [arXiv:1907.11896 [gr-qc]].

[107] Z. Yi, Q. Gao, Y. Gong and Z. h. Zhu, *Primordial black holes and secondary gravitational waves from inflationary model with a non-canonical kinetic term*, [arXiv:2011.10606 [astro-ph.CO]].

[108] Z. Yi, Y. Gong, B. Wang and Z. h. Zhu, *Primordial Black Holes and Secondary Gravitational Waves from Higgs field*, [arXiv:2007.09957 [gr-qc]].

[109] S. Pi, Y. Zhang, Q. G. Huang and M. Sasaki, *Scalaron from R^2-gravity as a Heavy Field*, JCAP **05** (2018) 042, [arXiv:1712.09896 [astro-ph.CO]]

[110] T. Harko, F. S. N. Lobo, E. N. Saridakis and M. Tsoukalas, *Cosmological models in modified gravity theories with extended nonminimal derivative couplings*, Phys. Rev. D **95**, no.4, 044019 (2017) [arXiv:1609.01503 [gr-qc]].

[111] D. S. Salopek, J. R. Bond and J. M. Bardeen, *Designing Density Fluctuation Spectra in Inflation*, Phys. Rev. D **40**, 1753 (1989).

[112] R. Fakir and W. G. Unruh, *Improvement on cosmological chaotic inflation through nonminimal coupling*, Phys. Rev. D **41**, 1783 (1990).

[113] D. I. Kaiser, *Primordial spectral indices from generalized Einstein theories*, Phys. Rev. D **52** (1995) 4295 [arXiv:astro-ph/9408044].

[114] E. Komatsu and T. Futamase, *Complete constraints on a nonminimally coupled chaotic inflationary scenario from the cosmic microwave background*, Phys. Rev. D **59** (1999) 064029, [arXiv:astro-ph/9901127].

[115] K. Nozari and S. D. Sadatian, *Non-Minimal Inflation after WMAP3*, Mod. Phys. Lett. A **23** (2008) 2933 [arXiv:0710.0058 [astro-ph]].

[116] S. C. Park and S. Yamaguchi, *Inflation by non-minimal coupling*, JCAP **08**, 009 (2008) [arXiv:0801.1722 [hep-ph]].

[117] F. L. Bezrukov and M. Shaposhnikov, *The Standard Model Higgs boson as the inflaton*, Phys. Lett. B **659**, 703 (2008), [arXiv:0710.3755 [hep-th]].

[118] A. O. Barvinsky, A. Y. Kamenshchik and A. A. Starobinsky, *Inflation scenario via the Standard Model Higgs boson and LHC*, JCAP **021** 0811 (2008), [arXiv:0809.2104 [hep-ph]].

[119] F. Bezrukov, D. Gorbunov and M. Shaposhnikov, *On initial conditions for the Hot Big Bang*, JCAP **06**, 029 (2009) [arXiv:0812.3622 [hep-ph]].

[120] J. Garcia-Bellido, D. G. Figueroa and J. Rubio, *Preheating in the Standard Model with the Higgs-Inflaton coupled to gravity*, Phys. Rev. D **79**, 063531 (2009) [arXiv:0812.4624 [hep-ph]].

[121] A. De Simone, M. P. Hertzberg and F. Wilczek, *Running Inflation in the Standard Model*, Phys. Lett. B **678**, 1-8 (2009) [arXiv:0812.4946 [hep-ph]].

[122] F. L. Bezrukov, A. Magnin and M. Shaposhnikov, *Standard Model Higgs boson mass from inflation*, Phys. Lett. B **675**, 88-92 (2009) [arXiv:0812.4950 [hep-ph]].

[123] C. P. Burgess, H. M. Lee and M. Trott, *Power-counting and the Validity of the Classical Approximation During Inflation*, JHEP **09**, 103 (2009) [arXiv:0902.4465 [hep-ph]].

[124] J. L. F. Barbon and J. R. Espinosa, *On the Naturalness of Higgs Inflation*, Phys. Rev. D **79**, 081302 (2009) [arXiv:0903.0355 [hep-ph]].

[125] F. Bezrukov and M. Shaposhnikov, *Standard Model Higgs boson mass from inflation: two loop analysis*, JHEP **07**, 089 (2009) [arXiv:0904.1537 [hep-ph]].

[126] A. O. Barvinsky, A. Y. Kamenshchik, C. Kiefer, A. A. Starobinsky and C. Steinwachs, *Asymptotic freedom in inflationary cosmology with a non-minimally coupled Higgs field*, JCAP **12**, 003 (2009) [arXiv:0904.1698 [hep-ph]].

[127] T. E. Clark, B. Liu, S. T. Love and T. ter Veldhuis, *The Standard Model Higgs Boson-Inflaton and Dark Matter*, Phys. Rev. D **80**, 075019 (2009) [arXiv:0906.5595 [hep-ph]].

[128] A. O. Barvinsky, A. Y. Kamenshchik, C. Kiefer, A. A. Starobinsky and C. F. Steinwachs, *Higgs boson, renormalization group, and naturalness in cosmology*, Eur. Phys. J. C **72**, 2219 (2012) [arXiv:0910.1041 [hep-ph]].

[129] M. B. Einhorn and D. R. T. Jones, *Inflation with Non-minimal Gravitational Couplings in Supergravity*, JHEP **03**, 026 (2010) [arXiv:0912.2718 [hep-ph]].

[130] R. N. Lerner and J. McDonald, *Higgs Inflation and Naturalness*, JCAP **04**, 015 (2010) [arXiv:0912.5463 [hep-ph]].

[131] C. P. Burgess, H. M. Lee and M. Trott, *Comment on Higgs Inflation and Naturalness*, JHEP **07**, 007 (2010) [arXiv:1002.2730 [hep-ph]].

[132] A. Mazumdar and J. Rocher, *Particle physics models of inflation and curvaton scenarios*, Phys. Rept. **497**, 85-215 (2011) [arXiv:1001.0993 [hep-ph]].

[133] C. Q. Geng, C. C. Lee, M. Sami, E. N. Saridakis and A. A. Starobinsky, *Observational constraints on successful model of quintessential Inflation*, JCAP **06**, 011 (2017) [arXiv:1705.01329 [gr-qc]].

[134] J. Fumagalli and M. Postma, *UV (in)sensitivity of Higgs inflation*, JHEP **05**, 049 2016, [arXiv:1602.07234[hep-ph]]

[135] M. P. Hertzberg, *On Inflation with Non-minimal Coupling*, JHEP **11**, 023 (2010) [arXiv:1002.2995 [hep-ph]].

[136] G. F. Giudice and H. M. Lee, *Unitarizing Higgs Inflation*, Phys. Lett. B **694**, 294-300 (2011) [arXiv:1010.1417 [hep-ph]].

[137] T. Tenkanen, *Resurrecting Quadratic Inflation with a non-minimal coupling to gravity*, JCAP **12**, 001 (2017) [arXiv:1710.02758 [astro-ph.CO]].

[138] J. McDonald, *Does Palatini Higgs Inflation Conserve Unitarity*, [arXiv:2007.04111 [hep-ph]]

[139] T. Tenkanen and E. Tomberg, *Initial conditions for plateau inflation: a case study*, JCAP **04**, 050 (2020) [arXiv:2002.02420 [astro-ph.CO]].

[140] R. N. Lerner and J. McDonald, *A Unitarity-Conserving Higgs Inflation Model*, Phys. Rev. D **82**, 103525 (2010) [arXiv:1005.2978 [hep-ph]].

[141] S. Lola, A. Lymperis and E. N. Saridakis, *Inflation with non-canonical scalar fields revisited*, Eur. Phys. J. C **81**, 719 (2021) [arXiv:2005.14069 [gr-qc]].

[142] E. Babichev and C. Charmousis, *Dressing a black hole with a time-dependent Galileon*, JHEP **08**, 106 (2014) [arXiv:1312.3204 [gr-qc]].

[143] A. Cisterna and C. Erices, *Asymptotically locally AdS and flat black holes in the presence of an electric field in the Horndeski scenario*, Phys. Rev. D **89**, 084038 (2014) [arXiv:1401.4479 [gr-qc]].

[144] C. Charmousis, T. Kolyvaris, E. Papantonopoulos and M. Tsoukalas, *Black Holes in Bi-scalar Extensions of Horndeski Theories*, JHEP **07**, 085 (2014) [arXiv:1404.1024 [gr-qc]].

[145] A. Anabalon, A. Cisterna and J. Oliva, *Asymptotically locally AdS and flat black holes in Horndeski Theory*, Phys. Rev. D **89**, 084050 (2014), [arXiv:1312.3597 [gr-qc]]

[146] A. Cisterna, T. Delsate and M. Rinaldi, *Neutron Stars in general second order scalar-tensor theory: the case of non-minimal derivative coupling*, Phys. Rev. D **92**, 044050 (2015), [arXiv:1504.05189 [gr-qc]]

[147] A. Cisterna, T. Delsate, L. Ducobu and M. Rinaldi, *Slowly rotating neutron stars in the nonminimal derivative coupling sector of Horndeski gravity*, Phys. Rev. D **93**, 084046 (2016), [arXiv:1602.06939 [gr-qc]]

[148] E. N. Saridakis and S. V. Sushkov, *Quintessence and phantom cosmology with non-minimal derivative coupling*, Phys. Rev. D **81**, 083510 (2010) [arXiv:1002.3478 [gr-qc]].

[149] J. B. Dent, S. Dutta, E. N. Saridakis and J. Q. Xia, *Cosmology with non-minimal derivative couplings:perturbation analysis and observational constraints*, JCAP **11**, 058 (2013) [arXiv:1309.4746 [astro-ph.CO]].

[150] H. Sheikhahmadi, E. N. Saridakis, A. Aghamohammadi and K. Saaidi, *Hamilton-Jacobi formalism for inflation with non-minimal derivative coupling*, JCAP **10**, 021 (2016) [arXiv:1603.03883 [gr-qc]].

[151] M. Atkins and X. Calmet, *Remarks on Higgs Inflation*, Phys. Lett. B **697**, 37-40 (2011) [arXiv:1011.4179 [hep-ph]].

[152] N. Yang, Q. Fei, Q. Gao and Y. Gong, *Inflationary models with non-minimally derivative coupling*, Class. Quant. Grav. **33**, no.20, 205001 (2016) [arXiv:1504.05839 [gr-qc]].

[153] Z. Yi and Y. Gong, *Nonminimal coupling and inflationary attractors*, Phys. Rev. D **94**, no.10, 103527 (2016) [arXiv:1608.05922 [gr-qc]].

[154] I. D. Gialamas, A. Karam, A. Lykkas and T. D. Pappas, *Palatini-Higgs inflation with nonminimal derivative coupling*, Phys. Rev. D **102**, no.6, 063522 (2020) [arXiv:2008.06371 [gr-qc]].

[155] I. Dalianis, S. Karydas and E. Papantonopoulos, *Generalized Non-Minimal Derivative Coupling: Application to Inflation and Primordial Black Hole Production*, JCAP **06**, 040 (2020) [arXiv:1910.00622 [astro-ph.CO]].

[156] P. A. González, M. Olivares, E. Papantonopoulos and Y. Vásquez, *Constraints on scalar–tensor theory of gravity by solar system tests*, Eur. Phys. J. C **80**, no.10, 981 (2020) [arXiv:2002.03394 [gr-qc]].

[157] J. Fumagalli, S. Mooij and M. Postma *Unitarity and Predictiveness in new Higgs inflation*, JHEP **03** 2018, 038, [arXiv:1711.08761[hep-ph]]

[158] J. Fumagalli, M. Postma and M. v. d. Bout *Matching and running sensitivity in non-renormalizable inflationary models*, JHEP **09** 2020, 114, [arXiv:2005.05905[hep-ph]]

[159] B. P. Abbott *et al.* [LIGO Scientific and Virgo Collaborations], *GW170817: Observation of Gravitational Waves from a Binary Neutron Star Inspiral*, Phys. Rev. Lett. **119**, no. 16, 161101 (2017) [arXiv:1710.05832 [gr-qc]].

[160] A. Goldstein *et al.*, *An Ordinary Short Gamma-Ray Burst with Extraordinary Implications: Fermi-GBM Detection of GRB 170817A*, Astrophys. J. **848**, no. 2, L14 (2017) [arXiv:1710.05446 [astro-ph.HE]].

[161] T. Kaluza, *On the Problem of Unity in Physics*, Sitzungsber. Preuss. Akad. Wiss. Berlin (Math. Phys.) **1921**, 966 (1921).

[162] O. Klein, *Quantum Theory and Five-Dimensional Theory of Relativity. (In German and English)*, Z. Phys. **37**, 895 (1926) [Surveys High Energ. Phys. **5**, 241 (1986)].

[163] L. Randall and R. Sundrum, *A large mass hierarchy from a small extra dimension*, Phys. Rev. Lett. **83**, 3370 (1999) [arXiv:9905221 [hep-ph]]; L. Randall and R. Sundrum, *An alternative to compactification*, Phys. Rev. Lett. **83**, 4690 (1999) [arXiv:9906064 [hep-th]].

[164] R. Maartens, *Brane-world gravity*, Living Rev. Rel. **7**, 7 (2004) [arXiv:0312059 [gr-qc]].

[165] E. Papantonopoulos, *Brane cosmology*, Lect. Notes Phys. **592** (2002) 458 [arXiv:0202044 [hep-th]]; U. Gunther and A. Zhuk, *Phenomenology of brane-worldcosmological models*, [arXiv:0410130 [gr-qc]]; D. Langlois, *Gravitation and cosmology in brane-worlds*, [arXiv:0410129 [gr-qc]].

[166] I. Antoniadis, *A Possible new dimension at a few TeV*, Phys. Lett. B **246**, 377 (1990).

[167] T. Appelquist, H. C. Cheng and B. A. Dobrescu, *Bounds on universal extra dimensions*, Phys. Rev. D **64**, 035002 (2001) [arXiv:0012100 [hep-ph]].

[168] D. Bailin, A. Love, *Kaluza-Klein Theories*, Rept. Prog. Phys., **50** 1087-1170, 1987

[169] J. M. Overduin, P. S. Wesson, *Kaluza-Klein Gravity*, Phys. Rept., **283** 303-380, 1997 [arXiv:9805018 [gr-qc]].

[170] G. Jungman, M. Kamionkowski and K. Griest, *Supersymmetric dark matter*, Phys. Rept. **267**, 195 (1996) [arXiv:9506380 [hep-ph]].

[171] G. Servant, T. M. P. Tait, *Is the Lightest Kaluza-Klein Particle a Viable Dark Matter Candidate*, [arXiv:0206071 [hep-ph]].

[172] T. Bringmann, M. Eriksson and M. Gustafsson, *Cosmological Evolution of Homogeneous Universal Extra Dimensions*, Phys. Rev. D **68**, 063516 (2003), [arXiv:0303497 [astro-ph]].

[173] A. I. Zhuk, *Conventional cosmology from multidimensional models*, [arXiv:0609126 [hep-th]].

[174] M. Eingorn and A. Zhuk, *Kaluza-Klein models: can we construct a viable example?*, Phys. Rev. D **83**, 044005 (2011) [arXiv:1010.5740 [gr-qc]].

[175] T. Bringmann and M. Eriksson, *Can homogeneous extra dimensions be stabilized during matter domination?*, JCAP 0310 **006** (2003), [arXiv:0308498v2 [astro-ph]].

[176] R. Brandenberger, C. Vafa, *Superstrings in the early Universe*, Nuclear Physics B **316**, (391-410), 1989.

[177] A. A. Tsetylin, C. Vafa, *Elements of string cosmology*, Nucl. Phys. B **372** 443-466, 1992. [arXiv:9109048 [hep-th]].

[178] R. H. Brandenberger, *Challenges for string gas Cosmology*, [arXiv:0509099 [hep-th]]; R. H. Brandenberger, *String Gas Cosmology*, [arXiv:0808.0746 [hep-th]]

[179] R. Easther, B. R. Greene, M. G. Jackson, D. N. Kabat, *Brane Gas Cosmology in M-Theory:Late- time behavior*, Phys. Rev. D **67**:123501, 2003, [arXiv:hep-th/0211124]; R. Easther, B. R. Greene, M. G. Jackson, D. N. Kabat, *Brane Gases in the early universe: Thermodynamics and Cosmology*, JCAP, 0401 **006**, 2004, [arXiv:hep-th/0307233]; R. Easther, B. R. Greene, M. G. Jackson, D. N. Kabat, *String windings in the early universe*, JCAP, 0502 **009**, 2005, [arXiv:hep-th/0409121];

[180] E. Kasner, *Geometrical theorems on Einstein's cosmological equations*, Am. J. Math. **43**, 217 (1921).

[181] A. Chodos and S. L. Detweiler, *Where Has the Fifth-Dimension Gone?*, Phys. Rev. D **21**, 2167 (1980).

[182] Je-An Gu, W-Y. P. Hwang, *Accelerating universe as from the evolution of extra dimensions*, Phys. Rev. D **66**, 024003 (2002), [arXiv:0112565v2 [astro-ph]].

[183] E. L. Ince, *Ordinary Differential Equations*, (1920).

[184] J. P. Uzan, *The fundamental constants and their variation: observational and theoretical status*, Reviews of Modern Physics, Vol. **75** (403), 2003.

[185] J. Cline and J. Vinet, *Problems with Time-Varying Extra Dimensions or Cardassian Expansion as alternatives to Dark Energy*, Phys. Rev. D **68** (2003) 025015, [arXiv:0211284v3 [hep-ph]].

[186] M. C. Bento, O. Bertolami, A. A. Sen, *Generalized Chaplygin Gas Model: Dark Matter- Dark Energy Unification and CMBR constraints*, Gen. Rel. Grav. **35** 2063-2069,2003, [arXiv:0305086 [gr-qc]]

[187] R. R. Caldwell, *A phantom menace*, Phys. Lett. B **545** 23-29,2002, [arXiv:9908168v2 [astro-ph]].

[188] R. R. Caldwell, M. Kamionkowski, N. Weinberg, *Phantom Energy and Cosmic Doomsday*, Phys.Rev.Lett. **91** (2003) 071301, [arXiv:0302506v1 [astro-ph]].

[189] N. Suzuki et al., *The Hubble Space Telescope Cluster Supernova Survey: V. Improving the Dark Energy Constraints above z=1 and building an Early-Type Hosted Supernova Sample*, Astrophys. J. **746**, 85, 2012.

[190] D. Sloan, P. Ferreira, *The Cosmology of an Infinite Dimensional Universe*, [arXiv:1612.02853v2 [gr-qc]]

[191] V.F. Mukhanov, H.A. Feldman, and R.H. Brandenberger, *Theory of Cosmological Perturbations*, Phys. Rep. **215**, 213 (1992)

[192] A.R. Liddle and D.H. Lyth: *Cosmological Inflation and Large-Scale Structure*, (Cambridge University Press 2000)

[193] J. Bardeen, *Gauge-invariant cosmological perturbations*, Phys. Rev. D **22**, 1789 (1980)

[194] R. L. Arnowitt, S. Deser and C. W. Misner, *The Dynamics of General Relativity*, Gen. Rel. Grav. **40** (2008) 1997 [arXiv:0405109 [gr-qc]]